A THREE DIMENSIONAL NUMERICAL INVESTIGATION OF HILLSLOPE FLOW PROCESSES

by

ANDREW MARK BINLEY

A Thesis Submitted for the Degree of

DOCTOR OF PHILOSOPHY

Department of Civil Engineering and Construction

The University of Aston in Birmingham

October 1986

THE UNIVERSITY OF ASTON IN BIRMINGHAM

A THREE DIMENSIONAL NUMERICAL INVESTIGATION OF HILLSLOPE FLOW PROCESSES

by

Andrew Mark Binley

A Thesis submitted for the Degree of

Doctor of Philosophy

October 1986

SUMMARY

Physically based distributed models of catchment hydrology are likely to be made available as engineering tools in the near future. Although these models are based on theoretically acceptable equations of continuity, there are still limitations in the present modelling strategy. Of interest to this thesis are the current modelling assumptions made concerning the effects of soil spatial variability, including formations producing distinct zones of preferential flow.

The thesis contains a review of current physically based modelling strategies and a field based assessment of soil spatial variability.

In order to investigate the effects of soil nonuniformity a fully three dimensional model of variably saturated flow in porous media is developed. The model is based on a Galerkin finite element approximation to Richards equation. Accessibility to a vector processor permits numerical solutions on grids containing several thousand node points.

The model is applied to a single hillslope segment under various degrees of soil spatial variability. Such variability is introduced by generating random fields of saturated hydraulic conductivity using the turning bands method. Similar experiments are performed under conditions of preferred soil moisture movement. The results show that the influence of soil variability on subsurface flow may be less significant than suggested in the literature, due to the integrating effects of three dimensional flow. Under conditions of widespread infiltration excess runoff, the results indicate a greater significance of soil nonuniformity. The recognition of zones of preferential flow is also shown to be an important factor in accurate rainfall-runoff modelling.

Using the results of various fields of soil variability, experiments are carried out to assess the validity of the commonly used concept of 'effective parameters'. The results of these experiments suggest that such a concept may be valid in modelling subsurface flow. However, the effective parameter is observed to be event dependent when the dominating mechanism is infiltration excess runoff.

Key words: Finite element, Computer modelling, Rainfall-runoff, soil variability, soil moisture.

Dedicated to the memory of my Mother

ACKNOWLEDGEMENTS

I would firstly like to thank my academic supervisor Dr. John Elgy for his help and encouragement throughout the period of this research.

I am indebted to Dr. Keith Beven of The University of Lancaster, formerly of The Institute of Hydrology, for showing great interest in this study and for providing expert guidance during the past two years.

I must also thank David Stops of the Computer Centre, Aston University for acting on many occasions as 'middle man' between UMRCC and myself.

Finally, thanks to Dawn for her lasting patience and understanding.

This research was financed by The Science and Engineering Research Council from whom the author was in receipt of a Research Studentship.

LIST OF CONTENTS

LIST OF CONTENTS (contd.)

LIST OF CONTENTS (contd.)

LIST OF TABLES

LIST OF TABLES (contd.)

LIST OF FIGURES

Chapter 1

Introduction

1.1 GENERAL

Control and management of the behaviour of water has always been of paramount importance to mankind. Devastating events such as floods and droughts necessitate the need to accurately describe the rainfall-runoff process. Such an understanding is also vital to predict the hydrological impact of man's changes to the environment and thus control any detrimental effects. Clearly it is impossible to make predictions of the hydrological cycle using the prototype, therefore models of the rainfall-runoff process are required.

Over the past decade a vast number of rainfall - runoff models have been developed and tested. These models are now becoming more complex and, according to the model authors, more accurate. However, even the most complex rainfall-runoff models show limitations due to a number of unresolved problems in modelling certain hydrological processes.

Hydrological models are formulated for various reasons, the principle purposes can be categorized as follows.

(i) Forecasting - Specific models may be used to obtain forecasts of extreme hydrological events, such as floods.

(ii) Operational simulation - Models may be used as decision making aids in water resources planning by evaluating the consequences of several alternative planning strategies.

(iii) Data fill-in and record extension - Synthetic data generation from a hydrological model may be used to provide missing values or extend an observed record.

(iv) Research - Hydrological models may be used to provide a greater understanding of the real system, if the model is assumed to be a reasonable descriptor of the real world processes.

This study is primarily concerned with using a hydrological model in the context of the latter category to examine the effects of certain phenomena on hillslope hydrology. In doing so an assessment of the limitations of current modelling techniques can be made.

1.2 THE HILLSLOPE HYDROLOGICAL CYCLE

Detailed descriptions of the complex hillslope hydrological processes can be found in many texts, in particular the classical work by Kirkby (1978). The current concept of the hillslope hydrological cycle can be briefly described as follows.

Rain that has not evaporated in the atmosphere has a number of possible destinations upon reaching the Earths surface (see figure 1.1). Rain falling directly into a stream adds to the channel flow whereas rain falling away from the channel may be intercepted by plant and tree leaves, open then to possible evaporation. Alternatively, the rain can fall on to the ground surface. Water on the soil surface will infiltrate into the soil in an attempt to reach a lower potential, however, if the rain intensity is higher than the infiltration capacity of the soil the surplus water will be held in storage on the soil surface or flow down the hillslope as overland flow. Some infiltrated water will be taken up by the roots of plants in the soil, the rest will continue its descent until an impeding layer is reached, for example another soil type. In general, lower soil horizons are less permeable than surface soils and therefore, depending on the infiltration rate, some water will be directed along the base of the upper soil horizons towards the channel. This flow of water is termed throughflow and can arrive at the stream channel during the storm, hence adding to the storm hydrograph. Under such conditions throughflow is often termed subsurface stormflow.

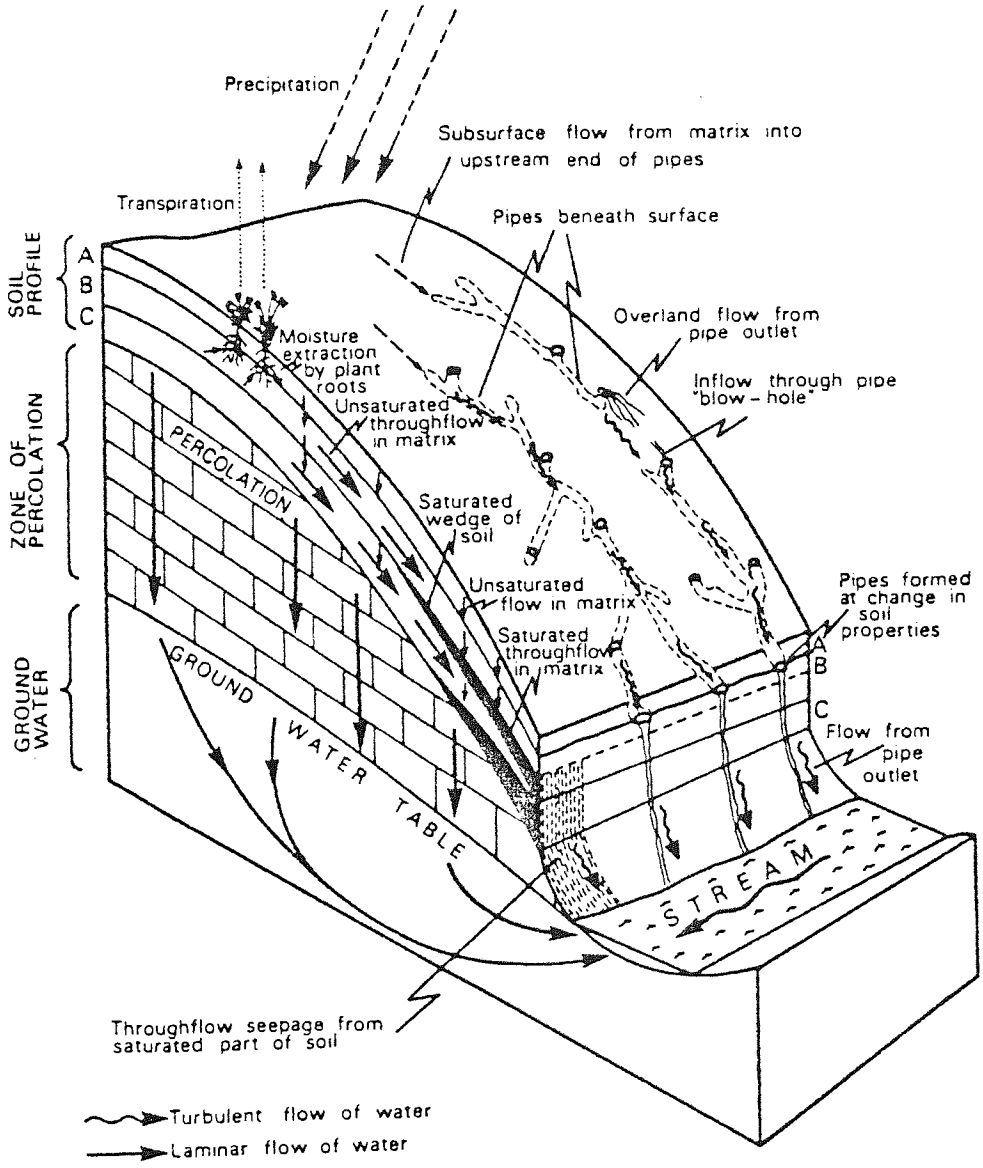

Figure 1.1 Hillslope flow routes, after Atkinson (1978).

As more water is resisted by the impeding layer a saturated zone builds up in the upper soil horizons which increases the speed of return to the channel. Should this saturated zone reach the soil surface water may be directed out of the soil mass as return flow, hence contributing to the overland flow.

Water that has percolated through the impeding layer, and any number of such layers, reaches the groundwater table and becomes part of the groundwater system. Groundwater flow is relatively slow due to the low conductivities of the base soils. This flow usually provides only base flow to the hydrograph.

The majority of water movement through the saturated-unsaturated soil is matrix flow, however the existence of large non capillary pores, or macropores, has been widely demonstrated in the literature. Macropores range from small cracks in the soil to large diameter pipes which are naturally formed. Figure 1.2 shows a section of an observed pipe in the Wye catchment, Wales (after Gilman and Newson ,1980). Such pores may cause preferential flow of soil water, allowing rapid transit and thus have a considerable effect on the storm hydrograph.

The response of the hillslope as a whole is therefore a complex interaction of many sub processes, which is further complicated by the nonuniformity of the system and the spatial and temporal variability of inputs.

1.3 MODELS OF HILLSLOPE HYDROLOGY

The idea of being able to model catchment behaviour is not new, in fact the early empirical models are thought to date back to the 17th Century. Little, if any, improvements were made until the early 20th Century when the classical model of the hillslope hydrological cycle was described by R.E. Horton.

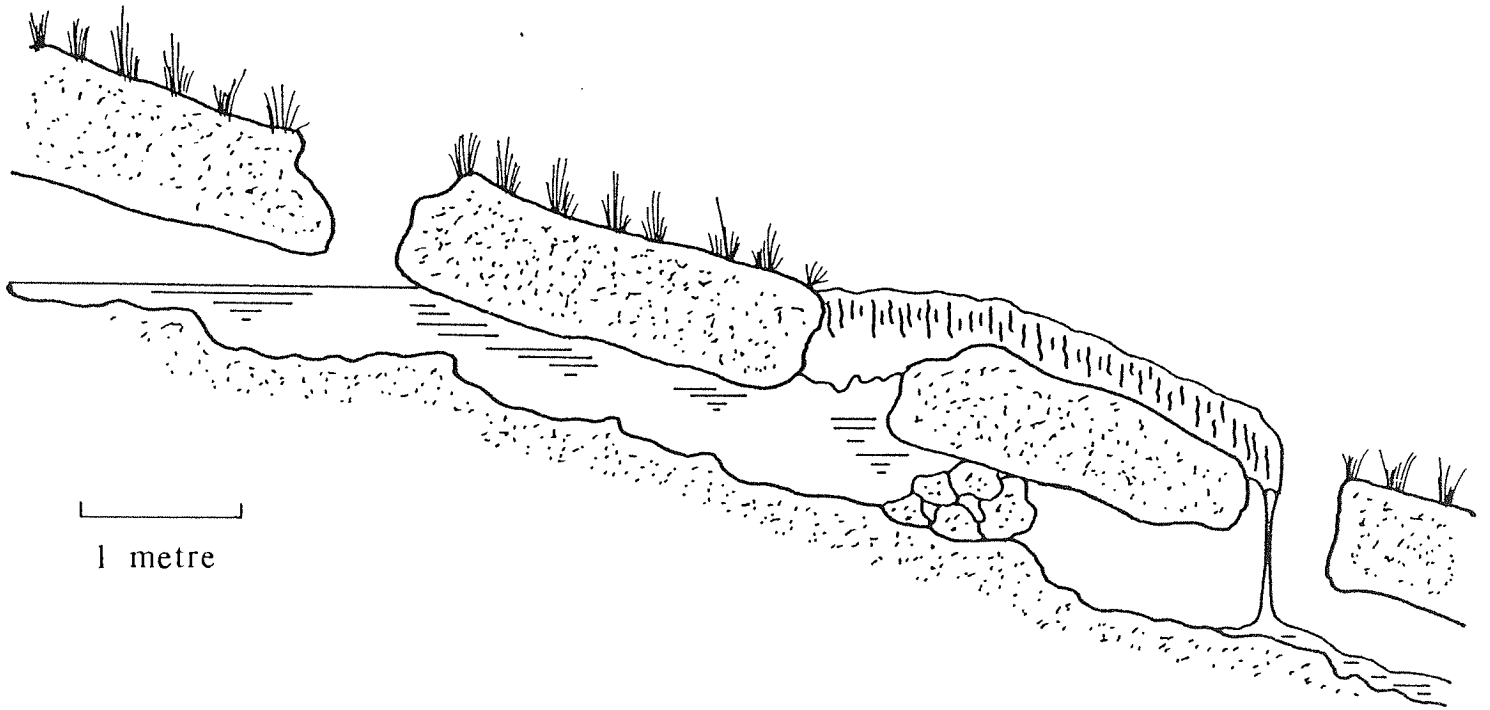

Figure 1.2 A longitudinal section of a perennial soil pipe in the Wye catchment, after Gilman and Newson (1980)

Rainfall-runoff models remained purely empirical until the 1950's when the availability of digital computers combined with a greater theoretical understanding of the processes enabled hydrologists to explore various modelling techniques.

There are a number of classifications which can be given to hydrological models. A model will be associated with at least one of the following categories.

Lumped - treats the processes in terms of average quantities over catchment areas. An example of one of the first lumped models is the Stanford Watershed Model (Linsey and Crawford, 1960).

Distributed - treats the catchment as a spatially variable system, for example Eraslan et al. (1981).

Deterministic - the model inputs and outputs are not subject to the laws of chance.

Stochastic - the model inputs and outputs are subject to uncertainties, that is, not deterministic.

Black box - the model is based on an appropriate mathematical function, or functions, which fit the data irrespective of the underlying process which it represents.

Conceptual - the model is designed using various simple empirical concepts describing the hydrological processes.

Physically based - the model is composed of a series of mathematical equations which represent the currently acceptable theory of the hydrological cycle.

Naef (1981) has compared the accuracy of a number of catchment models ranging from the unit hydrograph to complex conceptual models. Naef stated that a comparison of the results of these models revealed that none of the models tested actually described the process accurately since hydrological events could be found to fit the results of the models, as could events which would not fit the model simulations. These findings help to explain why the unit hydrograph is still one of the commonest techniques many years after its original development.

Physically based distributed models represent the latest generation of hydrological models. The mathematical equations used in these models are based on empirical relationships, for example Darcy's Law and Manning's equation, but offer the advantage over simpler models by the fact that parameters of the model are physically measurable in the field.

An important benefit of physically based modelling is that it allows an improved understanding of the hydrological behaviour of a watershed. More practical benefits from physically based models include the ability to analyze the effect of catchment changes and the capability of predicting the response of ungauged watersheds.

Since simpler models require calibration using previous hydrological records, the model itself is only valid if changes are not made to the system. Such changes include forest management, urbanization and agricultural changes. Physically based models allow the effects of these changes to be examined by the alteration of the model parameters. The physical significance of the model parameters within a physically based model also permit the modelling of ungauged catchments without the need for long records of hydrological data. Physically based models further allow the inclusion of pollutant and sediment transport equations in a distributed manner and therefore investigations into effects such as the dispersion of localized pollutant sources can be carried out.

The main limitations of physically based models can be categorized as follows.

(i) Computer limitations

(ii) Scarcity of data

(iii) Inadequacies in representing the real system

Limitations of types (i) and (ii) have restricted the few physically based modelling studies to research applications, although computer limitations are likely to diminish in future studies due to the rapid growth in computer technology.

Limitations of type (iii) include the assumptions made during the development of the governing equations, such as fluid incompressibility in the case of surface flow. At a more fundamental level, type (iii) limitations include the mis-representation of the actual mechanisms. For example, assuming sheet flow behaviour of overland flow is merely a conceptualized approximation to the real case of localized surface flow through rills and gullies over the soil surface. A further example of such a limitation, which is of interest to this study, is the assumption made in current models about the nonuniformity of soil properties over a catchment. The spatial and temporal variability of soil properties has been demonstrated by many field studies, however, limitations of type (ii) have, at present, precluded the inclusion of such effects in physically based models. The normal approach is to assume representive soil properties over areas of the flow domain, thus treating the distributed system in a lumped manner. However, there is little, if any, theoretical justification for such an assumption.

A further inadequacy in representing the real system lies in the way areas of preferred flow caused by natural soil pipes are treated. Again scarcity of data and limited hydrological understanding of the phenomenon has forced the same lumping process to be adopted to account for distinct zones of rapid soil water movement.

1.4 OBJECTIVES

The objectives of this study are twofold. Firstly, using a detailed physically based model of hillslope hydrology, developed for the purpose of this study, an investigation of the effects of soil spatial variability and zones of preferential flow on hillslope runoff generation can be made. Conclusions can then be drawn regarding the importance of such conditions in catchment modelling. Secondly, using the results of these numerical simulations, an assessment can be made of the validity of lumping physically based model parameters to represent various geomorphological phenomena.

1.5 OUTLINE OF THE THESIS

In order to define the problem in greater detail, Chapter 2 provides a review of the equations and principles used in physically based models of individual processes. A number of complete physically based catchment models are described and the problem of model calibration is addressed. In addition, a field assessment of soil spatial variability is made, including the results of a field measurement programme carried out for this thesis.

For the necessary hydrological simulations a three dimensional variably saturated flow model, based on the finite element method, is presented in Chapter 3, together with the results of a model verification test.

By considering two distinct dominating mechanisms of runoff generation, applications of the model to a single hillslope segment for various degrees of soil nonuniformity are provided in Chapter 4. Chapter 5 includes similar experiments under conditions of preferred soil water movement.

Using the results from Chapters 4 and 5, the question of the validity of lumping model parameters is addressed in Chapter 6 by assessing the suitability of 'equivalent' uniform soils representing a nonuniform formation. Finally, conclusions regarding the suitability of current modelling techniques and implications towards future modelling are presented in Chapter 7.

Chapter 2

Physically based modelling of catchment hydrology

Physically based models offer distinct advantages over simpler models, although there still exists a number of unresolved problems in the modelling of catchment hydrology. In applications to real systems, unavailability of data at a sufficiently fine spatial and temporal resolution and the correctness of the adopted descriptive equations present great threats to the suitability of current physically based modelling strategies.

2.1 MODELLING STRATEGY

Since the flow processes occuring within a catchment vary in space and time, the ideal physically based modelling strategy would be to solve acceptable continuum equations in a transient three dimensional system. At present such an approach is limited to small scale problems due to the immense computer requirements. It is therefore necessary to make certain simplifying assumptions about the hydrological processes within a catchment. Such assumptions lead to the reduction of the number of space dimensions in which the equations vary, such as one dimensional channel flow. The result is then a set of interacting one, two or three dimensional components each representing particular flow domains within the catchment. Figure 2.1 demonstrates such an approach. The catchment in this case is discretized into a series of hillslope and channel segments. By selecting the location of each hillslope segment such that each of its boundaries is either a channel segment, a catchment divide or a line normal to topographical contours, it may be possible to represent surface and subsurface flows within a hillslope using one or two dimensional equations.

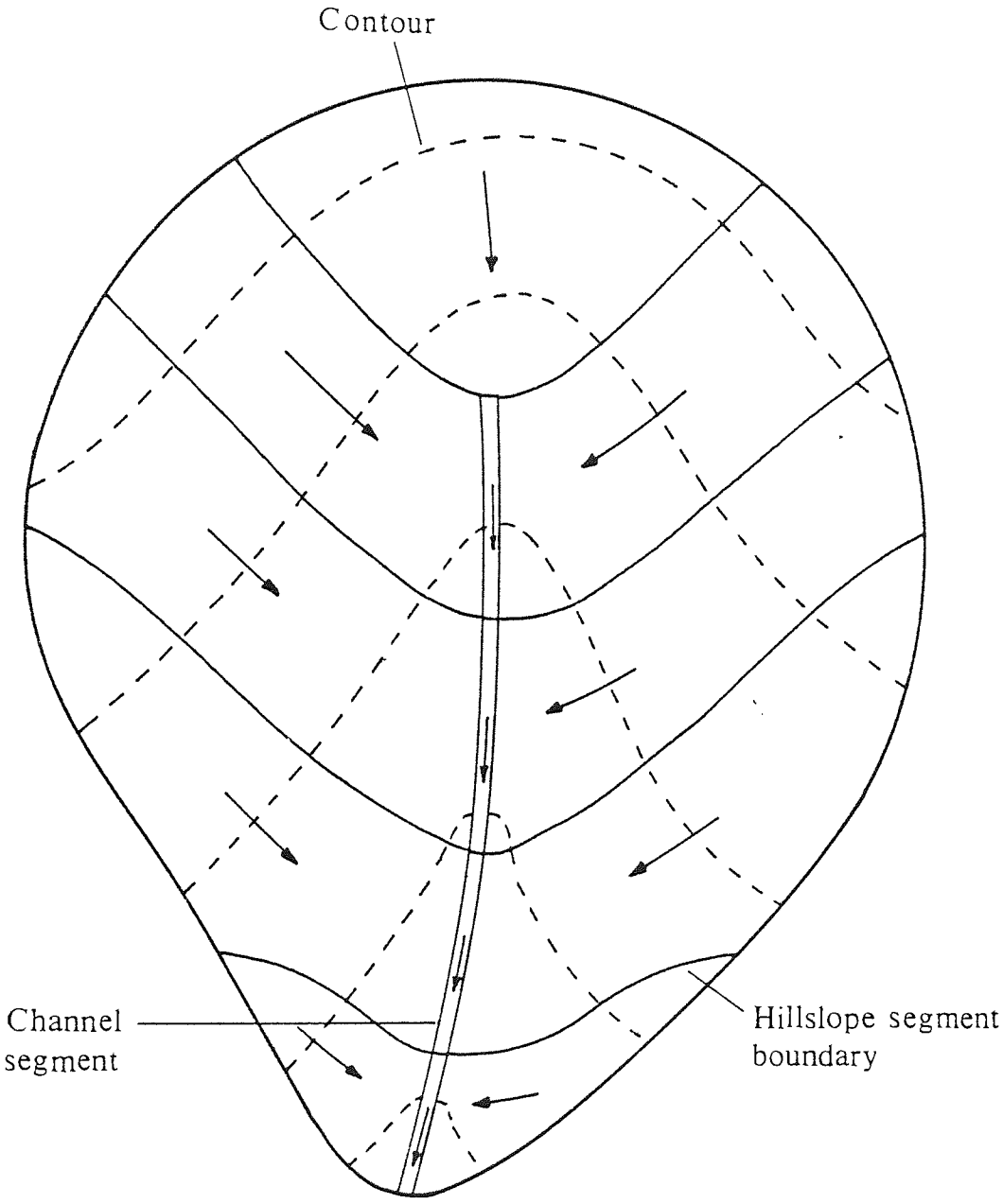

Figure 2.1 An example of physically based modelling catchment discretization, showing idealized flow routes

2.1.1 Model equations

2.1.1.1 Soil water flow

The movement of water through soil under conditions of variable saturation is described by (see for example Pinder and Gray, 1977),

$$\nabla . (K_S K_r (\psi) . \nabla h) - \{ \frac{\theta(\psi)}{n} (\alpha + n\beta) + C (\psi) \} \frac{\partial \psi}{\partial t} = 0 \qquad (2.1)$$

where, K_S = saturated hydraulic conductivity tensor

K_r = relative hydraulic conductivity ($0 < K_r \leq 1$)

ψ = pressure head

h = hydraulic head

θ = moisture content.

n = porosity

α = compressibility of the medium

β = water compressibility

t = time

C = specific moisture capacity = $\partial\theta(\psi) / \partial\psi$.

K_r, θ and C are nonlinear functions of ψ and for each soil type there exists two main curves for each function (wetting and drying). An infinite number of scanning curves

will lie between these two main curves, representing a transition from a wetting to a drying state or vice versa. This scanning is termed hysteresis and can be due to a number of reasons including; soil swelling and shrinking, entrapped air and the 'ink bottle effect' (Hillel, 1971, p 67).

Under unsaturated conditions, the effect of the compressibility of the medium and water is usually neglected due to the more dominating effects of moisture content variation (see for example Brutsaert and El-Kadi, 1984). The resulting equation is often called Richards equation, after Richards (1931).

In the saturated zone equation (2.1) is linear since for $\psi > 0$ it is normally assumed that

$K_r(\psi) = 1$, $C(\psi) = 0$ and $\theta(\psi) = n$.

2.1.1.2 Surface flow

Overland and channel flow may be described by the one dimensional form of the St. Venant equations (see for example Freeze, 1978). Assuming a rectangular channel, the equations of continuity and momentum, respectively, are,

$$\frac{\partial y}{\partial t} + y\frac{\partial v}{\partial x} + v\frac{\partial y}{\partial x} + \frac{vy}{B}\frac{\partial B}{\partial x} - r - \frac{q_i}{B} = 0 \qquad (2.2a)$$

$$\frac{\partial v}{\partial t} + v\frac{\partial v}{\partial x} + g\left(\frac{\partial y}{\partial x} - S_o + S_f\right) + \frac{v}{By}(rB + q_i) = 0 \qquad (2.2b)$$

where: v = velocity

x = distance along channel

y = depth of flow

r = effective rainfall

B = channel width

g = acceleration due to gravity

q_i = lateral inflow

S_o = bed slope

S_f = friction slope (obtained from Manning's or Chezy's formulae).

Equations (2.2) can be simplified to various degrees, for example, the diffusion model assumes that,

$$\left(\frac{\partial y}{\partial t} - S_o + S_f \right) = 0$$

Further simplification can be obtained using the kinematic wave assumption, that is,

$$S_o = S_f$$

The kinematic wave formation results in equations (2.2) being described by just one equation,

$$\frac{\partial y}{\partial t} + \frac{1}{B} \frac{\partial}{\partial x} (B \alpha y^m) - r - \frac{q_i}{B} = 0 \qquad (2.3)$$

where: $\alpha = \frac{\sqrt{S_o}}{n_{man}}$

m = 5/3 for turbulent flow

n_{man} = Manning's number.

A further advantage of the kinematic model is that only one boundary condition is required. In general, however, it is recognized that the complete (dynamic wave) equations are usually required to describe channel flow. The kinematic assumption is most appropriate for flow in steep channels or on steep slopes. Woolhiser and Ligget (1967) have shown that such an approximation is valid providing that a factor K is greater than 10,

where: $K = \frac{S_o L_o}{H_o F_o^2}$

L_o = length of plane

H_o = normal depth

F_o = Froude number = $v_o / \sqrt{gh}$

v_o = velocity at normal depth H_o = Q_{max} / H_o

Q_{max} = maximum outflow rate = $r_{max} L_o$

r_{max} = maximum rainfall rate.

For example, consider the case of surface flow on a 100 metre, 1 in 500 slope, Manning's number equal to 0.025 and rainfall rate equal to 20 millimetres per hour. The calculated value of K in the above equation is then 392.5.

In practice it has been well recognized that the condition suggested by Woolhiser and Ligget is generally true for overland flow and the kinematic model has been used in numerous overland flow studies, for example Overton (1971), Smith and Woolhiser (1971), Aparcio and Berezowky (1982).

2.1.1.3 Interception and evapotranspiration losses

Interception losses may be described in terms of leaf area index (area of leaf cover ÷ area of ground), see for example Jensen (1979). This percentage of precipitation which is retained by the plant surface may then evaporate or later drain to the soil surface. A comparison of a number of interception models can be found in Eriksson and Grip (1979).

The calculation of evapotranspiration is usually performed by determining the potential evapotranspiration which is then combined with soil plant characteristics and soil evaporation relationships to determine the actual evapotranspiration loss. A number of techniques are available (Saxton, 1981) and in general, the availability of data governs the choice of model. A comparison of the results of several evapotranspiration models is presented in Keller (1979).

2.1.2 **Solving the individual equations of flow**

Due to the complexity of the governing equations no analytical solutions exist without further simplifying the equation. Numerical solutions are therefore required. The most popular numerical techniques are the finite difference and the finite element methods, both of which lead to a set of algebraic equations which can be solved given initial and boundary conditions.

2.1.2.1 Variably saturated flow

2.1.2.1.1 Finite Difference Methods (FDM)

This technique is discussed extensively elsewhere, for example Remson et al. (1971) and will therefore not be described herein.

The first numerical models of multi-dimensional variably saturated flow were formulated using the FDM, Rubin (1968) being one of the pioneers in this field.

Rubin solved Richards equation for drainage of a block of soil and for horizontal infiltration into dry soil. For the latter case the Kirchoff integral transformation was also employed as he found that solving the equation in its original form could not account for the high nonlinearity of this example.

Rubin's work has been followed by numerous other variably saturated models using the FDM, for example Todsen (1973), Hornung and Messing (1979), Gillham et al. (1979), Vauclin et al. (1979) and Reeder et al. (1980). Remson et al. (1971) has provided an extensive list of earlier models using the FDM and Haverkamp and Vauclin (1981) have carried out a comparative study of the finite difference solution of three forms of Richards equation.

Freeze (1971) developed a three dimensional model of a groundwater basin including the unsaturated zone and coupled this model with a channel flow model (Freeze, 1972a,b). Freeze used the Line Successive Over Relaxation technique to solve the resulting finite difference equations. His model was applied to hypothetical catchments and rigorous tests were undertaken in order to examine the effects of different parameters and conditions. Freeze's model was the first of a very small number of models that, even under hypothetical conditions, have incorporated the full equations for variably saturated flow.

Rovey (1975) presented a similar model to that of Freeze and its application to a forty mile reach of the Arkansas valley of south eastern Colorada, USA.

A two dimensional finite difference model based on Richards equation, also similar to Freeze's model, has been developed by Akan and Yen (1981). The main area of

application of this model has been in infiltration modelling and to date, simulations of real events using this model are not evident in the literature.

The integrated finite difference method (IFDM) is considerably different to the usual FDM in that an arbitrary grid can be used. The method has been adopted for use in groundwater modelling since the early 1960's (Tyson and Weber, 1964; Cooley, 1971; Thomas, 1973). Narasimhan and Witherspoon (1976) developed a variably saturated flow model using the IFDM and then extended the model to account for flow in variably saturated deformable media (Narasimhan and Witherspoon, 1977, 1978; Narasimhan et al., 1978a).

In the IFDM each node is associated with a subregion, as in figure 2.2. A mass balance over each subregion is then made by integrating equation (2.1) over all subregions. These integrals are then approximated as a finite sum of finite differences. The IFDM has not been widely used in hydrology compared with the FDM and FEM. This is probably due to its requirement for a carefully designed mesh so that the boundary of the subregion of a node point corresponds to a series of perpendicular bisections of lines joining the node point and its surrounding nodes (see figure 2.2). Such a procedure is identical to the formation of Thiessen polygons for rainfall mapping.

2.1.2.1.2 The Finite Element Method (FEM)

Soon after the finite element method was introduced as a structural analysis method in the early 1960's, it was realized that the method could be used as a general technique for approximating the solution of partial differential equations. Initially the FEM relied on a variation principle and the Rayleigh-Ritz method was directly associated with the FEM. The problems that can be solved using the Rayleigh-Ritz method, however, represent a subsection of those solvable by a much more general method - the Method of Weighted Residuals (MWR). The MWR itself is a general class of tehniques: the

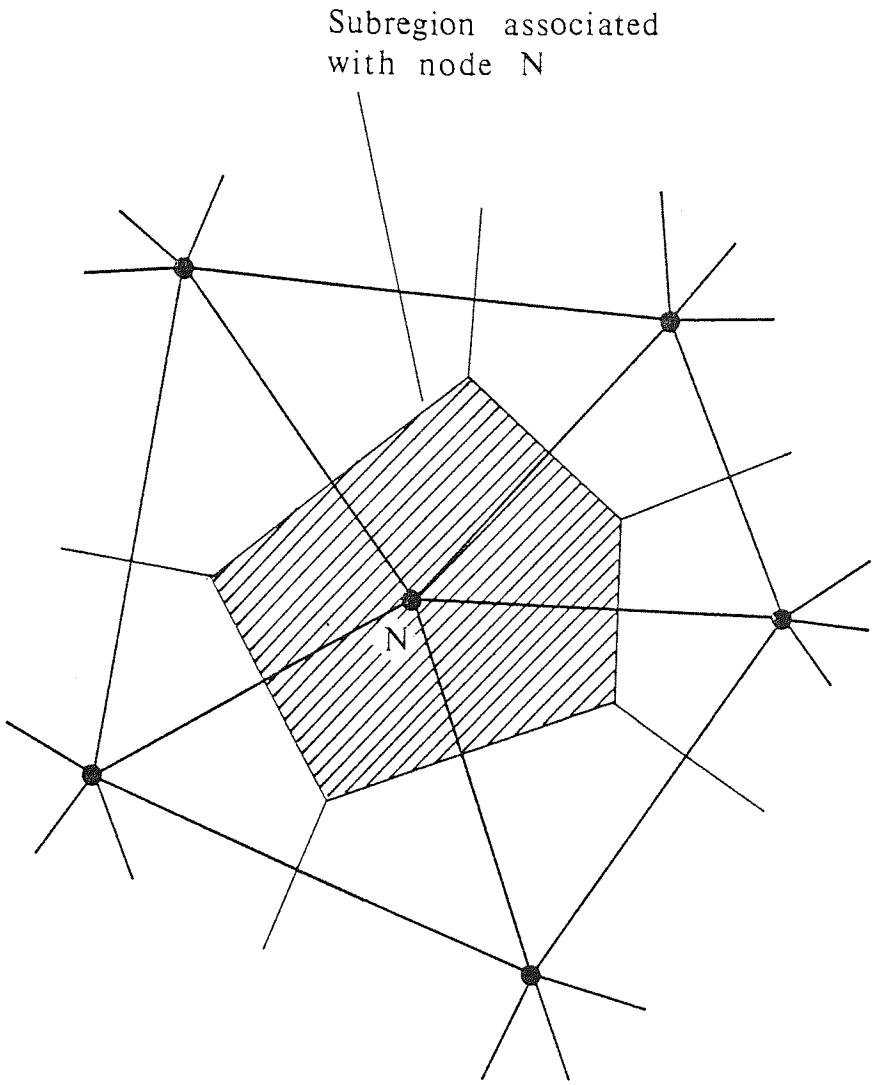

Figure 2.2 IFDM mesh geometry

Collocation, Least Squares, Subdomain and Galerkin's methods being the most commonly used (Pinder and Gray, 1977). In particular Galerkin's method has received much attention in the study of the hydrological processes. The major advantages of the FEM over the FDM are the ability to use higher order approximations, the ease of discretizing complex domains and the ease with which boundary conditions are introduced into the solution. Faust and Mercer (1980) have discussed the advantages and disadvantages of both methods.

The first stage of the procedure is to discretize the region into elements, the shapes of which are determined by node points (see figure 2.3). The variable of interest is approximated over the region by a series of products of the node point values and a corresponding interpolation function (also called a basis or shape function).

By substituting the series into the original differential equation, there will be some error between the exact and approximated solution. That is, if,

$$L\,u = f$$

is the original differential equation, where L is a differential operator, u is the unknown variable and f is a known function. Then the residual R is equal to,

$$R = L\,\hat{u} - f$$

where $\hat{u}$ is the approximated variable. The MWR essentially weights this residual over the region R. In the Galerkin's method the weights are chosen to be the interpolating functions.

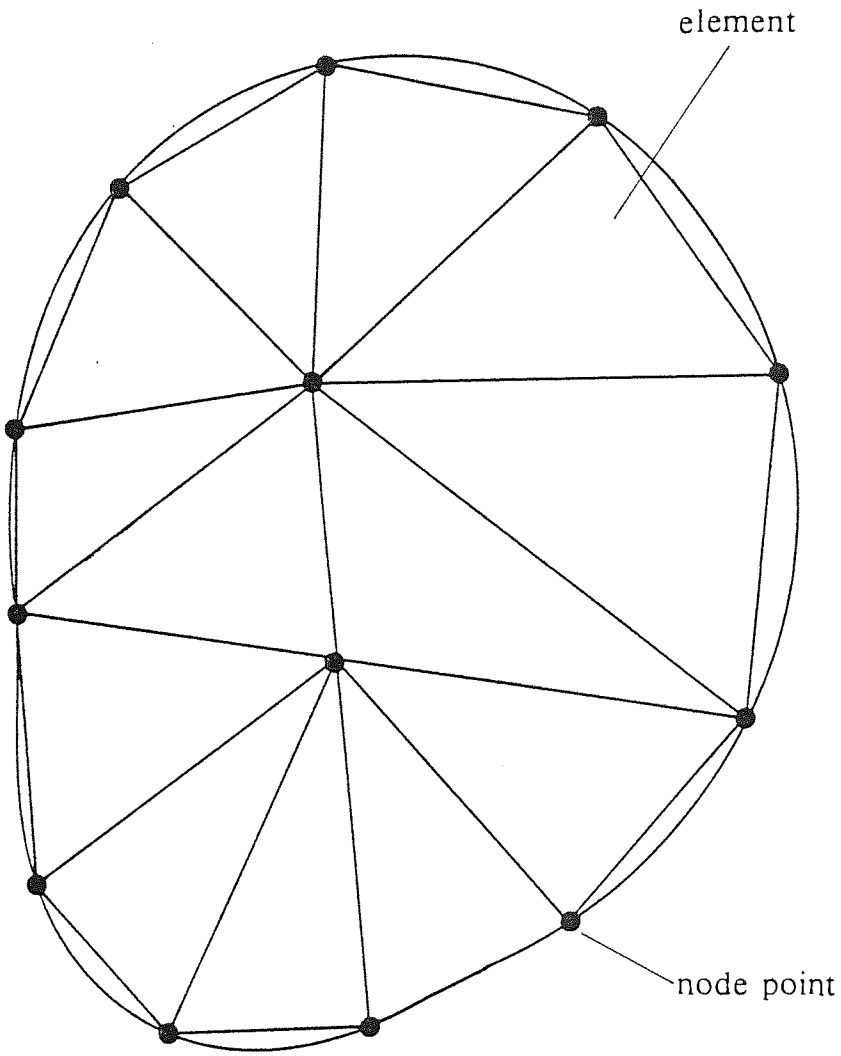

Figure 2.3 Domain discretization using finite elements.

The resulting equation is of the form,

$$\int_R R \; w_i \, dR = 0 \qquad i = 1, 2, \ldots n$$

where w_i is the weighting function and n is the number of node points.

The FEM therefore approximates the solution by an integral approach, whereas the FDM utilizes a differential approach.

The simplest form of the FEM results from the use of linear interpolation functions and simple element shapes. The only advantages of using a more complex shape, for example curvilinear triangles, is that an irregular region can be approximated with greater accuracy. This is of minor importance over large areas, as in the case of hydrological simulation, and therefore, the triangular and rectangular elements (for two dimensional equations) have become standard elements in this field.

The use of complex shape functions, for example cubic, is of more importance, particularly in the unsaturated zone. This is due to the high nonlinearity of the governing partial differential equation.

Neuman (1972, 1973) was one of the first to apply the FEM to flow in variably saturated porous media. Neuman applied Galerkin's method over the spatial derivatives using linear interpolation functions and a finite difference scheme to approximate the time derivatives.

Neuman's work was followed by many applications of similar models to two dimensional variably saturated flow problems. Examples include; Bruch (1976), Hayhoe (1978), Cusham et al. (1979), Yeh (1980), Gureghian (1981), Marino

(1981), Orlob and Ghorbanzadeh (1981), Zaslavsky and Sinai (1981), Stauffer and Job (1982), Herrling and Leisman (1984), and Lam and Fredlund (1984).

Due to the high nonlinearity of the governing equations of unsaturated flow, numerical problems, such as instability, may arise in a crude approximation to the complex system. Also unsaturated flow problems require large amounts of computing resources since the nonlinearity necessitates an iterative solution together with fine spatial and temporal discretization. Such economic considerations have led to various enhancements to the basic FEM. Modifications have been reported in Narasimhan et al. (1978b), Nieber (1980), Hromadka and Guymon (1980, 1981), Hromadka et al. (1981), Cooley (1983), Huyakorn et al. (1984) and Milly (1984).

More fundamental investigations have been carried out in studies of the effect of the inclusion of hysteresis in finite element models of variably saturated flow. Examples include; Pickens and Gillham (1980), Nieber and Walter (1981), and Milly (1982).

The hysteresis of the $\theta(\psi)$ function is usually expressed as a relationship between the boundary wetting and drying curves and the pressure head history, see for example Mualem (1974). Hysteresis in the $K_r(\psi)$ relationship is usually neglected. The studies mentioned have demonstrated that hysteresis can have a considerable effect, however, immense data requirements have prohibited the inclusion of such effects in applications under real conditions.

2.1.2.1.3 The Boundary Element Method (BEM)

The BEM was developed during the mid 1970's from much work on integral equations and the FEM. The theory behind this method will not be discussed here but can be found in a number of texts, for example Brebbia and Walker (1980) and Ligget and Lui (1983), the latter reference being specifically orientated towards analyzing flow through porous media.

Application of the BEM reduces the dimension of the problem and is therefore best suited to multi-dimensional problems. The resulting conductance matrix is full in comparison with the sparse structure in the FEM. The FEM, however, is more attractive in the study of anisotropic and nonlinear problems such as unsaturated flow.

A combination of both methods is possible, for example by approximating saturated flow by the BEM and the unsaturated flow region by the FEM (see figure 2.4), although this approach, as yet, has not received attention in modelling of catchment hydrology.

2.1.2.2 Saturated groundwater flow

By assuming strictly horizontal flow, a two dimensional form of equation (2.1), under saturated conditions, is normally adopted for models of aquifers.

Numerous solutions to saturated flow problems exist using the FDM (see for example Trescot et al., 1972; McDonald and Harbaugh, 1984) and the FEM (see for example Pinder and Frind, 1972; Jovic, 1977; Fog et al., 1979) . Dillon and Ligget (1983), amongst others, have formulated boundary element approximations to the governing equations. A review of the various solution methods can be found in Faust and Mercer (1980). The choice of numerical technique generally depends upon the individual preference of the model author.

2.1.2.3 Channel flow

To date, the commonest method of solution of the one dimensional St. Venant equations is the four point implicit finite difference approximation, for example Samuels and Price (1979). The FEM appears to offer no advatange over this technique (Fread, 1981).

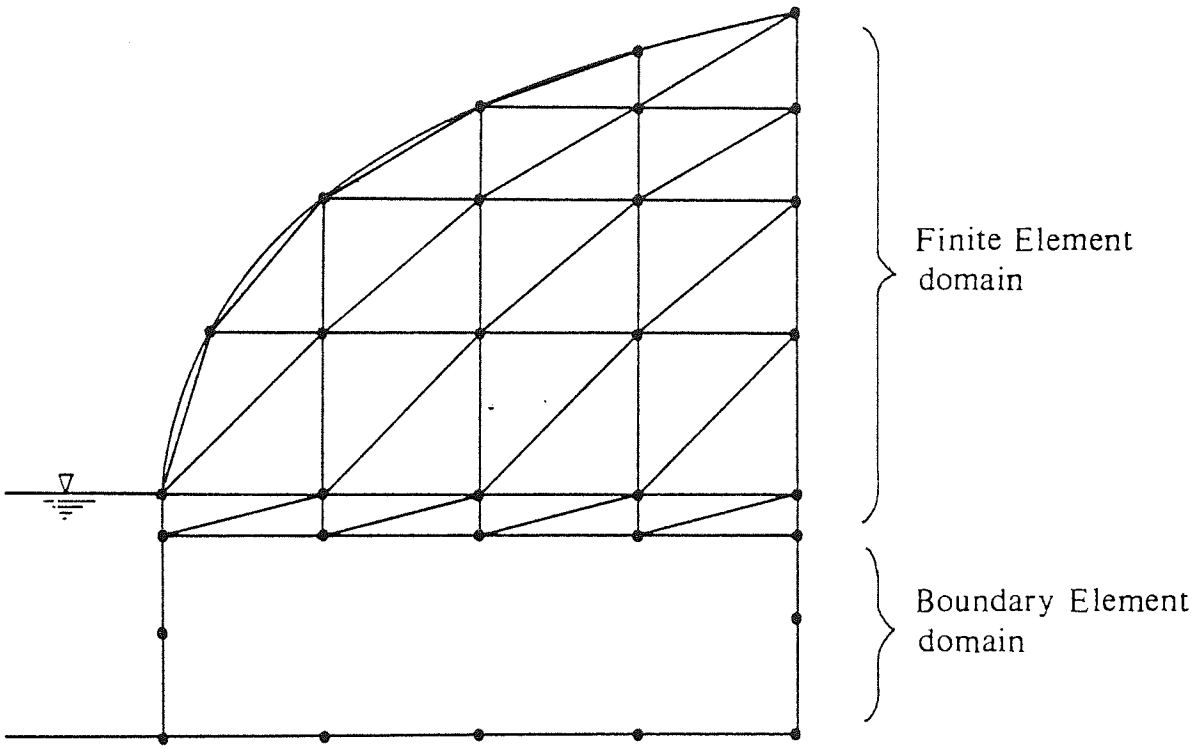

Figure 2.4 An example of combining the Finite Element and Boundary Element methods

The finite element method, however, is popular in the modelling of two dimensional problems, for example Samuels (1983), Hosseinipour and Amein (1984) and three dimensional unsteady flow, for example King (1985). Models such as these are only considered when a large amount of information is required, such as the modelling of estuaries, or when very irregular channel geometry is evident.

2.1.2.4 Overland flow

Many solutions of overland flow problems are presented in the literature. Both the FDM (for example, Brakensiek, 1966; Smith and Woolhiser, 1971) and the FEM (for example, Aparcio and Berezowsk, 1976; Taylor, 1976; Kawahara and Yokayama, 1980) have been utilized.

As in the case of channel flow modelling, finite element analysis of the one dimensional problem appears to offer no advantage over the FDM.

2.2 COMPLETE CATCHMENT MODELS

There have been numerous modelling studies of the individual components of catchment hydrology. Although several models of coupled components exist, only a small number have received applications to real world situations, in particular on the catchment scale.

2.2.1 The Finite Element Storm Hydrograph Model (FESHM)

The FESHM (Ross et al., 1979; Shantoltz et al., 1981; Heatwole et at, 1982) has been developed for application to catchments where Hortonian infiltration excess overland

flow dominates the storm hydrograph. Under such conditions subsurface flow is assumed to play a minor role and infiltration loss into the soil is the only recognition of the soil zone. Such losses are accounted for in the FESHM using the empirical Holtan equation (Holtan, 1961).

In the FESHM, model parameters are allowed to vary over the catchment by discretizing the watershed into land units having individual soil mapping and land use characterisitics. These areas are termed Hydraulic Response Units (HRU) (Li et al., 1977). A second discretization, independant of the first, is then performed in which the watershed is divided into finite elements for surface flow routing using the one dimensional kinematic wave model. Specifying precipitation inputs to the HRU's, infiltration excess is calculated knowing the current soil water state in each HRU. These values of overland flow recharge are then averaged over each finite element to provide boundary conditions to the finite element surface flow routing algorithm.

Figure 2.5 demonstrates the above discretization procedure for an application of the FESHM to Powells Creek, Virginia, USA (after Contractor et al., 1980). In this case the watershed is divided into 65 HRU's and flow routing is carried out on a finite element grid consisting of eight overland flow elements and four channel elements.

By treating catchments as ungauged, and then relying on measured model parameters, the FESHM has shown some success under conditions of large flood events, when the underlying assumptions of infiltration excess are reasonable.

2.2.2 Systême Hydrologique Européen (SHE)

A collaboration of the Danish Hydraulic Institute, SOGREAH (France) and the Institute of Hydrology (UK) has produced the Sytême Hydrologique Européen (SHE) physically based hydrological model (Jonch-Clausen, 1979; Beven et al., 1980).

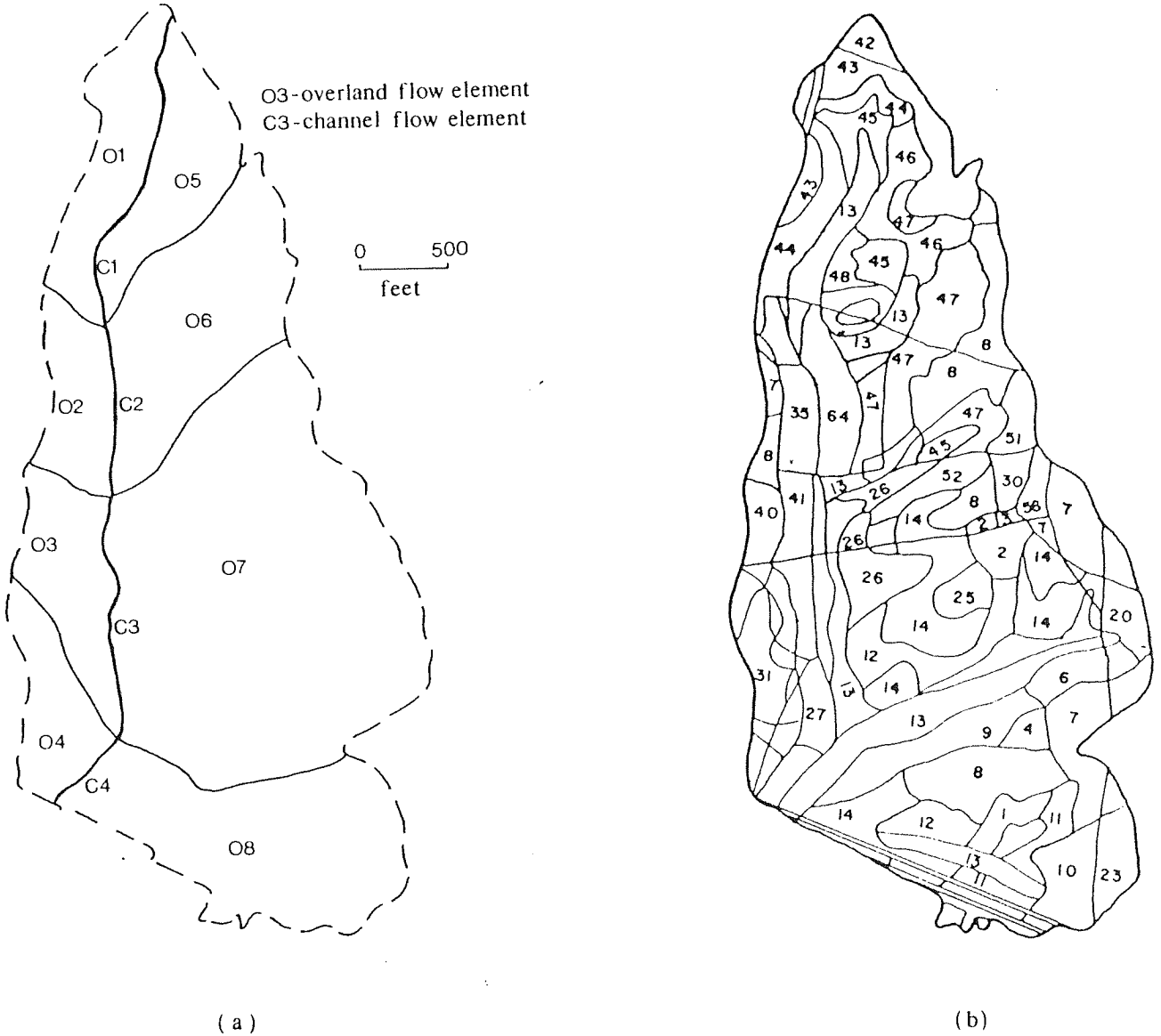

Figure 2.5 Discretization of Powell's Creek Watershed, after Contractor et al. (1980). (a) Finite element map, (b) HRU map

As shown in figure 2.6, the basic structure of the SHE model is an interaction of a two dimensional surface rectangular grid and a subsurface rectangular grid. Overland flow and channel flow are modelled on the surface grid using a simplified form of the St. Venant equations. The subsurface grid represents a single layer unconfined aquifer. An interaction between the surface flow components and the saturated groundwater component is allowed via a series of one dimensional vertical columns representing unsaturated soil water movement (Abbott et al., 1979). All flow equations are approximated using the FDM.

The SHE model recognizes interception and evapotranspiration losses (Jensen and Jonch-Clausen, 1981) and when appropriate, snowmelt (Morris and Godfrey, 1979).

Although the SHE model is intended to be used on grids of up to 2000 node points in the horizontal grids and 30 nodes in the vertical (Beven et al., 1980), the structure of the model does not permit fine resolution for areas of surface saturation close to channels, or for conditions when lateral unsaturated soil water movement is important. The applications of the SHE model are then best suited to cases where widespread infiltration excess overland flow occurs, as in the FESHM, or when regional groundwater movement is important.

A very similar model, in structure, to the SHE model is PREDIS (Gilding, 1983) which is under development by the Delft Hydraulic Laboratory, Netherlands. PREDIS allows recognition of both confined and unconfined aquifers which, as in SHE, are linked to the surface components using a vertical unsaturated flow model. The soil water equations in PREDIS are approximated using the FEM.

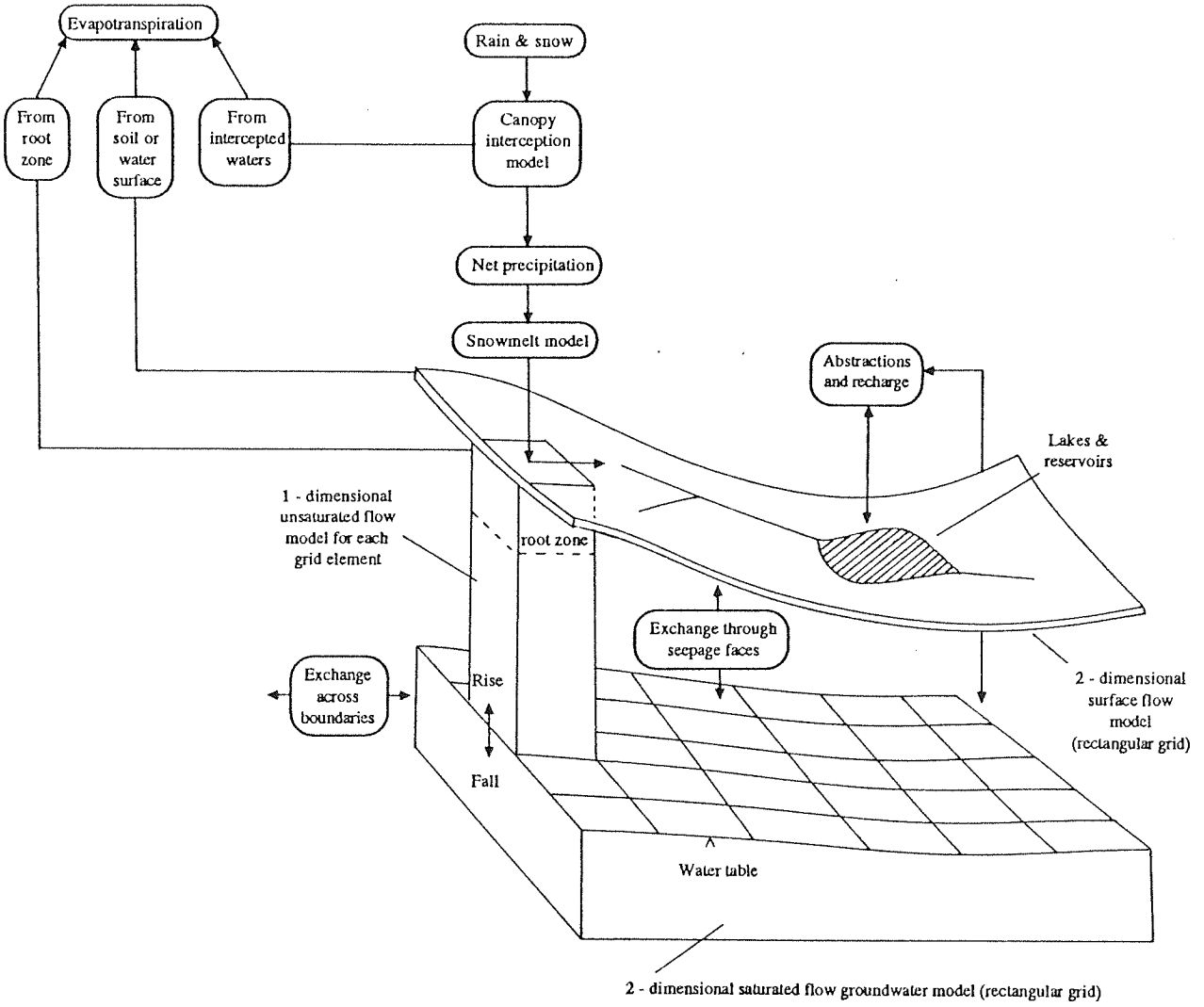

Figure 2.6 Schematic representation of the SHE model, after Beven et al. (1980).

2.2.3 The Institute of Hydrology Distributed Model (IHDM)

The Institute of Hydrology, UK has developed the IHDM (Beven and Morris, 1986) in a different framework to that of the SHE model in order to allow finer resolution at the hillslope scale. This permits the effects of hillslope divergence and convergence and the spread of local areas of saturation close to channels to be accounted for. In particular, the IHDM attempts to account for both vertical and downslope movement of water in unsaturated soils. The IHDM is therefore most suitable for the the modelling of upland catchments.

The process of catchment discretization in the IHDM is very similar to that of the FESHM in that the underlying structure is a series of hillslope segments providing inflow to a network of channel segments. Surface flow is accounted for using finite difference solutions to the kinematic wave equations, and when appropriate, the complete St. Venant equations are adopted for a more accurate description of channel flow.

Soil water flow is modelled in a two dimensional (vertical) slice using a finite element approximation to Richards equation. Also included in the IHDM are evapotranspiration, interception and snowmelt components.

The latest version of the IHDM has only recently been completed and sensitivity analyses are being carried out on the complete model (Rogers et al., 1985). The intended use of the IHDM is in the investigation of the effects of land-use changes and the predictions of the responses of ungauged catchments.

2.3 MODEL CALIBRATION

The development of model structure and solution strategy poses a minor problem in comparison to the application of the model to real world problems. Several physically based modelling studies have failed to produce accurate descripions of observed events.

One problem lies in the validity of the model equations used, one such possible source of error being the assumption of Darcian flow through soils, particularly when non capillary pores (macropores) are evident in the soil.

Macropores exist in various forms, ranging from small cracks in drying soils and wormholes to large diameter naturally formed pipe networks. The formation of these large pores can be governed by many factors, including soil flora and fauna, shrinking and swelling of the soil and soil erosion (Beven and Germann, 1982).

The importance of flow within macropores has been recognized by field studies (see for example Jones, 1971; Ehlers, 1975; Newson and Harrison, 1978; Gilman and Newson, 1980; Hammermesler et al., 1982); experimental investigations (for example Bouma and Dekker, 1981; Germann and Beven, 1981) and simplified theoretical studies (for example Scotter, 1978; Edwards et al., 1979; Beven and Germann, 1981; Bouma et al., 1982). However, due to the lack of suitable flow theories, the existence of macropores has received little attention in the modelling of catchment hydrology. Using current hydraulic theory the location and properties of individual macropores are required if a deterministic simulation is to be performed. This is clearly impractical, if not impossible, even for small scale simulations.

The occurence of macropores in soil has been used as an explanation for a number of unsuccessful simulations in previous physically based modelling studies, for example Jayawardena (1975), Beven (1975) and Mohsenisaravi (1981).

The model of Jayawardena (1975) accounted for surface soil water movement using a one dimensional (downslope) kinematic wave equation. The complete model was applied to two upland catchments in mid Wales and a number of recorded events were simulated. Insufficient data was available in the field and therefore Jayawardena intended to base model parameters on suitable values for the soil types present in the catchments. One such model parameter, the saturated hydraulic conductivity, estimated by Macfarlane (1969) for peat soils to lie within a range of 10^{-7} to 0.38 cm/s was adjusted by Jayawardena to lie within 1.0 and 10 cm/s in an attempt to account for macropores in the soil.

Although a number of observed events were satisfactorily simulated using Jayawardena's model, several predicted events were grossly in error. Clearly if such adjustment of model parameters is necessary, the model appears to have little physical resemblance to the real system.

The model of Beven (1975), which was probably a forerunner to the IHDM, was applied to the East Twin Catchment, UK. Beven attempted to choose 'best' parameters to fit the observed hydrographs. Close agreement between simulated and observed events was not obtained. By comparing predicted and recorded soil moisture profiles it was evident that not enough water was being lost from the hillslope during the simulations. Beven concluded that the influence of macropores within the soil layer was probably a major contribution to the poorly simulated hydrographs.

Mohsenisaravi (1981) attempted to simulate subsurface flow hydrographs on a single hillslope of the Pine Creek Watersheds, Idaho, USA. Mohsenisaravi used the two dimensional variably saturated flow model of Neuman et al. (1974) which was based on the original work of Neuman (1973) and included an evapotranspiration component. Mohsenisaravi calibrated this model from a series of events taken from one years records, the model was then applied to a number of storms during the next

two years. Mohsenisaravi found that the saturated hydraulic conductivity of the soil was the most influential model parameter and once calibrated the model failed to provide results of sufficient accuracy, suggesting a possible time dependence of the hydraulic conductivity. The causes of such time dependency could include the effects of decaying flora and the formation of macropores.

A further problem of predicting hydrological events using physically based models lies in the data requirements of such a model. In theory, since the model equations are solved on a grid of node points, each node point or nodal area may be associated with a model parameter, such as the saturated hydraulic conductivity. Therefore, the spatial (and temporal) variability of model parameters can be described. However, since such information is unlikely to be available , the current modelling practice assumes that areas of the flow domain can be represented by constant parameter values, implying that some 'equivalent parameter' can be used.

2.3.1 Field evidence of soil spatial variability

Field evidence of spatial variability of soil properties, in particular the saturated hydraulic conductivity, has been demonstrated by many studies. Myers (1967) has shown considerable variation of soil hydraulic properties across a 200 m hillslope site using infiltrometer data.

Significant variation in unsaturated hydraulic conductivity has been shown by Stockton (1971) and Carvallo et al. (1976). Stockton's observations were based on a series of measurements at a depth of 50 cm over a 40 ha site of Pima Clay Loam. A much smaller study area (0.01 ha) was used in the investigation by Carvallo et al. (1976).

The probability density function for hydraulic conductivity has been shown, in

Table 2.1 Some published statistical parameters for lognormal frequency distributions of hydraulic conductivity (K in cm/s)

Source	μ_{lnK}	σ_{lnK}
Law (1944)	-10.046	0.433
	-11.221	0.884
	-12.205	0.814
Rogowski (1972)	-7.162	1.5
	-5.968	0.9
	-8.533	1.0
	-6.653	1.6
Nielsen (1973)	-8.786	1.01
Smith (1978)	-1.403	0.504
Sharma et al (1980)†	-7.289	0.659
Russo and Bresler (1981b)	-5.964	1.015

† Based on final infiltration rate.

general, to be log normal. Law (1944) was one of the first to propose such a distribution using core data from an oil field reservoir. Other field studies verifying such a distribution for hydraulic conductivity or related infiltration properties include Rogowski (1972), Nielsen et al. (1973), Baker and Bouma (1976) and Babalola (1978). Further evidence is also provided in Freeze (1975). A number of published estimates of spatial variability of hydraulic conductivity are presented in table 2.1.

There appears to be little agreement in the literature about the amount of spatial correlation of soil hydraulic properties. Smith (1978) measured porosity and saturated hydraulic conductivity on two 30 m transects, samples being taken at 0.3 m intervals. The correlograms of Smith suggested little spatial correlation. Also no obvious pattern in the distribution of infiltration parameters with respect to position has been observed by Sharma et al. (1979) and Mapa (1984).

Experimental data from Vierra et al. (1981) and Russo and Bresler (1982) has suggested significant variance structure extending to tens of metres. Measurements of soil properties such as clay content and pH, along a 3 km transect, by Webster and Cuanalo (1975) have implied the possiblity of correlation at distances of hundreds of metres.

2.3.1.1 Eastergrounds study

In order to obtain more information of the variability of soil hydraulic properties within a single hillslope, a series of measurements were made on the Easterground field of the Slapton Wood Catchment (Troake and Walling, 1983; Trudgill, 1983) during March 1985. Topographic variation in the field is shown in figure 2.7. The site is approximately 1.5 ha in size.

Using a single ring infiltrometer (Burt, 1978) a series of 72 soil surface infiltrometer plots were selected, 32 of which were placed on a triangular grid (see figure 2.7). The

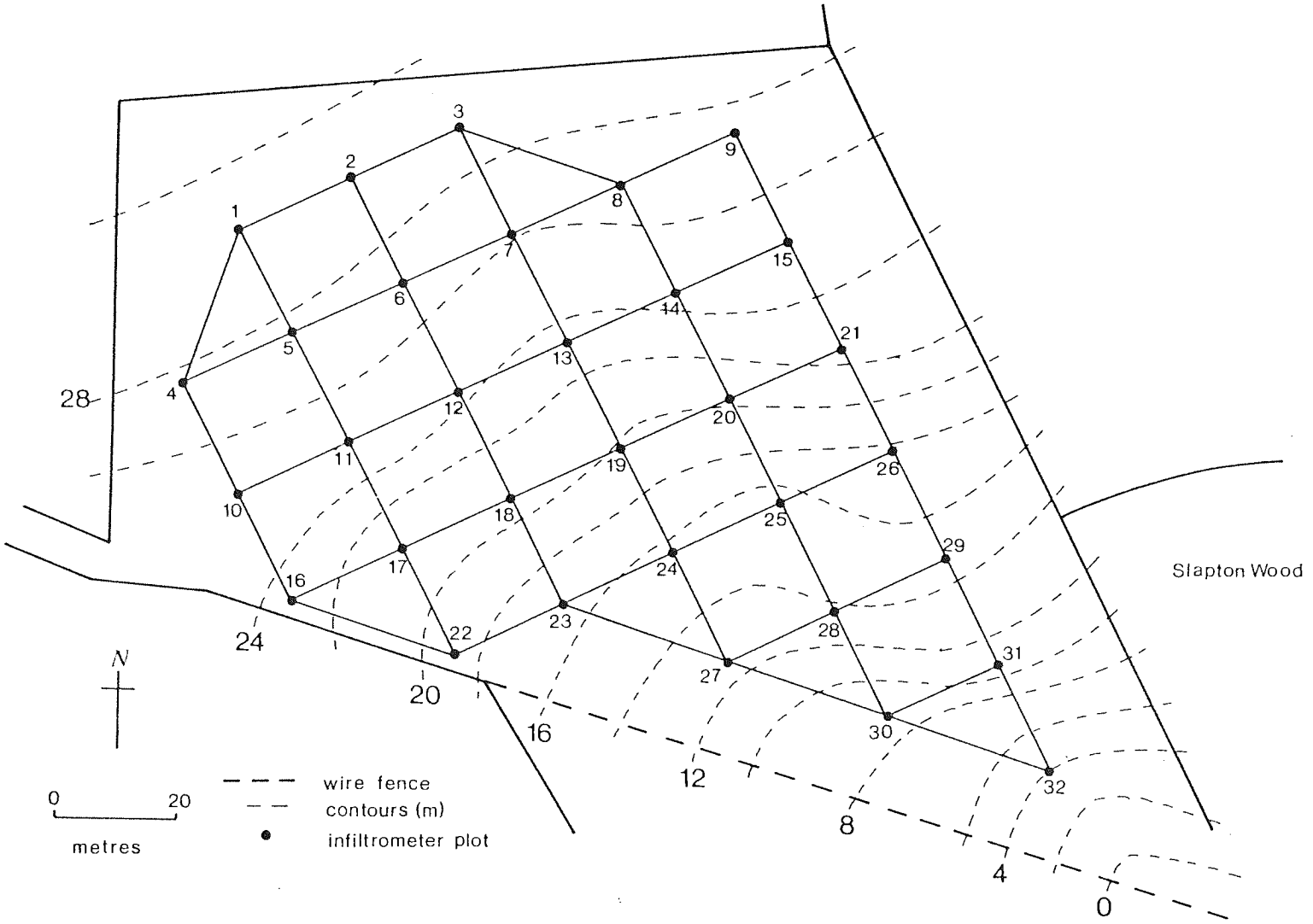

Figure 2.7 Topographical variation of Eastergrounds field.

remaining 40 plots were located along a 50 m transect between the mid points of 4 and 5 and 8 and 9 (figure 2.7).

At each infiltrometer site readings were taken of infiltration rates with time until a near steady infiltration rate was observed.

There are several mathematical expressions describing vertical infiltration, for example Green and Ampt (1911), Philip (1957) and Holtan (1961). For this study, the widely recognized Philip's equation was used. Philip's equation can be written in the form,

$$i = A + B\, t^{-1/2} \qquad (2.4)$$

where: i = infiltration rate at time t

A = final infiltration rate

B = Sorptivity = constant

A least squares fit of equation (2.4) to the observed data was made in order to obtain values of the final infiltration rates over the field. An example of such a fit is shown in figure 2.8. The calculated final infiltration rates for the 72 plots are tabulated in appendix 1.

Analysis of the 32 final infiltration rates over the field show a normal distribution of ln (A) with mean ln (A) = -7.776 (A in cm/s) and a standard deviation of 1.282 at the 80 % confidence level (see figure 2.9). It has been suggested in the literature that the value of A in Philip's equation lies between one third and two thirds of the saturated hydraulic conductivity of the surface soil (see for example Youngs, 1968; Philip, 1969). An appropriate estimate of the mean saturated hydraulic conductivity is then 8.4×10^{-4} cm/s.

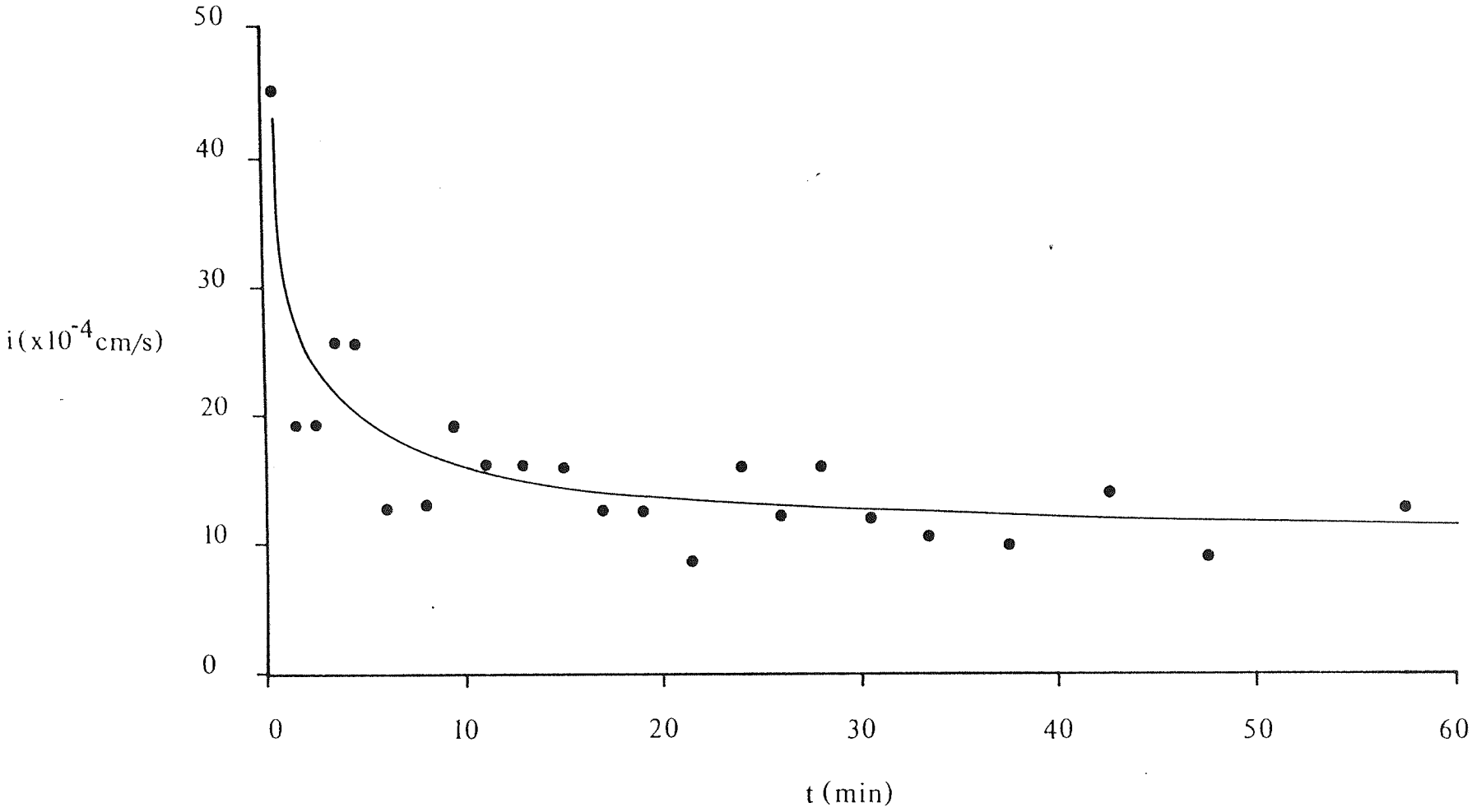

Figure 2.8 Least squares fit to infiltrometer data. • indicates field observations.

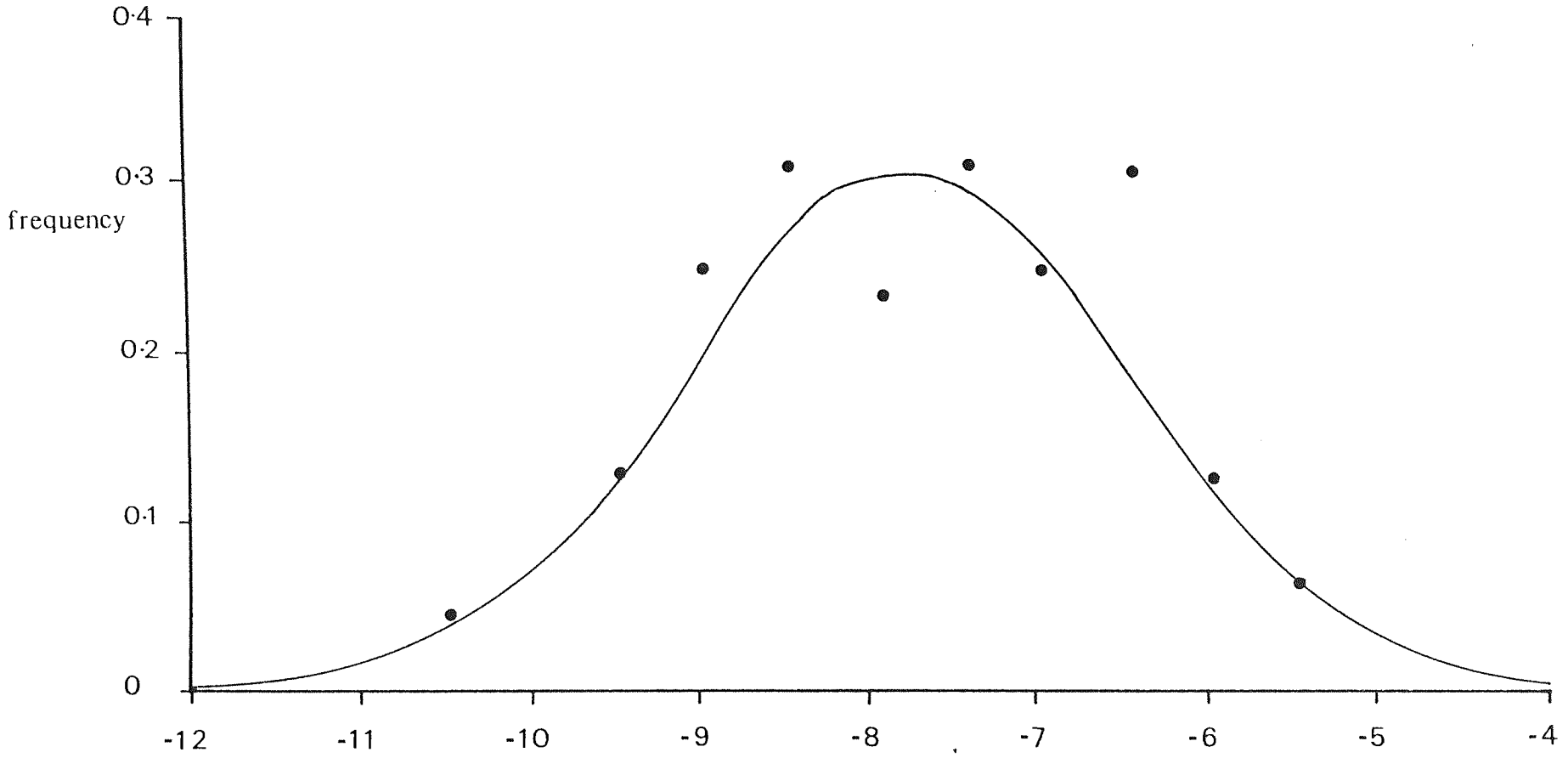

Figure 2.9 Frequency distribution of final infiltration rates. ● indicates observed frequency, solid line represents a theoretical normal distribution of ln A with mean of -7.776 and standard deviation of 1.282.

Variation of ln (A) along a 50 m transect is shown in figure 2.10. Significant noise is evident. The autocorrelation at various lags ι may be evaluated using,

$$\rho_\iota = \frac{\frac{1}{n-\iota}\sum_{i=1}^{n-\iota}(Y_i - \bar{Y}_i)(Y_{i+\iota} - \bar{Y}_{i+\iota})}{\frac{1}{n-\iota}\sum_{i=1}^{n-\iota}(Y_i - \bar{Y}_i)^2 \cdot \frac{1}{n-\iota}\sum_{i=1}^{n-\iota}(Y_{i+\iota} - \bar{Y}_{i+\iota})^2}$$

where:
$$\bar{Y}_i = \frac{1}{n-\iota}\sum_{i=1}^{n-\iota} Y_i$$

$$\bar{Y}_{i+\iota} = \frac{1}{n-\iota}\sum_{i=1}^{n-\iota} Y_{i+\iota}$$

$Y = \ln (A)$

n = number of data points

Inspection of the correlogram (figure 2.11) reveals little variance structure which is further demonstrated by the inclusion of the 95% confidence limits for a purely random process.

The soil in the Easterground field is very stoney (Butcher, 1986) and the soil surface has received considerable compaction from grazing animals and the many previous field studies. These two factors help to explain the insignificant variance structure observed.

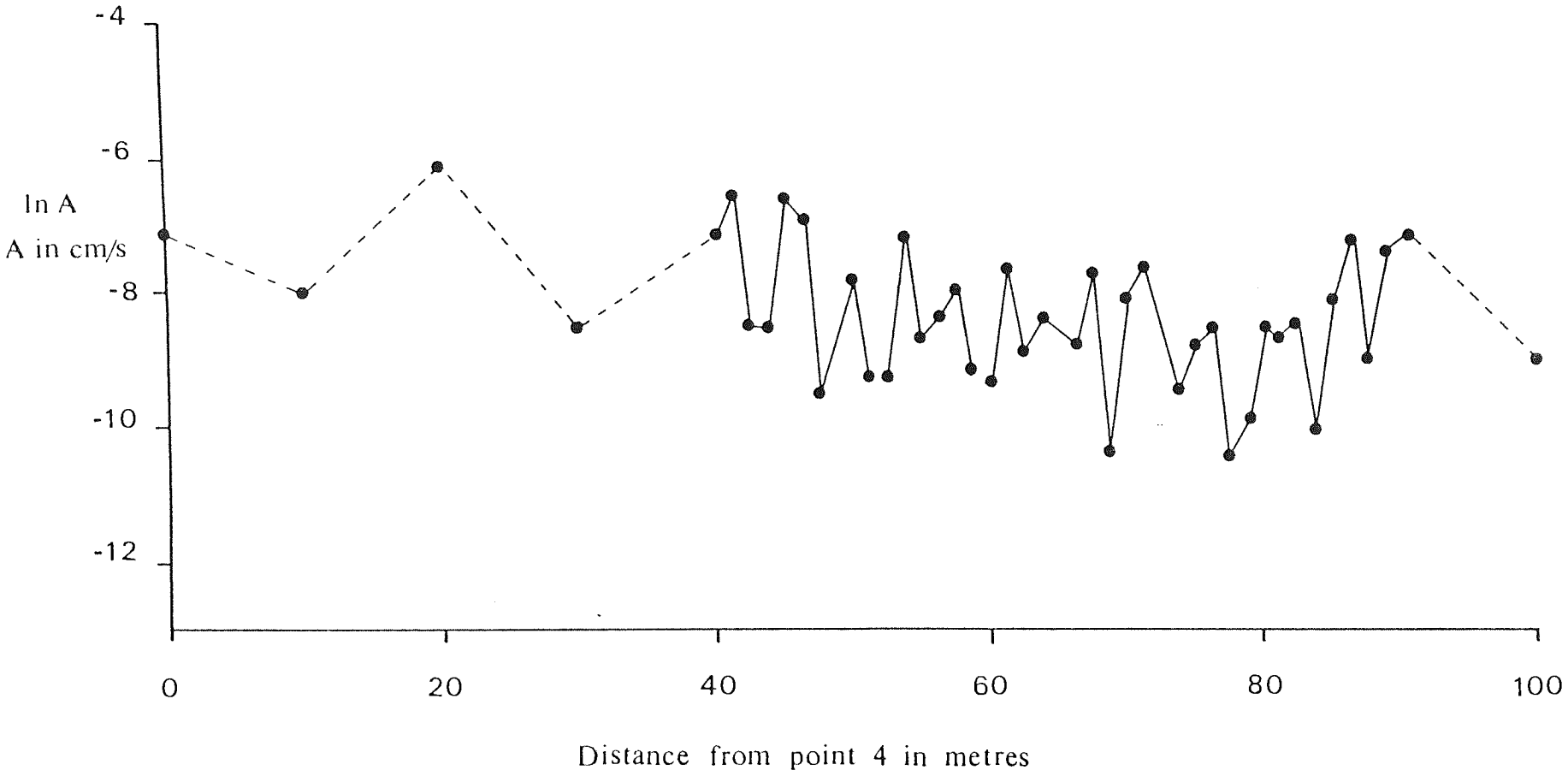

Figure 2.10 Variation of ln A between infiltrometer plots 4 and 9.

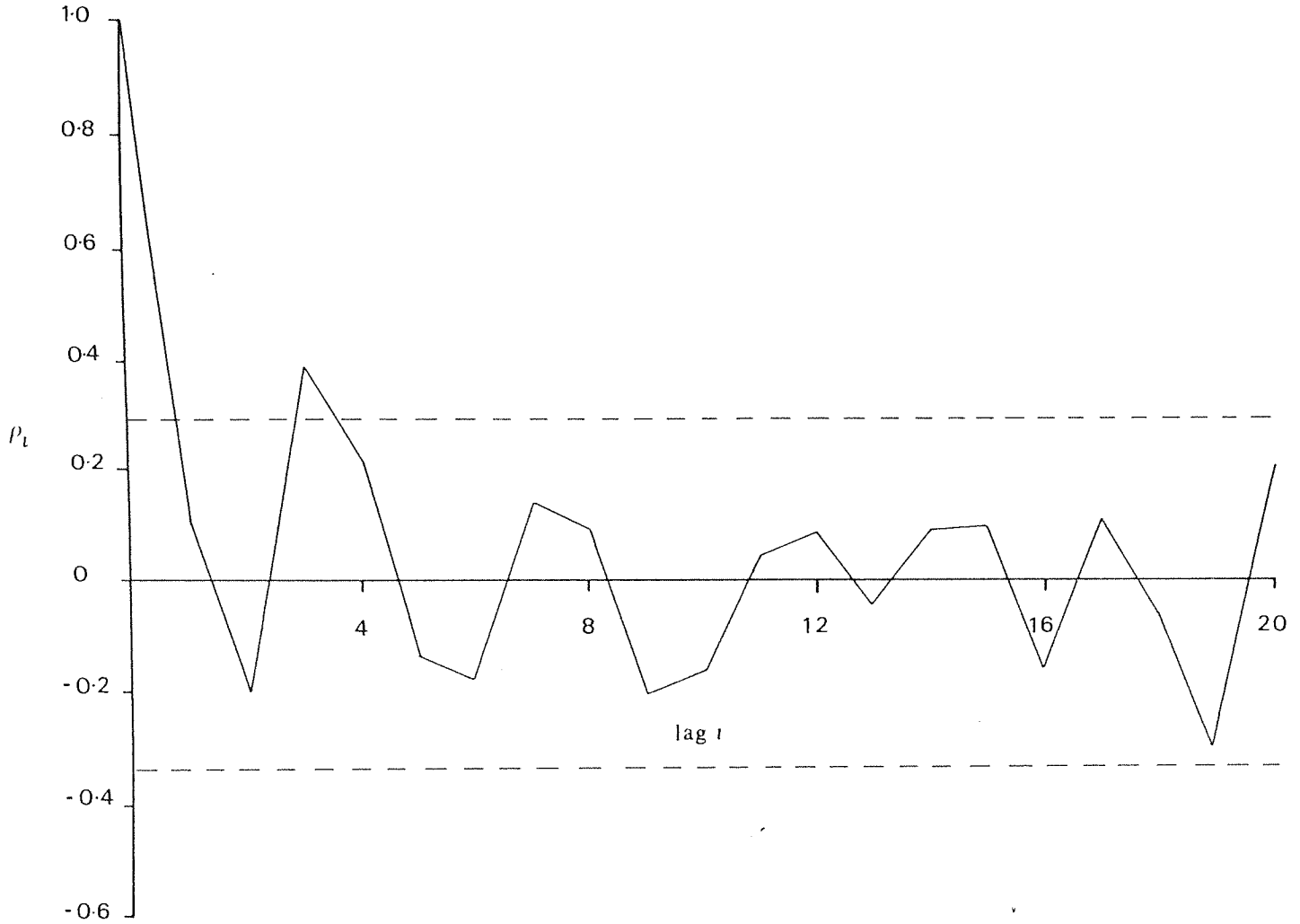

Figure 2.11 Correlogram of final infiltration rates along 50 metre transect. Lag of one equals 1.25 metres. Dashed line indicates 95% confidence limits for a purely random process.

A series of undisturbed soil cores were also taken along a different transect in the field and at two locations at various depths. However, the very stoney nature of the soil made it extremely difficult to measure reasonable estimates of saturated hydraulic conductivity in the laboratory.

Butcher (1986) has measured infiltration rates at various depths in the Eastergrounds field which have shown a distinct increasing trend with soil depth. This demonstrates the heavily compacted nature of the soil surface.

2.4 SUMMARY AND CONCLUSIONS

Current physically based modelling strategy involves the simulation of the complex interaction of individual hydrological processes using theoretically acceptable continuum equations. The governing equations of flow are usually presented in the form of partial differential equations which require a numerical solution to specific boundary and initial conditions. Methods such as the FDM and FEM have been popular for the modelling of such processes.

Application of sub process models, in particular those representing variably saturated flow, to real systems have received limited success. Phenomena such as soil spatial and temporal variability and non-capillary soil moisture movement are generally neglected in any physically based framework. There is ample evidence of soil spatial variability in the literature including suggested frequency distributions of individual properties. Extent of variability has been shown to vary between soil types and sites, so too has the amount of recorded variance structure. Several field investigations, including the one carried out for this thesis, have found little, if any, autocorrelation of soil properties, whereas others have reported significant correlation between properties over tens of metres. There is a need for more site investigations such as these to

provide sufficient information to evaluate the likely extent of soil variability. It is clear that the influence of such variability must be investigated in order to assess the limitations of current models. Moreover, complete catchment models are becoming available to practicing engineers without forewarning of the oversimplification of the hydrological systems.

Chapter 3

A three dimensional finite element model of variably saturated flow in porous media

3.1 INTRODUCTION

In order to carry out a detailed analysis of the effects of soil spatial variability it was necessary to develop a three dimensional model of variably saturated flow. Although the development of such a model is a relatively simple extension of two dimensional analysis, several problems have restricted such an approach in applications to real situations. The computing requirements (both storage and processing time) for a three dimensional solution are considerably greater than a two dimensional model, in particular where a large portion of the flow domain is unsaturated, since the nonlinear governing equations require an iterative solution. A further restriction lies in the data preparation required for three dimensional grids, such as mesh geometry, initial conditions and boundary conditions.

As stated in 2.2.2.1, the finite difference model of Freeze (1971) was probably the first fully three dimensional solution to the problem of variably saturated flow through porous media, albeit under hypothetical conditions.

The FEM has received attention in the modelling of three dimensional saturated groundwater movement, for example Gupta and Tanji (1976). More recently, Frind and Verge (1978) presented a finite element solution to three dimensional saturated-unsaturated flow.

The model of Frind and Verge was applied to a real system in a study of groundwater movement within the Whiteshell Nuclear Research Establishment site, Manitoba, Canada. The computing requirements of their study suggest that three dimensional modelling of groundwater basins is a practical option. However, in such an application detailed modelling of unsaturated flow is not required and thus any unsaturated elements merely serve as a link between surface inputs and saturated groundwater flow. This is clearly demonstrated in Frind and Verge's study since the

element sizes are in the order of hundreds of metres in plan and several metres with depth. These values are at least an order of magnitude greater than those required in detailed unsaturated flow modelling.

It is worth drawing attention to the three dimensional groundwater transport model of Babu and Pinder (1984). In their model a finite element-finite difference scheme was employed in the three space dimensions. The approach was based upon a horizontal-vertical splitting algorithm in which the horizontal plane was treated using finite elements and finite differences were used to approximate the vertical flow. The mesh layout in such a formulation appears to restrict the application of this model, furthermore, the stability of the method under conditions of predominantly unsaturated flow is yet to be demonstrated.

3.2 SOLUTION STRATEGY

Neglecting compressibility effects and assuming isotropic conditions, equation (2.1) can be written,

$$K_s \frac{\partial}{\partial x}\left(K_r \frac{\partial \psi}{\partial x}\right) + K_s \frac{\partial}{\partial y}\left(K_r \frac{\partial \psi}{\partial y}\right) + K_s \frac{\partial}{\partial z}\left(K_r \frac{\partial \psi}{\partial z}\right) + K_s \frac{\partial K_r}{\partial z} - C \frac{\partial \psi}{\partial t} = 0 \qquad (3.1)$$

The value of ψ over the region R is approximated by,

$$\psi(x,y,z,t) \approx \hat{\psi}(x,y,z,t) = \sum_{i=1}^{n} \psi_i(t)\, N_i(x,y,z)$$

where n is the number of node points and N_i are the interpolation functions.

Applying Galerkin's method (2.1.2.1.2) to equation (3.1) at a given instant in time,

$$\int_R [\{ K_s \frac{\partial}{\partial x}(K_r \frac{\partial}{\partial x}) + K_s \frac{\partial}{\partial y}(K_r \frac{\partial}{\partial y}) + K_s \frac{\partial}{\partial z}(K_r \frac{\partial}{\partial z}) \} \sum_{i=1}^{n} \psi_i N_i +$$

$$K_s \frac{\partial K_r}{\partial z}] N_j \, dR - \sum_{i=1}^{n} \frac{\partial \psi_i}{\partial t} \int_R C N_j \, dR = 0 \qquad j = 1,2,..n \qquad (3.2)$$

Where the time derivatives of the nodal values of $\partial\psi_i / \partial t$ have been defined as weighted averages over R, that is,

$$\frac{\partial \psi_i}{\partial t} = \frac{\int_R C \frac{\partial \psi}{\partial t} N_j \, dR}{\int_R C N_j \, dR}$$

The use of this weighting process has been termed mass lumping and was first used in unsaturated flow modelling by Neuman (1972) to improve convergence of the solution. The method has also been employed in other nonlinear problems, for example heat flow (Becker et al., 1974).

The application of Green's theorem to equation (3.2) reduces the order of the integrand. Green's theorem can be written in the form,

$$\int_R \Phi \nabla^2\Theta \, dR = -\int_R \nabla\Phi \nabla\Theta \, dR + \int_S \Phi \nabla\Theta \upsilon \, dS$$

Where υ is the outward normal to the boundary S.

Equation (3.2) then becomes:

$$-\int_R \{ \frac{\partial N_j}{\partial x} \sum_{i=1}^{n} K_s K_r \frac{\partial N_i}{\partial x} + \frac{\partial N_j}{\partial y} \sum_{i=1}^{n} K_s K_r \frac{\partial N_i}{\partial y} + \frac{\partial N_j}{\partial z} \sum_{i=1}^{n} K_s K_r \frac{\partial N_i}{\partial z} \} \psi_i \, dR$$

$$+\int_S V N_j \, dS - \sum_{i=1}^{n} \frac{\partial \psi_i}{\partial t} \int_R C N_j \, dR - \int_R K_s K_r \frac{\partial N_j}{\partial z} dR = 0 \qquad (3.3)$$

$i,j = 1,2,...n$

Where the second term in equation (3.3) has been obtained from Darcy's law and V is the velocity of the flow entering the system.

If the shape functions N are chosen such that,

$$\int_R dR = \sum_e \int_{R^e} dR^e$$

and

$$\int_S dS = \sum_{se} \int_{S^e} dS^e$$

where e and se are the number of elements and surface elements respectively. R^e is the region of element e and S^e is the surface of boundary element se.

Equation (3.3) then becomes,

$$A_{ij}\,\psi_j + F_{ij}\,\frac{\partial \psi_j}{\partial t} = Q_i - B_i \qquad (3.4)$$

$$i,j = 1,2,...n$$

where,

$$A_{ij} = \sum_e K_s \int_{R^e} K_r \frac{\partial N_i}{\partial x}\frac{\partial N_j}{\partial x}\,dR^e + \sum_e K_s \int_{R^e} K_r \frac{\partial N_i}{\partial y}\frac{\partial N_j}{\partial y}\,dR^e + \sum_e K_s \int_{R^e} K_r \frac{\partial N_i}{\partial z}\frac{\partial N_j}{\partial z}\,dR^e \qquad (3.5a)$$

$$F_{ij} = \delta_{ij} \sum_e \int_{R^e} C\,N_i\,dR^e \qquad (3.5b)$$

$$Q_i = \sum_{se} \int_{S^e} V\,N_i\,dS^e \qquad (3.5c)$$

$$B_i = \sum_e K_s \int_{R^e} K_r \frac{\partial N_i}{\partial z}\,dR^e \qquad (3.5d)$$

δ_{ij} in equation (3.5b) is the Kronecker delta.

The basic linear isoparametric element shape was selected for this study. Unfortunately analytical solutions to the integrals in equations (3.5) cannot be found for such elements therefore numerical integration is required. In order to carry out the integrations a transformation from global (x,y,z) coordinates to local (ε,η,ζ) is made (see figure 3.1).

The integrals then become,

$$A_{ij} = \sum_{e} \int_{-1}^{1}\int_{-1}^{1}\int_{-1}^{1} K_s K_r \left(\frac{\partial N_i}{\partial x}\frac{\partial N_j}{\partial x} + \frac{\partial N_i}{\partial y}\frac{\partial N_j}{\partial y} + \frac{\partial N_i}{\partial z}\frac{\partial N_j}{\partial z} \right) |J| \, d\varepsilon \, d\eta \, d\zeta \qquad (3.6a)$$

$$F_{ij} = \delta_{ij} \sum_{e} \int_{-1}^{1}\int_{-1}^{1}\int_{-1}^{1} C N_i |J| \, d\varepsilon \, d\eta \, d\zeta \qquad (3.6b)$$

$$B_i = \sum_{e} \int_{-1}^{1}\int_{-1}^{1}\int_{-1}^{1} K_s K_r \frac{\partial N_i}{\partial z} |J| \, d\varepsilon \, d\eta \, d\zeta \qquad (3.6c)$$

where **J** is the Jacobian of the coordinate transformation.

The numerical integration scheme adopted is Gauss quadrature using four points in the predominant direction of flow, which is vertical. By evaluating the unsaturated soil properties $K_r(\psi)$ and $C(\psi)$ at each Gauss point, a good representation of the variation of these functions within each element is achieved. This has been demonstrated in a number of two dimensional finite element studies, in particular Nieber (1980).

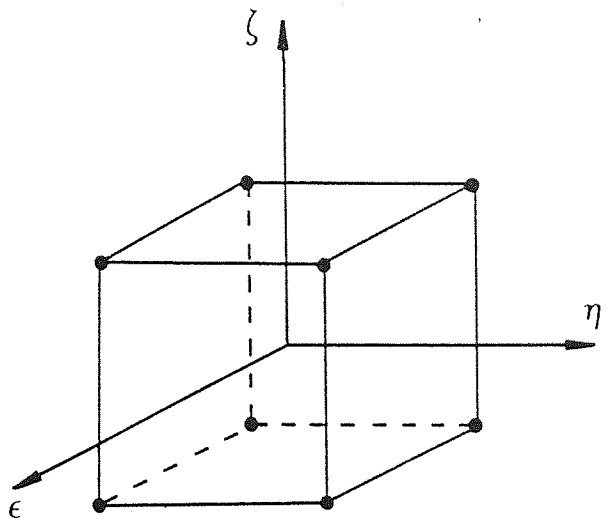

Figure 3.1a Three dimensional isoparametric element in local coordinates.

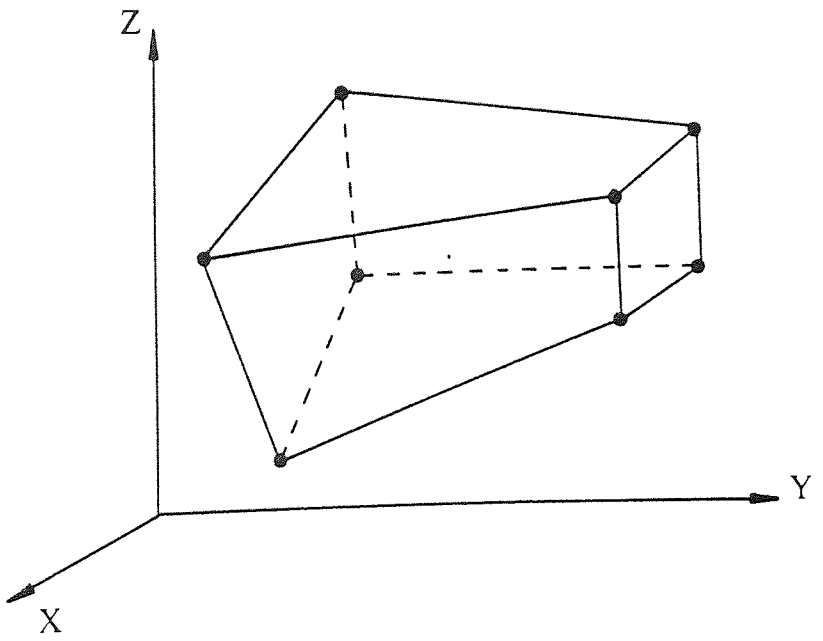

Figure 3.1b Three dimensional isoparametric element in global coordinates.

Since m Gauss points are required to exactly integrate a polynomial of degree 2m - 1, in this study cubic variation of the terms in equations (3.6a-c) is assumed in two directions of flow and linear variation in the third.

The resulting elemental contributions to equation (3.4) become,

$$A_{ij}^{e} = K_s \sum_{g=1}^{4} K_r(\psi_g)\left\{ \left(\frac{\partial N_i}{\partial x}\frac{\partial N_j}{\partial x} + \frac{\partial N_i}{\partial y}\frac{\partial N_j}{\partial y} + \frac{\partial N_i}{\partial z}\frac{\partial N_j}{\partial z} \right) |J| W_\varepsilon W_\eta W_\zeta \right\}_g \quad (3.7a)$$

$$F_{ij}^{e} = \sum_{g=1}^{4} C(\psi_g)\left\{ N_i |J| W_\varepsilon W_\eta W_\zeta \right\}_g \qquad i = j$$

(3.7b)

$$F_{ij}^{e} = 0 \qquad i \neq j$$

$$B_i^{e} = K_s \sum K_r(\psi_g)\left\{ \frac{\partial N_i}{\partial z} |J| W_\varepsilon W_\eta W_\zeta \right\}_g \quad (3.7c)$$

where W_ε, W_η, and W_ζ are the weight coefficients at each Gauss point g.

The linear basis functions are given by ,

$$N_i = \frac{1}{8}(1+\varepsilon\varepsilon_i)(1+\eta\eta_i)(1+\zeta\zeta_i)$$

$$\varepsilon_i = \pm 1\,,\ \eta_i = \pm 1\,,\ \zeta_i = \pm 1$$

therefore,

$$\frac{\partial N_i}{\partial \varepsilon} = \frac{1}{8}\varepsilon_i(1+\eta\eta_i)(1+\zeta\zeta_i)$$

$$\frac{\partial N_i}{\partial \eta} = \frac{1}{8}\eta_i(1+\varepsilon\varepsilon_i)(1+\zeta\zeta_i)$$

$$\frac{\partial N_i}{\partial \zeta} = \frac{1}{8}\zeta_i(1+\varepsilon\varepsilon_i)(1+\eta\eta_i)$$

The derivatives of the basis functions with respect to the global coordinate system are obtained using the Jacobian matrix,

$$\begin{bmatrix} \frac{\partial N_i}{\partial x} \\ \frac{\partial N_i}{\partial y} \\ \frac{\partial N_i}{\partial z} \end{bmatrix} = \mathbf{J}^{-1} \begin{bmatrix} \frac{\partial N_i}{\partial \varepsilon} \\ \frac{\partial N_i}{\partial \eta} \\ \frac{\partial N_i}{\partial \zeta} \end{bmatrix}$$

where,

$$\mathbf{J} = \begin{bmatrix} \frac{\partial x}{\partial \varepsilon} & \frac{\partial y}{\partial \varepsilon} & \frac{\partial z}{\partial \varepsilon} \\ \frac{\partial x}{\partial \eta} & \frac{\partial y}{\partial \eta} & \frac{\partial z}{\partial \eta} \\ \frac{\partial x}{\partial \zeta} & \frac{\partial y}{\partial \zeta} & \frac{\partial z}{\partial \zeta} \end{bmatrix}$$

For elements of arbitrary shape it is necessary to evaluate $\mathbf{J}^{-1}$ and $|\mathbf{J}|$ at each Gauss point of each element. However, for simple element shapes computer requirements

can be reduced. Consider the parallelapiped element of constant width x_e in figure 3.2. It is easily shown that the Jacobian is constant throughout the element and is given by,

$$J = \frac{1}{2} \begin{bmatrix} x^e & 0 & 0 \\ 0 & y^e & w^e \\ 0 & 0 & z^e \end{bmatrix}$$

and

$$|J| = \frac{1}{8} x^e y^e z^e$$

Therefore, by employing an element shape index and given the geometric properties w^e, x^e, y^e and z^e, an array of the derivatives of the basis functions with respect to the global coordinates can be formed for each element shape. Furthermore, the local element matrices in equation (3.7) can be evaluated *a priori* for saturated elements without significant increase in computer storage, provided the number of element shapes is low

Discretization in time is performed using a fully implicit backward difference scheme of the form:

$$\left(A_{ij}^{k+1/2} + \frac{1}{\Delta t_k} F_{ij}^{k+1/2} \right) \psi_j^{k+1} = Q_i^{k+1/2} - B_i^{k+1/2} + \frac{1}{\Delta t_k} F_{ij}^{k+1/2} \psi_j^{k} \qquad (3.8)$$

$i,j = 1,2,....n$

Where k refers to a point t^k in time and $\Delta t_k = t^{k+1} - t^k$. Evaluating the coefficients at half the time step (k+1/2) in equation (3.8) is carried out in order to under relax the system (Neuman, 1973).

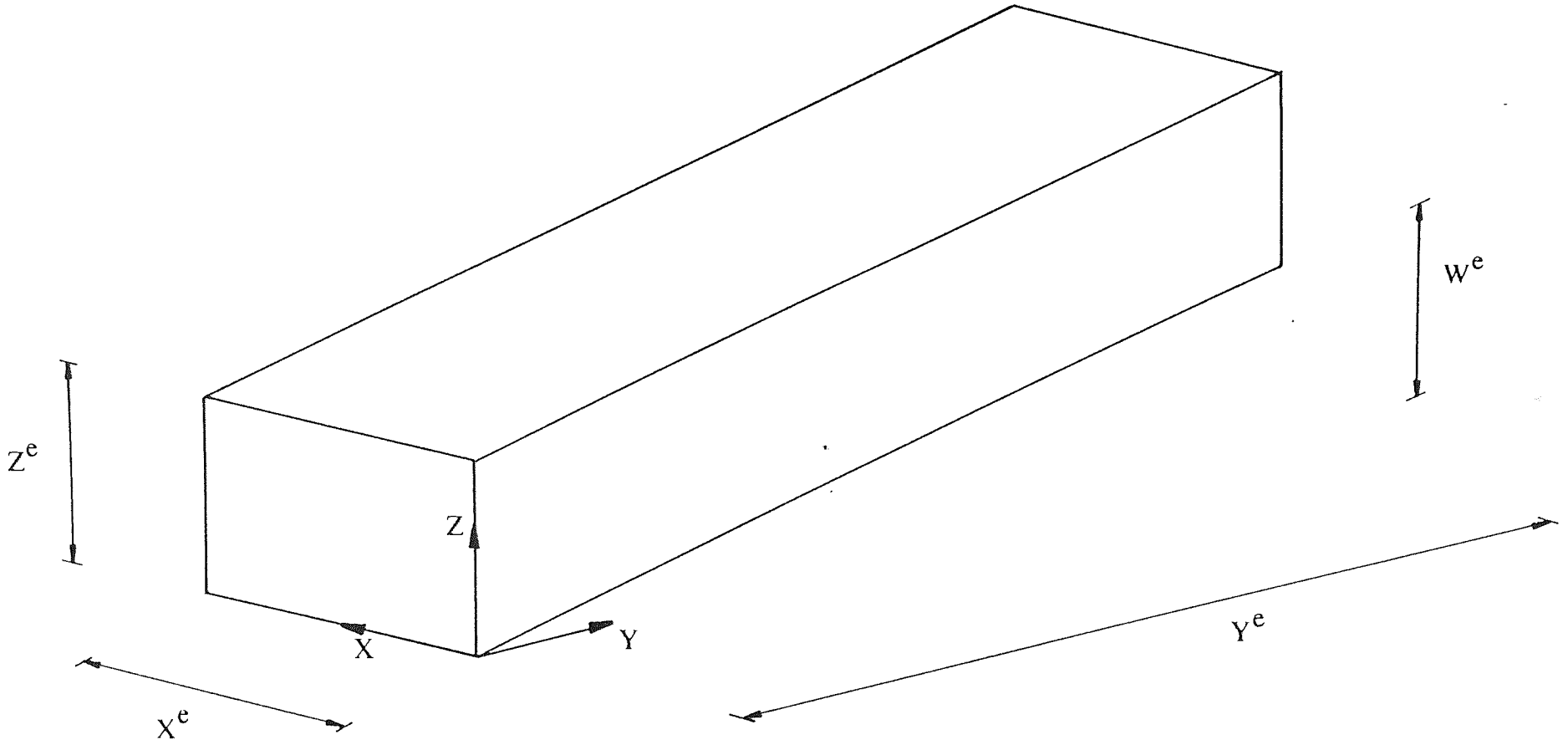

Figure 3.2 Parallelapiped element geometry.

At the beginning of each time step, the values of $\psi^{k+1/2}$ are predicted by extrapolation from the previously calculated values, using,

$$\psi_i^{k+1/2} = \psi_i^k + \frac{\Delta t_k}{2\Delta t_{k-1}} (\psi_i^k - \psi_i^{k-1}) \qquad k < 3 \qquad (3.9a)$$

$$\psi_i^{k+1/2} = \psi_i^k + \{ \frac{\log t_{k+1/2} - \log t_k}{\log t_k - \log t_{k-1}} \} (\psi_i^k - \psi_i^{k-1}) \qquad k \geq 3 \qquad (3.9b)$$

Equation (3.8) is the solved for ψ^{k+1} at all nodes. These values are then averaged with ψ^k using,

$$\psi_i^{k+1/2} = \frac{1}{2} (\psi_i^k + \psi_i^{k+1}) \qquad k=1 \qquad (3.10a)$$

$$\psi_i^{k+1/2} = \psi_i^{k+1} + \{ \frac{\log t_{k+1} - \log t_{k+1/2}}{\log t_{k+1} - \log t_k} \} (\psi_i^k - \psi_i^{k+1}) \qquad k > 1 \qquad (3.10b)$$

The cycle continues until satisfactory convergence is achieved. Equation (3.9b) was used by Huyakorn et al. (1984) to improve convergence rates. Experience has shown that log based time also enhances convergence when determining nodal pressure heads at mid time steps (equation, 3.10b).

The solution of the simultaneous equations in equation (3.8) represents a major portion of the computational effort. Frind and Verge (1978) presented two schemes in their three dimensional model, Gaussian elimination and Cholesky factorization. Frind and

Verge compared the efficiencies of the two methods and suggested the Gaussian elimination to be the best choice under most conditions. The Gaussian elimination algorithm used by Frind and Verge (1978) is that of Neuman et al. (1974). This was claimed, by Frind and Verge, to take advantage of the sparseness of the conductance matrix **A**, by bypassing operations on the zero terms. A slightly modified version of the Cholesky algorithm of Felippa (1975), which adopts envelope (or skyline) storage of the conductance matrix **A**, was found to be more efficient for this study. In particular, a number of operations within this method can be represented by hardware vector functions of computers with vector processing architecture such as the CDC Cyber 205. For example, rather than bypassing zero terms along a series of bandwidth calculations, the operation is treated as a single vector operation thus utilizing the greater speed of the vector processor.

Having determined the values of ψ_i^{k+1} at all nodes, the nodal fluxes $Q_i^{k+1/2}$ can be obtained explicitly from equation (3.8). The mass balance of the solution is greatly improved by such a procedure rather than calculating boundary fluxes using estimated hydraulic conductives and potential gradients, as in for example Beven (1975). In order to calculate the nodal fluxes, the relevant elements of the conductance matrix **A** need to be stored before solving the system of equations. Clearly if the entire matrix is duplicated as in two dimensional models such as Neuman (1972), there will be a significant waste of computer resources. For this reason. a compact form of the conductance matrix is utilized for nodal flux calculations.

To reduce computational effort a domain restriction method is adopted as follows. After the second iteration of each time step, all nodes that have converged to a specified tolerance become prescribed head nodes for the remainder of that time step. Therefore areas of the flow domain not affected by the wetting front are not included in the solution of the equations. The method is not as sophisticated as that of Stauffer

and Job (1982) but, unlike their procedure, vector processor instructions can be utilized.

Due to inadequate spatial and temporal discretization and the high nonlinearality of the unsaturated soil properties, convergence problems may occur resulting in oscillation about the solution. This tendency has been noted in particular when elements change from an entirely unsaturated state to a partially saturated state. Techniques to combat such oscillation are presented in the literature, in fact the under relaxation of equation (3.8) described earlier is for this purpose. Cooley (1983) suggested a method of determining damping parameters to maintain stability of the solution. This technique was tested together with Cooley's backward difference scheme. Little, if any, advantage was evident from employing such an approach and it was felt that the under relaxed system in equation (3.8) was the most attractive strategy. As in Beven (1975), if oscillations do occur the average of the nodal values at two successive iterations is used as an estimate of the solution.

Various functional relationships for unsaturated soil properties are suggested in the literature. For example Gillham et al. (1976) adopted a hyperbolic cosine function, Frind and Verge (1978) used a cubic spline representation and Beven and Morris (1986) used the Brooks and Corey relationships (Brooks and Corey, 1964). In this study the relative hydraulic conductivity is represented in the following form,

$$K_r(\psi) = \frac{a}{a + |\psi|^b}$$

where a and b are constants.

The following relationships are used to represent the moisture content and specific moisture capacity functions,

$$\theta(\psi) = \theta_{res} + (\theta_s - \theta_{res}) \frac{A}{A + |\psi|^B} \qquad (3.11a)$$

$$\psi \leq \psi_o$$

$$C(\psi) = (\theta_s - \theta_{res}) \frac{A B |\psi|^{B-1}}{(A + |\psi|^B)^2} \qquad (3.11b)$$

$$\theta(\psi) = \theta_s (1 + \beta\psi - \gamma\psi^2) \qquad (3.12a)$$

$$\psi_o \leq \psi < 0$$

$$C(\psi) = \theta_s (\beta - 2\gamma\psi) \qquad (3.12b)$$

$$\theta(\psi) = \theta_s (1 + \beta\psi) \qquad (3.13a)$$

$$\psi \geq 0$$

$$C(\psi) = \theta_s \beta \qquad (3.13b)$$

where,

θ_{res} = residual moisture content

A, B, β, γ, ψ_o = constants.

A small non-zero specific moisture capacity in the saturated zone (equation, 3.13b) implies recognition of the soil matrix compressibility. Beven and Morris (1986) stated that the inclusion of such a property within the IHDM has improved the stability of the variably saturated flow equations.

Values of A, B and θ_{res} can be obtained by fitting equation (3.11a) to experimental data. By selecting a value of β in equation (3.13b) γ and ψ_o can be obtained from equations (3.12) to ensure a continuous functional relationship.

Hysteresis of the unsaturated soil properties is not included in the current form of the model since the necessary data is unlikely to be available. However, the implementation of hysteretic relationships within the code is straightforward.

At the end of each time step an approximation of the continuity error over the domain is obtained using the following multiple integral,

$$E = \sum_{e} \int_{R^e} \int_{0}^{\Delta t} \frac{\partial \theta}{\partial t} \, dt \, dR^e - \Delta t \sum_{i=1}^{n} Q_i^{t+\Delta t/2} \qquad (3.14)$$

Using a four point Gauss quadrature integration scheme, equation (3.14) is estimated by,

$$E = \sum_{e} \sum_{g=1}^{4} (\theta(\psi_g^{t+\Delta t}) - \theta(\psi_g^{t})) \{ | J | W_\varepsilon W_\eta W_\zeta \}_g - \Delta t \sum_{i=1}^{n} Q_i^{t+\Delta t/2} \qquad (3.15)$$

A percentage continuity error is then evaluated as,

$$E_{cont} = 100 \times E / \Delta t \sum_{i=1}^{n} Q_i^{t+\Delta t/2}$$

If the calculated percentage error E_{cont} is greater than a specified value then the time step size is automatically reduced for the next time step. During the simulation, the value of Δt is also allowed to vary in magnitude depending upon the number of iterations during the previous time step. Thus too large a step length requiring many iterations and an excessive number of time steps which are too small are eliminated. The basic structure of the described algorithm is shown in figure 3.3. A listing of the code, written in FORTRAN 200, is provided in appendix 2.

3.3 MODEL VERIFICATION

The finite element method has been shown to be suitable for solving the equations of variably saturated flow under ideal conditions, by numerous previous studies. However, each individual model requires evidence of verification. The example presented herein is a water table recharge problem.

The data is taken from the results of an experimental and numerical study presented in Vauclin et al. (1979). The flow domain is shown in figure 3.4 and consists of a rectangular slab (dimensions 3m x 2m x 5cm) of fine river sand.

The height of the water table is initially 65cm above the base of the slab. Recharge to the water table is provided by a constant flux of 14.8 cm/hr applied to the upper boundary of the flow domain.

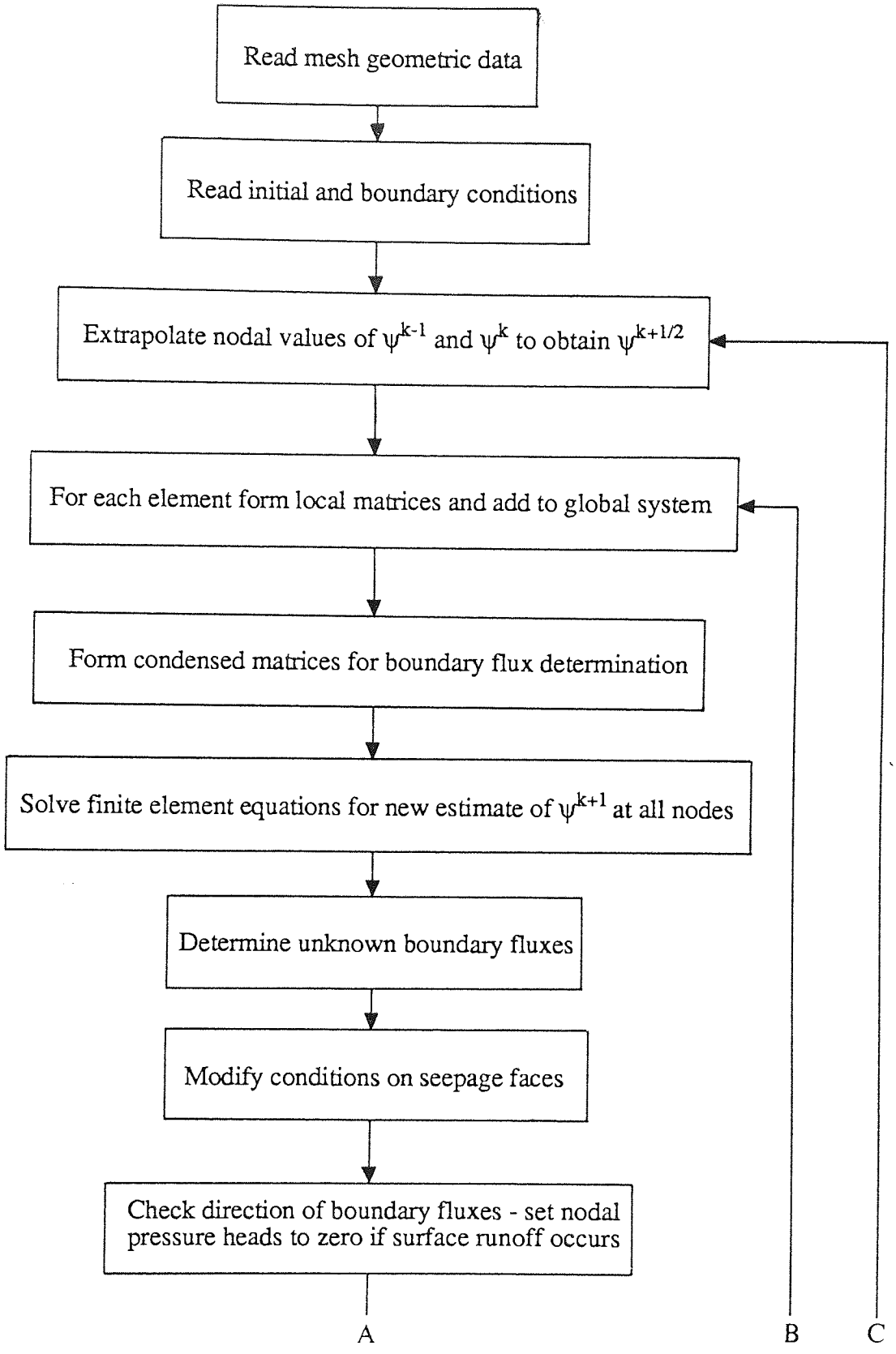

Figure 3.3 Flow chart for the finite element algorithm

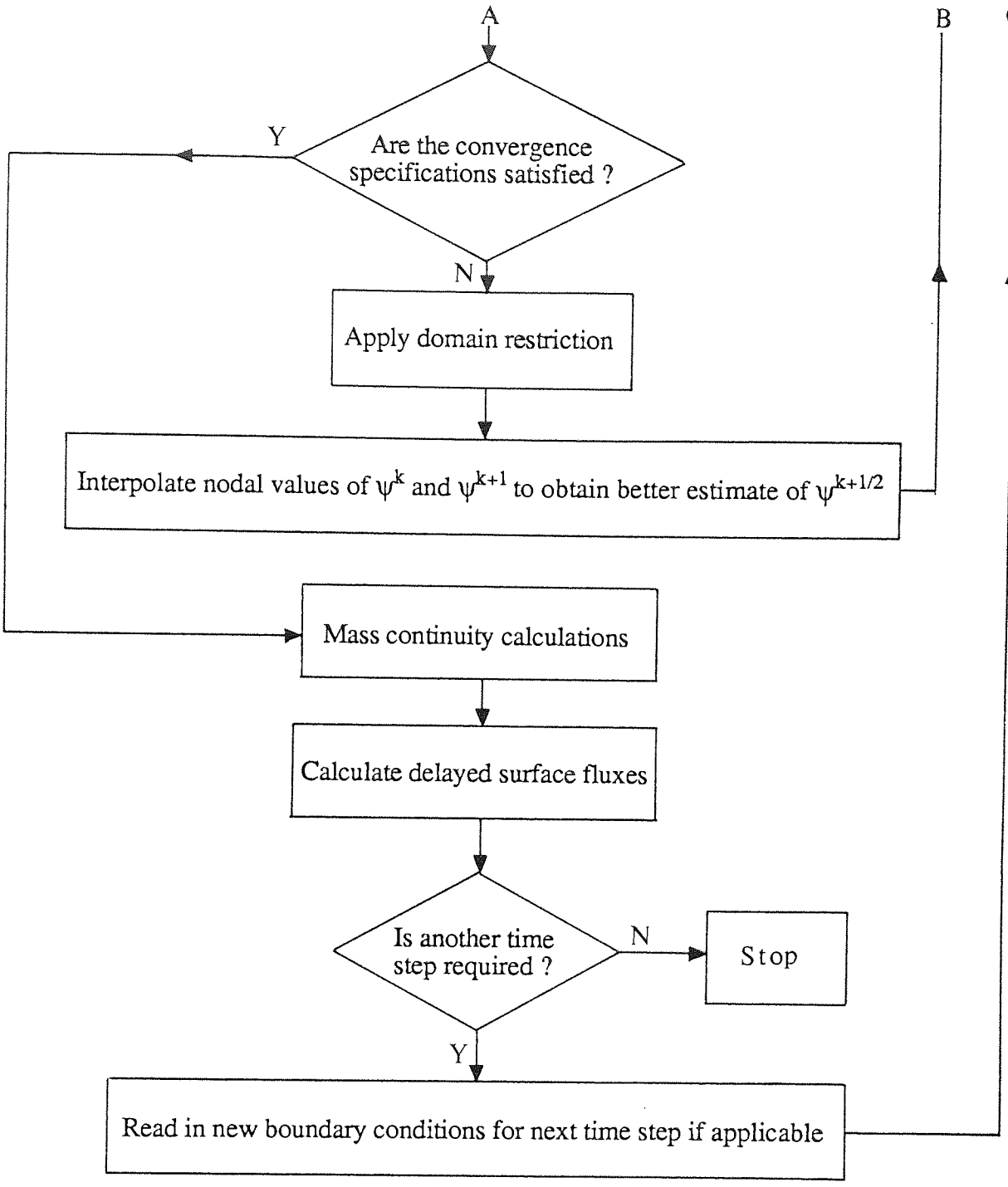

Figure 3.3 (continued)

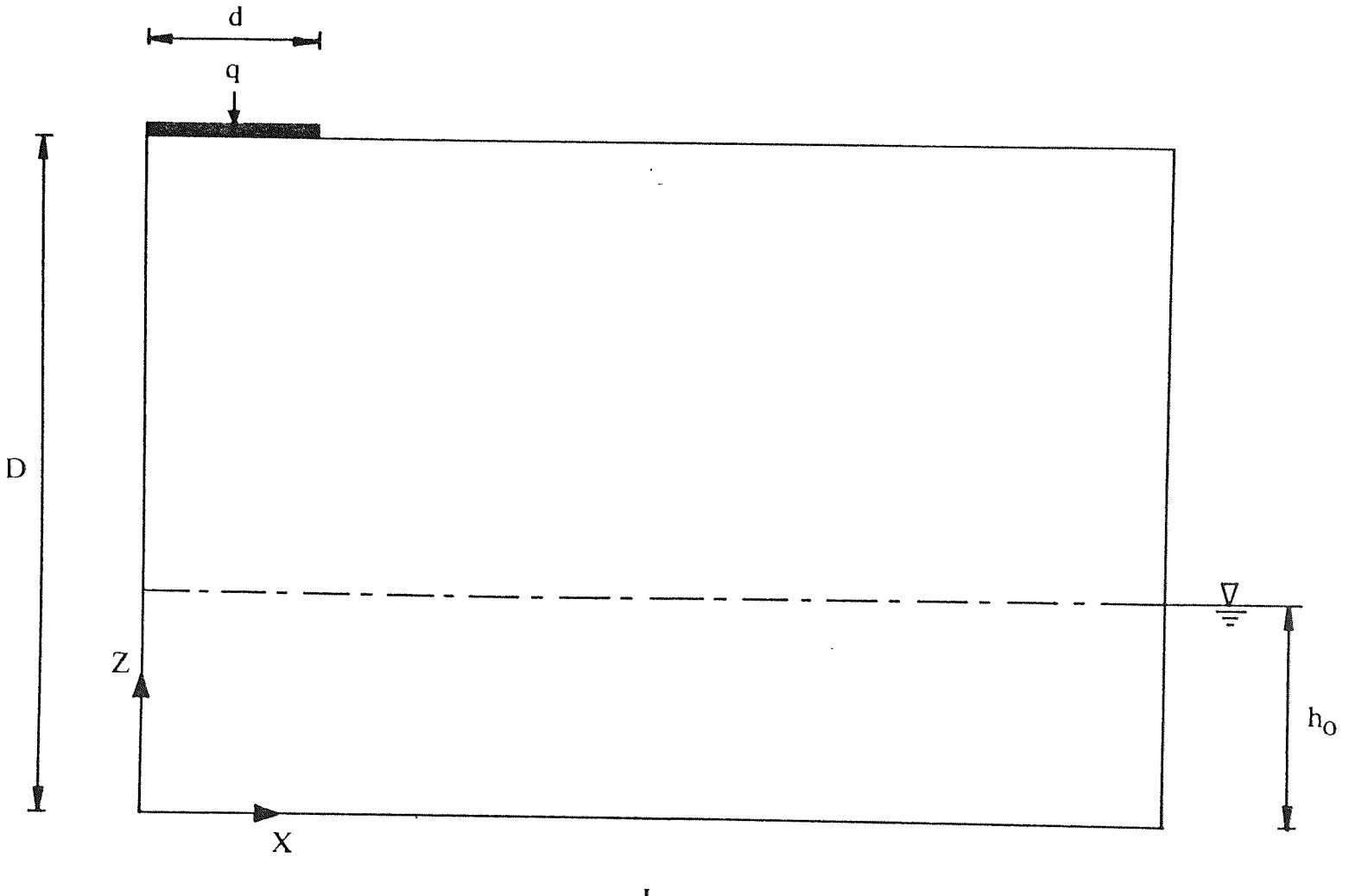

Figure 3.4 Flow domain for water table recharge problem.

The initial and boundary conditions are:

(i)	$\psi = 65 - z$	$0 \leq x \leq L$	$0 < z \leq 115$	$t = 0$
(ii)	$\psi = 6.8 - 0.494\ z$	$0 \leq x \leq L$	$115 < z \leq D$	$t = 0$
(iii)	$h = h_o$	$x = L$	$0 \leq z \leq h_o$	$t > 0$
(iv)	$\frac{\partial h}{\partial z} = 0$	$0 < x < L$	$z = 0$	$t \geq 0$
(v)	$\frac{\partial h}{\partial x} = 0$	$x = 0$	$0 \leq z < D$	$t \geq 0$
(vi)	$-K_s\frac{\partial h}{\partial z} = q$	$0 \leq x \leq d$	$z = D$	$t \geq 0$
(vii)	$\frac{\partial h}{\partial z} = 0$	$d < x \leq L$	$z = D$	$t \geq 0$
(viii)	$\frac{\partial h}{\partial x} = 0$	$x = L$	$z_s < z \leq D$	$t > 0$
(ix)	$h = z$	$x = L$	$h_o < z \leq z_s$	$t > 0$

where z_s is the height of the seepage face.

Conditions (i) and (ii) are taken from the experimental readings of Vauclin et al. Condition (ii) demonstrates that the initial conditions are not static over the entire flow domain. Conditions (viii) and (ix) refer to the seepage face at the right-most boundary.

The unsaturated soil characteristics are given by:

$$\theta(\psi) = \theta_s \frac{A}{A + |\psi|^B} \qquad \psi < 0$$

$$\theta(\psi) = \theta_s \qquad \psi \geq 0$$

$$K_r(\psi) = \frac{a}{a + |\psi|^b} \qquad \psi < 0$$

$$K_r(\psi) = 1 \qquad \psi \geq 0$$

where:

θ_s = 0.3 cm cm^{-1}

A = 4.0×10^4 $cm^{2.9}$

B = 2.9

a = 2.99×10^6 cm^5

b = 5.0

The saturated hydraulic conductivity is assumed constant throughout the flow domain and is equal to 35.0 cm/hr.

Vauclin et al. (1979) simulated the problem numerically in two stages. Until the wetting front reached the water table, the governing equations were only solved in the unsaturated zone. The method used was a combined Kirchoff transformation/finite difference scheme as used by Rubin (1968). The finite difference grid dimensions adopted were $\Delta x = \Delta z = 10$cm and $\Delta t = 10$s.

For time greater than 1.75 hours, the complete flow domain was solved using a finite difference scheme without the Kirchoff transformation. An iteration tolerance of 0.01 cm and a mesh consisting of 396 nodes were employed. Variable time steps were used in the second stage of the simulation, the size of the step length being determined from a stability equation. Values in the order of 20s appear to have been used for this stage of the numerical study.

In order to solve the same problem using the finite element method, a 3D finite element mesh consisting of 130 elements was used (figure 3.5). The eight hour simulation period was discretized into eighty seven time steps which varied between 6s and 600s. An average of 3 to 4 iterations per time step were required to satisfy an iteration tolerance of 0.01 cm. The entire simulation required 13.5 minutes CPU time† on the DEC VAX 11/750 at Aston University's Computer Centre.

The water table positions calculated using the finite element scheme together with the experimental results are shown in figure 3.6. Close agreement is evident.

Figure 3.7 illustrates the change in outflow, inflow and storage of water within the soil mass with time from both the experimental findings and the finite element scheme. The volume of storage was obtained from the integral in equation (3.14). Overall the numerical results are in close agreement with the experimental observations.

In order to verify the simulation of flow in the third (minor) dimension, the same problem was analyzed using identical spatial and temporal discretization with two Gauss points per element, as opposed to four, in the predominant direction of flow. Similar, but less accurate, results were obtained . However, in the intended application of the model much smaller potential gradients are likely to be encountered in the third dimension.

It is important to note that much coarser spatial and temporal discretization was possible using the described finite element formulation in comparison with the finite difference method adopted by Vauclin et al. (1979). Frind and Verge (1978) reported similar findings in a comparison of their model with the finite difference model of Freeze (1971). Freeze discretized a small groundwater basin into 8788 node points

† Clearly the CPU time would be considerably less if a two dimensional equivalent code was used.

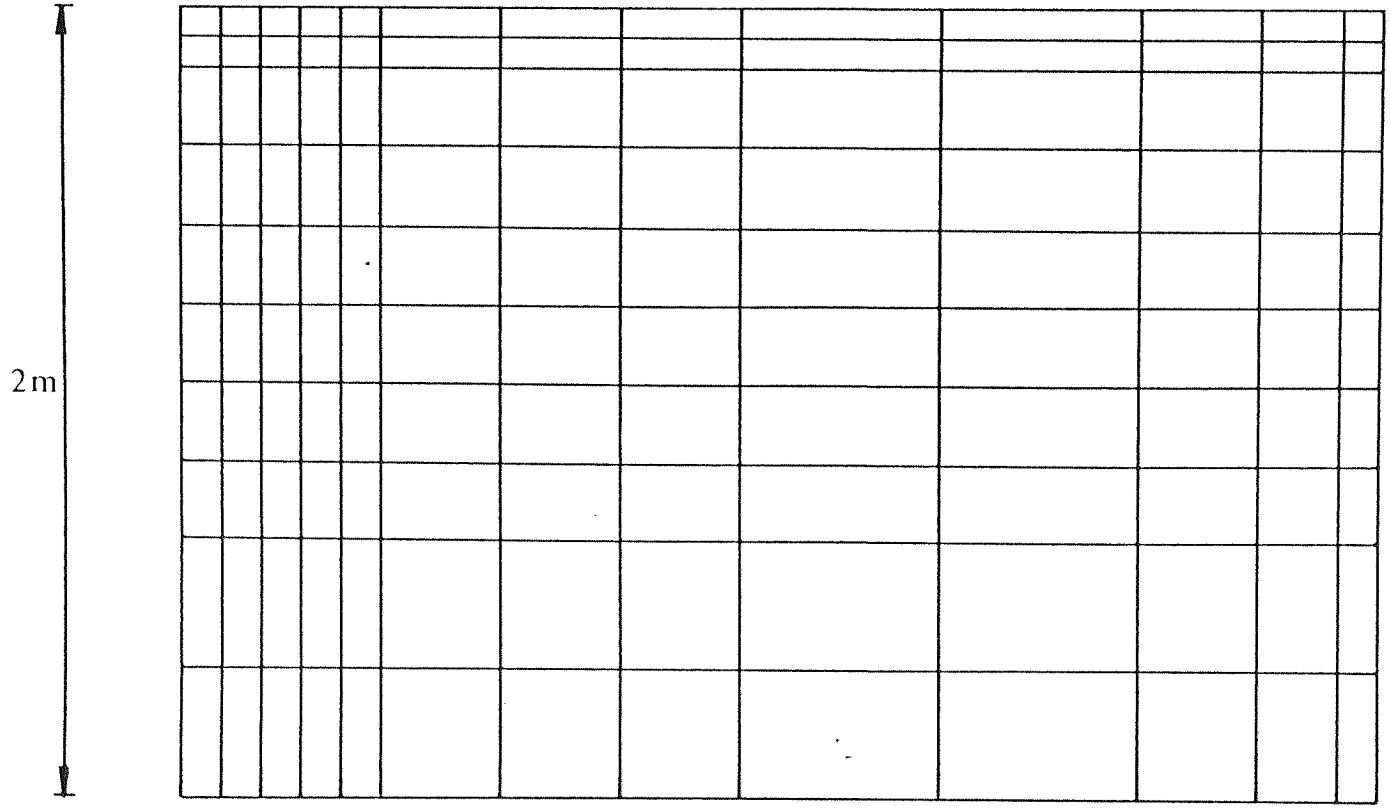

Figure 3.5 Finite element discretization for the water table recharge problem.

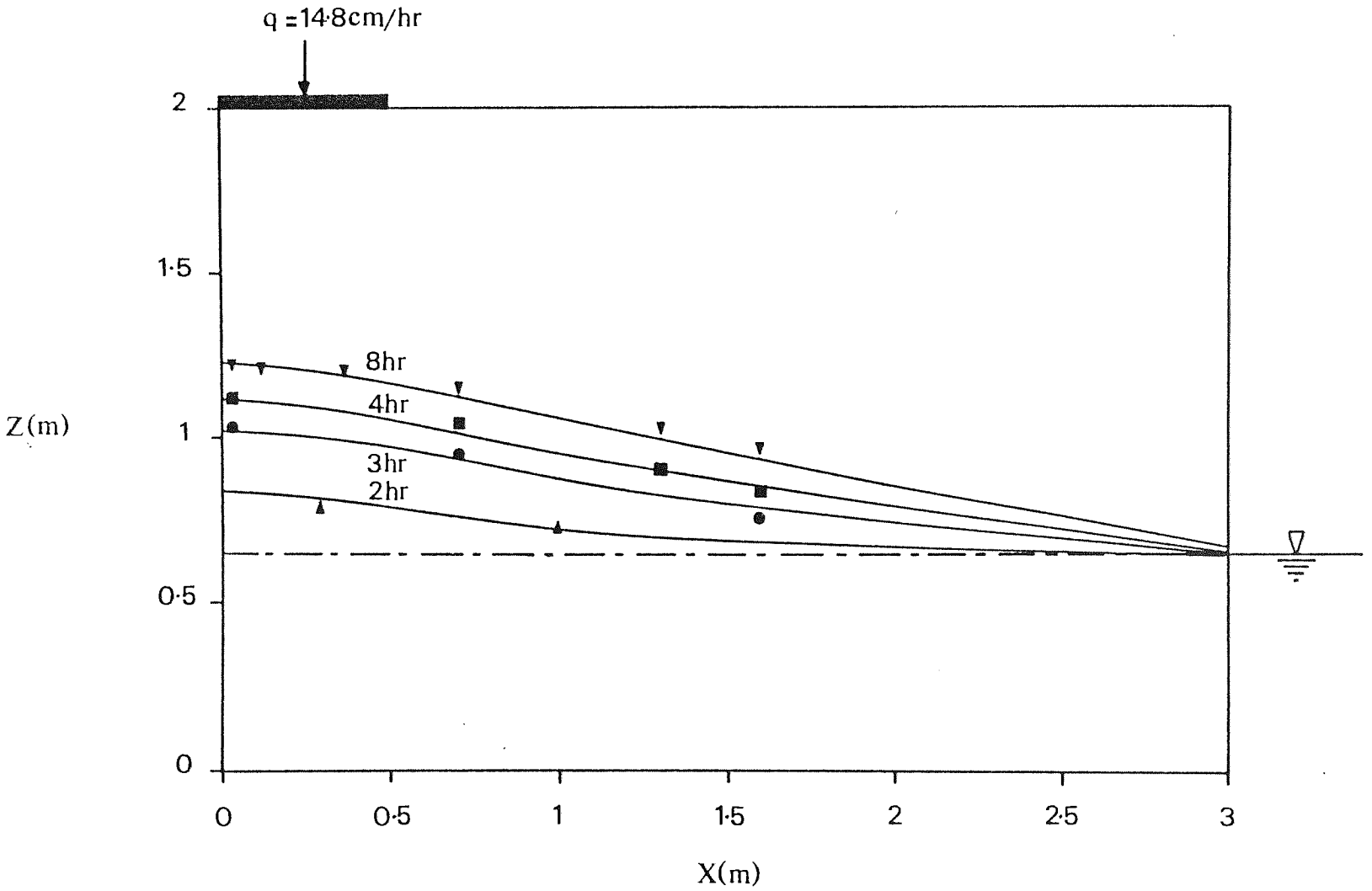

Figure 3.6 Measured and calculated water table elevations. Symbols indicate experimental observations by Vauclin et al. (1979).

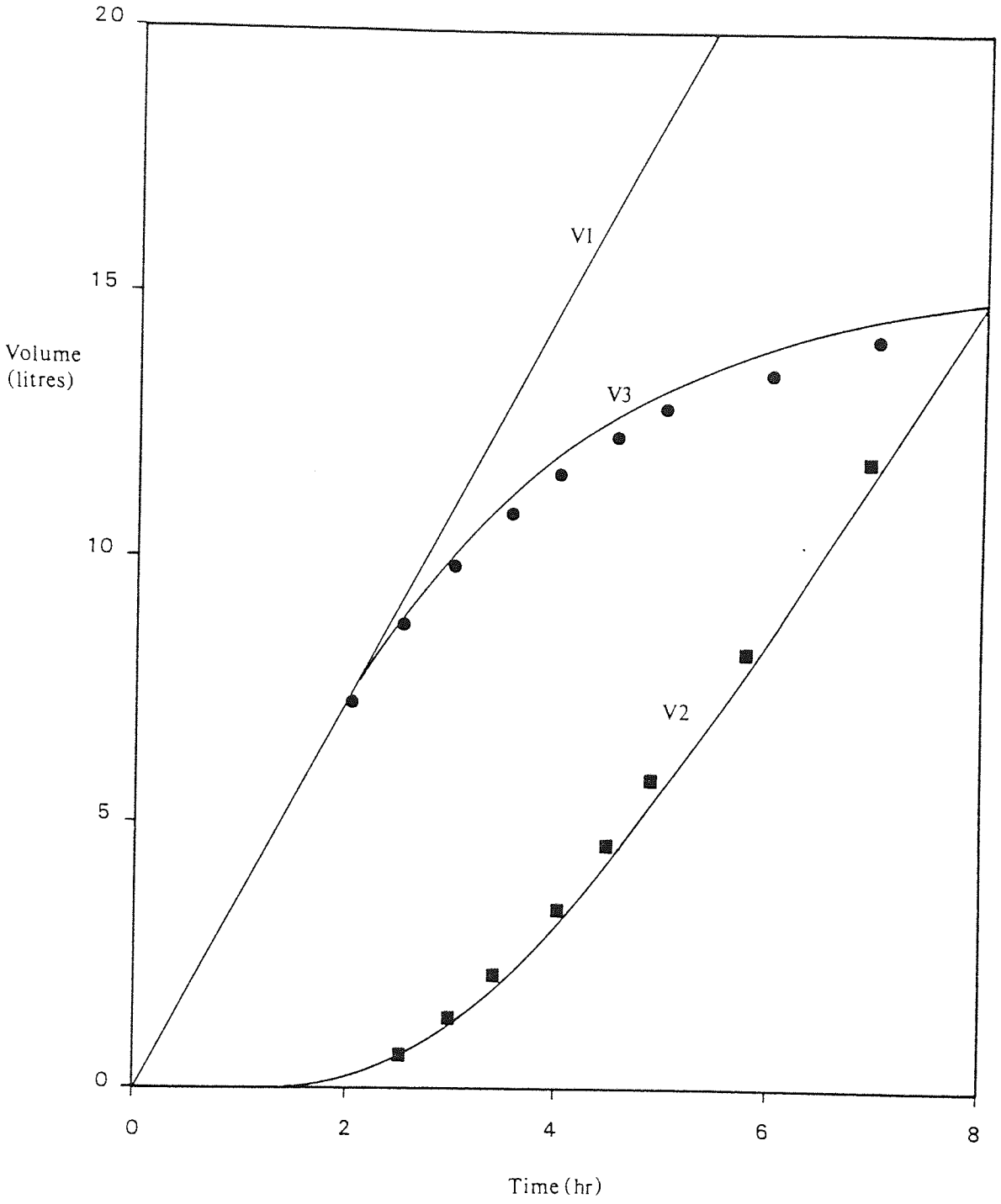

Figure 3.7 Comparison of experimental and numerical volumetric observations. V1 indicates volume of water entering the slab, V2 indicates volume of water leaving the slab and V3 indicates change in storage. Symbols represent experimental results from Vauclin et al. (1979).

and needed 200 time steps to simulate a 47 hour period. The model of Frind and Verge, using a simpler integration scheme than the methods presented here, solved the same problem using 400 finite elements and 13 time steps. Frind and Verge (1978) concluded that the implicit nature of the finite element scheme permitted such a coarse discretization.

3.4 SUMMARY AND CONCLUSIONS

A model of three dimensional flow in variably saturated porous media has been developed based on the Galerkin's approximation to the finite element method. The model utilizes four point Gauss quadrature integration which permits a more accurate representation of the nonlinear system in comparison to linear finite element or finite difference schemes. A number of operations within the algorithm have been programmed in the explicit vector syntax of CDC's FORTRAN 200. In doing so the portability of the code is removed, although it is felt that such manufacturer extensions are likely to be standard features of future versions of the FORTRAN language.

Verification of the model was carried out using the experimental data of a water table recharge problem presented in Vauclin et al. (1979). Close agreement between observed and predicted responses was evident. Furthermore, the FEM scheme adopted permitted coarser spatial and temporal discretization, in comparison to the finite difference analysis of the same problem also presented in Vauclin et al. (1979).

Chapter 4

The hydrological effects of soil spatial variability

The evidence of spatial variability of soil properties, in particular the hydraulic conductivity, is now well established. However, the influence of such variability on hydrological processes has not been fully assessed but may help to explain the limited success of a number of previous physically based modelling studies. The majority of studies examining the effect of spatial variability have concentrated on generalized flow domains, little work has been carried out specifically directed towards soil moisture movement on hillslopes. Furthermore, the fully three dimensional variably saturated transient system has not been examined.

4.1 PREVIOUS INVESTIGATIONS

Previous analyses of spatial variability have followed two distinct paths in the literature. One approach is to derive analytical expressions describing the moments (means, variances, covariances) of the output variables, such as hydraulic head, given the moments of the soil property distribution.

The second approach utilizes Monte Carlo simulations which have a wider range of applicability than the analytical approach since under numerous conditions, analytical descriptions of the output moments cannot be found. Furthermore, Monte Carlo analysis allows the entire probability distribution of the output variables to be ascertained.

4.1.1 Analytical investigations

Bakr et al. (1978) analyzed steady state, saturated groundwater flow in a statistically homogeneous, isotropic media. The hydraulic conductivity was treated as a stochastic process in an infinite domain. Bakr et al. first considered the case of unidirectional

saturated steady flow, that is,

$$\frac{d}{dx}\left[K_s(x) \frac{dh}{dx} \right] = 0$$

where $K_s(x)$ is the saturated hydraulic conductivity at any point x and h is the hydraulic head. By expressing the variables in the above equation in terms of a mean and a perturbation,

$$h = h + \tilde{h} \qquad h = E\{h\} \qquad E\{\tilde{h}\} = 0$$

$$\ln K_S = Y + \tilde{Y} \qquad Y = E\{\ln K_S\} \qquad E\{\tilde{Y}\} = 0$$

and expanding the governing equation (neglecting products of the perturbations) Bakr et al. were able to use spectral analysis to analytically derive variance and covariance expressions for the resulting hydraulic head distribution. A comparison of these expressions for one and three dimensional flows in an infinite domain shows that the variance of hydraulic head in a three dimensional system is only 5 per cent of that in the corresponding one dimensional case.

Gutjhar and Gelhar (1981) enhanced the method used by Bakr et al. (1978) to investigate steady saturated flow in finite domains.

Other investigations of steady state, saturated flow in spatially variable media, using perturbation methods, include Dagan (1982a) in a study of conditional simulation. Such an approach involves conditioning field measured values of the variable field, the remaining values in the field are then allowed to fluctuate randomly. Mizzel et al. (1982) have also used a combination of perturbation and spectral analysis to study two dimensional steady flow in a confined aquifer. Analytical solutions to the problem of unsteady saturated flow are presented in Dagan (1982b).

Unsaturated flow in spatially variable fields was investigated by Bresler and Dagan (1983a) using approximate flow equations for unsteady unidirectional flow (Dagan and Bresler, 1983). Their analytical solutions were based on perturbation methods, which were extended further to study one dimensional solute transport (Bresler and Dagan, 1983b).

Yeh et al. (1985a) studied the effect of soil variability on steady, unsaturated flow in an infinite domain. Unlike the earlier work of Bresler and Dagan (1983a), Yeh et al. accounted for autocorrelation in the spatially variable media. In this study the functional representation of unsaturated conductivity was,

$$K_r(\psi) = \exp(-\alpha\psi)$$

after Gardner (1958), where α is a parameter representing the relative rate of decrease of hydraulic conductivity with increasing pressure head. Assuming α constant, Yeh et al. compared head variances under one and three dimensional flows. Their results showed that for small $\alpha\lambda$, where λ is a measure of the variance structure of the hydraulic conductivity distribution, there was a considerable difference between the head variance in the one and three dimensional system, as in the saturated case (Bakr et al., 1978). For large values of $\alpha\lambda$, which may be associated with coarse textured soils, similar variances of hydraulic head were reported for one and three dimensional flows.

Yeh et al. (1985b) extended their study to account for anisotropic soils with variable α.

All of the analytical investigations discussed so far have been based on perturbation techniques. A limitation of this approach is that since high order terms of the fluctuations are neglected in the expanded series representing the governing equations of flow, then large amplitude problems, that is domains of high variability, cannot be

studied. Cusham (1983), Gelhar and Axness (1983) and Gutjhar (1984) discussed the validity of the perturbation method. Anderson and Shapiro (1983) have compared 'exact' Monte Carlo results with analytical equations based on perturbation methods for unidirectional, steady state unsaturated flow. Their results suggested that, even under conditions of large variability, perturbation methods may be appropriate. However, Anderson and Shapiro recognized that their one dimensional study has serious limitations and that the same conclusions may not arise from multidimensional analyses.

It is worth noting an alternative method of analyzing spatial variability for transient saturated groundwater flow presented in Sagar (1978) and Dettinger and Wilson (1981). The method does not produce analytical expressions describing the moments of the output variables, these values are obtained by forming a series of equations approximating the flow equations, using some numerical procedure such as finite elements. The solution of these stochastic equations is then obtained by Taylor expansion around the expected values and independent variables. Since the Taylor series is truncated at some level, this method has the same limitation as the previously described techniques, as the results can only be assumed 'exact' for fields of low variability.

4.1.2 Monte Carlo investigations

Monte Carlo analysis allows specific bounded domain problems to be studied. The flow domain is discretized into a series of discrete homogeneous blocks of different soil properties. The values assigned to each block are taken from frequency distributions of specified moments. By applying the same problem to a number of realizations of soil variability, the uncertainty of all the output variables can be extracted, if the number of realizations is considered large enough. Since numerical methods are normally required to solve each flow problem, large amounts of computing resources are invariably needed. This method has the advantage that, unlike perturbation and similar

techniques, there are no restrictions on the extent of variability considered, also the results of Monte Carlo simulations are more easily interpreted.

Probably the earliest example of a Monte Carlo analysis of the effect of soil spatial variability, is that of Warren and Price (1961). They used a finite difference model of saturated groundwater flow to investigate the influence of several possible frequency distributions of hydraulic conductivity. The investigations were limited to steady state quasi-linear and quasi-radial flow geometries and to a transient quasi-radial flow system.

Freeze (1975) examined the effect of nonuniformity of hydraulic conductivity on one dimensional, steady state, saturated flow. Freeze used the analytical solution to this boundary value problem, within a Monte Carlo analysis. He recognized more realistic variabilities of soil properties that those used by Warren and Price (1961). An example of Freeze's results is shown in figure 4.1. This demonstrates the influence of the variability of hydraulic conductivity on the uncertainty in hydraulic head throughout the one dimensional column. Freeze's results suggested that nonuniformity could have a significant effect on groundwater hydrology, although Freeze (1975) admitted that limiting the study to one dimensional analysis could be partially responsible for such claims. In the same work, Freeze also investigated the multivariate problem of one dimensional transient consolidation. Hydraulic conductivity, porosity and media compressibility values for each homogeneous block were generated from suggested frequency distributions. Freeze concluded from the results of the transient simulations that the variances of the soil property distributions are just as important as the mean values as an index property for nonuniform soils.

Smith and Freeze (1979a) extended the work of Freeze (1975) by examining the effect of autocorrelation of hydraulic conductivity in a Monte Carlo study of one dimensional, steady state, saturated flow; under the same conditions as the earlier study of Freeze. Autocorrelated properties were generated by a simple nearest neighbour method

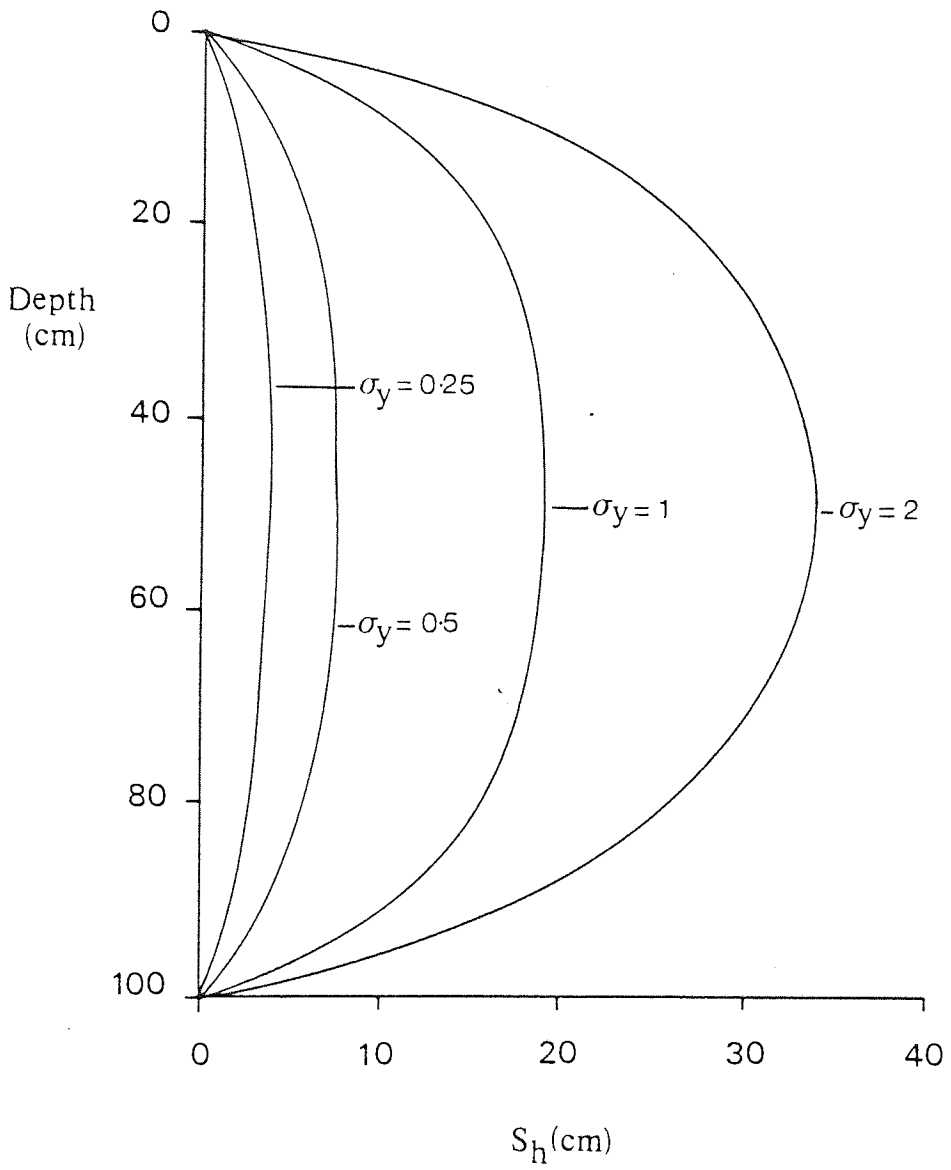

Figure 4.1 Influence of the standard deviation σ_y ($y=\log_{10}K_s$) of the hydraulic conductivity distribution on the standard deviation S_h of the predicted hydraulic head distribution throughout a 100 centimetre vertical column, after Freeze (1975).

(Bartlett, 1975). Using realistic descriptions of the nonuniformity, calculated values of the standard deviation of hydraulic head were as high as thirty per cent of the difference in head throughout the soil column.

Recognizing the possible limitations of a one dimensional study, Smith and Freeze (1979b) analyzed the effect of spatial variability of hydraulic conductivity on two dimensional steady flow. A comparison of the variability of hydraulic head in their one and two dimensional studies showed a reduction in the standard deviation of slightly less than one half for the two dimensional system. Such a small reduction conflicts with the analytical results reported in Gelhar (1976), who found an order of magnitude difference in one and two dimensional flow in an infinite domain, although Smith and Freeze recognized that the small difference suggested in their study is probably due to the bounded nature of the flow domain.

Using algebraic infiltration models, Smith and Hebbert (1979) carried out Monte Carlo simulations in a study of the effect of random distributions of soil properties on the resulting distribution of ponding times and infiltration rates. Smith and Hebbert generated a large number of homogeneous soil blocks from a random distribution of hydraulic conductivity. A constant rainfall event was then applied to each soil block independently. Therefore, no hydrological interaction of soil blocks was permitted. Furthermore, autocorrelation of the hydraulic conductivities was neglected. Smith and Hebbert presented the composite mean infiltration pattern for a range of variation of soil properties under two different rainfall intensities. Their results suggested that under low rainfall intensity, random variability of soil properties can have a significant effect on the resulting hydrological response. The conclusions of Smith and Hebbert's study, however, are restricted to events characterized by the Hortonian mechanism.

The study presented in Freeze (1980) is unarguably the most important analysis to date, of the effect of spatial variability on hillslope flow process. Freeze adopted a 'stochastic - conceptual' analysis of the response of a hypothetical quasi-three

dimensional hillslope.

The hillslope in plan was discretized into 200 soil blocks, each 10m square. When rainfall was applied to each block the infiltration rate was determined, using algebraic equations, at each time step of the event. The rainfall excess was then evaluated and routed directly to the channel, assuming constant overland flow velocity. Channel flow was treated in the same manner as overland flow.

One complete Monte Carlo experiment of Freeze involved the simulation of one hundred events, each consisting of sixty time steps. For each experiment, surface topography, hydraulic conductivity, porosity and a soil moisture storage parameter were generated using the algorithm of Mejia and Rodriguez-Iturbe (1974). These four stochastic processes were generated with specific autocorrelations, although cross correlation of the soil properties was neglected. For each independent event antecedant conditions and external storm properties, such as duration and intensity were generated. An autocorrelated rainfall intensity pattern was then generated for each time step of the event.

Freeze's study did not recognize subsurface storm flow, although base flow was incorporated in a simplified manner by recognizing the elevation of a generated water table. The incorporation of a water table position in Freeze's study allowed both Hortonian and Dunne mechanisms of overland flow to occur during an event. However, Freeze admitted that :

> "... the transient propogation of this water table rise into adjacent elements is not considered; the moisture conditions in the soil column of each element are considered independently".

In fact, this is a serious limitation of Freeze's experiments, since, although autocorrelation of soil properties is recognized, the localizing of a highly correlated spatial structure is not simulated due to the independent nature of Freeze's calculations.

Freeze carried out several investigations on different permutations of the 'major' underlying statistical distributions, for example increasing the variance of the hydraulic conductivity distribution, other parameters remaining fixed. By comparing the resulting hydrograph distributions of several experiments, Freeze concluded, that μ_Y, the mean of the log transformed hydraulic conductivities, σ_Y, the standard deviation and α_Y, an autocorrelation parameter, have a significant influence on the hydrological response of the hillslope. Freeze suggested that the order of importance of these statistical parameters is μ_Y, σ_Y, α_Y. In particular, for conductivity fields with high mean values, a large variance of the distribution can have a striking effect due to the inclusion of areas of conductivity less than the rainfall intensity, although for low mean conductivity distributions, the results shown in Table 2 of Freeze (1980) demonstrate that the autocorrelation of the distribution is just as important as the variance. However, since Freeze's soil block calculations were evaluated independently, it is difficult to see how autocorrelation of soil properties can have such an effect. A possible explanation is that each Monte Carlo experiment of Freeze used a single realization of spatial variability, an analysis of multiple realizations in Freeze's study may remove any 'chance' effects.

Beven (1983) has investigated the effect of spatial variability of hydraulic conductivity within the semi-distributed, variable contributing area model TOPMODEL (Beven and Kirkby, 1979). The model was applied to a representation of a 3.25 km^2 catchment under various uncorrelated distributions of saturated hydraulic conductivity. Beven examined the effect of variability on different catchment scales and concluded that only at the small catchment scale or hillslope scale will the pattern of variability have a significant effect on runoff generation.

A number of experiments on the effect of variability in a small sloping soil block representing a single hillslope segment have been performed by Sai (1983). The

'hillslope' was 1.83 m long, 1.22 m deep and 0.13 m wide. A two dimensional (vertical slice) finite element model was used to compare the effect of hydraulic conductivity distributions on the hydraulic head field produced by transient variably saturated flow. Sai investigated changes in mean, variance and autocorrelation of the conductivity distributions but limited his study to only six permutations of these statistical parameters. Sai restricted his study to low variability under a small range of mean conductivity (0.713 cm/min - 0.813 cm/min) and further failed to consider multiple realizations of the underlying statistical distributions. Sai concluded that under the conditions examined, changes in mean and variance of the conductivity patterns have only a significant effect at long times, when steady state conditions are approached. Changes in autocorrelation had little effect on the resulting hydraulic head distribution, even under steady flow.

El-Kadi and Brutsaert (1985) have also examined hydraulic conductivity variability in a two dimensional flow domain. They applied a transient two dimensional model of saturated flow (neglecting vertical flow), based on the linearized form of the Boussinesq equations, to a hypothetical study of the drainage of an unconfined aquifer. Using Monte Carlo simulations, El-Kadi and Brutsaert analyzed the effect of various conductivity distributions on the resulting water table elevations and outflow rates. Analysis of the results of the multiple realizations showed that the variability of the water table elevations and outflow rates were significantly affected by the degree of variability of the hydraulic conductivity and were functions of time, although the variability of the outflow rate relative to the mean flux remained virtually constant throughout the simulation period. A comparison of the results of various degrees of autocorrelation between the conductivity values by El-kadi and Brutsaert, demonstrated that increasing the correlation increases the uncertainty of the output variable. However, the effects of such changes were not as large as those produced by changes in the variance of conductivity distribution.

4.1.3 Summary

Several investigations of the effect of spatial variability of hydraulic conductivity on various hydrological processes are evident in the literature. The two distinct methods of such analyses are analytical derivations and Monte Carlo simulation, the advantages of which have been discussed. Various degrees of complexity of groundwater movement have been studied, ranging from one dimensional, steady state, saturated flow to three dimensional, steady, unsaturated flow and two dimensional, transient, variably saturated soil water movement. Also, a number of studies on overland flow generation within spatially variable fields are presented in the literature. Very little work has been carried out on specific flow domains, in particular, hillslope runoff generation. Furthermore, the fully three dimensional, transient, variably saturated flow problem has not been examined, even in a generalized system. It is clear that increasing the number of spatial dimensions of groundwater analysis will reduce the effect of soil spatial variability, since the restriction of flow in localized low conductivity areas in one or two dimensional systems will be reduced. This reduction has been demonstrated by several investigators, although implications of such a reduction in hydrological modelling have not been fully assessed.

4.2 THE EFFECTS OF SPATIAL VARIABILITY OF SATURATED HYDRAULIC CONDUCTIVITY ON THE RESPONSE OF A SINGLE HILLSLOPE SEGMENT

In order to investigate the effects of soil spatial variability on hillslope runoff generation, it was decided to concentrate the experiments on a hypothetical straight hillslope. In doing so, the effects of topographic variation (Freeze, 1972b) and slope divergence or convergence (Beven, 1977) would not be encountered and thus more general conclusions could be drawn from the results of the investigation.

The geometry of the hillslope selected for this study is shown in figure 4.2. The hillslope is 150 metres wide and 100 metres long. An isotropic soil, 1 metre thick, lies on an impermeable 1 in 6 slope.

Faces ABFE, EFGH, and DCGH are also considered impermeable. ABCD is a potential seepage face, the pressure head along AD being prescribed as atmospheric. Under certain conditions the water table will rise to the surface of the soil layer. If this occurs the pressure head is set to zero, neglecting a small depth of surface flow caused by the the onset of surface saturation. During the simulation of a rainfall event, all node points of the finite element mesh on the soil surface (face BCGF) have prescribed flux values. These values are reduced automatically in the finite element code if surface saturation or infiltration excess overland flow occurs.

In order to solve the boundary value problem, the hillslope was discretized into 3024 node points and 2380 elements (figure 4.3). Due to the immense data requirements of such a mesh, a code was developed to generate the necessary information for the finite element code.

4.2.1 Soil properties

It was originally intended to extend the hypothetical investigation to a real hillslope, namely the Eastergrounds field of the Slapton Wood catchment described in 2.3.1.1, therefore unsaturated soil-water properties resembling those in the Eastergrounds field were used for this study. Soil moisture characteristics were made available† for a silty clay loam at Loworthy Farm, Slapton, which was considered very similar to the soil in the Eastergrounds site. Using a least squares algorithm the functional form of the

† N Coles (1985). Personal communication

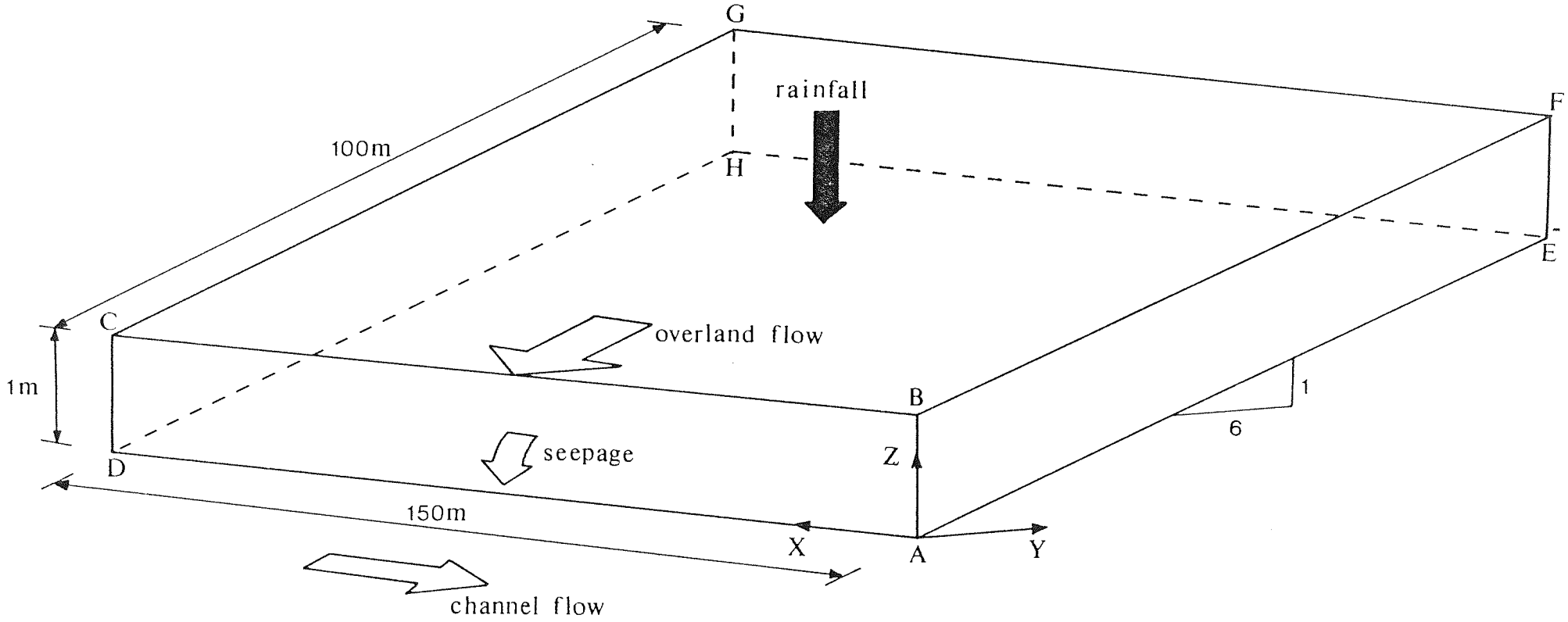

Figure 4.2 Hypothetical straight hillslope.

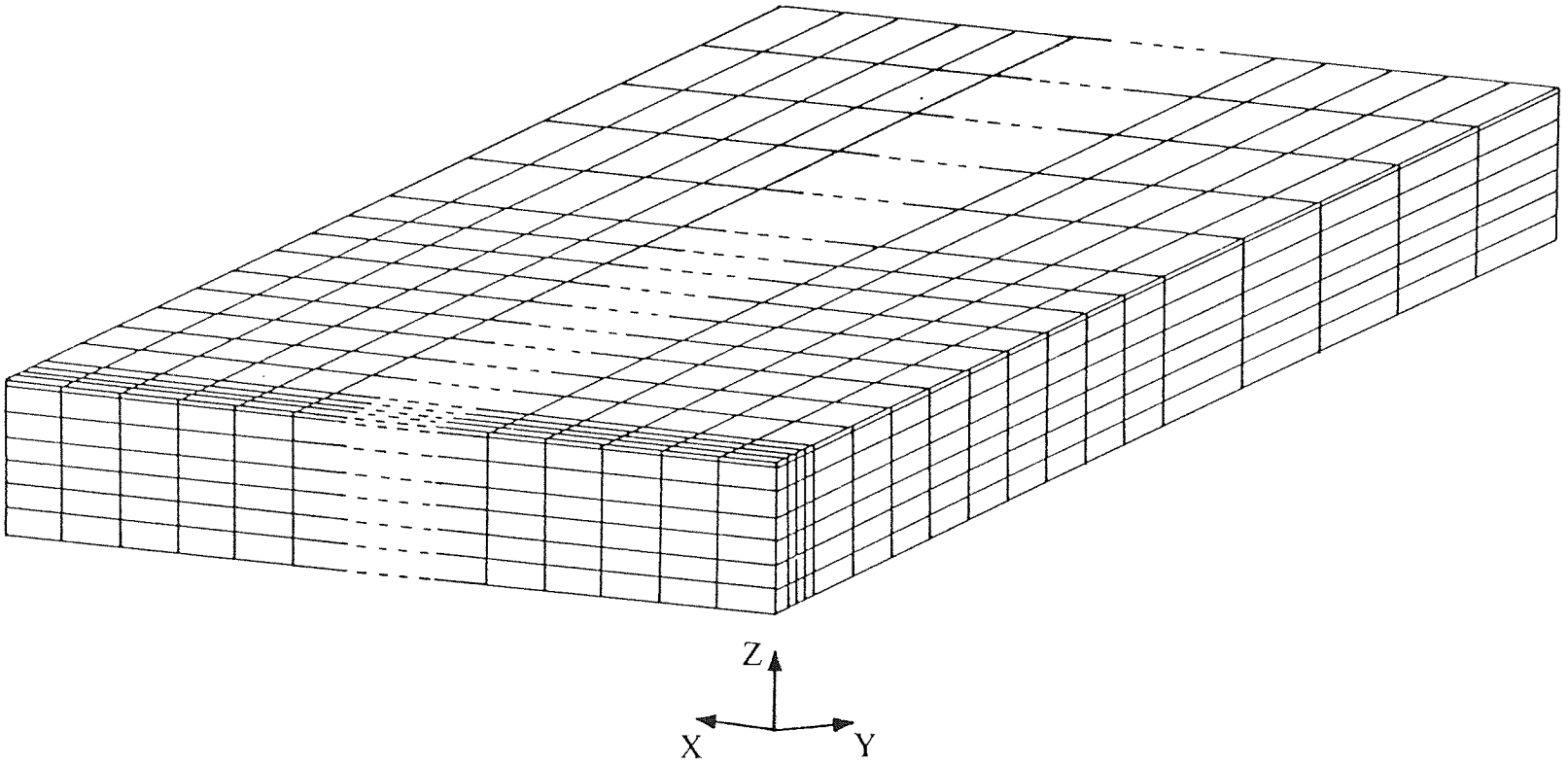

Figure 4.3 Finite element discretization of the hillslope.

retention curve in equation (3.11a) was fitted to the data (figure 4.4). Rewriting equation (3.11a),

$$\theta(\psi) = \theta_{res} + (\theta_s - \theta_{res}) \frac{A}{A + |\psi|^B}$$

the best fit parameters were:

θ_s = 0.57 $cm^3\ cm^{-3}$

θ_{res} = 0.245 $cm^3 cm^{-3}$

A = 1924.8 $cm^{1.247}$

B = 1.247

It is important to note that the unrealistically high value of residual moisture content was selected to fit the data over a range of suction values likely to be encountered throughout the simulations.

The values of β, γ and ψ_o in equations (3.12) were evaluated to be 1.745 x 10^5 cm^{-1}, 0.1702 cm^{-2} and -3.382 x 10^{-5} cm respectively, which produce a constant value of specific moisture capacity, in the saturated zone, equal to 1.0 x 10^{-5} cm^{-1}.

Unfortunately data describing the unsaturated hydraulic conductivity characteristic was not available for the same soil. It was decided to use the permeability model first proposed by Childs and Collis-George (1950) to produce a functional form of the unsaturated hydraulic conductivity corresponding to the previously described soil moisture curve.

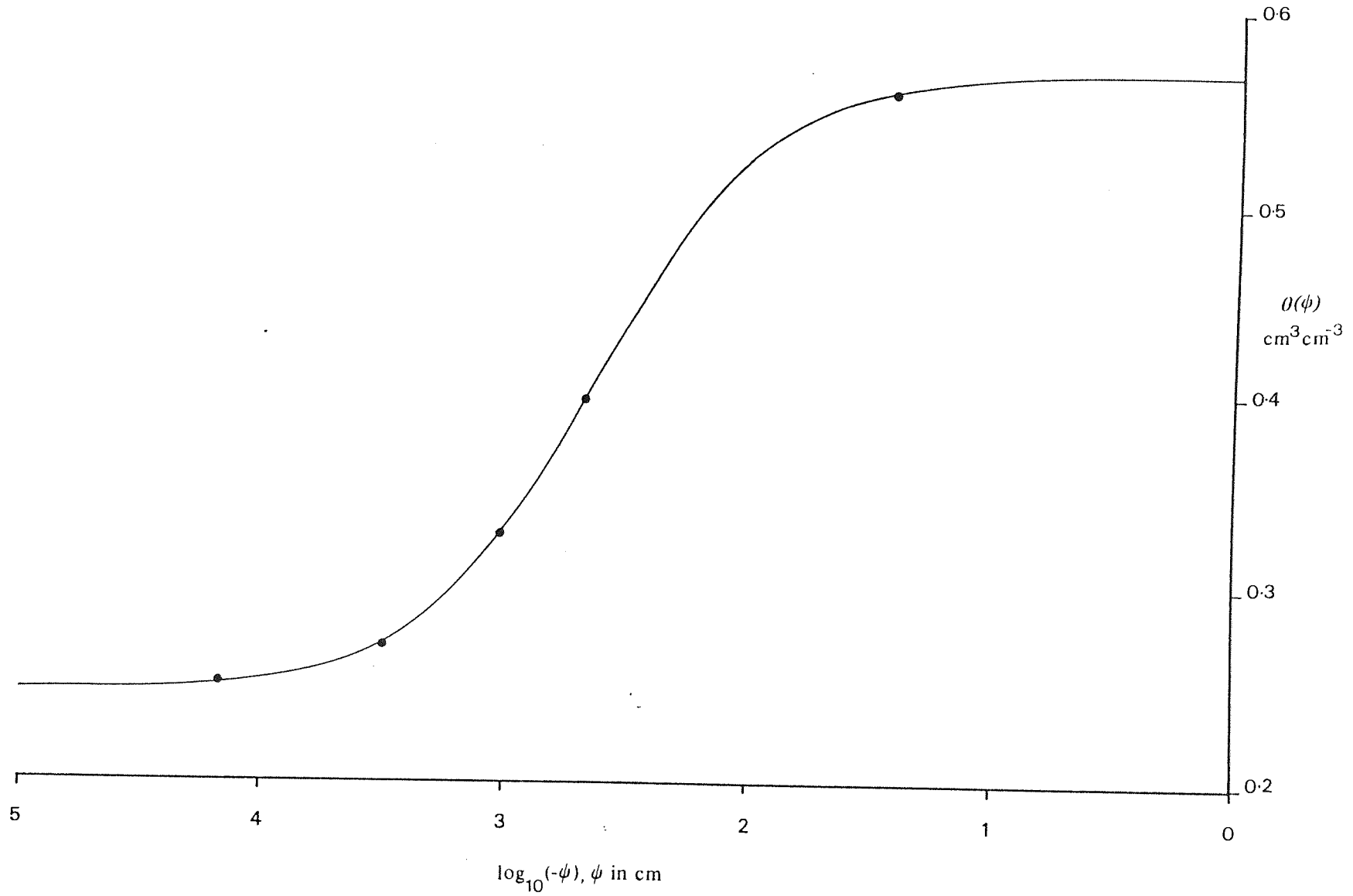

Figure 4.4 Observed (●) and estimated (—) soil water characteristics.

The effective saturation, S_e, is defined as:

$$S_e = \frac{S - S_r}{1 - S_r} = \frac{A}{A + |\psi|^B} \qquad (4.1)$$

where: S = saturation

S_r = residual saturation = θ_{res} / θ_s

Note that the second equality in equation (4.1) only refers to the functional relationship as given in equation (3.11a).

Assuming the soil to consist of capillaries of various radii r, the effective pore size density function $s_e(r)$ is given by (Brutsaert, 1966):

$$s_e(r) = \frac{d}{dr} S_e(r) = \frac{B\, d\, r^{B-1}}{(d + r^B)^2} \qquad (4.2)$$

where: $d = \frac{0.149^B}{A}$

That is, given the soil moisture characteristics, the corresponding pore size distribution can be determined via equation (4.2). This distribution for the given retention curve is shown in figure 4.5.

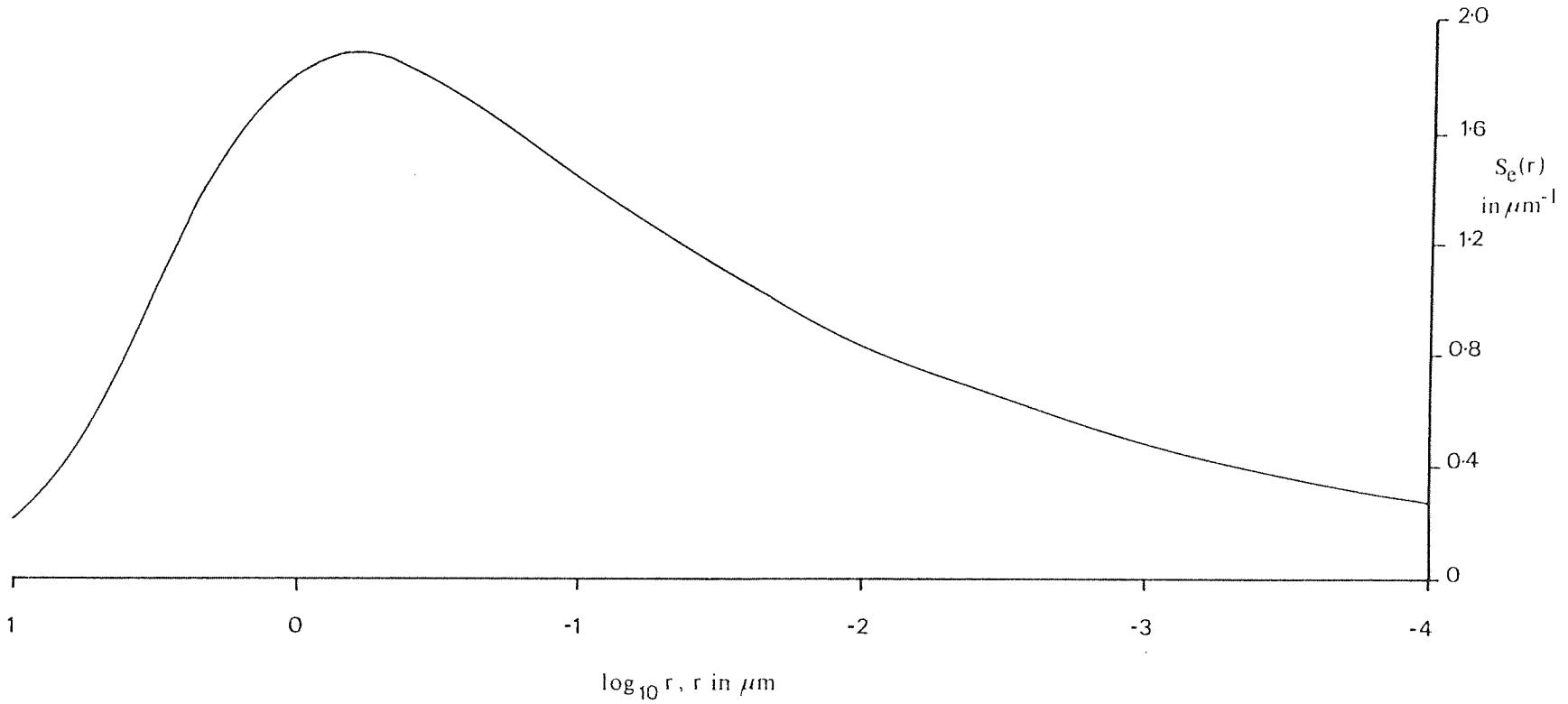

Figure 4.5 Pore size distribution from equation (4.2).

Adopting a series - parallel permeability model, the intrinsic permeability, k, is given by (Brutsaert, 1968):

$$k(\psi) = [\, \theta_s^2 (1 - S_r)^2 / 8 \,] \,.\, k'(\psi) \qquad (4.3)$$

where:

$$k'(\psi) = 2d^{2/B} \left[S_e(\psi) \int_0^{S_e(\psi)} x^{2/B} (1 - x)^{-2/B} \, dx - \int_0^{S_e(\psi)} x^{(2+B)/B} (1 - x)^{-2/B} \, dx \right]$$

and the intrinsic permeability is related to the hydraulic conductivity by:

$$k(\psi) = K_S \, K_r(\psi) \frac{\mu}{\gamma}$$

where: γ is the specific weight of water

μ is the viscosity of water.

To obtain the relative hydraulic conductivity curve, equation (4.3) was evaluated at various values of ψ using numerical integration. The resulting relationship is shown in figure 4.6.

It is interesting to note that the calculated value of k in equation (4.3) at saturation is equal to 5.08×10^{-9} cm^2 which corresponds to a saturated hydraulic conductivity of 4.98×10^{-4} cm/s (at 20°C), which compares well with the mean hydraulic conductivity of 8.4×10^{-4} cm/s for the Eastergrounds field suggested in 2.3.1.1.

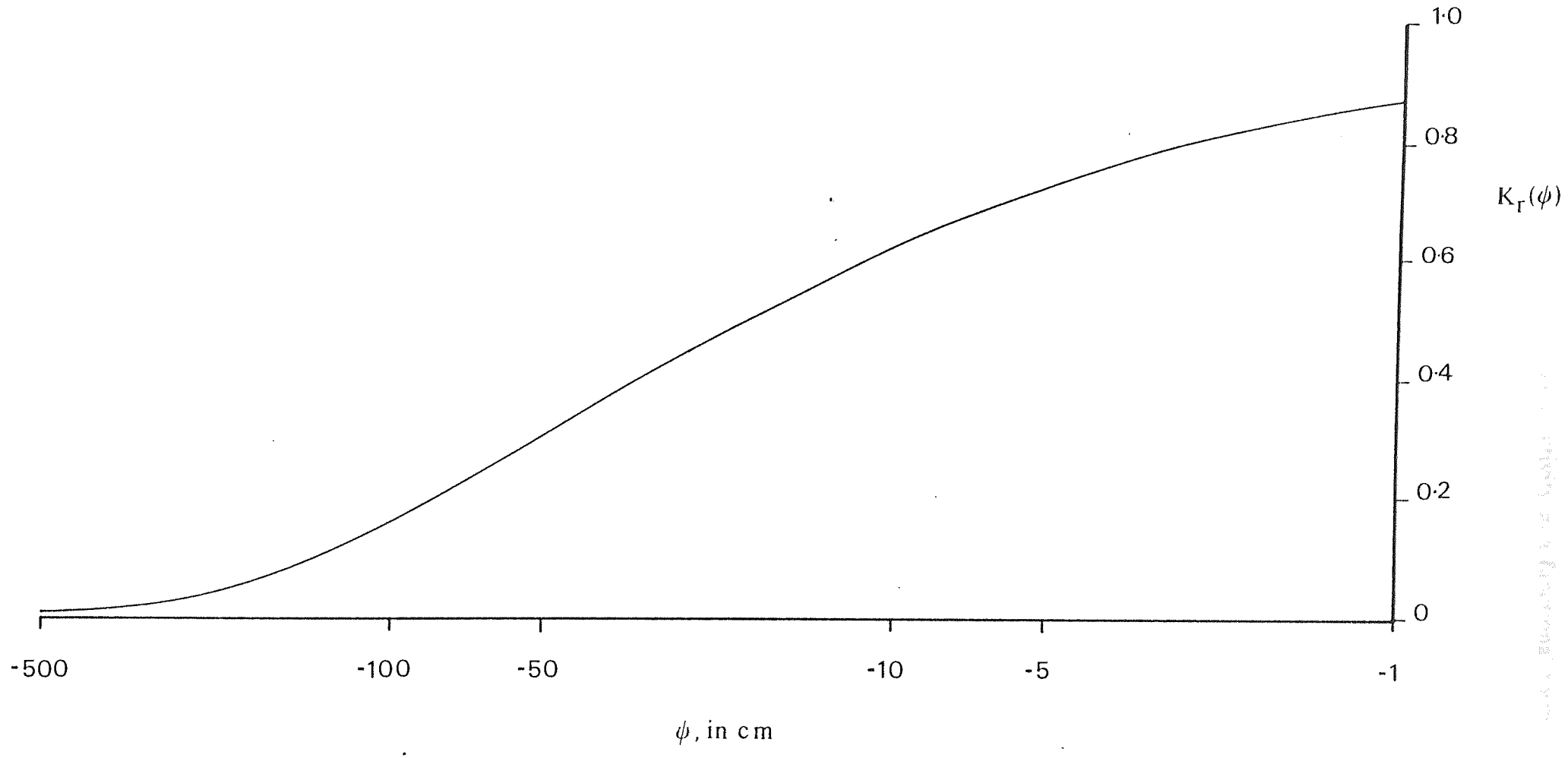

Figure 4.6 Estimated unsaturated hydraulic conductivity relationship.

In order to describe the relative hydraulic conductivity in a functional form, a least squares fit was made of the equation,

$$K_r(\psi) = \frac{a}{a + |\psi|^b}$$

The 'best' parameters were evaluated as:

$$a = 14.752 \text{ cm}^{0.957}$$

$$b = 0.957$$

4.2.2 Generation of hydraulic conductivity fields

There are several techniques available for the generation of multidimensional random fields. Matrix models describe the field only at specified discrete points, one such model is the nearest neighbour method (Whittle, 1954; Bartlett, 1975) which has been used in a number of Monte Carlo simulations of hydrological processes. A less expensive and more popular method is based on multidimensional spectral analysis of random fields such as Mejia and Rodriguez-Iturbe (1974). Recently, Mantoglou and Wilson (1982) have demonstrated that a different technique, the turning bands method, may be more attractive for Monte Carlo simulations in hydrology.

The turning bands method (TBM), which was first introduced by Matheron (1973), is based on representing a multidimensional field as a sum of a series of unidimensional processes. The generation procedure for a two dimensional field is shown diagramatically in figure 4.7. In the two dimensional case, lines are generated along a series of uniformly distributed direction vectors **u** within the unit circle of arbitrary origin. A discrete unidimensional process having zero mean and covariance function $c(\tau)$ is generated along each line i, where τ is the coordinate along that line. For each

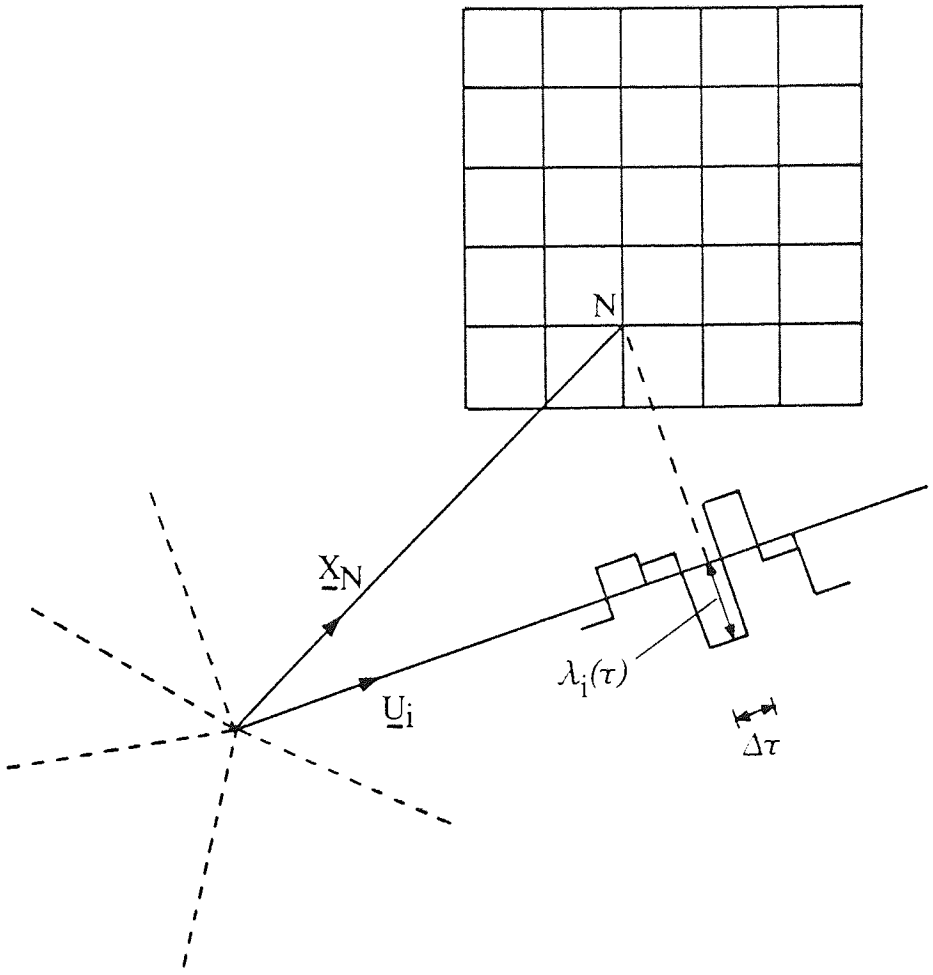

Figure 4.7 The generation of a two dimensional field using the turning bands method.

point in the two dimensional field an orthogonal projection is made onto the line i. The value of the discrete process is then assigned to the corresponding location in the two dimensional field. The procedure is repeated for L lines such as i. The value of the generated field at point N with location vector X_N is then evaluated as:

$$\lambda_s(X_N) = \frac{1}{\sqrt{L}} \sum_{i=1}^{L} \lambda_i (X_N.u_i)$$

where $\lambda_i(X_N.u_i)$ is the value of the discrete process.

The mean of the generated process is zero. Mantoglou and Wilson (1981) have shown the relationship between the line covariance function $c(\tau)$ and the generated covariance function for isotropic and anisotropic fields.

In order to produce correlated conductivity fields, a code based on the TBM was made available by the Institute of Hydrology, UK. The code produces a random field in three dimensions, two space and one time. For the purpose of this study the vertical space dimension z was represented by the time axis. An isotropic field was generated in the x-y plane by specifying a specimen distance r_s and the autocorrelation at that distance $\rho_{xy}(r_s)$. The correlation function generated obeys power law decay, that is $\rho(r)$ is proportional to r^{α}, where α is a specified constant. A specimen distance was also required in the z axis (z_s) together with a correlation at that distance ($\rho_z(z_s)$).

Examples of two realizations of conductivity fields are shown in figures 4.8 and 4.9. The statistics of these fields, in terms of the log transformed values ($Y = \ln K_s$) are; μ_Y = 0.2 cm/min, $\sigma_Y^2 = 0.5$, $\alpha = 1.0$, $\rho_{xy}(10m) = 0.7$, $\rho_z(0.1m) = 0.8$.

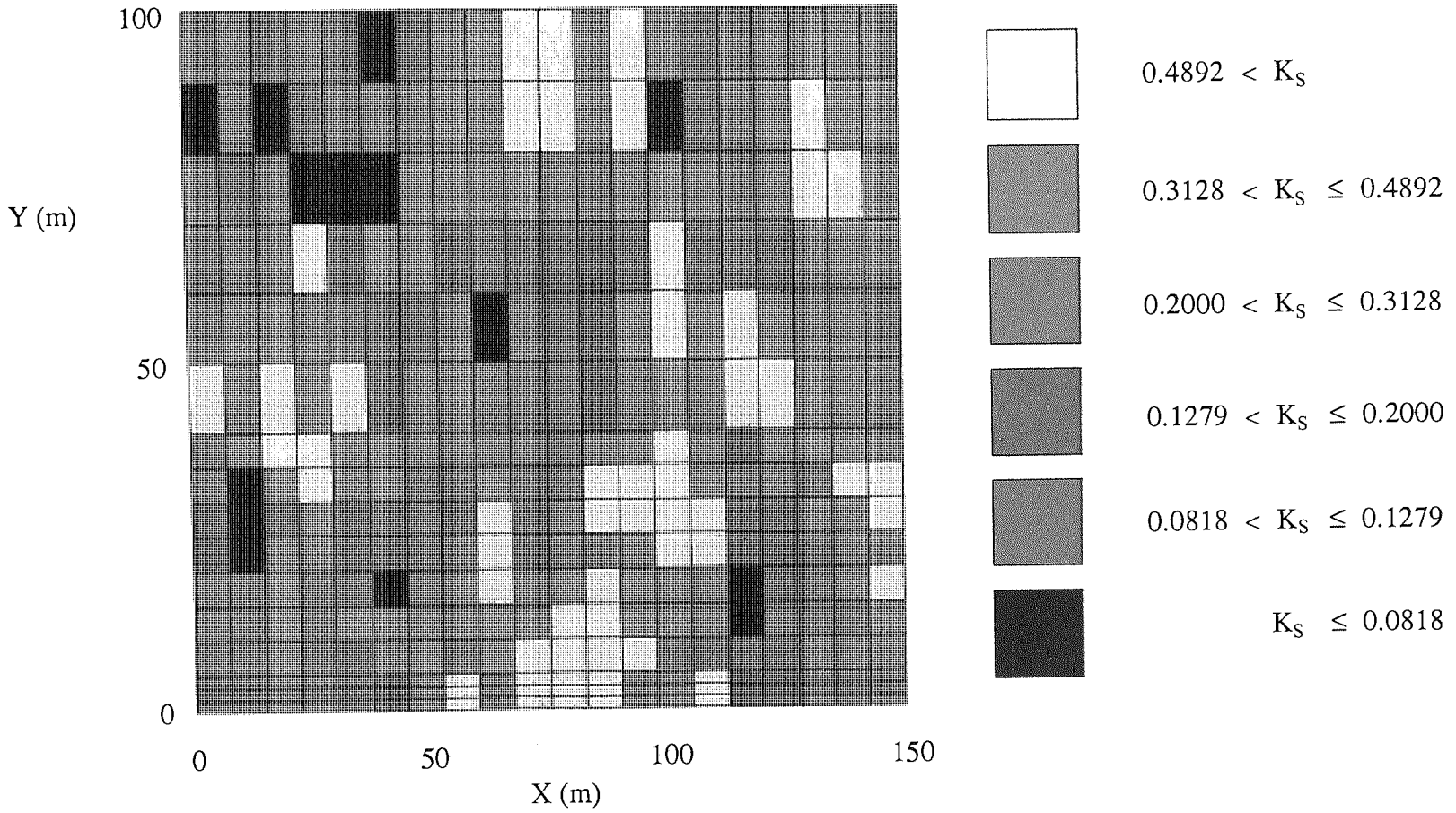

Figure 4.8 Single realization of a correlated distribution of hydraulic conductivity (in cm/min) over the soil surface. Refer to text for details of the statistics of the field.

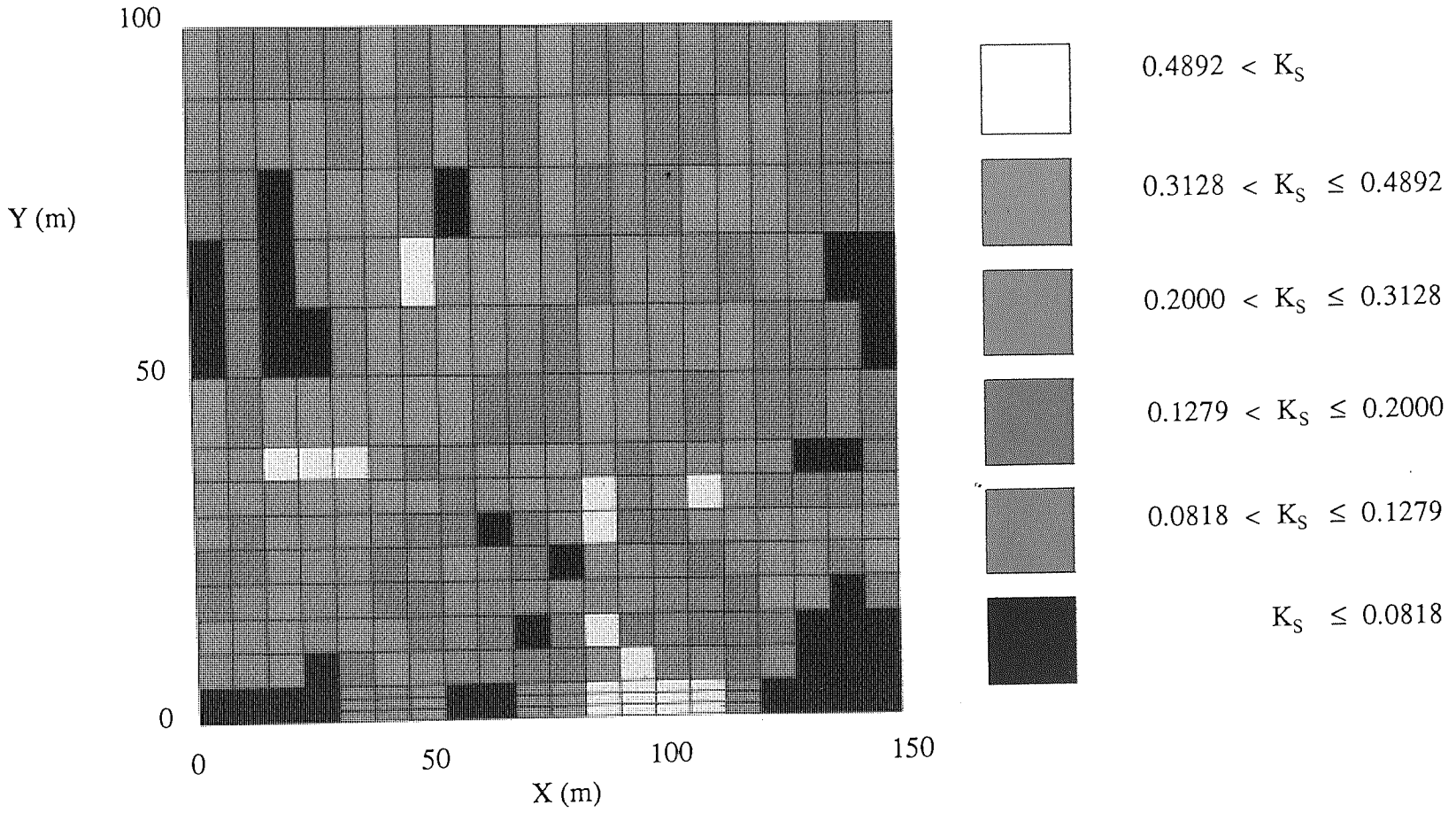

Figure 4.9 Single realization of a correlated distribution of hydraulic conductivity (in cm/min) over the soil surface. Refer to text for details of the statistics of the field.

Uncorrelated random fields were generated using a standard random number generator (Numerical Algorithms Group routine G05DDF). It is recognized that these fields will not be strictly uncorrelated due to the finite size of the elements used in the numerical simulations, however, for the remainder of this study the term uncorrelated will be used.

4.2.3 Initial conditions

Initial values of pressure head at all nodes in the finite element mesh are required prior to solving the transient problem. Clearly the commonly used assumption of static conditions is not valid if the hillslope exhibits soil spatial variability. Furthermore, under such conditions the soil will be under extremely high suctions at the top of the slope and, as was noted by Beven (1975), only a small portion of the hillslope may effect the generation of subsurface flow. Another possible initial condition is the assumption that the soil has reached 'field capacity' over the entire slope. Again such conditions are invalid for a highly variable soil, also the unsaturated characterisitics used in this study would define a very dry state for the 'field capacity'. An alternative approach, which was used for this investigation, is that of steady state conditions. In order to produce a steady state simulation the nodal values of pressure head at the soil surface were predefined. Equation (3.4), with time dependent terms omitted, was then solved to obtain the pressure head distribution over the hillslope. Therefore, prior to the transient simulation, a steady state run was made for each realization of a hydraulic conductivity field. The predefined surface pressure head values used throughout the remainder of this chapter follow a linear decrease from -80 to -550 cm water. An example of a steady state solution is shown in figure 4.10 for a uniform homogeneous soil with hydraulic conductivity equal to 0.1 cm/min.

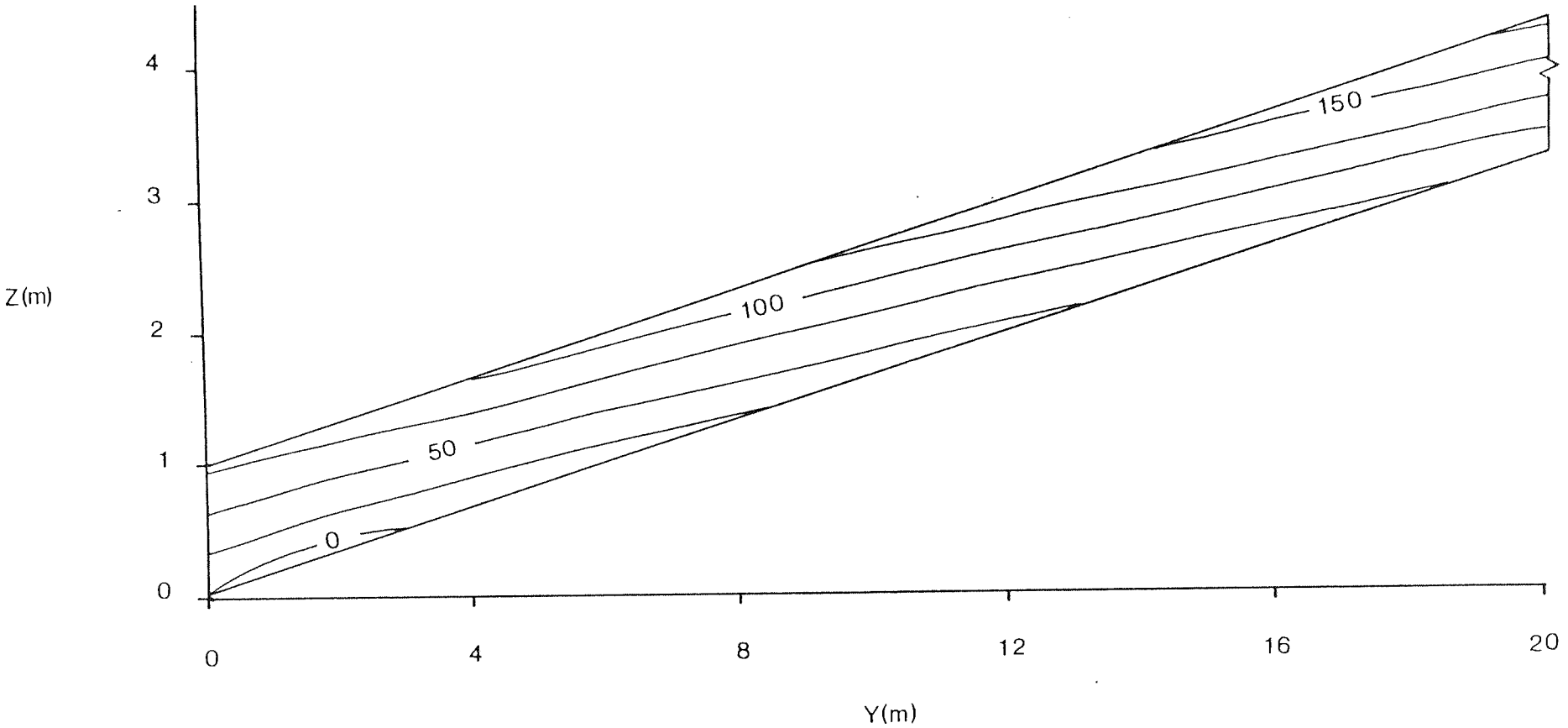

Figure 4.10 Steady state pressure head distribution for a uniform homogeneous soil. Contours indicate suction values in centimetres of water.

4.2.4 The response to a single event

The hypothetical deterministic event selected for this part of the study consisted of 5 hours of drainage followed by 8 hours constant rainfall intensity equal to 0.00667 cm/min (4 mm/hr) which preceded 10 hours of drainage. The inital 5 hour drainage period was included to filter out the effects of the inital conditions, which can have a dramatic effect on the resulting discharge hydrograph (see for example Beven, 1975).

Due to the immense computing requirements of three dimensional analysis it was impossible to perform complete Monte Carlo experiments, in fact in describing his own model, Freeze (1980) remarked,

> "These calculations do not consist of a numerical solution of the three dimensional boundary value problem representing transient, saturated - unsaturated, subsuface flow on a hillslope. The computer time required for such an approach in a Monte Carlo analysis would be much too large".

Rather than carrying out several hundred Monte Carlo simulations, it was decided to only consider ten realizations of the underlying variability. The limitations of such a restriction are recognized, however it is felt that a suitable comparison of different variabilities could be drawn from the results.

Instead of limiting the investigation to a single mechanism of runoff generation, as in several previous studies, a range of mean hydraulic conductivities was chosen in order to allow two distinct mechanisms to volumetrically dominate the storm hydrograph, namely subsurface stormflow and Hortonian overland flow.

In order to route surface flow a simple travel time approach was adopted, for which a constant overland flow velocity was assumed. Unless otherwise stated, a value of 250 cm/min (0.042 m/s) was used for the simulations presented in this study. This value

lies within the range suggested by Emmet (1978). Travel times of channel flow were neglected because the majority of streamflow is likely to travel the 150 metre reach during a typical time step of several minutes.

For each realization of a given variability, output was produced in the form of two hydrographs, subsurface flow and total (subsurface plus surface) flow and pressure head distributions at selected times. In order to compare the results of each distribution two numerical quantities were used to characterize the hydrographs, these were q, the peak flow and Q, the volumetric flow. Each realization required approximately 1000 seconds of CPU time on the CDC Cyber 205 at the University of Manchester Regional Computer Centre using an explicitly vectorized form of the code. Running the code entirely on the scalar processor required approximately five timesmore CPU time. Equivalent central processing times on a DEC VAX 11/750, which is often regarded as a standard unit of computer power was approximately 18 hours, demonstrating the restrictions of fully three dimensional analysis. The average value of the mass balance error in equation (3.15) of all these simulations was approximately 0.002 per cent.

4.2.4.1 High permeability soils

Three mean hydraulic conductivity values were selected for analysis of predominantly subsurface flow responses, these were 0.05, 0.1 and 0.2 cm/min. The subsurface flow hydrograph results of nine experiments on uncorrelated distributions are presented in table 4.1. Referring to this table, $\overline{Q}$ is the arithmetic mean of ten realizations, S_Q is the standard deviation and CV_Q is the coefficient of variation. Table 4.2 shows the corresponding total flow hydrograph results. No overland flow occured in cases G, H and I , the results of these cases have therefore been omitted from table 4.2.

The results in table 4.1 and 4.2 show little variation with respect to the mean peak or volumetric flow for all cases. A comparison of the responses of the nonuniform cases

Table 4.1 A comparison of cases (A-I) showing the effect of hydraulic conductivity distribution on the subsurface flow hydrograph

CASE	μ_Y (cm/min)	σ_Y^2	PEAK FLOW			VOLUMETRIC FLOW		
			$\bar{q}$ (l/min)	S_q (l/min)	CV_q (%)	$\bar{Q}$ ($x10^3$l)	S_Q ($x10^3$l)	CV_Q (%)
A	0.05	0.00	33.592			17.658		
B	0.05	0.25	34.360	0.423	1.231	17.928	0.246	1.430
C	0.10	0.00	44.508			25.895		
D	0.10	0.25	46.160	0.512	1.110	26.205	0.317	1.211
E	0.10	0.50	46.259	0.231	0.500	26.489	0.456	1.723
F	0.10	1.00	47.334	0.498	1.051	27.081	0.669	2.469
G	0.20	0.00	56.459			36.360		
H	0.20	0.25	57.105	0.447	0.783	36.811	0.414	1.126
I	0.20	0.50	57.643	0.666	1.156	37.225	0.600	1.612

Table 4.2 A comparison of cases (A-F) showing the effect of hydraulic conductivity distribution on the total flow hydrograph

CASE	μ_Y (cm/min)	σ_Y^2	PEAK FLOW			VOLUMETRIC FLOW		
			$\bar{q}$ (l/min)	S_q (l/min)	CV_q (%)	$\bar{Q}$ ($x10^3$l)	S_Q ($x10^3$l)	CV_Q (%)
A	0.05	0.00	73.593			19.772		
B	0.05	0.25	74.163	0.480	0.648	20.019	0.159	0.785
C	0.10	0.00	44.508			25.895		
D	0.10	0.25	50.539	1.994	3.945	26.252	0.299	1.139
E	0.10	0.50	51.119	2.423	4.739	26.544	0.434	1.635
F	0.10	1.00	51.816	2.108	4.068	27.147	0.645	2.377

with the corresponding results for the uniform cases in table 4.1 suggests that spatial variability has little effect on subsurface flow generation in an uncorrelated media. The net effect in all cases is increasing peak and volumetric flows with increasing variability.

By referring to tables 4.1 and 4.2 it can be seen that the sensitivity of total flow to σ_Y^2 is dependent on the mean hydraulic conductivity (μ_Y). In particular, the peak total flow of the nonuniform cases D, E and F are significantly greater than the respective value for the uniform case C. This is due to the fact that for the event selected, a hydraulic conductivity of 0.1 cm/min is just greater than a threshold value for a uniform homogeneous media. Below this threshold, surface saturation occurs and overland flow is generated (as in case A).

Figure 4.11 shows the range of subsurface flow hydrographs for case E. It is clear from this diagram that there is little difference between the results of the ten realizations at any given time. This is further demonstrated in figure 4.12 which shows the changes in the coefficient of variation of total flow with time. It can be seen from this diagram that during the two drying periods, the coefficient of variation is roughly constant, this is in agreement with the findings of El-Kadi and Brutsaert (1985) in their study of aquifer drainage. After the onset of rainfall at t = 5 hours, CV_q increases slightly due to the variations in the response times of the ten realizations. After a steady decrease, a sharp peak in CV_q is produced just before the cessation of rainfall at t = 13 hours. This dramatic increase in CV_q is caused by the onset of surface saturation and hence overland flow for several of the realizations.

The results of five experiments on correlated media are presented in tables 4.3 and 4.4. For all cases, the autocorrelation parameters (see section 4.2.2) are, α = 1.0 and

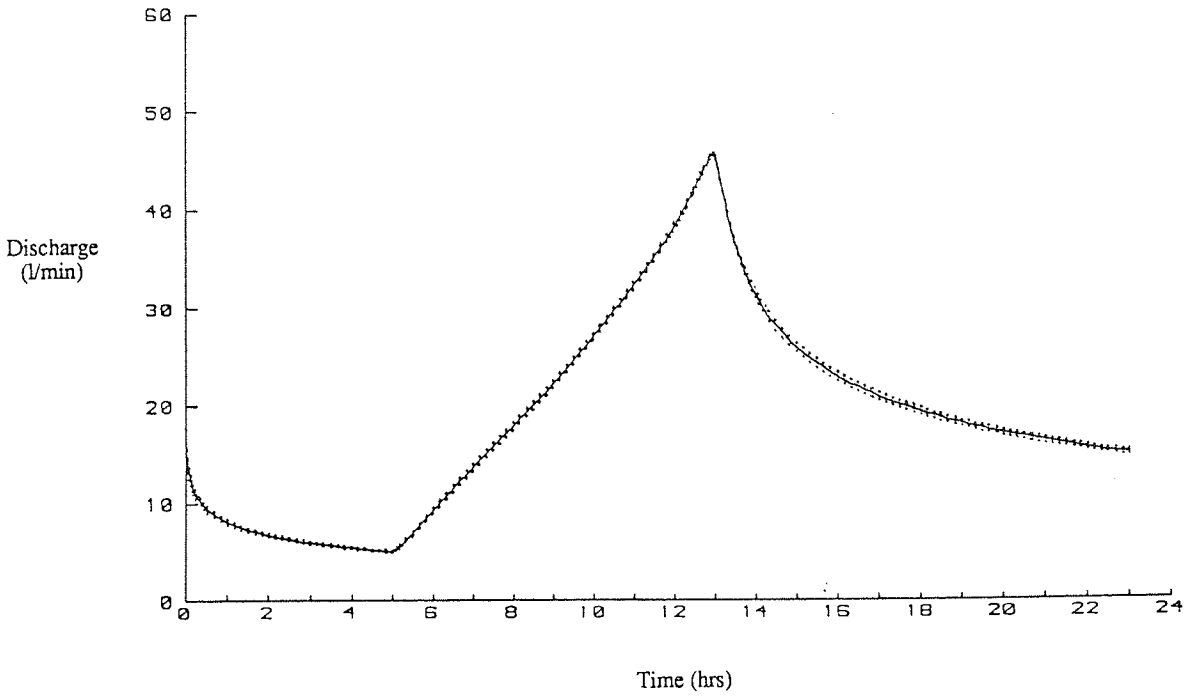

Figure 4.11 Range of subsurface flow hydrographs for case E. Solid line indicates mean hydrograph, dotted line indicates mean ± one standard deviation.

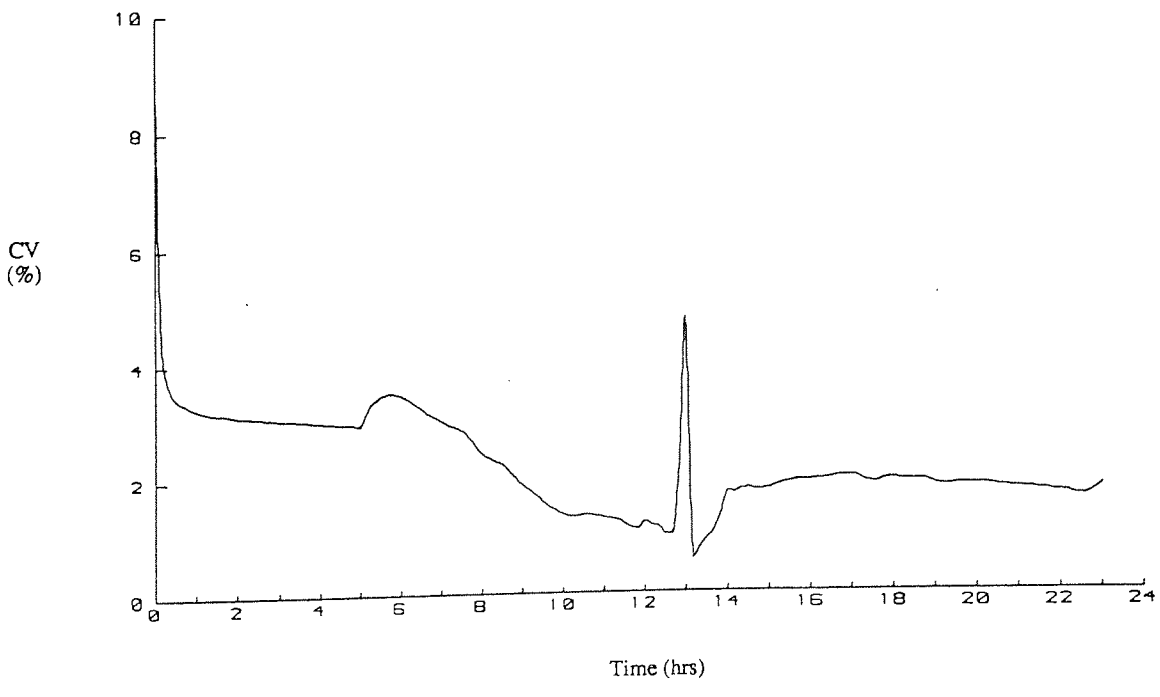

Figure 4.12 Change in the coefficient of variation of total flow with time for case E.

$\rho_{xy}(10m) = 0.7$. Cases J, K, M and N refer to conductivity fields where $\rho_z(0.1m) =$ 0.8. Case L has a greater autocorrelation in the vertical axis ($\rho_z(0.5m) = 0.8$).

A comparison of the peak and volumetric flows for correlated and uncorrelated media suggests that the mean values of ten realizations are less sensitive to the extent of correlation than to the amount of variability. For example, referring to table 4.1, a 100 per cent change in σ_Y (cases D and F) produces a 2.5 per cent change in the peak subsurface flow, whereas, the difference between the same result for the highly correlated media of case J and the uncorrelated soil of equal variance (case D) is only 0.5 per cent. The influence of the degree of correlation on mean flows is also demonstrated by comparing the results of Case K within the greater correlated Case L.

The hydrograph variance of the ten realizations is significantly increased for the correlated cases. A comparison of tables 4.1 and 4.3 shows that the coefficients of variation of subsurface flow (CV_q and CV_Q) differ by nearly an order of magnitude. The range of subsurface flow hydrographs can be seen in figures 4.13 and 4.14 for cases K and N respectively. The total flow hydrograph range for case K is also shown in figure 4.15. The sensitivity of runoff variation to the extent of autocorrelation is due to the fact that areas at the base of the hillslope make a greater contribution to the overall response than do upslope regions. Since in a highly correlated media one may expect to find a large region of the base of the slope displaying soils of low (or high) conductivity, the entire hillslope will behave similar to a homogeneous hillslope of low (or high) permeability. Therefore, several realizations of soil variability will include a wider range of responses with increasing autocorrelation of soil properties. As the degree of correlation decreases, the effect of variability is averaged out, as shown by the results in tables 4.1 and 4.2.

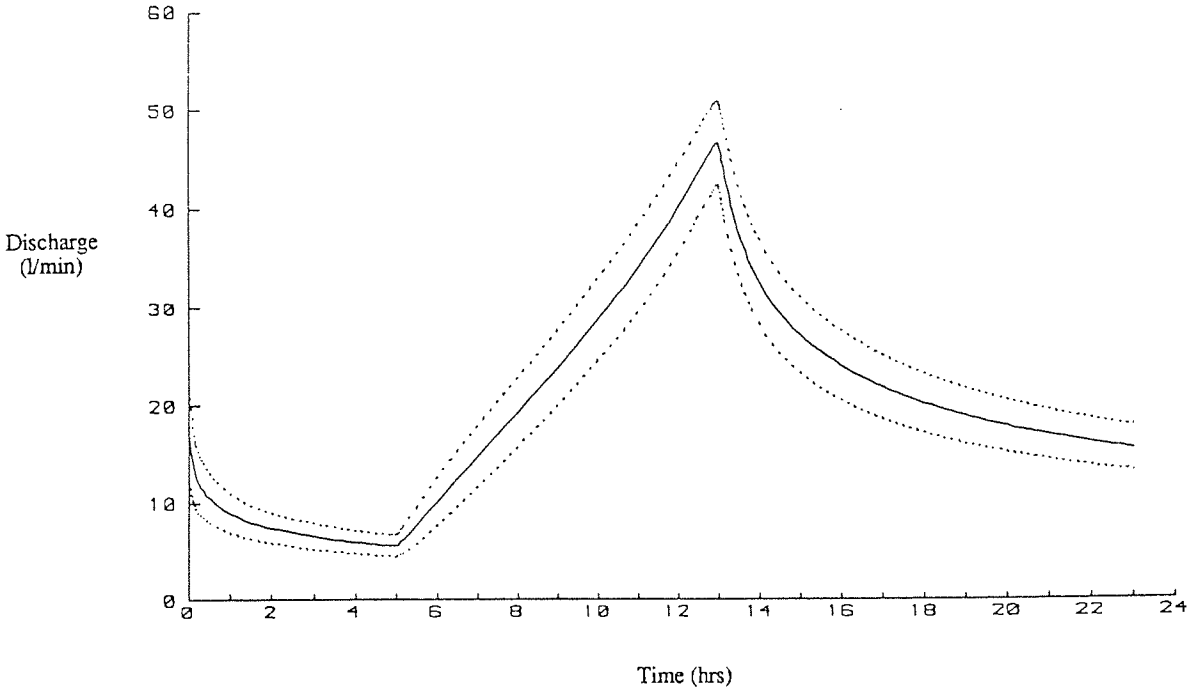

Figure 4.13 Range of subsurface flow hydrographs for case K. Solid line indicates mean hydrograph, dotted line indicates mean ± one standard deviation.

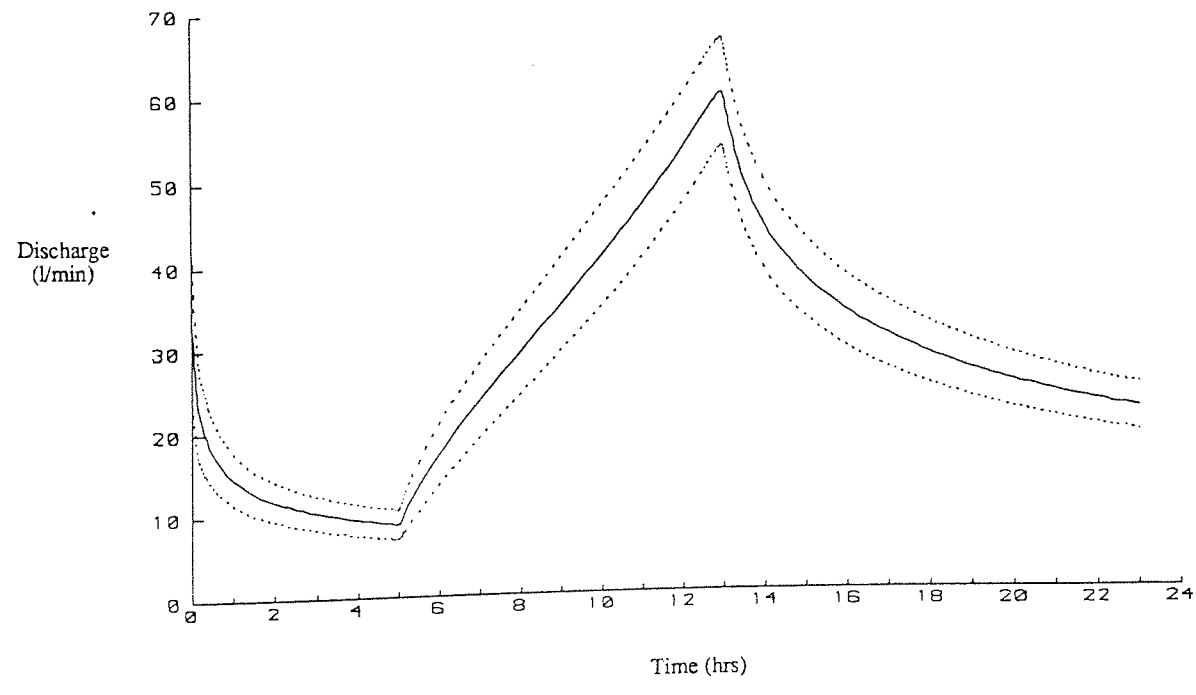

Figure 4.14 Range of subsurface flow hydrographs for case N. Solid line indicates mean hydrograph, dotted line indicates mean ± one standard deviation.

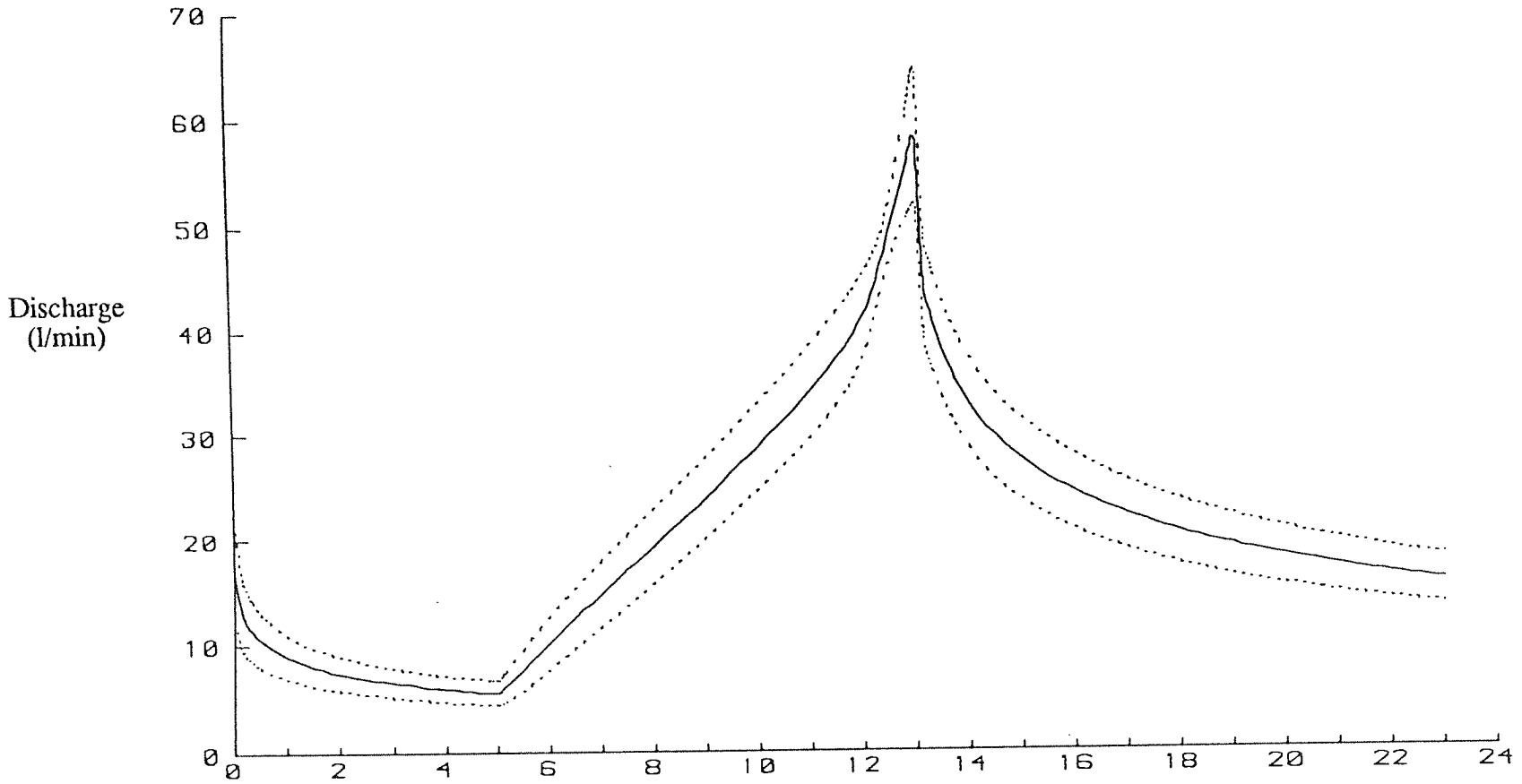

Figure 4.15 Range of total flow hydrographs for case K. Solid line indicates mean hydrograph, dotted line indicates mean ± one standard deviation.

Table 4.3 A comparison of cases (J-N) showing the effect of hydraulic conductivity distribution on the subsurface flow hydrograph

CASE	μ_Y (cm/min)	σ_Y^2	PEAK FLOW			VOLUMETRIC FLOW		
			$\bar{q}$ (l/min)	S_q (l/min)	CV_q (%)	$\bar{Q}$ ($x10^3$l)	S_Q ($x10^3$l)	CV_Q (%)
J	0.10	0.25	46.405	2.786	6.003	26.977	2.868	10.632
K	0.10	0.50	47.304	4.316	9.124	27.888	4.187	15.014
L	0.10	0.50	46.928	5.537	11.798	27.596	4.860	17.613
M	0.20	0.25	58.300	4.268	7.320	38.001	3.912	10.294
N	0.20	0.50	59.987	6.437	10.731	39.274	5.682	14.468

Table 4.4 A comparison of cases (J-N) showing the effect of hydraulic conductivity distribution on the total flow hydrograph

CASE	μ_Y (cm/min)	σ_Y^2	PEAK FLOW			VOLUMETRIC FLOW		
			$\bar{q}$ (l/min)	S_q (l/min)	CV_q (%)	$\bar{Q}$ ($x10^3$l)	S_Q ($x10^3$l)	CV_Q (%)
J	0.10	0.25	56.871	6.794	11.946	27.248	2.642	9.695
K	0.10	0.50	58.431	6.307	10.794	28.250	3.888	13.763
L	0.10	0.50	61.332	5.460	8.902	28.131	4.441	15.785
M	0.20	0.25	58.400	4.212	7.212	38.002	3.911	10.292
N	0.20	0.50	60.542	6.134	10.133	39.286	5.674	14.442

The effect of soil variability on pressure head distribution is shown in figures 4.16 and 4.17. Figure 4.16 is a contour map of the mean pressure head ($\bar{\psi}$) at the soil surface for case E, averaged over the ten realizations, at the end of the rainfall period (t = 13 hours). Figure 4.17 is the corresponding map for the correlated case K. Both maps show little difference from the uniform homogeneous result (figure 4.18), the uncorrelated case being closest in agreement. The majority of fluctuations along contour lines in figures 4.16 and 4.17 and indeed those presented in the remainder of this study, would be expected to diminish if the number of realizations were increased, and the finite element mesh were made finer (allowing much smoother transitions for the contouring routine).

The variability of head, expressed as the standard deviation (S_ψ) is shown in figure 4.19 for case K at time t = 13 hours. It was noticed that this variability changed considerably throughout the event. At the end of the 10 hour drainage period (t = 23 hours), S_ψ was calculated to be less than 4.0 cm at any point more than 20 metres away from the base of the slope. The variation in $\bar{\psi}$ over the soil surface for the same case at time t = 23 hours is shown in figure 4.20, which is virtually identical to the corresponding map for the uniform field (figure 4.21).

Figure 4.22 shows the variation of pressure head, at a constant depth of 20 cm from the soil surface, at the end of the storm, for a single realization from case E. The equivalent diagram for a single realization from the correlated case K is shown in figure 4.23. As expected, there is a significant difference between the two results. The equipotentials of the uncorrelated field generally appear as random fluctuations from parallel lines, whereas the effect of large areas of low hydraulic conductivity resisting water movement can be seen in the corresponding diagram for the correlated field (figure 4.23).

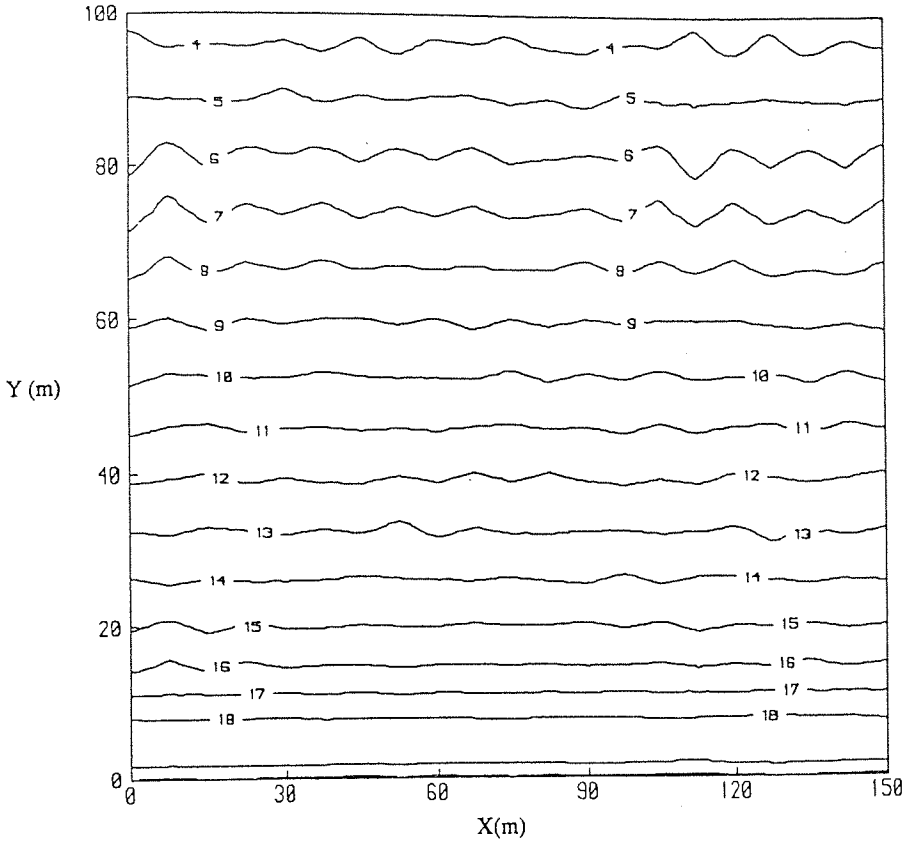

CONTOUR KEY	
1	-450.00
2	-425.00
3	-400.00
4	-375.00
5	-350.00
6	-325.00
7	-300.00
8	-275.00
9	-250.00
10	-225.00
11	-200.00
12	-175.00
13	-150.00
14	-125.00
15	-100.00
16	-75.00
17	-50.00
18	-25.00
19	0.00
20	25.00
21	50.00

Figure 4.16 Variation of $\bar{\psi}$ in cm over the soil surface for case E at time t = 13 hours.

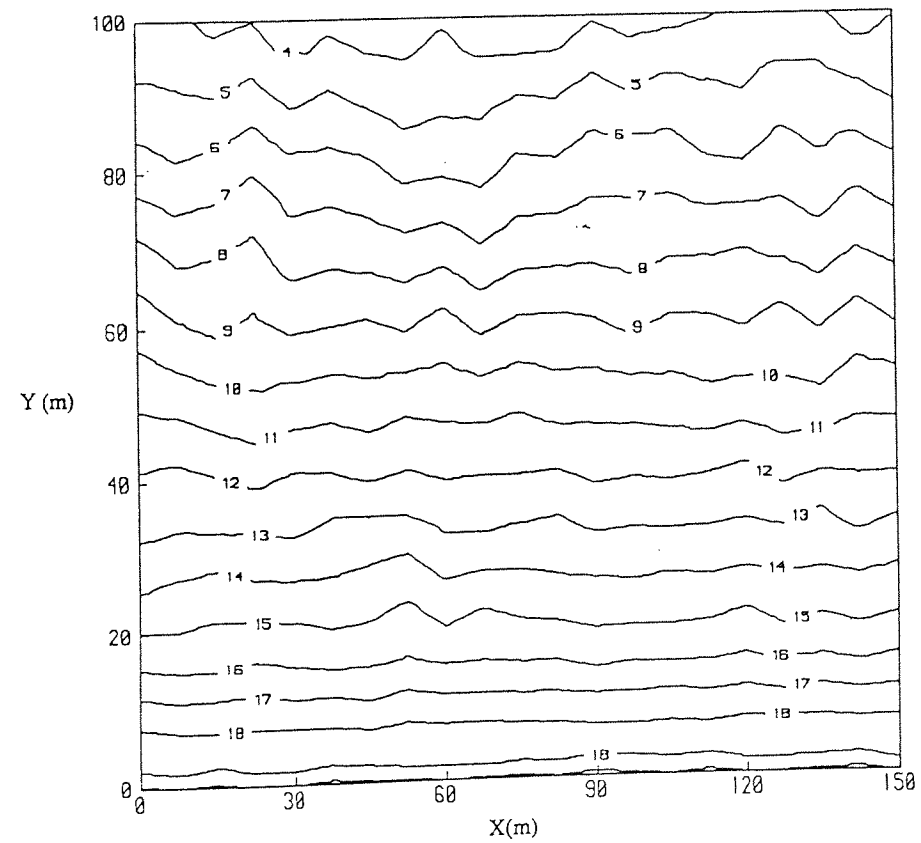

CONTOUR KEY	
1	-450.00
2	-425.00
3	-400.00
4	-375.00
5	-350.00
6	-325.00
7	-300.00
8	-275.00
9	-250.00
10	-225.00
11	-200.00
12	-175.00
13	-150.00
14	-125.00
15	-100.00
16	-75.00
17	-50.00
18	-25.00
19	0.00
20	25.00
21	50.00

Figure 4.17 Variation of $\bar{\psi}$ in cm over the soil surface for case K at time t = 13 hours.

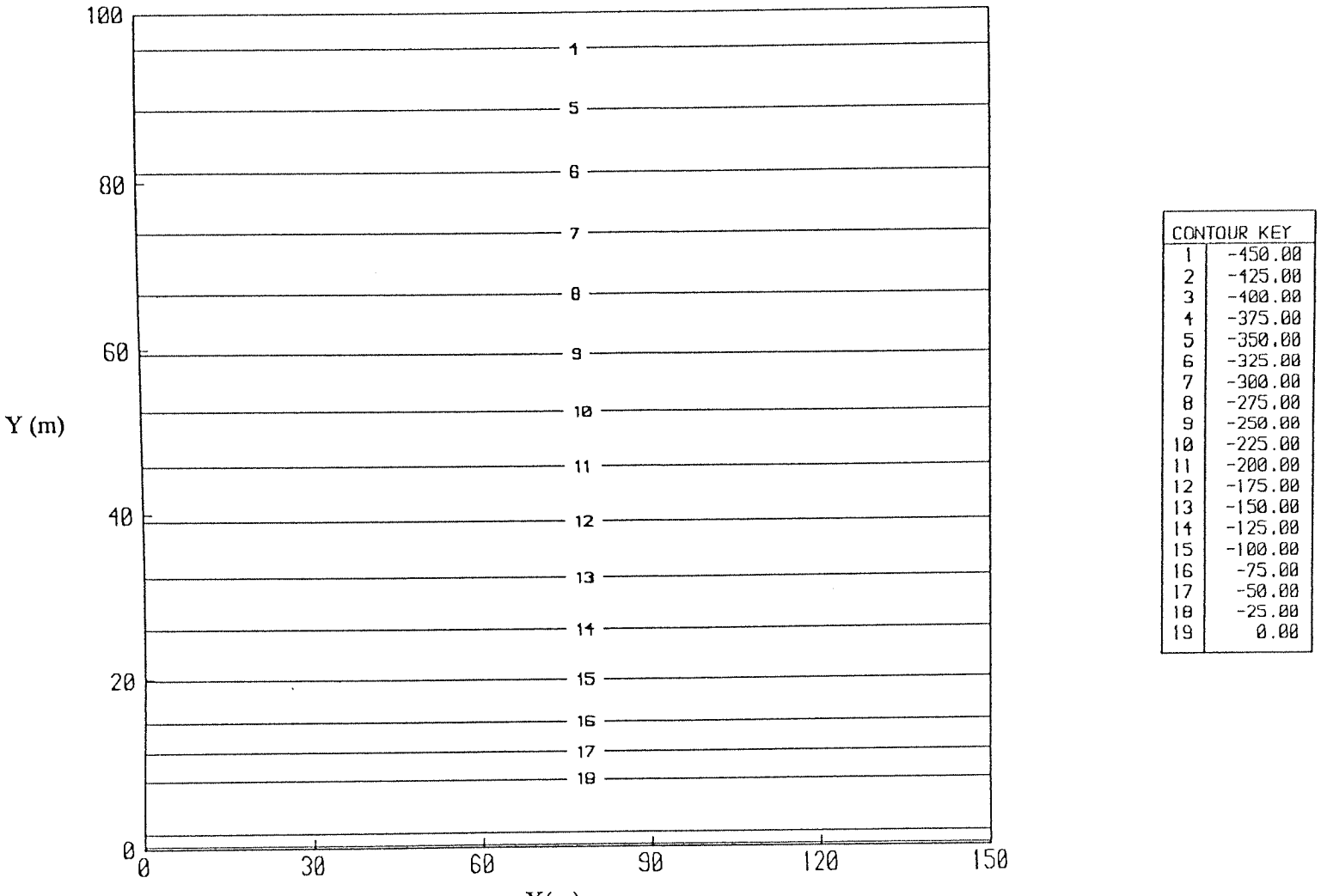

Figure 4.18 Variation of ϕ in cm over the soil surface for case C at time t = 13 hours.

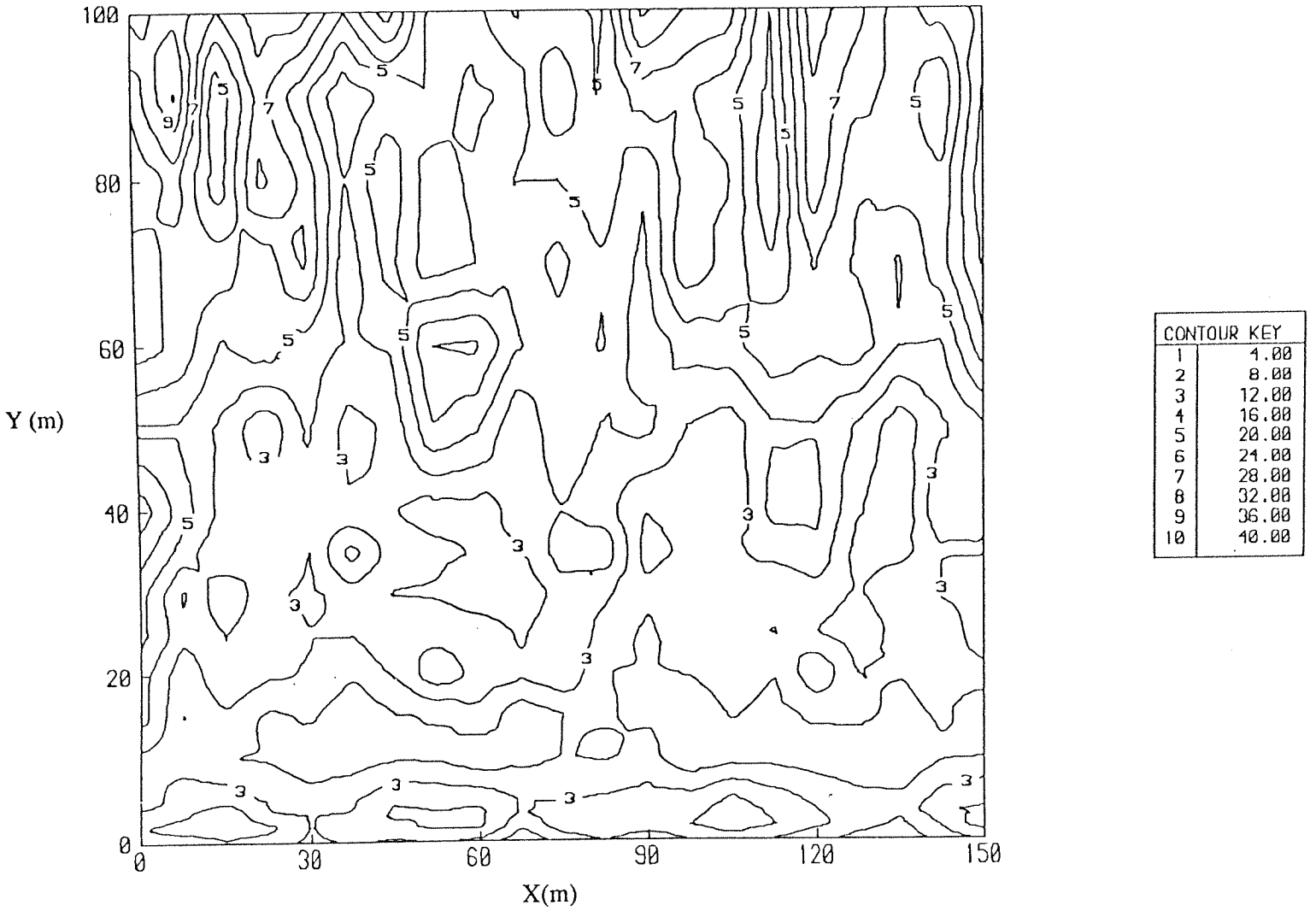

Figure 4.19 Variation of S_ψ in cm over the soil surface for case K at time t = 13 hours.

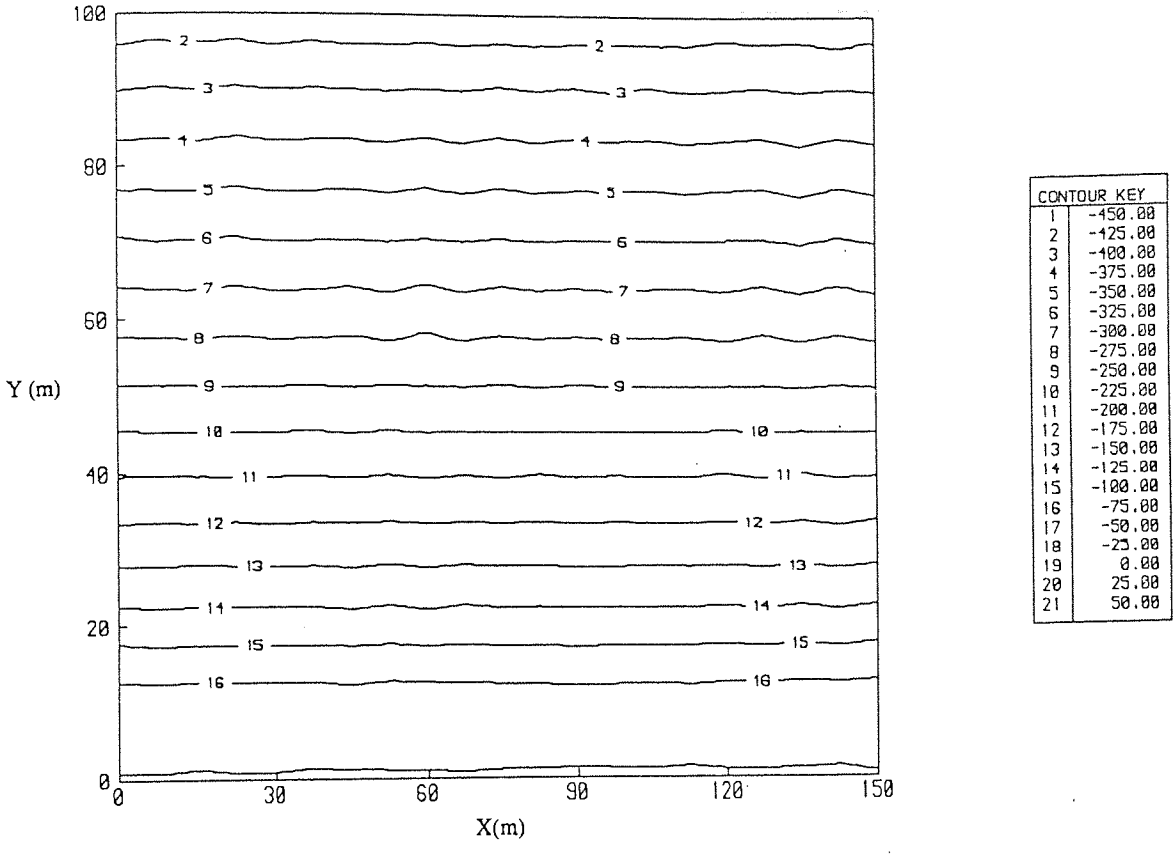

Figure 4.20 Variation of $\bar{\psi}$ in cm over the soil surface for case K at time t = 23 hours.

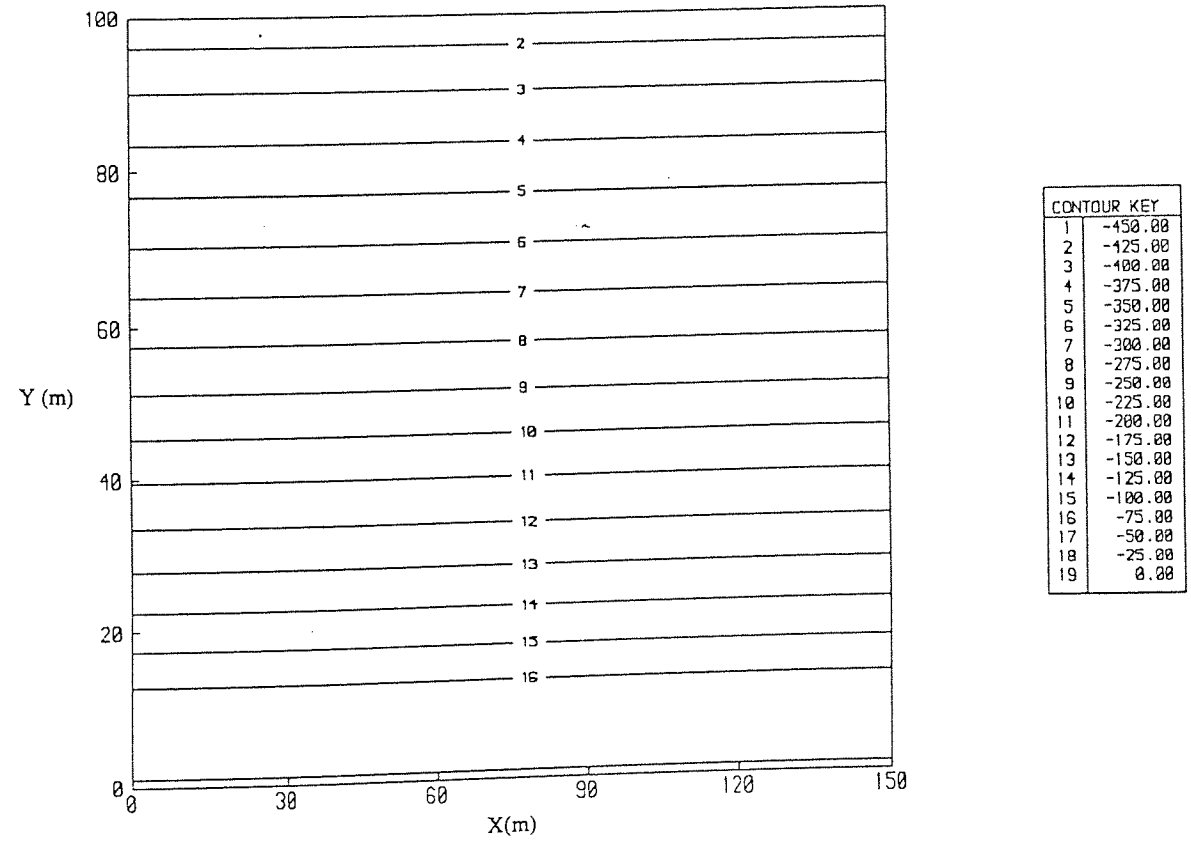

Figure 4.21 Variation of ψ in cm over the soil surface for case C at time t = 23 hours.

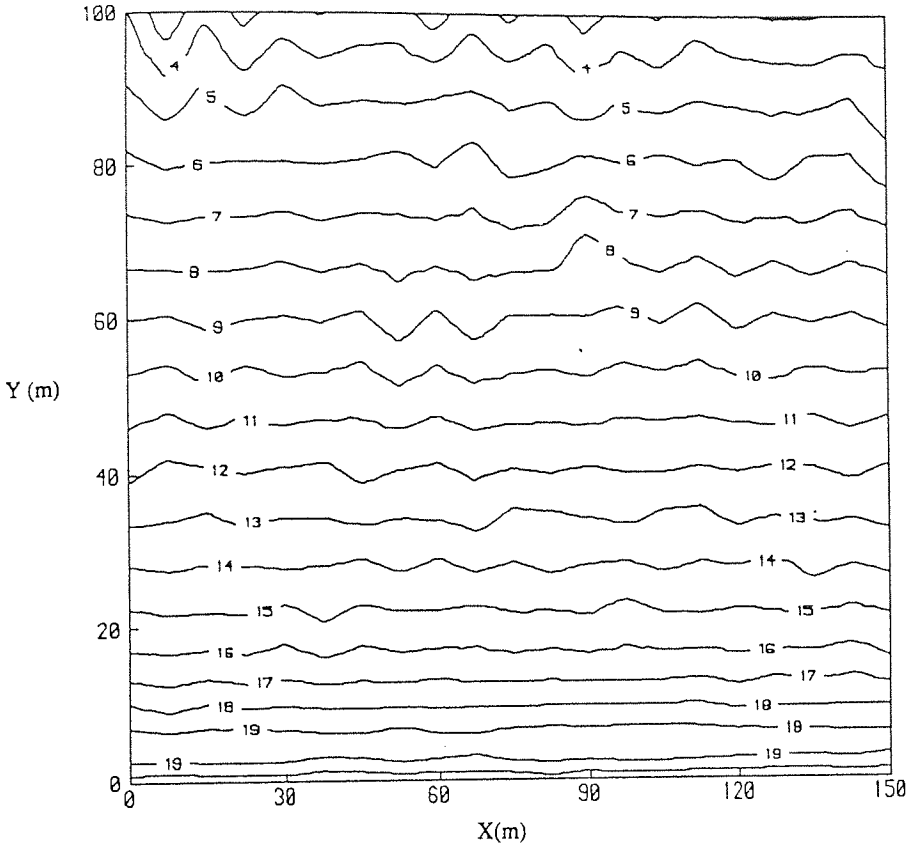

CONTOUR KEY	
1	-450.00
2	-425.00
3	-400.00
4	-375.00
5	-350.00
6	-325.00
7	-300.00
8	-275.00
9	-250.00
10	-225.00
11	-200.00
12	-175.00
13	-150.00
14	-125.00
15	-100.00
16	-75.00
17	-50.00
18	-25.00
19	0.00
20	25.00
21	50.00

Figure 4.22 Distribution of ψ in cm at a constant depth of 20 cm for a single realization from case E at time t = 13 hours.

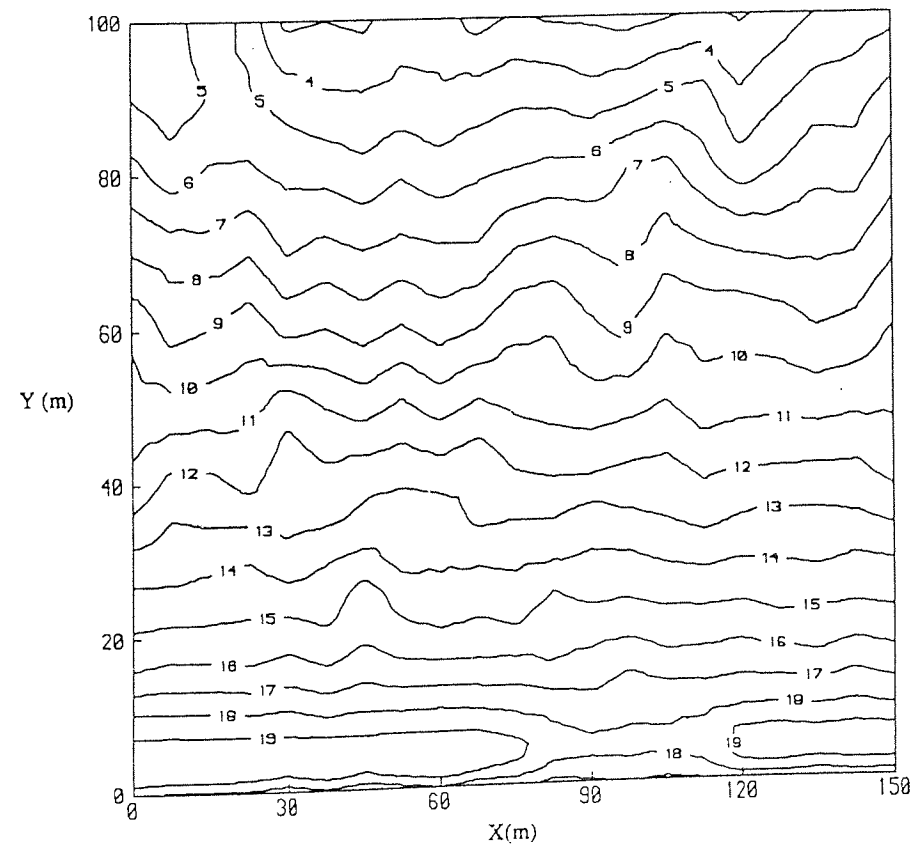

CONTOUR KEY	
1	-450.00
2	-425.00
3	-400.00
4	-375.00
5	-350.00
6	-325.00
7	-300.00
8	-275.00
9	-250.00
10	-225.00
11	-200.00
12	-175.00
13	-150.00
14	-125.00
15	-100.00
16	-75.00
17	-50.00
18	-25.00
19	0.00
20	25.00
21	50.00

Figure 4.23 Distribution of ψ in cm at a constant depth of 20 cm for a single realization from case K at time t = 13 hours.

4.2.4.2 Low permeability soils

In order to investigate the effect of spatial variability of hydraulic conductivity on runoff generation dominated by infiltration excess overland flow, five conductivity fields of different structure were defined (cases O, P, Q, R and S). All cases possess a mean conductivity of 0.005 cm/min (= 3/4 rainfall intensity). The results of the five cases are presented in tables 4.5 and 4.6. Cases P and Q are uncorrelated distributions, Cases R and S have a correlation structure identical to the high permeability fields J, K, M and N defined in 4.2.4.1.

It can be seen from these results that, as in the high permeability soils, increasing the variability of the soil has a general effect of increasing the average peak and volumetric flows. The autocorrelation of the soil also has the same effect as noted in 4.2.4.1, that is, increasing the amount of spatial correlation produces a result equivalent to increasing the variability of the soil. However, this effect is considerably greater for the low permeability soils. The spread of results, quantified by the values of CV_q and CV_Q in tables 4.5 and 4.6 are also substantially greater than those reported earlier. Taking the results of Cases H, I and M (μ_Y = 0.2 cm/min) from tables 4.1 and 4.4 for comparative purposes, a change in σ_Y^2 from 0.25 to 0.5 produces an increase in volume of total flow by 1.13 per cent. For the same mean conductivity, the increase in volume of total flow produced by the change from an uncorrelated to a correlated structure, of the same variance, is 3.24 per cent. The corresponding calculations for the low permeability soils in table 4.6 reveal increases by 7.91 per cent and 26.26 per cent respectively. That is, the sensitivity of total flow to spatial variability is seven times more for the low permeability soils. The higher sensitivity is due to the nature of the dominating runoff mechanism since in the case of infiltration excess overland flow, the variability of soil properties over the surface of the hillslope will control the extent of surface runoff,

Table 4.5 A comparison of cases (O-S) showing the effect of hydraulic conductivity distribution on the subsurface flow hydrograph

CASE	μ_Y (cm/min)	σ_Y^2	PEAK FLOW			VOLUMETRIC FLOW		
			$\bar{q}$ (l/min)	S_q (l/min)	CV_q (%)	$\bar{Q}$ ($x10^3$l)	S_Q ($x10^3$l)	CV_Q (%)
O	0.005	0.00	6.719			3.694		
P	0.005	0.25	6.827	0.192	2.818	3.700	0.100	2.712
Q	0.005	0.50	6.803	0.302	4.432	3.676	0.146	3.960
R	0.005	0.25	7.150	1.439	20.130	3.834	0.785	20.469
S	0.005	0.50	7.383	2.175	29.462	3.947	1.137	28.796

Table 4.6 A comparison of cases (O-S) showing the effect of hydraulic conductivity distribution on the total flow hydrograph

CASE	μ_Y (cm/min)	σ_Y^2	PEAK FLOW			VOLUMETRIC FLOW		
			$\bar{q}$ (l/min)	S_q (l/min)	CV_q (%)	$\bar{Q}$ ($x10^3$l)	S_Q ($x10^3$l)	CV_Q (%)
O	0.005	0.00	84.810			14.721		
P	0.005	0.25	88.896	3.519	3.959	15.934	0.471	2.954
Q	0.005	0.50	91.573	3.203	3.506	17.195	0.566	3.289
R	0.005	0.25	104.703	17.086	16.318	20.118	4.096	20.362
S	0.005	0.50	121.187	26.444	21.821	24.873	6.670	26.817

although the finite size of the soil blocks, used in studies such as this, leads to an over emphasis of the importance of surface soil variability. Also, since subsurface flow is directly affected by the restriction of soil water recharge from the surface, then both surface and subsurface flows are, to some extent, controlled by two dimensional variability, thus the averaging out effect noted in the case of high permeability soils is less apparent.

The range of total flow hydrographs produced for cases Q and S are shown in figures 4.25 and 4.26 (note the change of vertical scale in figure 4.26). The effect of variability can be seen by comparing these hydrographs with the result from the uniform case O (figure 4.24).

It is worth noting that in all of the previously presented hydrographs there appears to be little if any time delay after the cessation of rainfall to the peak of subsurface flow, even for soils of very low saturated hydraulic conductivities. For the soil properties used herein, a significant time delay was not evident for hydraulic conductivities greater than 0.001 cm/min. The effect of soil-water properties, such as porosity, on subsurface flow peak time delays is discussed in Beven (1975).

The time dependence of the coefficient of variation of subsurface flow for case S is shown in figure 4.27. As with the high permeability soils, CV_q gradually decreases during the drainage periods, in fact $d(CV_q)/dt$ appears virtually constant during the drying stages and equal for the two periods. After an average time delay of 2.5 hours from the beginning of the storm to the onset of subsurface flow, CV_q rises to maximum at about t = 9 hours, which characterizes the average time at which the water table has risen to the soil surface at the base of the slope. Any return flow produced by this surface saturation is routed as overland flow, the subsurface flow hydrograph therefore reaches a limiting value and thus CV_q decreases with time.

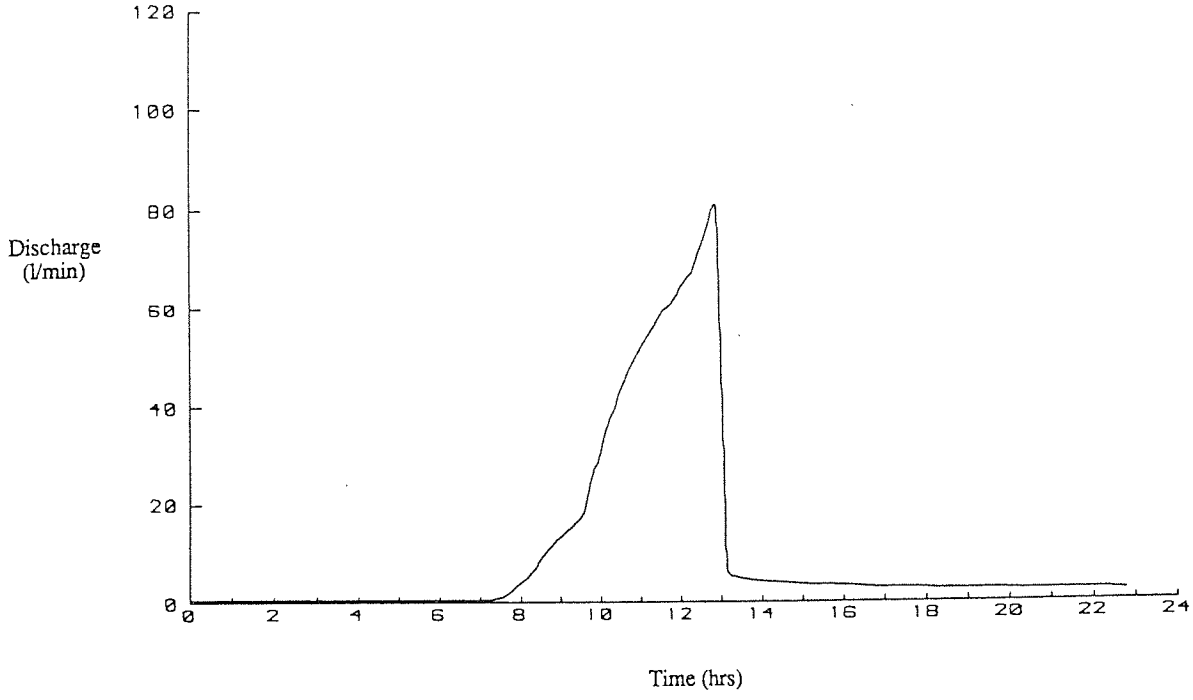

Figure 4.24 Total flow hydrograph for case O.

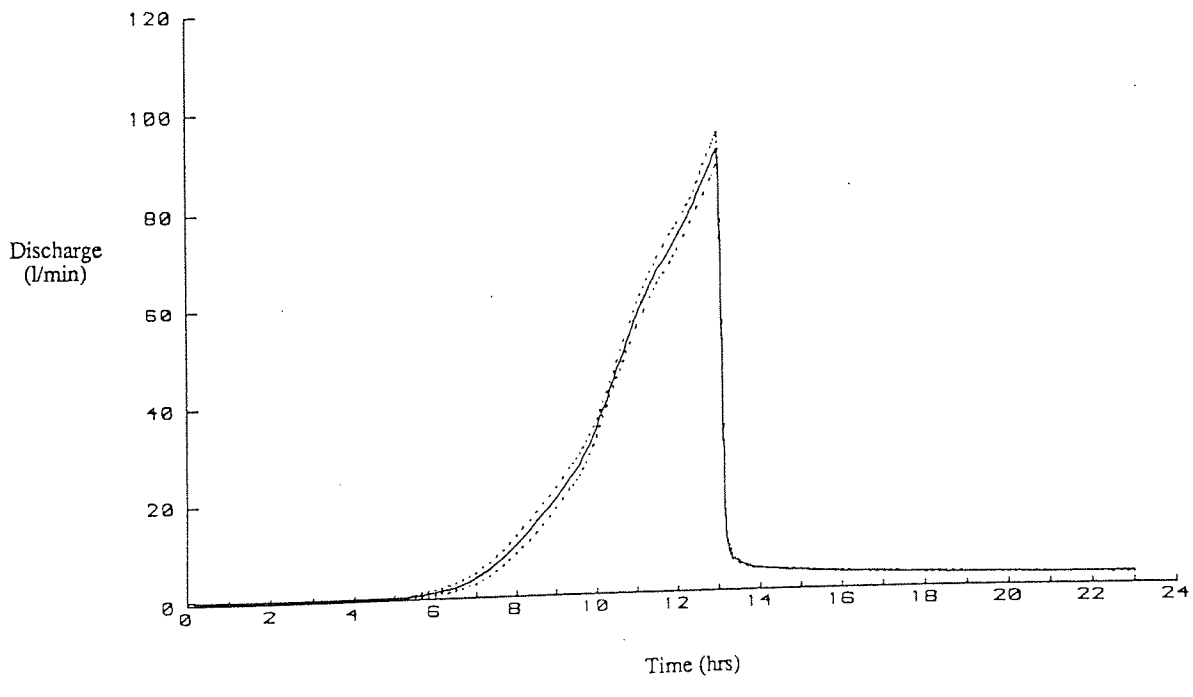

Figure 4.25 Range of total flow hydrographs for case Q. Solid line indicates mean hydrograph, dotted line indicates mean ± one standard deviation.

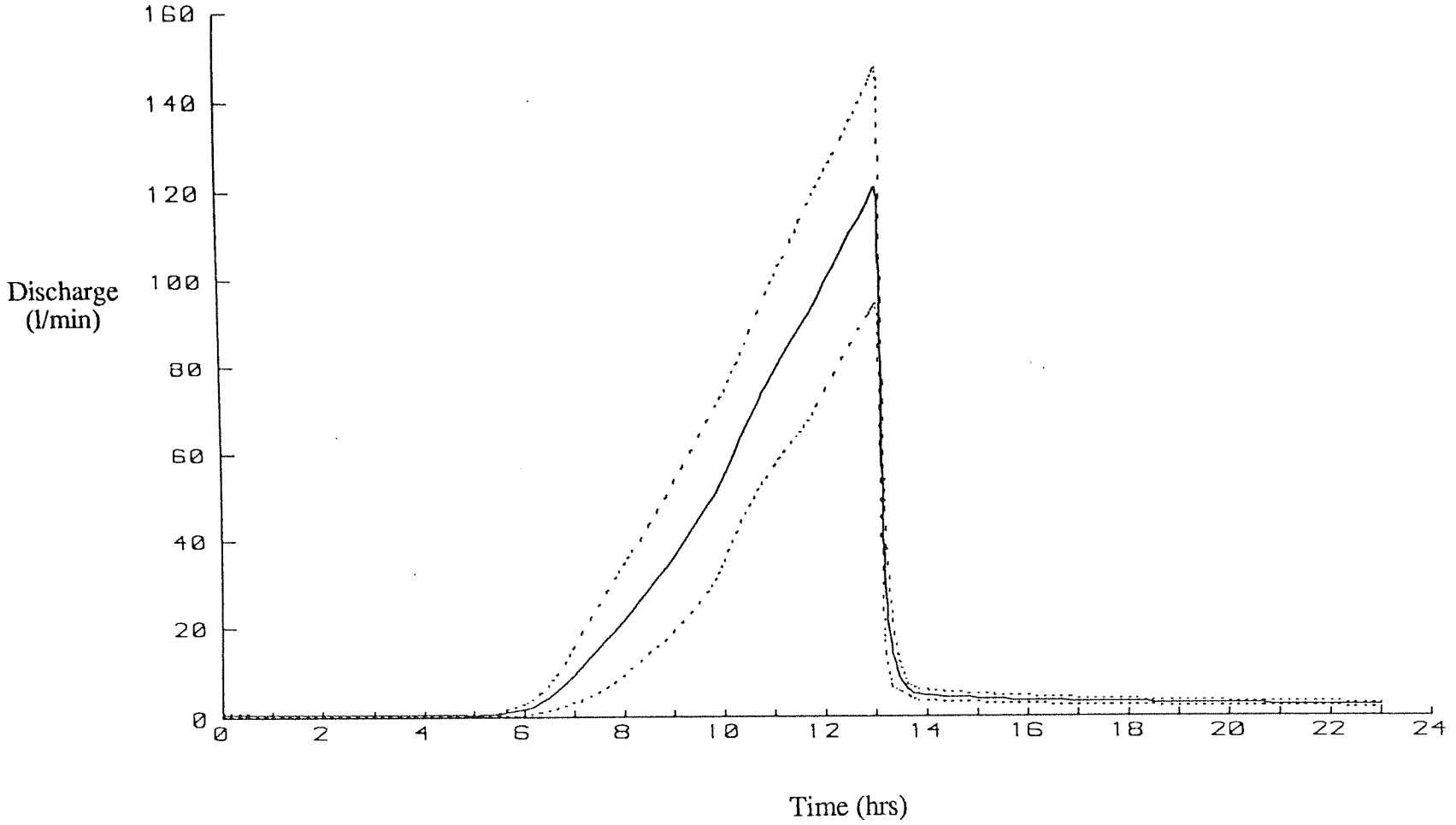

Figure 4.26 Range of total flow hydrographs for case S. Solid line indicates mean hydrograph, dotted line indicates mean ± one standard deviation.

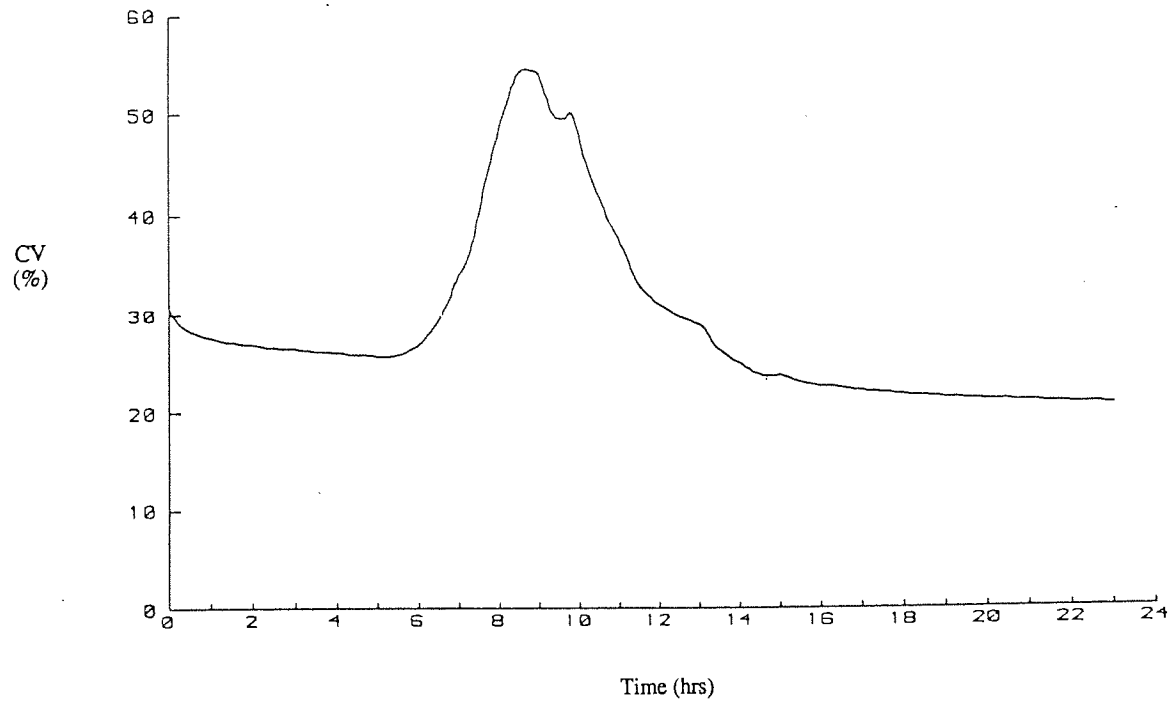

Figure 4.27 Change in the coefficient of variation of subsurface flow with time for case S.

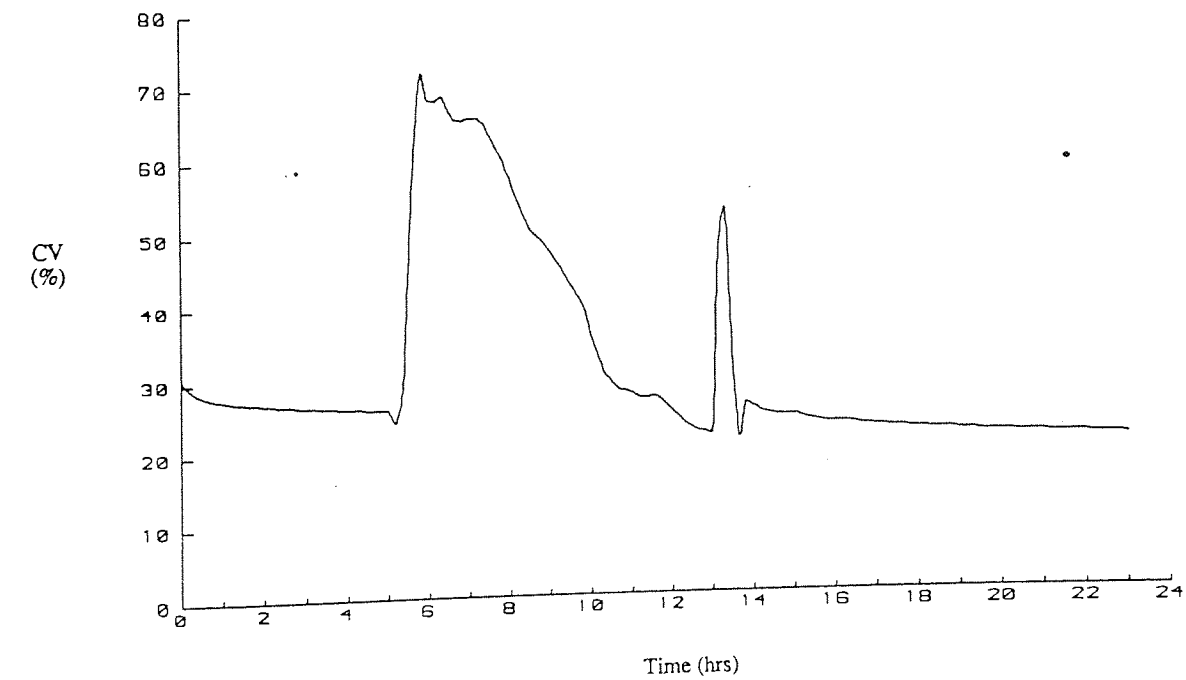

Figure 4.28 Change in the coefficient of variation of total flow with time for case S.

Figure 4.28 shows the variation of CV_q for total flow with time. The onset of overland flow can be seen clearly to occur at about t = 6 hours. The sharp peak at approximately t = 13.5 hours indicates the variation in the recession of the hydrographs at the end of the storm.

The variation of S_ψ over the soils surface for case S at the end of the rainfall period is shown in figure 4.29. The values are approximately double those presented in figure 4.19 for the high permeability case K. The difference between the coefficient of variation of pressure head (CV_ψ) for the two cases is greater still since the soil surface is much drier in the high permeability soils.

The variation of pressure head at a depth of 20 cm from the soils surface at t = 13 hours for a single realization of case Q (uncorrelated) is presented in figure 4.31, figure 4.30 is the corresponding diagram for the uniform case O. The effect of spatial variability is more striking that that noted for the high permeability soils (cf. figure 4.22).

The effect of spatial variability on pressure head contours at various depths for an individual realization from the correlated case S can be seen in figures 4.32 to 4.34.

The significant variations in ψ at the soils surface (figure 4.34) showing distinct local peaks of high suction, becomes less apparent at greater depths. At a depth of 64 cm (figure 4.32) the equipotentials show gradual trends, caused by the correlated structure of the soil. A comparison of figure 4.34 and the corresponding diagram for the uniform field (figure 4.35) demonstrates clearly two completely different responses of the same event.

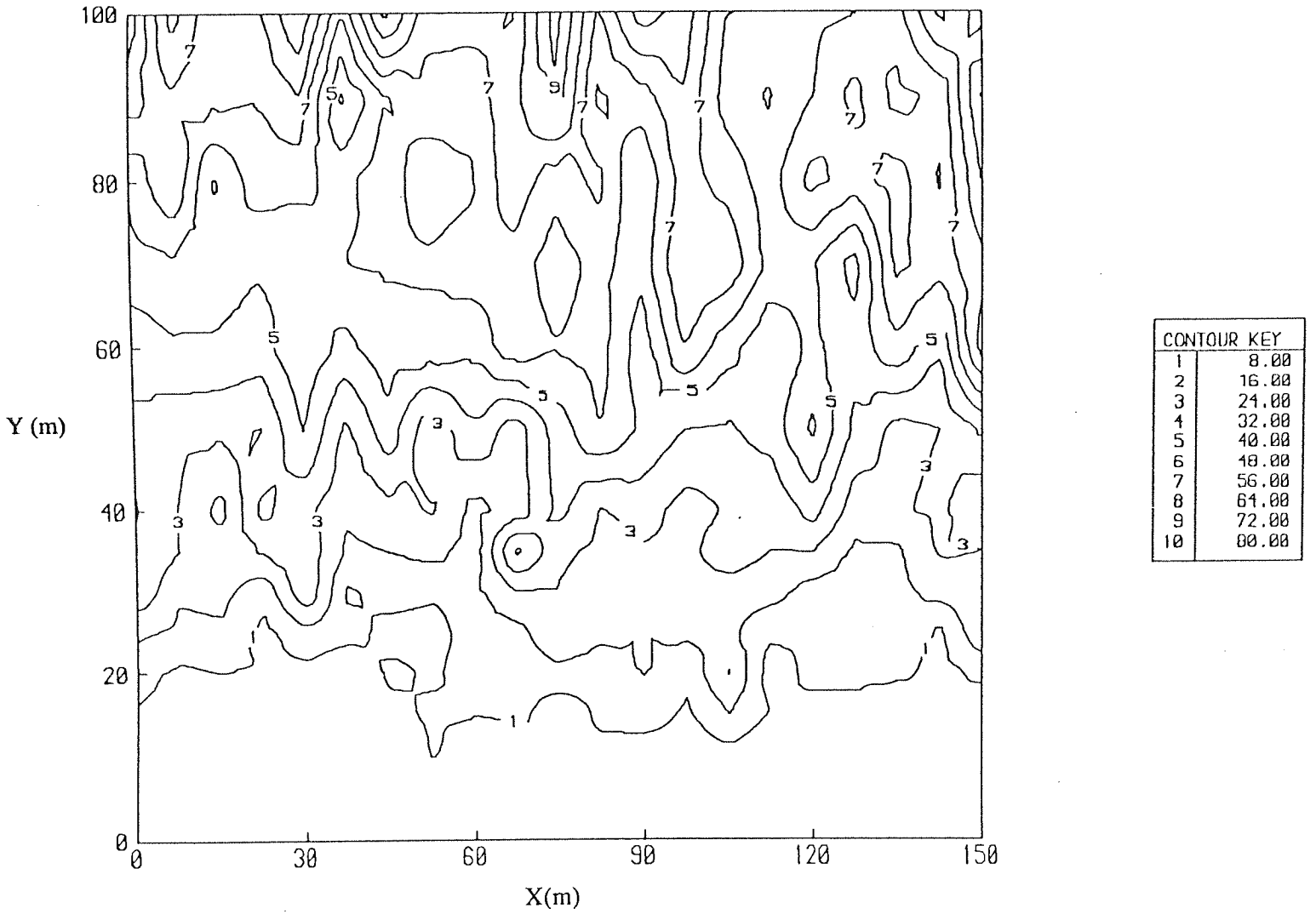

Figure 4.29 Variation of S_{ψ} in cm over the soil surface for case S at time t = 13 hours.

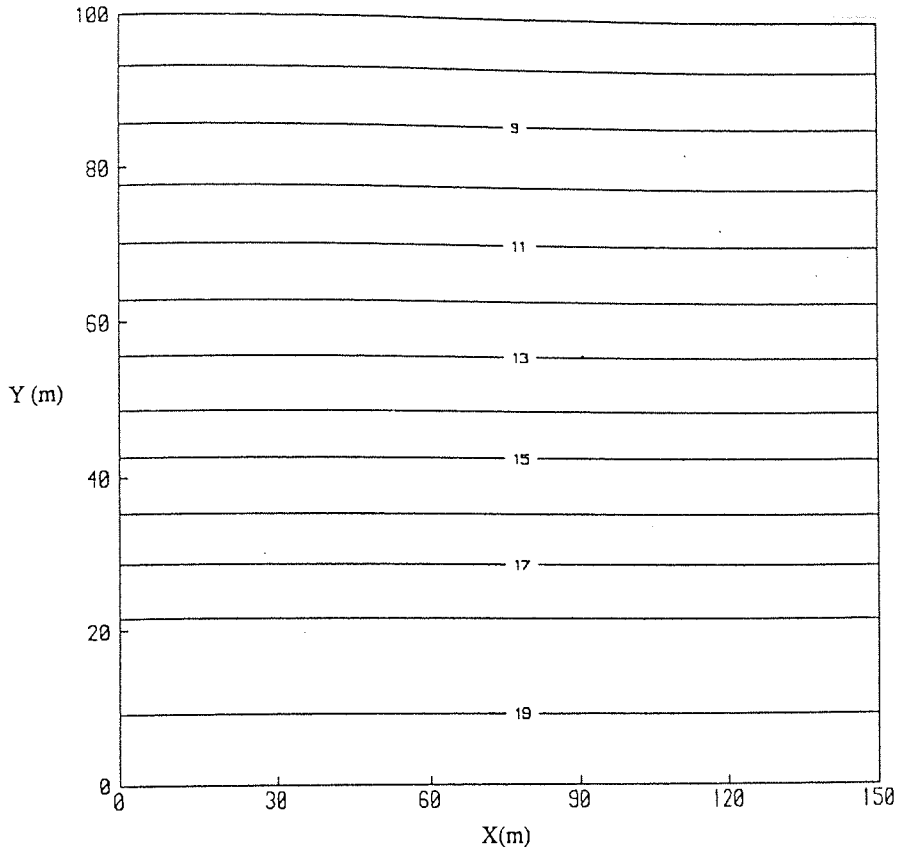

CONTOUR KEY	
1	-450.00
2	-425.00
3	-400.00
4	-375.00
5	-350.00
6	-325.00
7	-300.00
8	-275.00
9	-250.00
10	-225.00
11	-200.00
12	-175.00
13	-150.00
14	-125.00
15	-100.00
16	-75.00
17	-50.00
18	-25.00
19	0.00
20	25.00
21	50.00

Figure 4.30 Distribution of ψ in cm at a constant depth of 20 cm for a single realization from case O at time t = 13 hours.

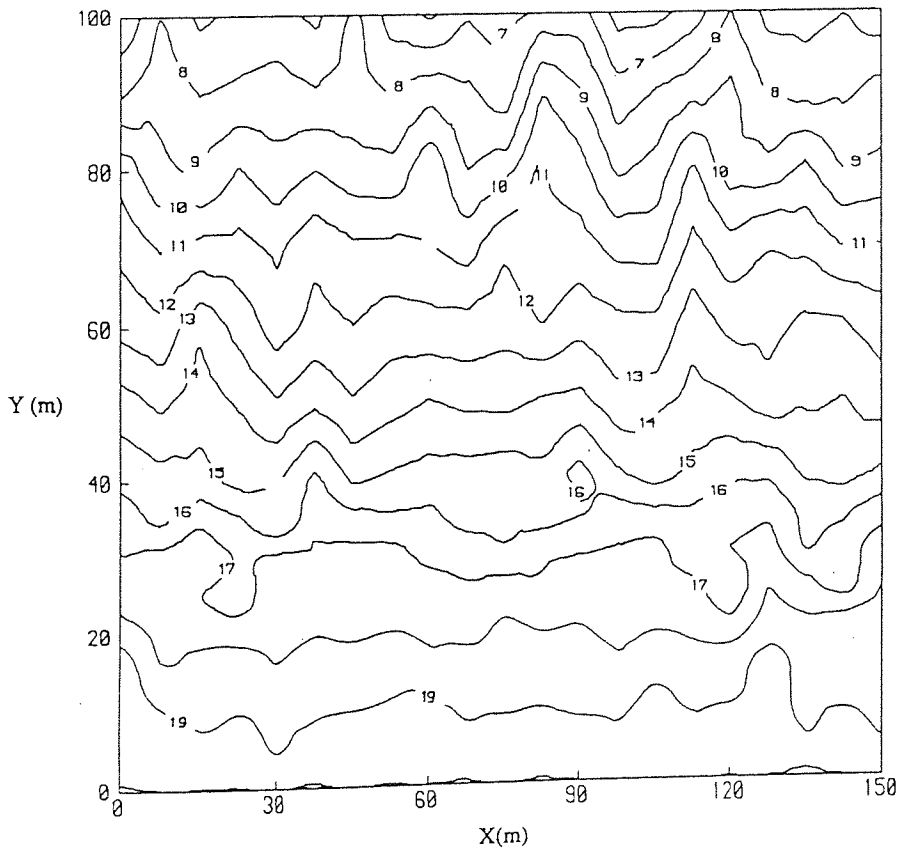

CONTOUR KEY	
1	-450.00
2	-425.00
3	-400.00
4	-375.00
5	-350.00
6	-325.00
7	-300.00
8	-275.00
9	-250.00
10	-225.00
11	-200.00
12	-175.00
13	-150.00
14	-125.00
15	-100.00
16	-75.00
17	-50.00
18	-25.00
19	0.00
20	25.00
21	50.00

Figure 4.31 Distribution of ψ in cm at a constant depth of 20 cm for a single realization from case Q at time t = 13 hours.

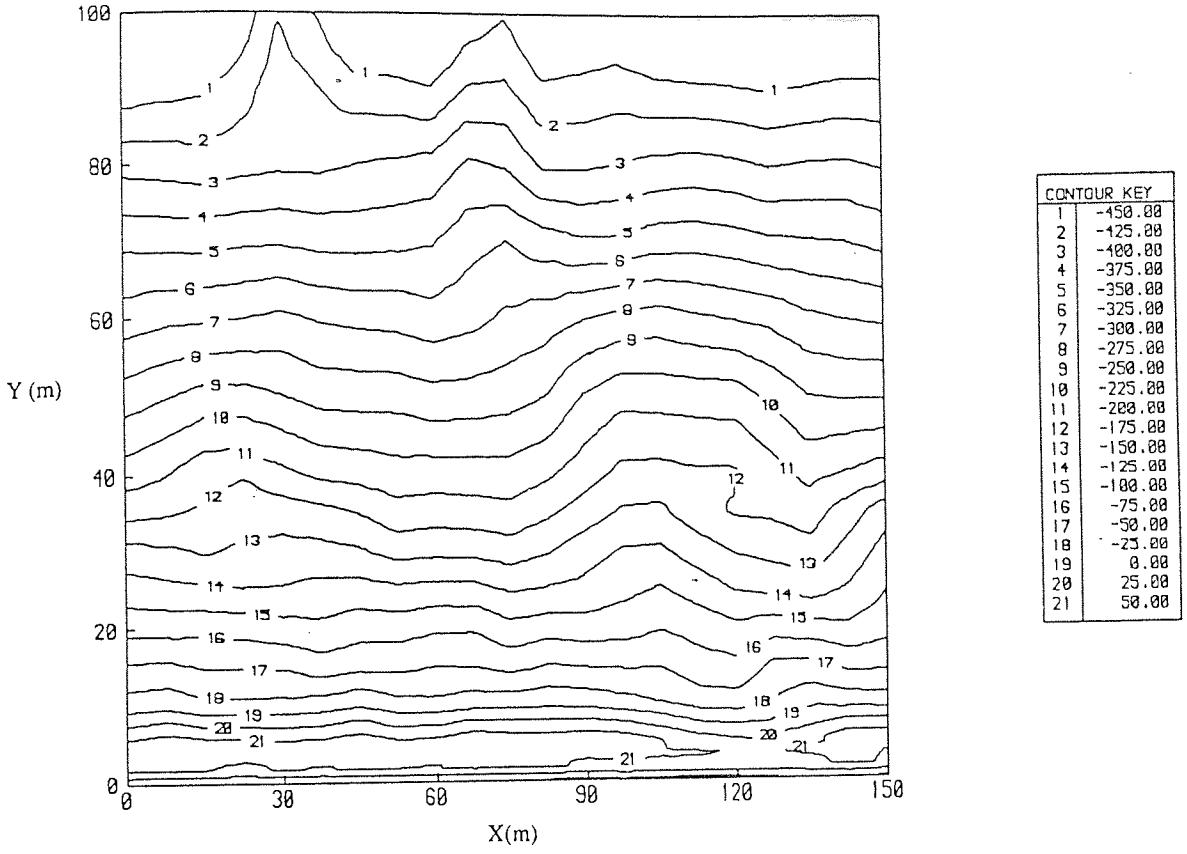

Figure 4.32 Distribution of ϕ in cm at a constant depth of 64 cm for a single realization from case S at time t = 13 hours.

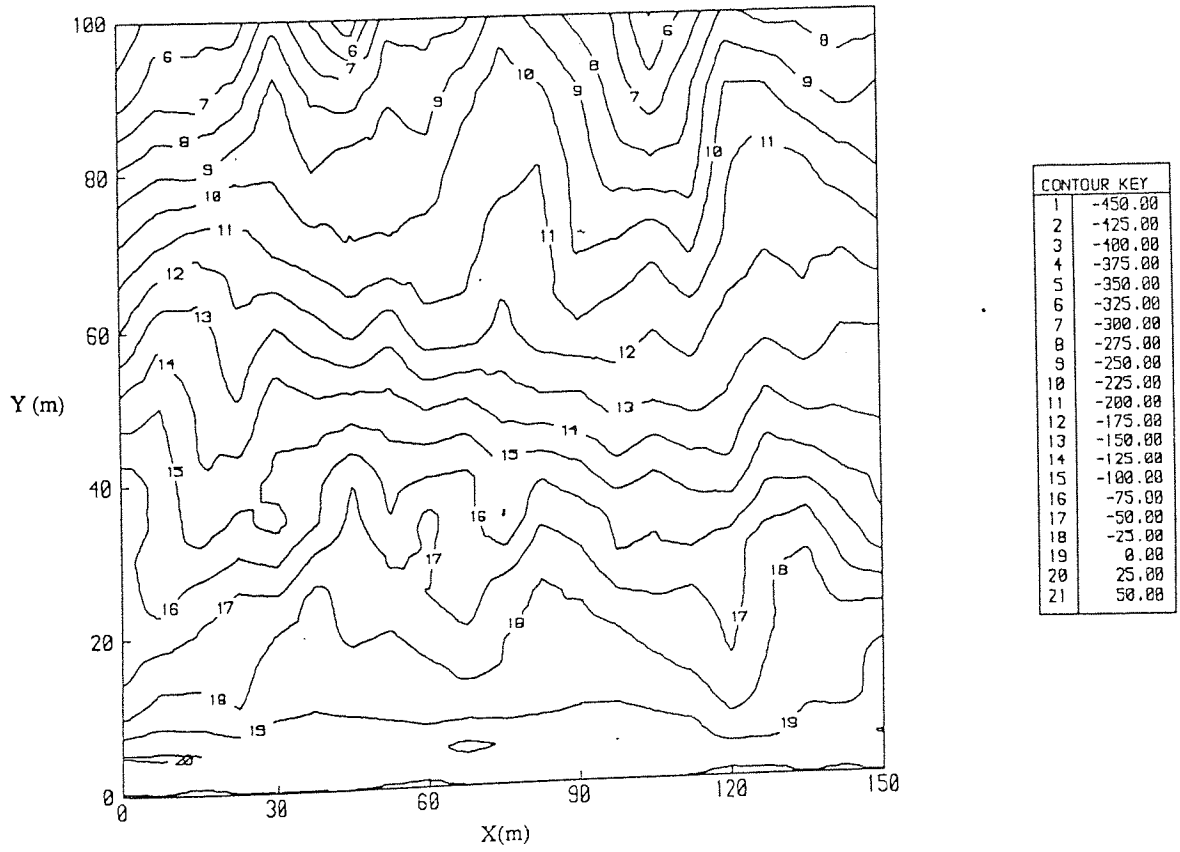

Figure 4.33 Distribution of ϕ in cm at a constant depth of 20 cm for a single realization from case S at time t = 13 hours.

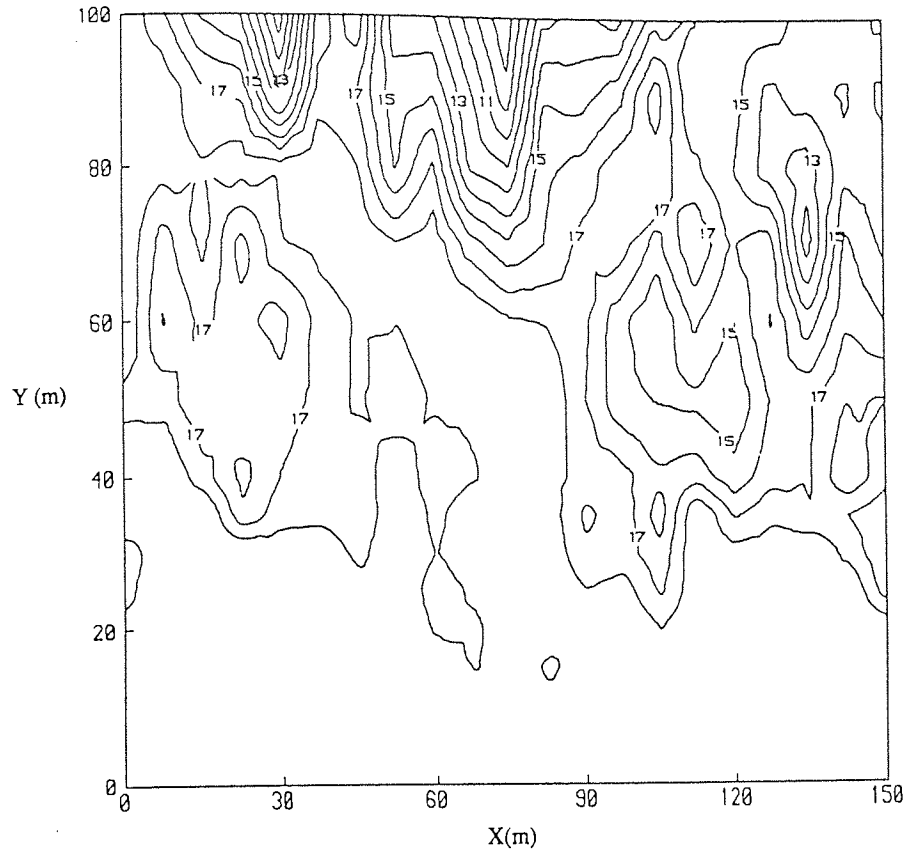

CONTOUR KEY	
1	-450.00
2	-425.00
3	-400.00
4	-375.00
5	-350.00
6	-325.00
7	-300.00
8	-275.00
9	-250.00
10	-225.00
11	-200.00
12	-175.00
13	-150.00
14	-125.00
15	-100.00
16	-75.00
17	-50.00
18	-25.00

Figure 4.34 Distribution of ψ in cm over the soil surface for a single realization from case S at time t = 13 hours.

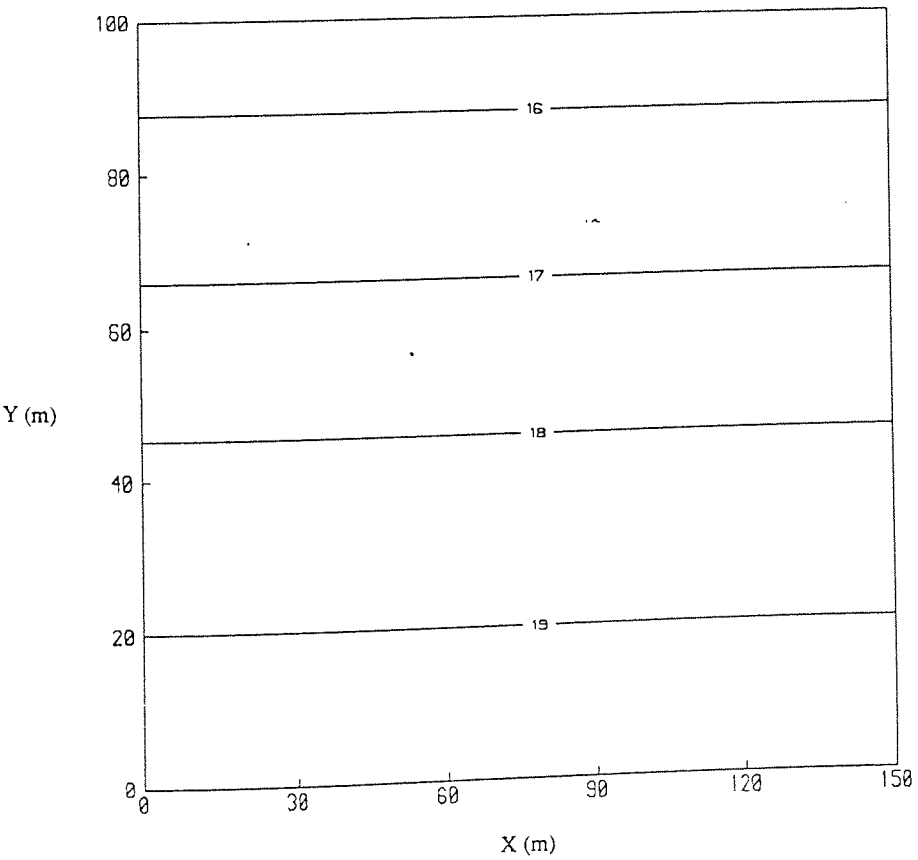

CONTOUR KEY	
1	-450.00
2	-425.00
3	-400.00
4	-375.00
5	-350.00
6	-325.00
7	-300.00
8	-275.00
9	-250.00
10	-225.00
11	-200.00
12	-175.00
13	-150.00
14	-125.00
15	-100.00
16	-75.00
17	-50.00
18	-25.00
19	0.00

Figure 4.35 Distribution of ψ in cm over the soil surface for case O at time t = 13 hours.

4.3 SUMMARY AND CONCLUSIONS

The majority of earlier investigations of the effect of soil spatial variability have limited their analyses to one or two dimensional flow domains. This investigation is the first to be directed towards the problem of three dimensional variably saturated flow in a spatially variable media and has concentrated on assessing the effect of such variability on hillslope runoff generation, which has direct implications towards the current form of physically based models of catchment hydrology.

Suitably realistic soil properties were adopted for this study, including a range of statistical parameters of the log normal hydraulic conductivity distribution, suggested in the literature. Random fields of conductivity were generated within a hypothetical hillslope using the turning bands method (4.2.2) and the response of the hillslope to a single event was evaluated for several fields, using the three dimensional finite element model described in Chapter 3.

The increase in the amount of computing resources required for fully three dimensional analysis posed severe restrictions on the experiments carried out. The main restriction was that of a rather crude Monte Carlo analysis based on only ten realizations of possible hydraulic conductivity fields, the limitations of which have been discussed.

Two distinct mechanisms of hillslope runoff generation have been addressed. In the first case, categorized by high permeability soils, subsurface flow volumetrically dominates the hydrograph. Sharp peaks of the hydrograph may be caused by the onset of overland flow, due to rising of the water table to the soil surface. In the second category, low permeability soils lead to infiltration excess overland flow dominating the hydrograph.

For soils of high permeability, the effect of spatial variability was less significant than originally anticipated. The overall response of the entire hillslope appears to integrate the effects of three dimensional variability, in particular for uncorrelated media. In a highly correlated soil, the variability of the hydrograph peak was recorded to be as high as 12 per cent of the mean peak flow, although this figure is likely to be reduced somewhat with an increased number of realizations in the Monte Carlo analysis. The variability of flows was shown to be highly dependent of time during the wetting period. During the periods of drainage the coefficient of variation of fluxes followed a steady decline, in agreement with the results of El-Kadi and Brutsaert (1985). The variability of head over the flow domain has also been shown to be dependent of time.

In the case of low permeability soils, the effect of spatial variability is more striking. The coefficient of variation of the hydrograph peak was approximately 22 per cent for the highly correlated soils, that is nearly double the figure recorded for the high permeability case. The variance of head was also shown to be considerably greater for soils of low hydraulic conductivity. The effect of correlation of the soil properties was also shown to be of greater significance, both on the hydrograph and the head distribution, under conditions of widespread infiltration excess runoff.

The investigation has been limited to a single rainfall event, therefore, generalized conclusions cannot be drawn from these results. Furthermore, the effect of spatial variability in soils of different soil-water characteristics needs to be assessed. Nevertheless, it is felt that the results of this study have shown that the effect of soil spatial variability on hillslope runoff generation may be less significant than suggested in the literature. Under conditions of high autocorrelation of soil properties the effects of spatial variability may be striking. However, a number of previous field investigations have reported insignificant variance structures. For such cases the effects of uncertainty in measured parameter values will probably outweigh the consequences of spatial variability

Chapter 5

The hydrological effects of zones of preferential flow

The occurrence of naturally formed pipes within the soil matix has been recognized by several authors. The consequences of water movement in such areas of preferred flow, however, has in general remained neglected within models of catchment hydrology.

5.1 PREVIOUS INVESTIGATIONS

The phenomenon of natural soil pipes is evident in various soil types and has been shown to occur in both humid climates, for example Jones (1971) and semi-arid or arid climates, for example Parker (1963). Several theories describing the formation of soil pipes have been postulated, these include formation due to the erosive action of high velocity subsurface flow. This is likely to occur in highly permeable soils, such as peats, under steep hydraulic gradients. The susceptibility to cracking of peat soils during dry periods has also been suggested as a possible mechanism of pipe formation. Devegetation and burrowing of animals are also recognized as contributory factors.

The size of pipes range from several millimetres to over one metre in diameter. Pipes in the peaty soil of the Plylimon Catchments, Wales form extensive networks of a globally discontinous nature (Atkinson, 1978). Recorded flow velocities in these pipes have shown to be three orders of magnitude greater than flow through the soil matrix. Similar observations are also noted in Mosely (1979). The influence of soil pipes is clearly dependent on the location of the pipe. Connections at both ends of the pipe to the soil surface may lead to a flashy response to storm conditions, wheras an isolated macropore may have little effect on the storm hydrograph. Surface connections of the pipe may not necessarily be the pipe itself, Jones (1975), among others, has identified cracks in the soil connecting pipes to the soil surface.

Very few studies have attempted to investigate the influence of soil pipes in a theoretical framework. Gilman and Newson (1980) optimized a simple, four parameter, linear reservoir pipeflow model at various locations in the Nant Gerig catchment, Wales, for a number of recorded pipe discharge hydrographs. The variation of their optimized parameters, both spatially and temporally, suggests that current hydraulic theory may be inadequate to describe such a phenomenon, even if the exact location of individual pipes were known.

Barcelo and Nieber (1981) investigated the signficance of pipe flow on a hypothetical hillslope segment. The matrix flow was analyzed using a two dimensional (vertical slice) model of variably saturated flow. Using the steady state tile drain formula after Kirkham (1949), Barcelo and Nieber compared the response of a single soil pipe located at two positions under two different rainfall events. The hillslope of their study measured 5 metres long, 1 metre deep and 1 metre wide. The size of the constant diameter pipe was 2 metres long with a diameter of 0.051 metres. Barcelo and Nieber admitted that, using the said tile drain formula, the only mechansim considered for the generation of pipe flow was that of seepage from a surrounding saturated matrix. Vertical recharge to the pipe was therefore neglected. Their results showed that increasing the rainfall application rate or decreasing the elevation of the pipe increased the relative significance of the soil pipe. Increased pipe response with decreased elevation is a direct consequence of the form of the tile drain formula used. The maximum effect of pipe flow, under the conditions examined, was to increase the peak of the hydrograph by one hundred per cent.

Barcelo and Nieber (1982) extended their earlier work by investigating the contribution of a pipe network to the response of a hillslope segment. In order to model the movement of water through the soil matrix, a two dimensional (in plan) approximation was adopted neglecting any time delay associated with infiltration. The location of the pipe network in Barcelo and Nieber's hypothetical hillslope is shown in figure 5.1.

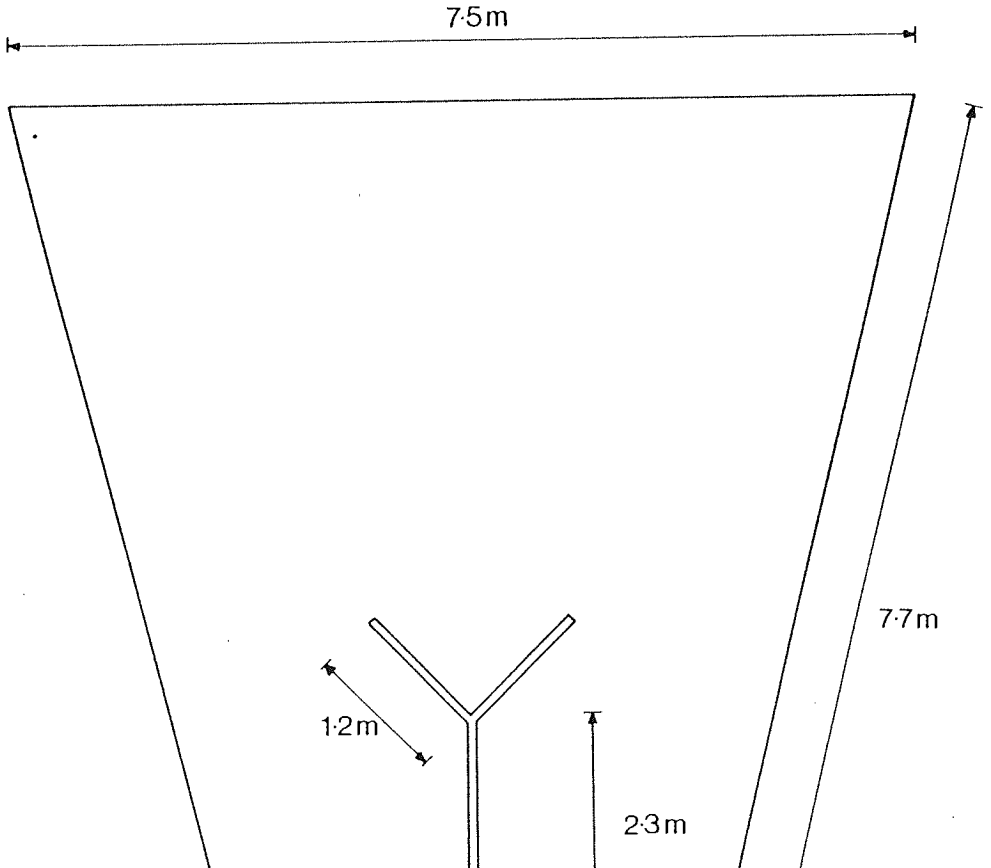

Figure 5.1 Plan view of the hypothetical hillslope used by Barcelo and Nieber (1982).

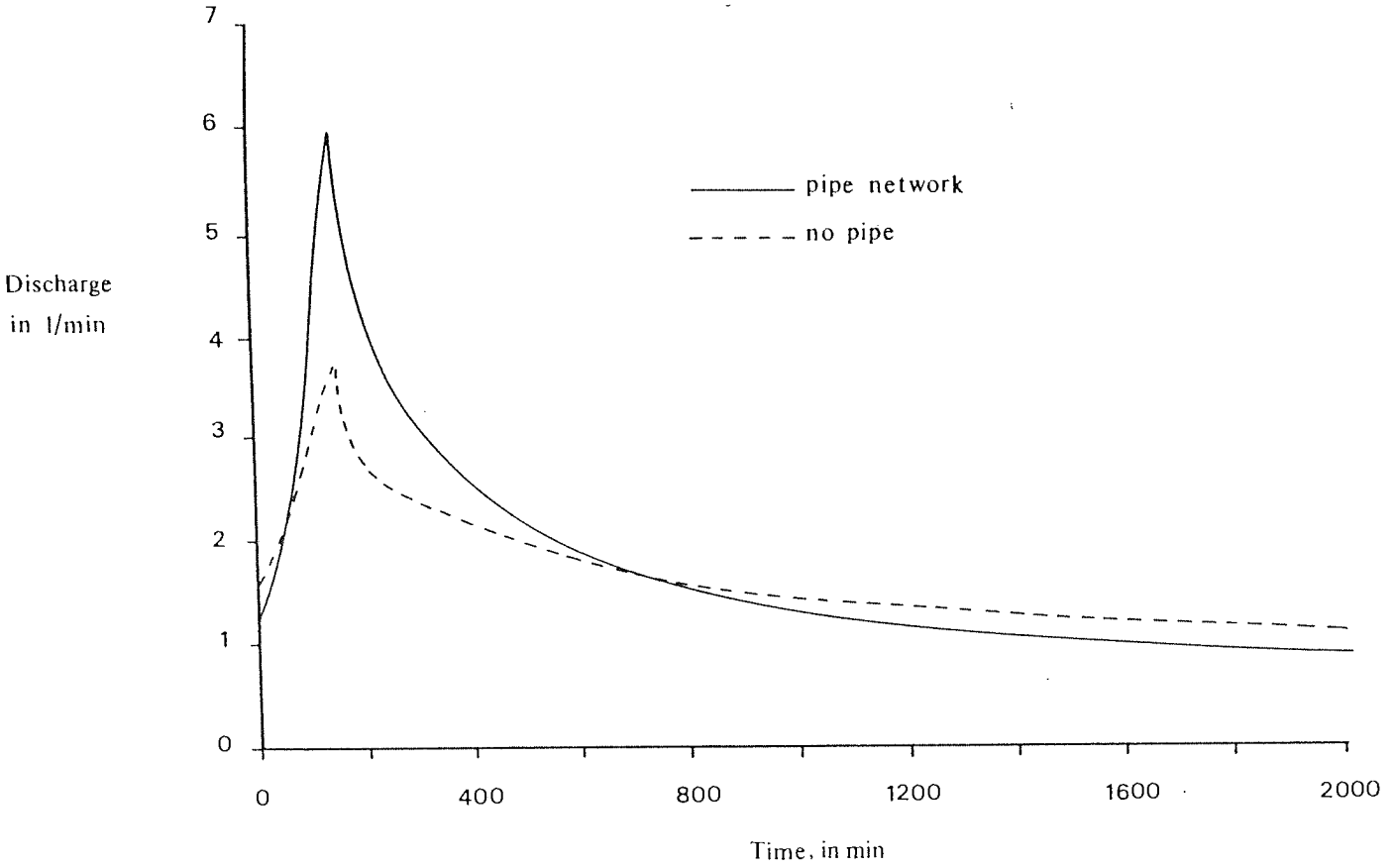

Figure 5.2 Comparison of total flow hydrographs in a piped and unpiped hillslope, after Barcelo and Nieber (1982).

The network is situated at mid depth of a 1 metre deep soil bed. Flow through the soil pipes was described using the same formula as in their earlier work.

A comparison of the runoff hydrographs resulting from the piped and unpiped hillslope under the same conditions is shown in figure 5.2. Referring to this diagram, it can be seen that the network makes a significant contribution to the storm hydrograph. The resulting soil moisture distributions in the hillslope, presented in Barcelo and Nieber (1982), also show considerable differences between the piped and unpiped hillslopes.

5.2 INVESTIGATION PROCEDURE

There are several possible schemes for examining preferential flow on hillslope runoff generation. One possible approach is to synthetically generate a number of individual pipes (or networks) within a hillslope segment. For example, each pipe may be expressed in terms of a length, average diameter, orientation and position. A suitable method is then required to couple the pipe flow to the conditions of the soil matrix. By using the sink (or source) terms in the governing equations of matrix flow, the influence of each pipe may be expressed as an average loss (or gain) of flux to the node points of the matrix flow system. Several problems are apparent with this approach. Firstly, due to the lack of suitable theory, assumptions of serious limitations are needed in order to route the flow of water through the soil pipes, as was noted in Barcelo and Nieber (1981). Secondly, it may be necessary to perform a large number of realizations of the given stochastic process in order to evaluate the average effect of the underlying pipe network distribution. Finally, problems of numerical instability are almost inevitable due to the coupling of the two flow processes. Barcelo and Nieber noted conspicuous oscillations of the pipe flow hydrograph in their analysis of a single pipe (see figure 6.11 of Barcelo and Nieber, 1981). These problems are largely resolved when examining fissured flow in saturated media, the

problem is clearly more complex when dealing with unsaturated flow.

A second possible approach is to discretize the flow domain in such a way that groups of relatively small finite elements represent natural pipes in the soil. By prescribing very high permeabilities to these 'pipe elements', the effect of areas of preferred flow may be ascertained without the need of a coupled solution. However, instabilities of the finite element solution may arise due to significant difference of soil types at 'pipe' boundaries. Furthermore, a finite element mesh consisting of a large number of nodes would be required for an analysis of this type, data preparation time would also be considerable.

An alternative method, used for this study, is to consider distinct global trends of permeability over the flow domain. By specifying some functional form of the hydraulic conductivity distribution, an area of high permeability may be introduced into an otherwise homogeneous soil. In fact such a representation is similar to the 'seepage lines', or 'percolines', observed by Bunting (1961) in which downslope movement of the water is concentrated.

Adopting the same hypothetical hillslope segment as in section 4.2, the form of the trend in hydraulic conductivity used was that of increasing permeability towards the centre of the slope. Variation with depth was also included - increasing towards mid depth followed by a decline to the base of the slope. Added to a general increase in permeability down slope, a three dimensional functional representation of the trend in hydraulic conductivity was required. Using a linear variation downslope and an exponential decline in the other two space dimensions, the functional form adopted was,

$$K_s(x, y, z) = K_o + (K_{max}(y) - K_o) \exp(-\alpha X - \beta Z) \qquad (5.1)$$

where K_o is the saturated conductivity of the soil surrounding the area of preferred flow α and β are constants defining the decay of permeability. X and Z are shifted coordinate axes given by $X = x - (x_{max} / 2)$ and $Z = z - (z_{max}/2)$ (refer to figure 4.2 for the location of the x, y, z axes). Since $K_{max}(y)$, the maximum hydraulic conductivity at the centre of the slope, is taken as a linear function, it can be represented by,

$$K_{max}(y) = K_2 - (K_2 - K_1) \frac{y}{y_{max}}$$

where K_2 is the saturated hydraulic conductivity at $y = 0$, $X = 0$, $Z = 0$ and K_1 is the corresponding value at $y = y_{max}$, $X = 0$, $Z = 0$.

Therefore, by selecting values of α, β, K_o, K_1 and K_2, a three dimensional variation in hydraulic conductivity is achieved. An example of a conductivity surface defined in equation (5.1) is shown in figure 5.3 for variation in the x-z plane at the base of the slope, with parameters $\alpha = 0.0307$ m^{-2}, $\beta = 27.6310$ m^{-2}, $K_o = 0.05$ cm/min, $K_2 = 5.0$ cm/min.

In order to compare the effects of this area of preferred flow with those noted in a spatially variable field in section 4.2 a random component of specified variance was added to the log transformed value of $K_s(x, y, z)$ in equation (5.1). Two conductivity fields were studied, cases T and U, the parameters of which are presented in table 5.1. If the areas of preferred flow were omited from these cases, then both fields would be identical to that of case B in section 4.2.4.1, that is, $\mu_Y = 0.05$ cm/min, $\sigma_Y^2 = 0.25$.

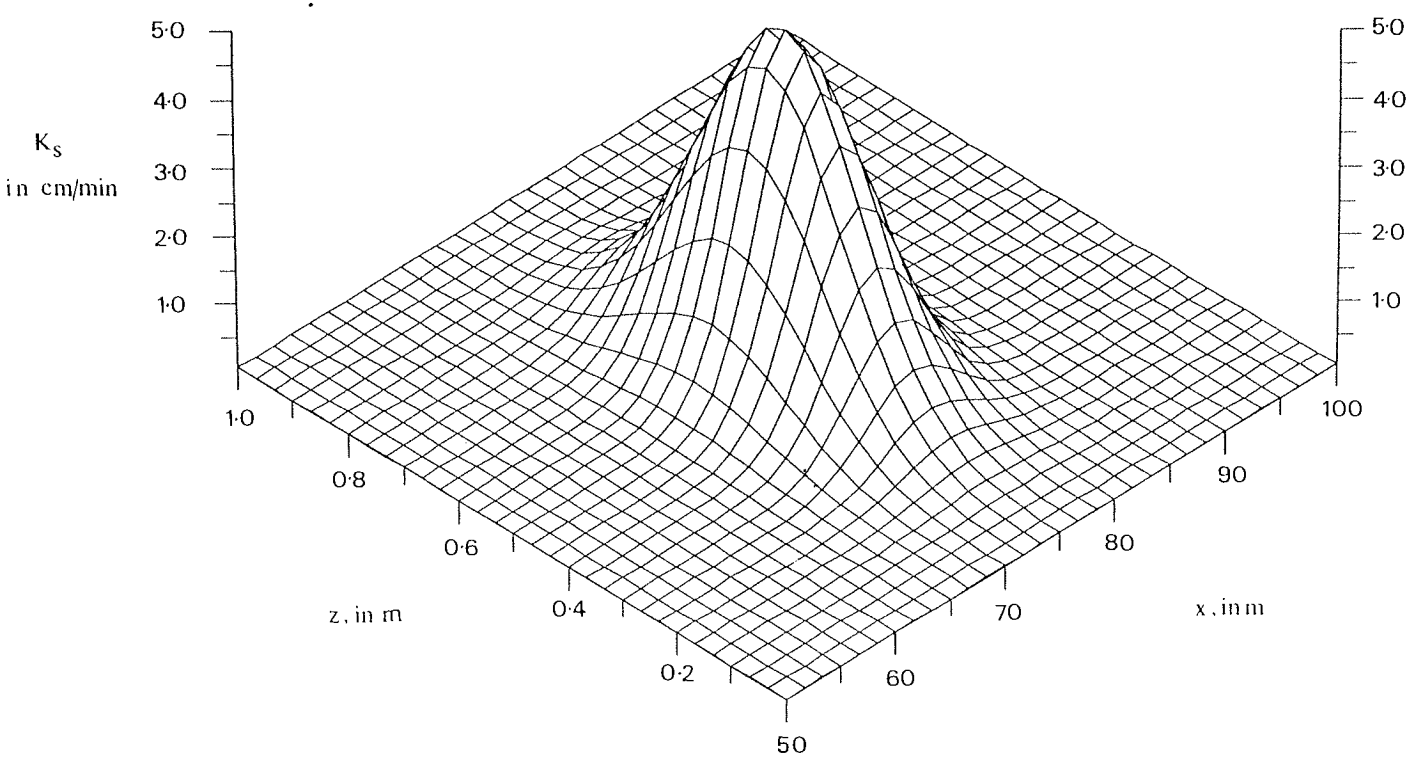

Figure 5.3 Variation in saturated hydraulic conductivity over the (x-z) plane at the base of the slope. Refer to text for the parameters of the field.

Table 5.1 Hydraulic conductivity distribution parameters for cases T and U

CASE	K_0 (cm/min)	K_2 (cm/min)	K_1 (cm/min)	α (m^{-2})	β (m^{-2})	σ_Y^2
T	0.05	5.00	2.50	0.03070	27.6310	0.25
U	0.05	1.00	0.50	0.00768	27.6310	0.25

As in the previous analysis, ten realizations were generated for each field, examples of the variation over the slope at mid soil depth can be seen in figures 5.4 and 5.5 for cases T and U respectively. Referring to these diagrams, it can be seen that the variation across the slope is much more gradual in case U, in comparison with that of T, although the increase in permeability is greater in case T.

The initial conditions and storm event adopted were those used in the earlier study (see section 4.2). Hydrographs and pressure head distributions, were obtained from the finite element solution for analysis of results.

5.3 DISCUSSION OF RESULTS

The results of ten realizations of each conductivity distribution are presented in tables 5.2 and 5.3 for subsurface flow and total flow hydrographs respectively. For comparison, the results from section 4.2.4.1 for cases A ($\mu_Y = 0.05$ cm/min, $\sigma_Y^2 = 0.0$) and B ($\mu_Y = 0.05$ cm/min, $\sigma_Y^2 = 0.25$) are also included.

The values in table 5.2 show that the zone of preferred flow in case T causes an increase in peak subsurface flow by 28 per cent, in relation to case B. The corresponding increase in peak total flow, however, is an order of magnitude smaller (table 5.3). This is due to the reduced area of surface saturation in the preferred flow case, although it is interesting to note that both conductivity fields retain similar surface conductivity values. The overall effect of the area of high conductivity is to increase the volume of total (subsurface plus surface) runoff by approximately 30 per cent. The zone of preferential flow in case U, affects the resulting hydrographs to a lesser extent. In fact, in comparison with case B, the peak total flow rate is reduced by nearly 5 per cent as a result of the more widespread area of high permeability.

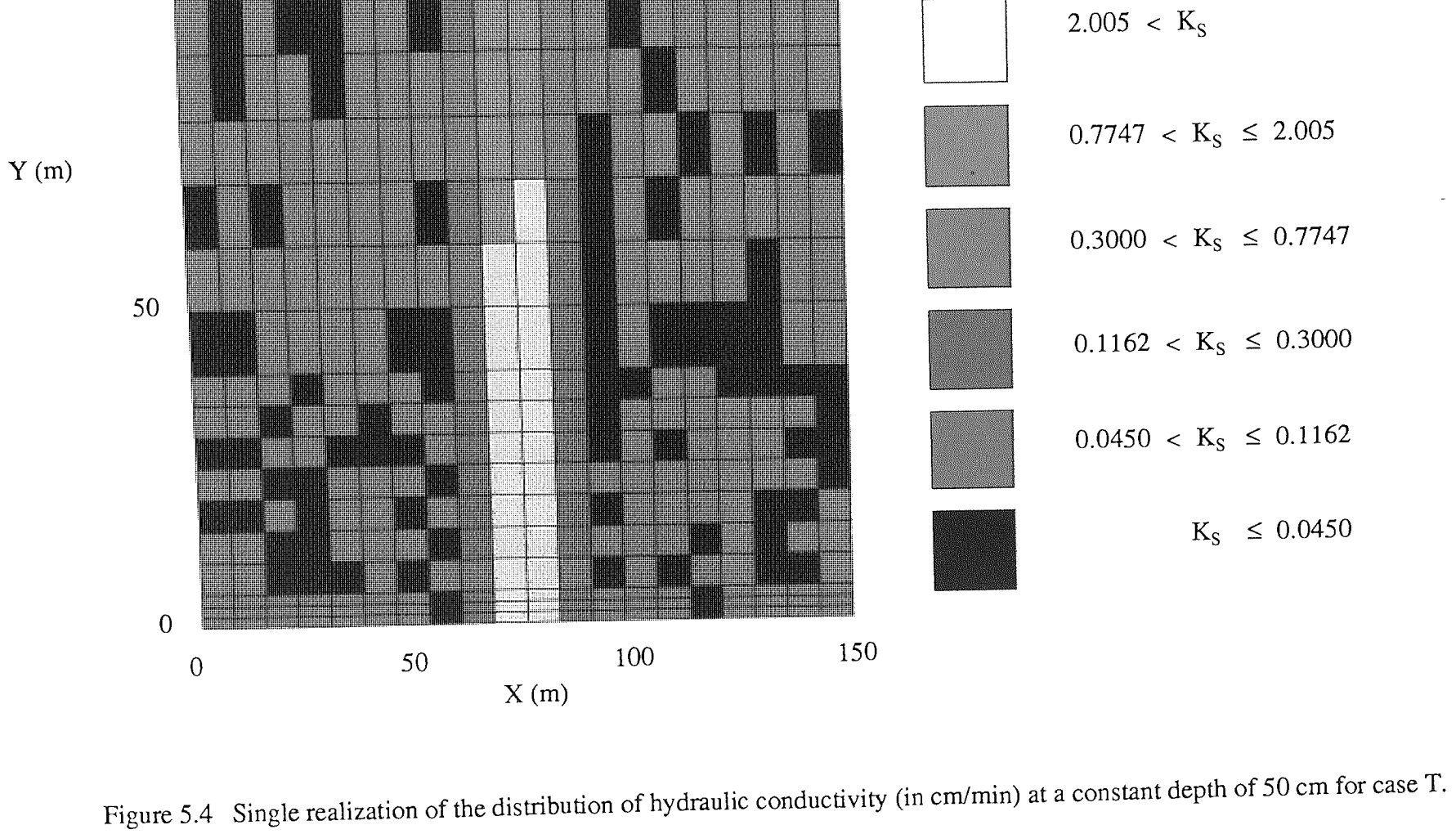

Figure 5.4 Single realization of the distribution of hydraulic conductivity (in cm/min) at a constant depth of 50 cm for case T.

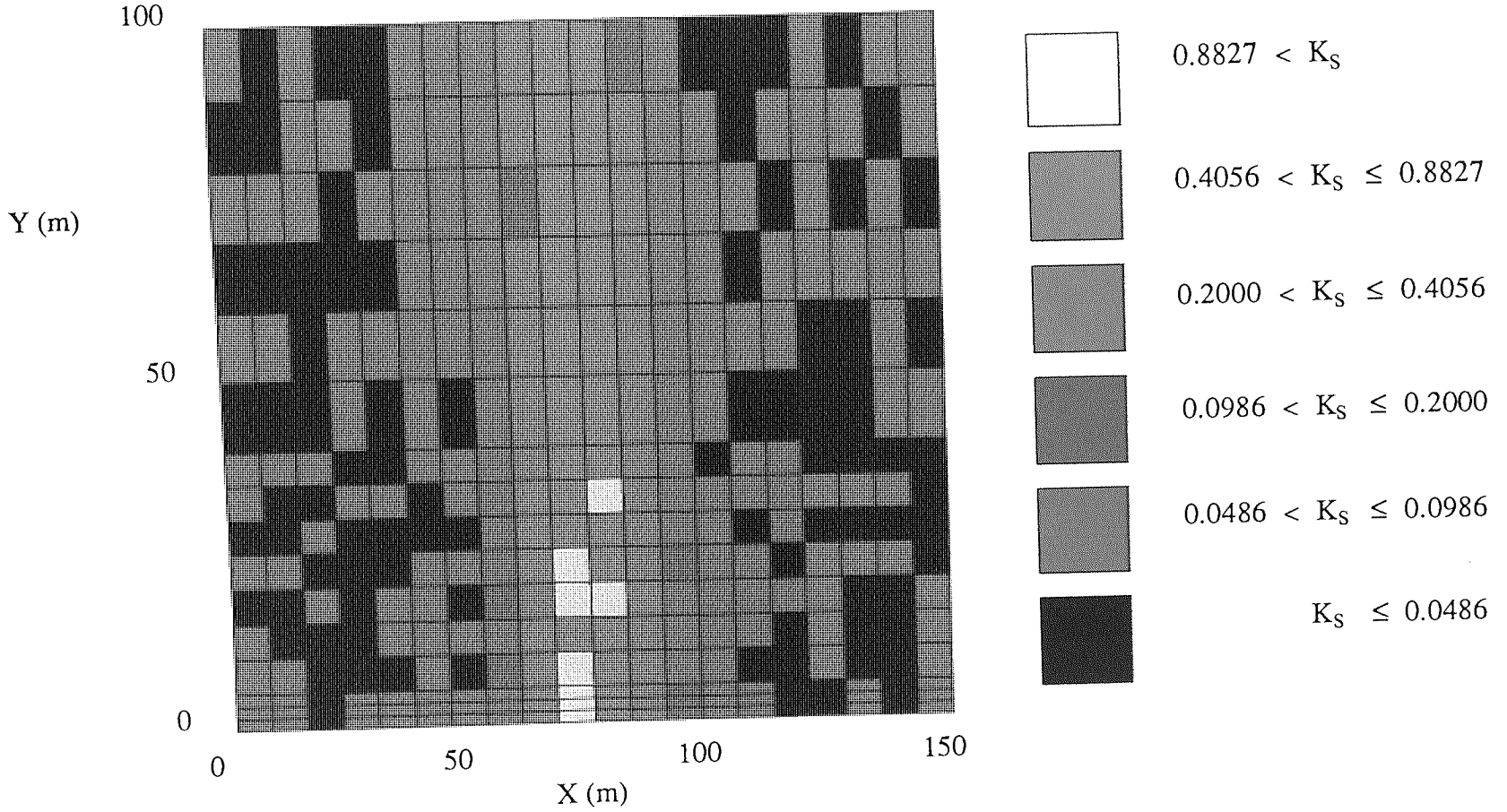

Figure 5.5 Single realization of the distribution of hydraulic conductivity (in cm/min) at a constant depth of 50 cm for case U.

Table 5.2 A comparison of cases A,B,T and U showing the effect of hydraulic conductivity distribution on the subsurface flow hydrograph

CASE	σ_Y^2	PEAK FLOW			VOLUMETRIC FLOW		
		$\bar{q}$ (l/min)	S_q (l/min)	CV_q (%)	$\bar{Q}$ ($x10^3$l)	S_Q ($x10^3$l)	CV_Q (%)
A	0.00	33.592			17.658		
B	0.25	34.360	0.423	1.231	17.928	0.246	1.430
T	0.25	43.976	0.303	0.690	24.345	0.253	1.040
U	0.25	41.268	0.368	0.891	22.186	0.228	1.025

Table 5.3 A comparison of cases A,B,T and U showing the effect of hydraulic conductivity distribution on the total flow hydrograph

CASE	σ_Y^2	PEAK FLOW			VOLUMETRIC FLOW		
		$\bar{q}$ (l/min)	S_q (l/min)	CV_q (%)	$\bar{Q}$ ($x10^3$l)	S_Q ($x10^3$l)	CV_Q (%)
A	0.00	73.593			19.772		
B	0.25	74.163	0.480	0.648	20.019	0.159	0.785
T	0.25	76.184	0.882	1.157	25.939	0.201	0.774
U	0.25	70.516	0.608	0.862	23.649	0.172	0.726

It is also evident from the figures presented in tables 5.2 and 5.3 that there is little difference between the results of each realization, the variability of hydraulic conductivity within the highly permeable area apparently has little effect on the variation of results. The mean hydrographs for cases T and U are shown in figures 5.6 and 5.7 respectively. Figures 5.8 and 5.9 show the corresponding hydrographs for cases A and B respectively. A comparison of these diagrams reveals little difference in the overall shape of the hydrogaphs. A slightly steeper rising limb of the subsurface hydrograph is noticeable in the cases of preferred flow. The reduced volume of surface runoff is also clearly visible.

The effect of the area of high permeability on the resulting pressure head distribution can be seen in figures 5.10 to 5.12 at various depths for a single realization of case T at the end of the rainfall period. Near the soil surface (figure 5.10) the moisture tends to move towards the centre of the slope as the surrounding low permeability soil impedes vertical flow. Towards the bed of the soil layer (figure 5.12) the situation changes. Water now moves away from the centre of the slope as a result of the impeding layer at the base of the high conductance zone. The position of the water table near the surface of the soil (contour 19 in figure 5.10) distinguishes the contributing areas of surface runoff at this stage of the event. For comparison of the uniform distribution, figure 5.13 shows the pressure head distribution at a constant depth of 16 centimetres at the end of the storm.

The effect of impeded flow is more noticeable in the map of equipotentials over a vertical slice located 80 metres from the base of the slope (figure 5.14). Together with the corresponding map of pressure head distribution (figure 5.15), the movement of water discussed can be seen clearly. It must be noted that these vertical slice contour maps are subject to some error due to the few data points used in the contour generating algorithm. The area of high conductivity apparently affects the movement of moisture to a lesser extent towards the base of the slope (figure 5.16).

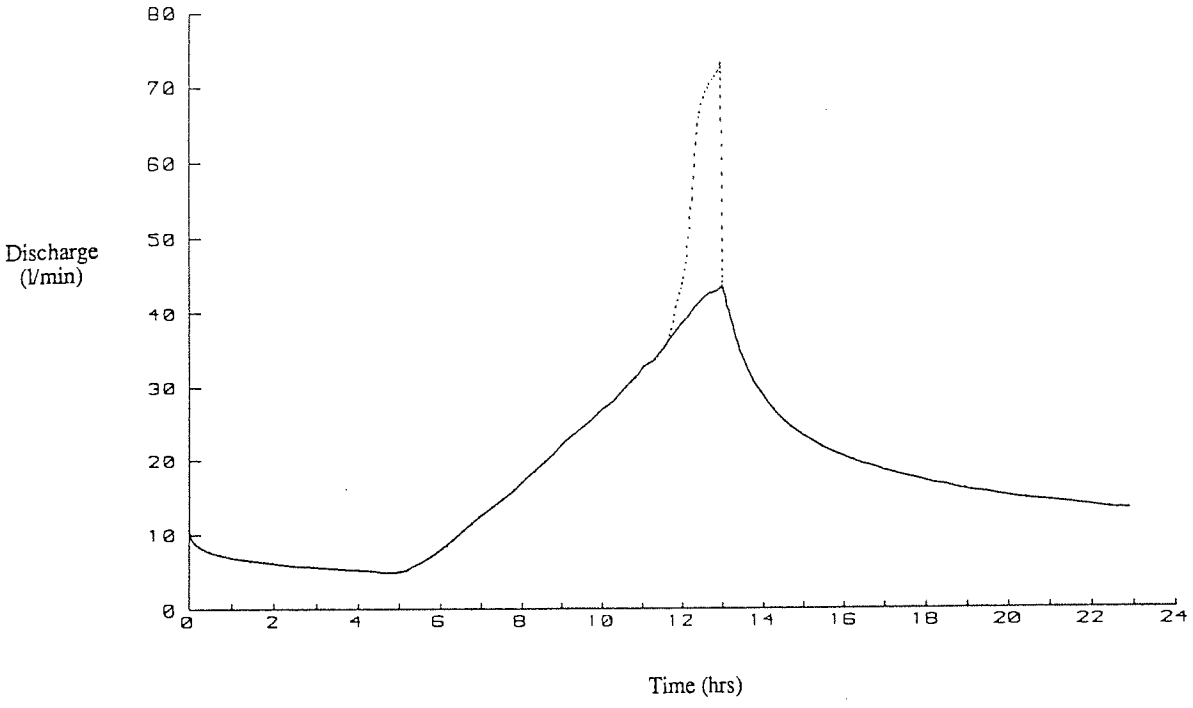

Figure 5.6 Mean hydrograph response for case T. Solid line indicates subsurface flow, dotted line indicates total flow

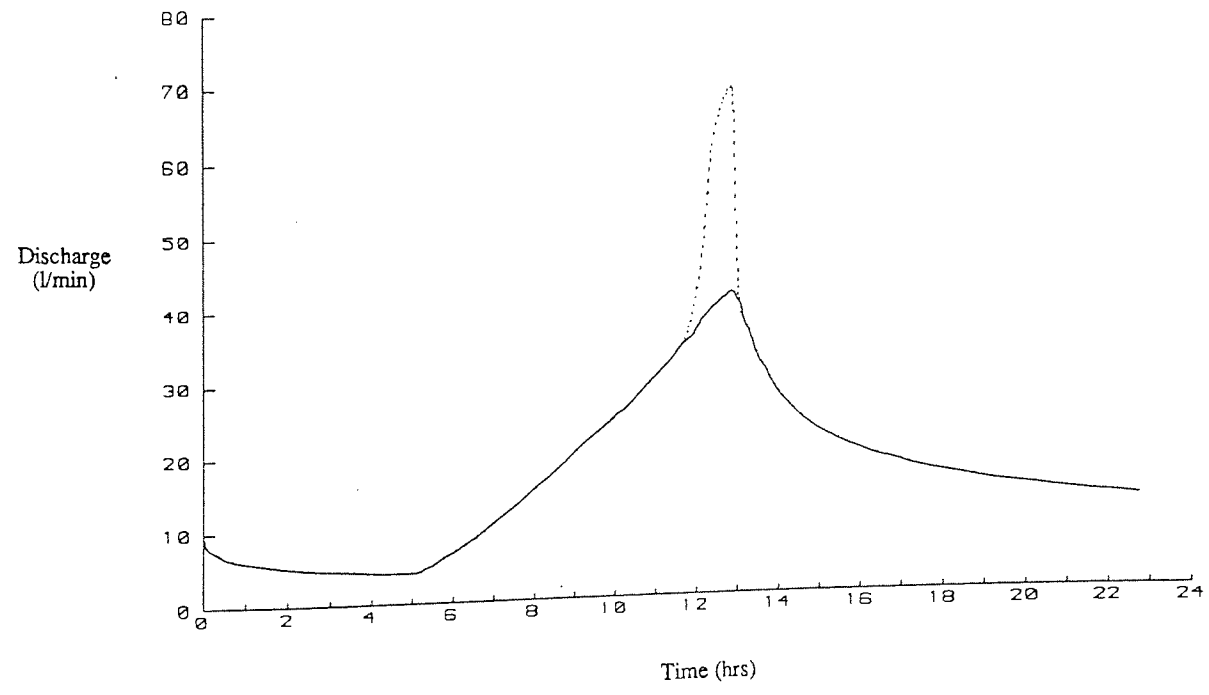

Figure 5.7 Mean hydrograph response for case U. Solid line indicates subsurface flow, dotted line indicates total flow

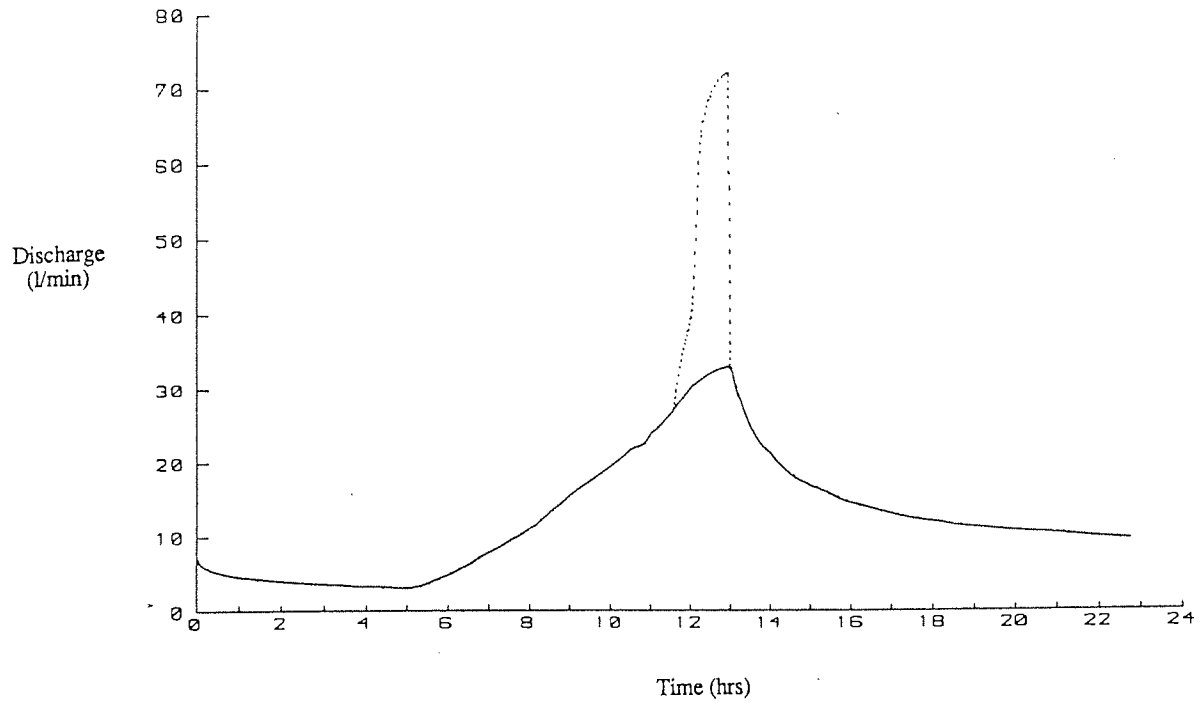

Figure 5.8 Hydrograph response for case A. Solid line indicates subsurface flow, dotted line indicates total flow

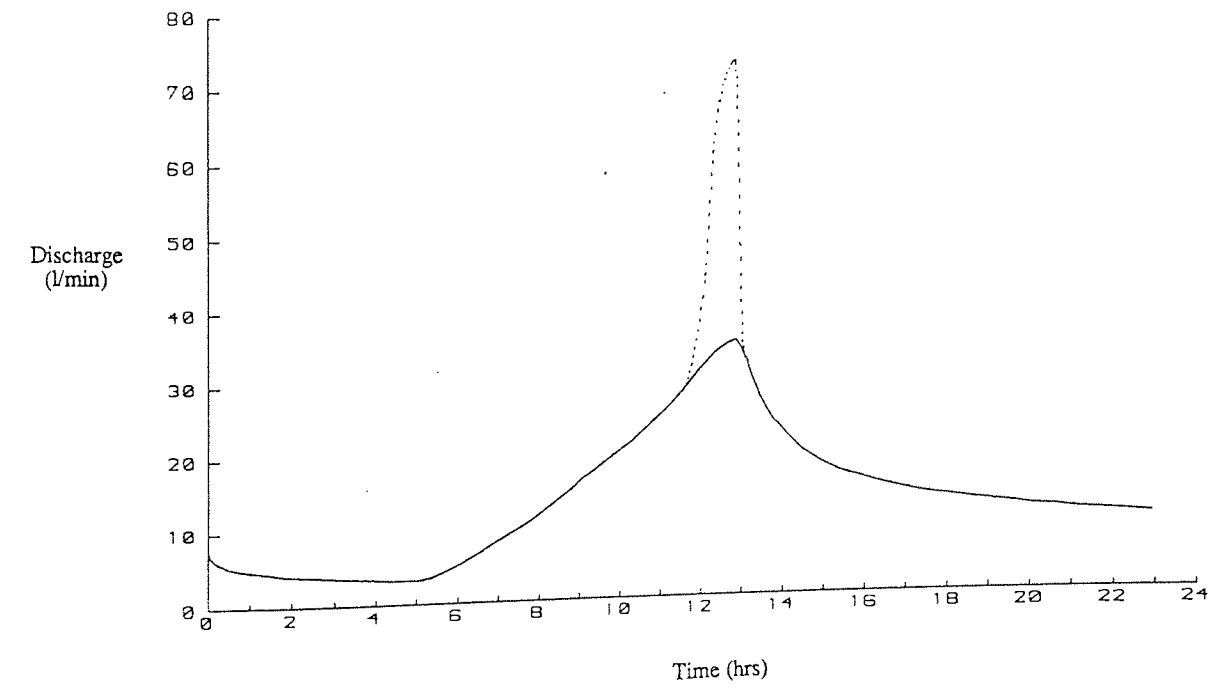

Figure 5.9 Mean hydrograph response for case B. Solid line indicates subsurface flow, dotted line indicates total flow

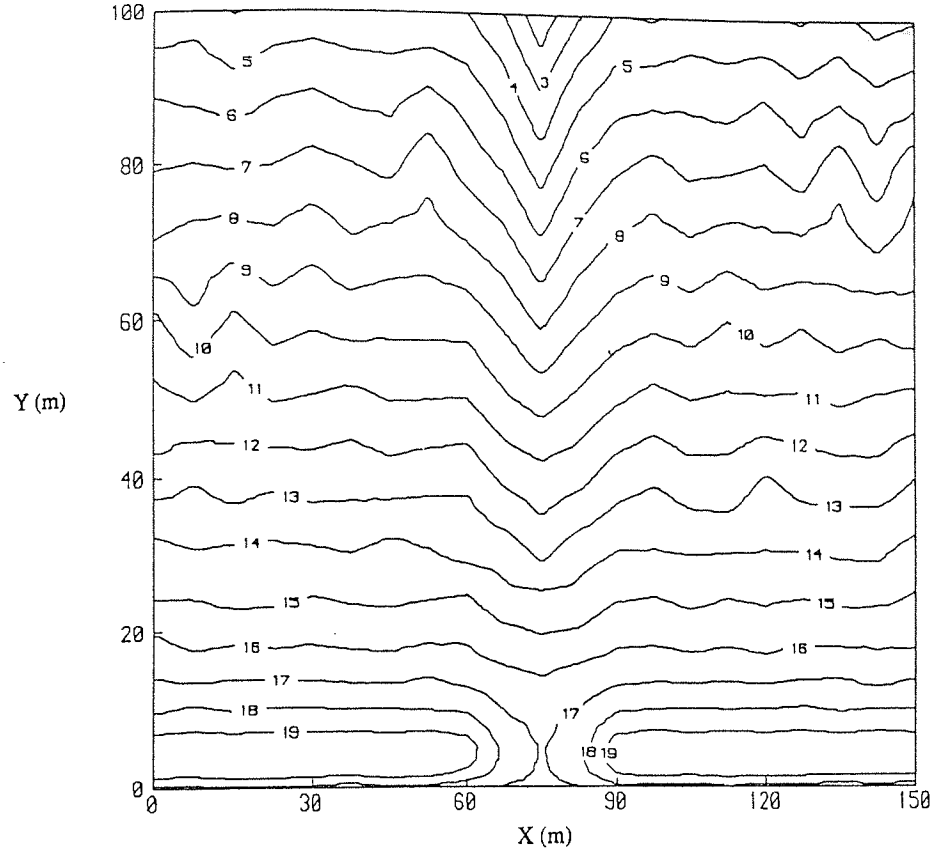

CONTOUR KEY	
1	-450.00
2	-425.00
3	-400.00
4	-375.00
5	-350.00
6	-325.00
7	-300.00
8	-275.00
9	-250.00
10	-225.00
11	-200.00
12	-175.00
13	-150.00
14	-125.00
15	-100.00
16	-75.00
17	-50.00
18	-25.00
19	0.00
20	25.00
21	50.00
22	75.00
23	100.00

Figure 5.10 Distribution of ψ in cm at a constant depth of 16 cm for a single realization from case T at time t = 13 hours.

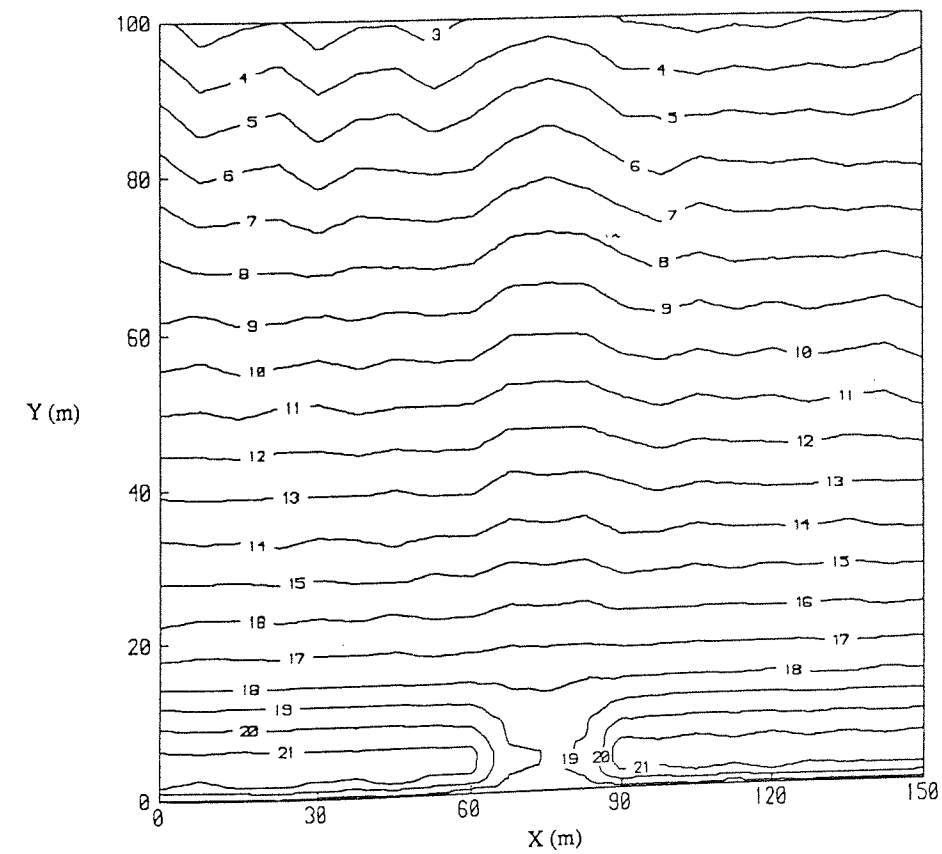

CONTOUR KEY	
1	-450.00
2	-425.00
3	-400.00
4	-375.00
5	-350.00
6	-325.00
7	-300.00
8	-275.00
9	-250.00
10	-225.00
11	-200.00
12	-175.00
13	-150.00
14	-125.00
15	-100.00
16	-75.00
17	-50.00
18	-25.00
19	0.00
20	25.00
21	50.00
22	75.00
23	100.00

Figure 5.11 Distribution of ψ in cm at a constant depth of 40 cm for a single realization from case T at time t = 13 hours.

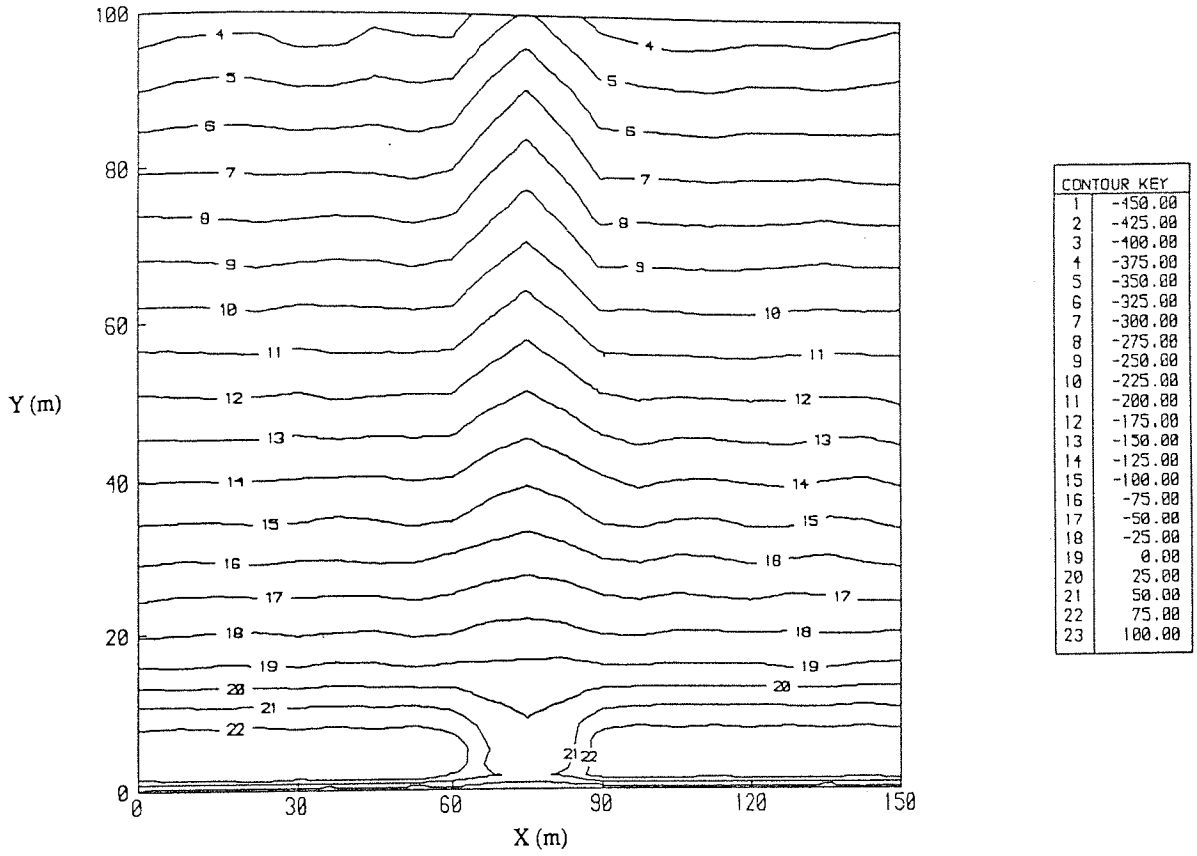

Figure 5.12 Distribution of ψ in cm at a constant depth of 100 cm for a single realization from case T at time t = 13 hours.

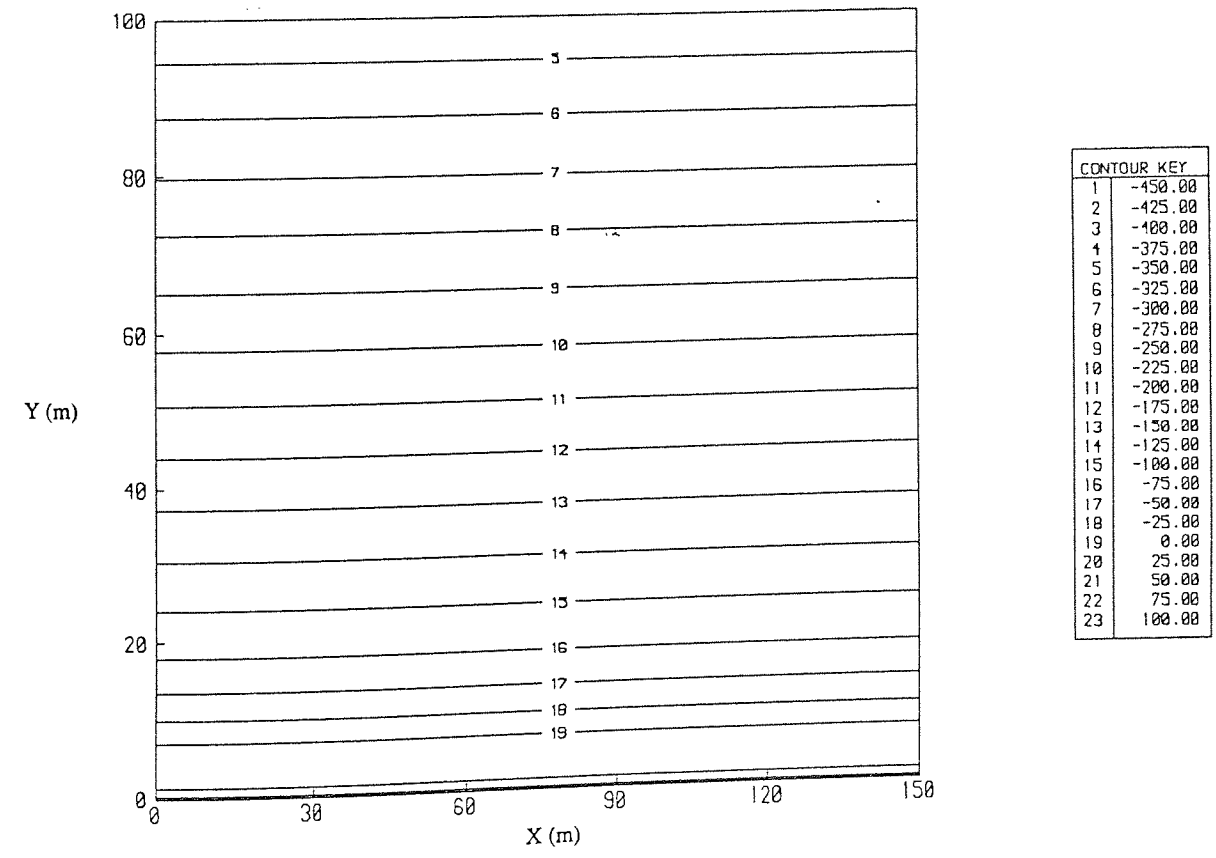

Figure 5.13 Distribution of ψ in cm at a constant depth of 16 cm for a single realization from case A at time t = 13 hours.

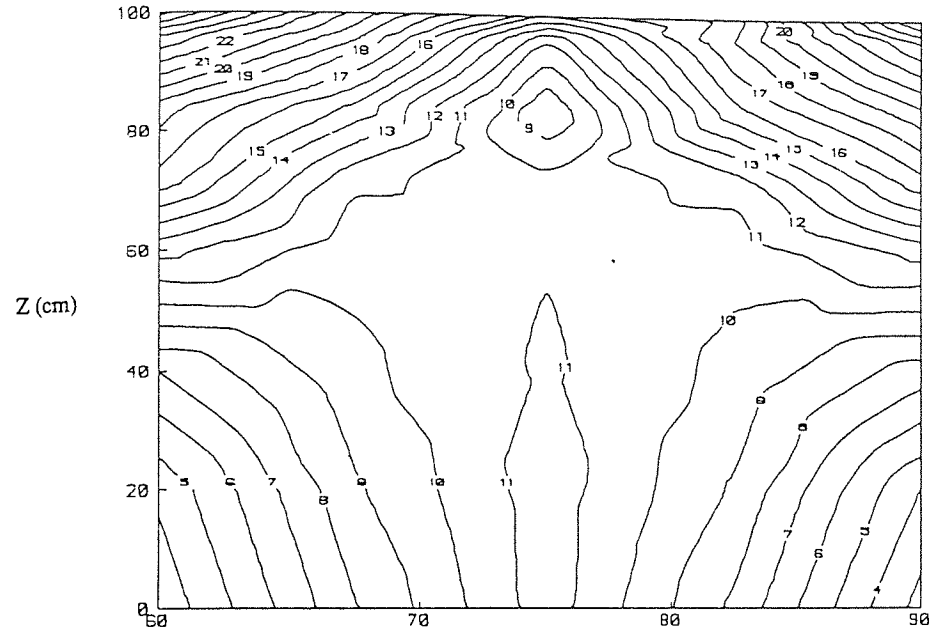

CONTOUR KEY	
1	1020.00
2	1025.00
3	1030.00
4	1035.00
5	1040.00
6	1045.00
7	1050.00
8	1055.00
9	1060.00
10	1065.00
11	1070.00
12	1075.00
13	1080.00
14	1085.00
15	1090.00
16	1095.00
17	1100.00
18	1105.00
19	1110.00
20	1115.00
21	1120.00
22	1125.00
23	1130.00
24	1135.00
25	1140.00
26	1145.00
27	1150.00

Figure 5.14 Distribution of h = ψ + Z in cm in a vertical slice in the (X-Z) plane at Y = 80 m for a single realization from case T at time t = 13 hours.

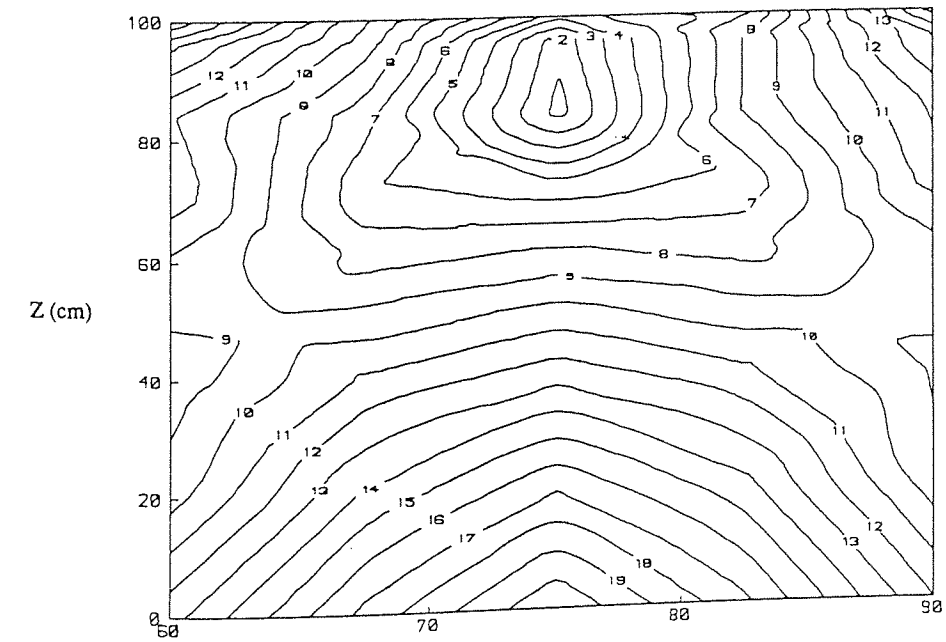

CONTOUR KEY	
1	-360.00
2	-355.00
3	-350.00
4	-345.00
5	-340.00
6	-335.00
7	-330.00
8	-325.00
9	-320.00
10	-315.00
11	-310.00
12	-305.00
13	-300.00
14	-295.00
15	-290.00
16	-285.00
17	-280.00
18	-275.00
19	-270.00
20	-265.00
21	-260.00

Figure 5.15 Distribution of ψ in cm in a vertical slice in the (X-Z) plane at Y = 80 m for a single realization from case T at time t = 13 hours.

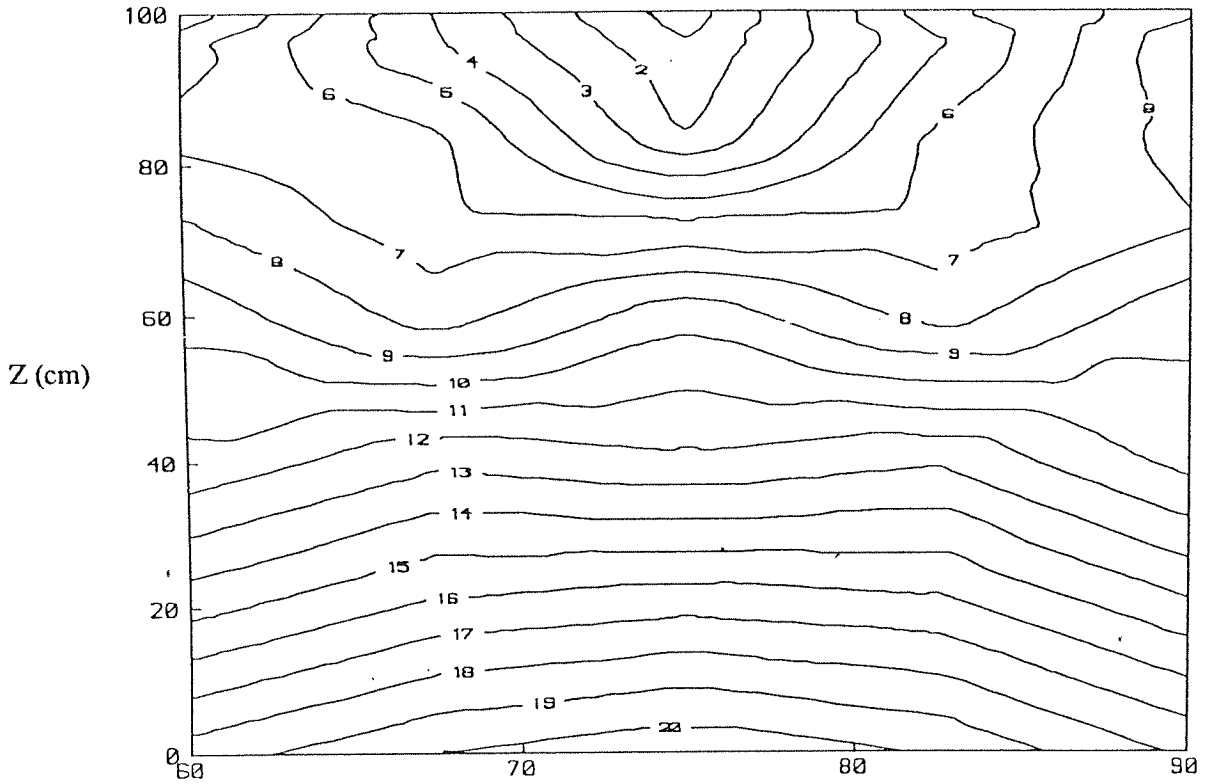

CONTOUR KEY	
1	-160.00
2	-155.00
3	-150.00
4	-145.00
5	-140.00
6	-135.00
7	-130.00
8	-125.00
9	-120.00
10	-115.00
11	-110.00
12	-105.00
13	-100.00
14	-95.00
15	-90.00
16	-85.00
17	-80.00
18	-75.00
19	-70.00
20	-65.00
21	-60.00

Figure 5.16 Distribution of ψ in cm in a vertical slice in the (X-Z) plane at Y = 30 m for a single realization from case T at time t = 13 hours.

Contour maps of the pressure head distribution at two depths at the end of the period of rainfall are shown in figures 5.17 and 5.18 for a single realization of case U. The result of the more widespread area of preferred flow can be seen clearly in these diagrams. It is interesting to note that a comparison of figures 5.17 and 5.10, which are based on identical realizations of the hydraulic conductivity distribution in the areas of low permeability, reveals that the zone of preferred flow has a limited influence to the mid-third of the domain, since outside this area the equipotentials are virtually identical.

A significant result, evident from the comparison of figures 5.19 and 5.20 which show the pressure head distribution at equal depths at the end of the event (t =23 hours) for cases T and B respectively, is that the area of high permeability has little influence on the moisture profiles at distances over 30 meters away from the base of the slope. The discharge in case T at this time, however, is 34 per cent greater than that of case B, which demonstrates the significance of the high permeabilities near the base of the slope in case T.

5.4 SUMMARY AND CONCLUSIONS

Very few studies have attempted to assess the importance of zones of preferential flow on hillslope runoff generation using numerical simulation. It is recognized that the conditions analyzed herein are somewhat artificial, however, it is felt that the results provide further evidence that areas of preferred flow, in the form of natural soil pipes or associated with 'percolines' (Bunting, 1961), may exert a significant influence on the runoff rate and volume from a hillslope. The resulting moisture profiles within the hillslope were also found to be considerably different from those attributed to homogeneous soil permeability formations.

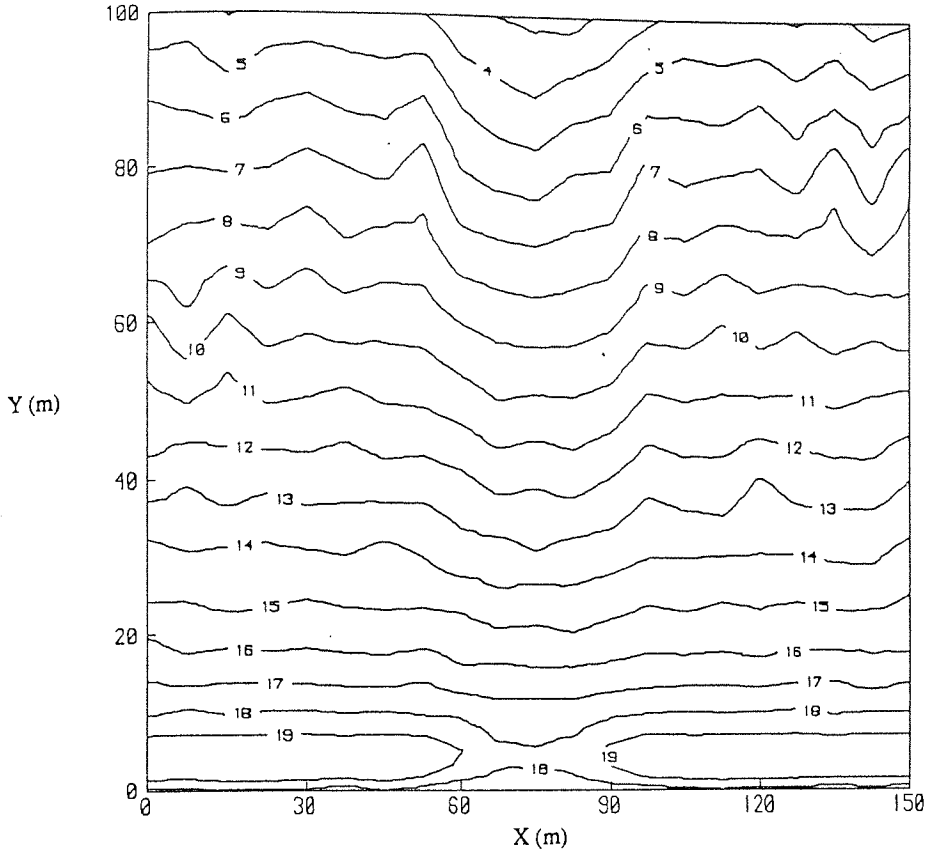

CONTOUR KEY	
1	-450.00
2	-425.00
3	-400.00
4	-375.00
5	-350.00
6	-325.00
7	-300.00
8	-275.00
9	-250.00
10	-225.00
11	-200.00
12	-175.00
13	-150.00
14	-125.00
15	-100.00
16	-75.00
17	-50.00
18	-25.00
19	0.00
20	25.00
21	50.00
22	75.00
23	100.00

Figure 5.17 Distribution of ψ in cm at a constant depth of 16 cm for a single realization from case U at time t = 13 hours.

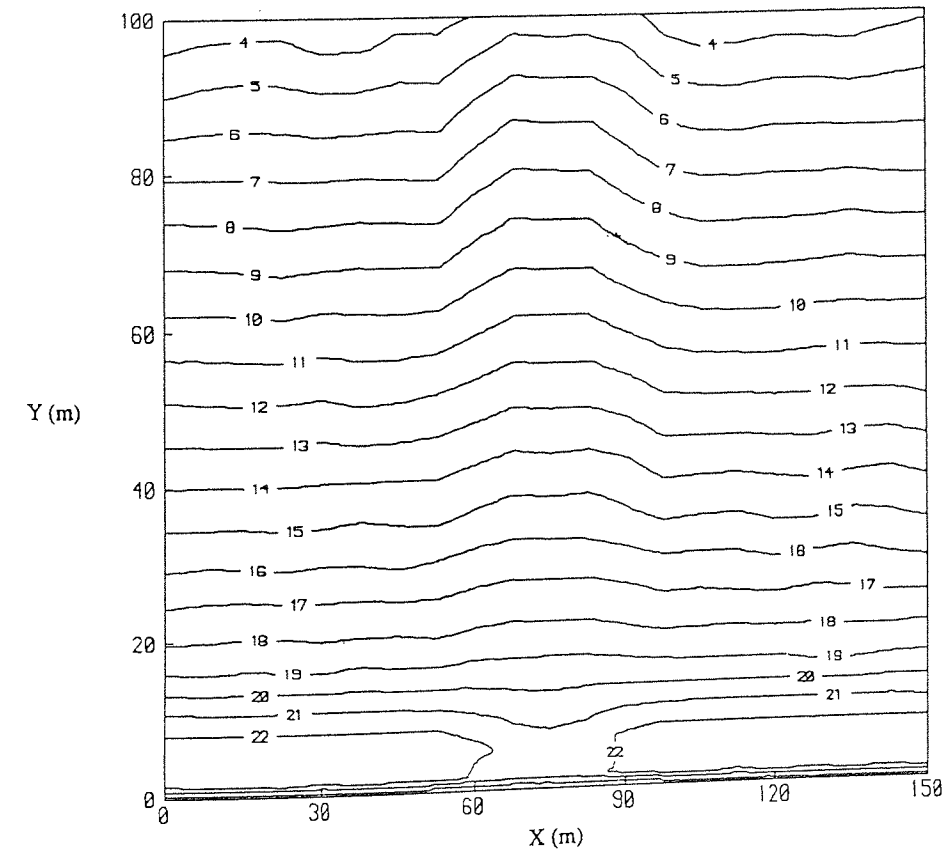

CONTOUR KEY	
1	-450.00
2	-425.00
3	-400.00
4	-375.00
5	-350.00
6	-325.00
7	-300.00
8	-275.00
9	-250.00
10	-225.00
11	-200.00
12	-175.00
13	-150.00
14	-125.00
15	-100.00
16	-75.00
17	-50.00
18	-25.00
19	0.00
20	25.00
21	50.00
22	75.00
23	100.00

Figure 5.18 Distribution of ψ in cm at a constant depth of 100 cm for a single realization from case U at time t = 13 hours.

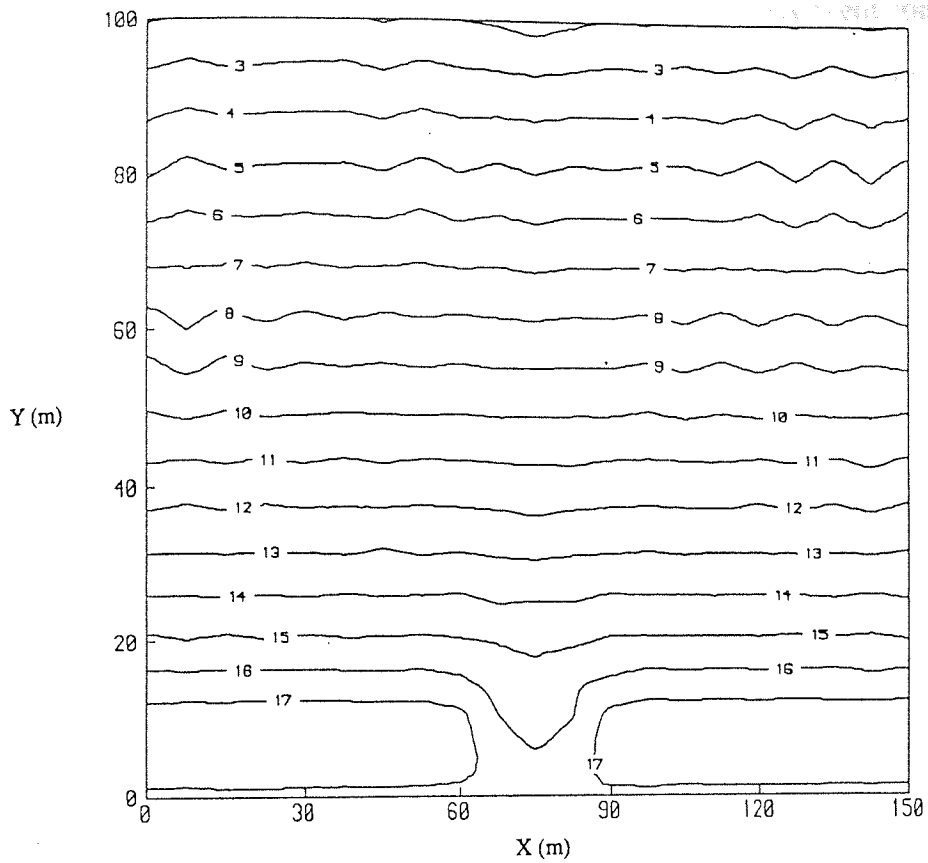

Figure 5.19 Distribution of ϕ in cm at a constant depth of 16 cm for a single realization from case T at time t = 23 hours.

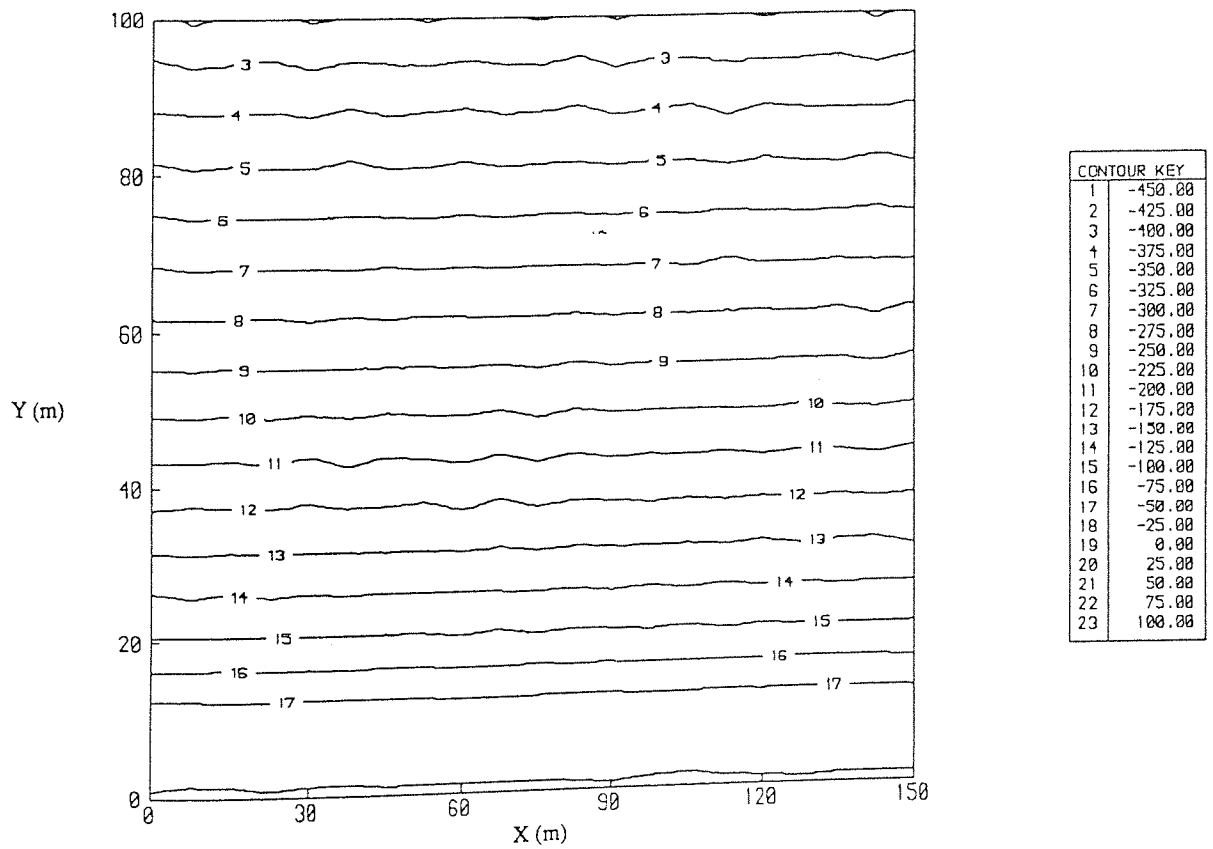

Figure 5.20 Distribution of ϕ in cm at a constant depth of 16 cm for a single realization from case B at time t = 23 hours.

Clearly a more detailed analysis is required under various event conditions. The effect of zones of preferential flow within different soil types and hillslope geometry also needs addressing. Perhaps the results of more field studies may permit an investigation based on observed data. However, if one is to analyze flow through natural soil pipes using current hydraulic theory then vast quantities of information are required from the field in order to assess parameters such as pipe friction factors.

As in the case of soil spatial variability, an important question arises with respect to the validity of current catchment modelling techniques. Is it justifiable to represent areas of the flow domain using equivalent model parameter values? In the context of this chapter, can a single hillslope, showing distinct areas of high permeability, be represented by a hillslope of uniform homogeneous soil properties? The following chapter addresses such questions.

Chapter 6

Effective parameters

The concept of effective (or equivalent) parameters is of fundamental importance in catchment modelling. Practical applications of current physically based models rely on the assumption that areas of the flow domain can be represented by some equivalent model parameter. However there is little (if any) theoretical evidence supporting such an approach. Of particular interest is the validity of effective saturated hydraulic conductivities as many previous modelling studies have demonstrated the high sensitivity of this model parameter.

6.1 PREVIOUS STUDIES OF EQUIVALENT HYDRAULIC CONDUCTIVITY

The simplest and one of the earliest examples of effective hydraulic conductivity determination is presented in Cardwell and Parsons (1945). They considered three basic situations of soil heterogeneity by representing a square block of soil as a composition of four smaller square blocks, two of which have a hydraulic conductivity of K1 and the other two a hydraulic conductivity of K2. Figure 6.1 shows the possible arrangements of such a system. Under saturated conditions, if a pressure drop from left to right causes fluid movement, then it is easily shown that the equivalent hydraulic conductivity for the first case (figure 6.1a) is equal to the arithmetic mean of K1 and K2. Similarly, the response of the composite block in figure 6.1b can be represented by the harmonic mean of K1 and K2. The calculation of the effective hydraulic conductivity for the oblique flow case in figure 6.1c is not as straightforward. Cardwell and Parsons, using an electrical analogy experiment, showed that the equivalent value for this case lies between the harmonic and arithmetic means. Their experimental results are shown in figure 6.2. Cardwell and Parsons failed to notice that their electrical analogy results are close to the geometric mean of K1 and K2 (see figure 6.2). In fact for this condition of heterogeneity, the geometric mean appears to be a suitable equivalent parameter.

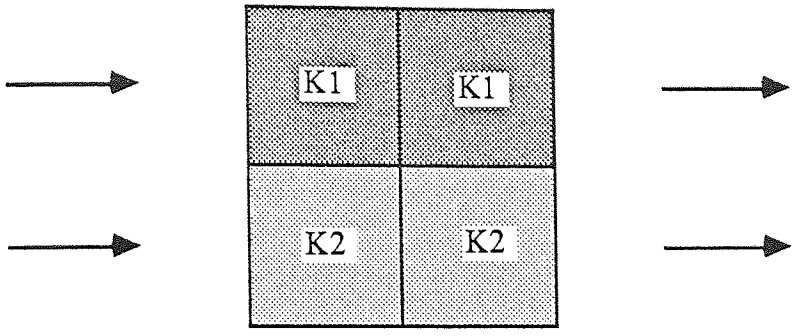

(a)

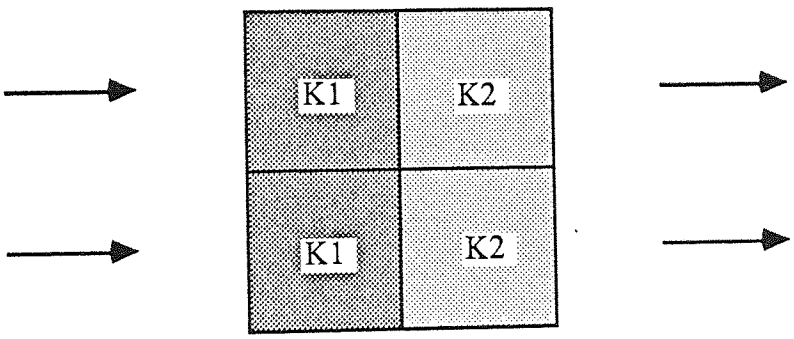

(b)

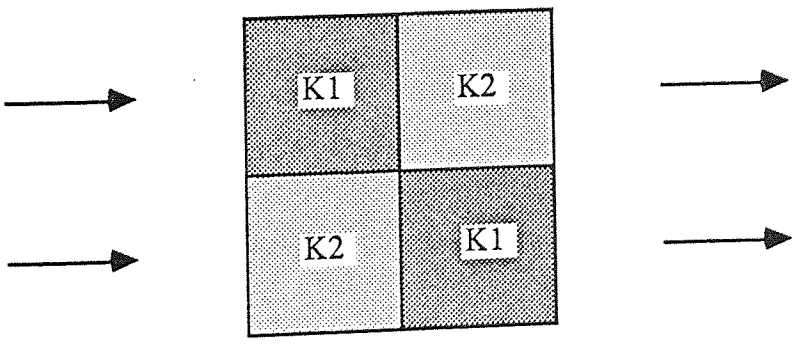

(c)

Figure 6.1 Cases (a), (b) and (c) of a soil block composed of four squares having two different permeabilities.

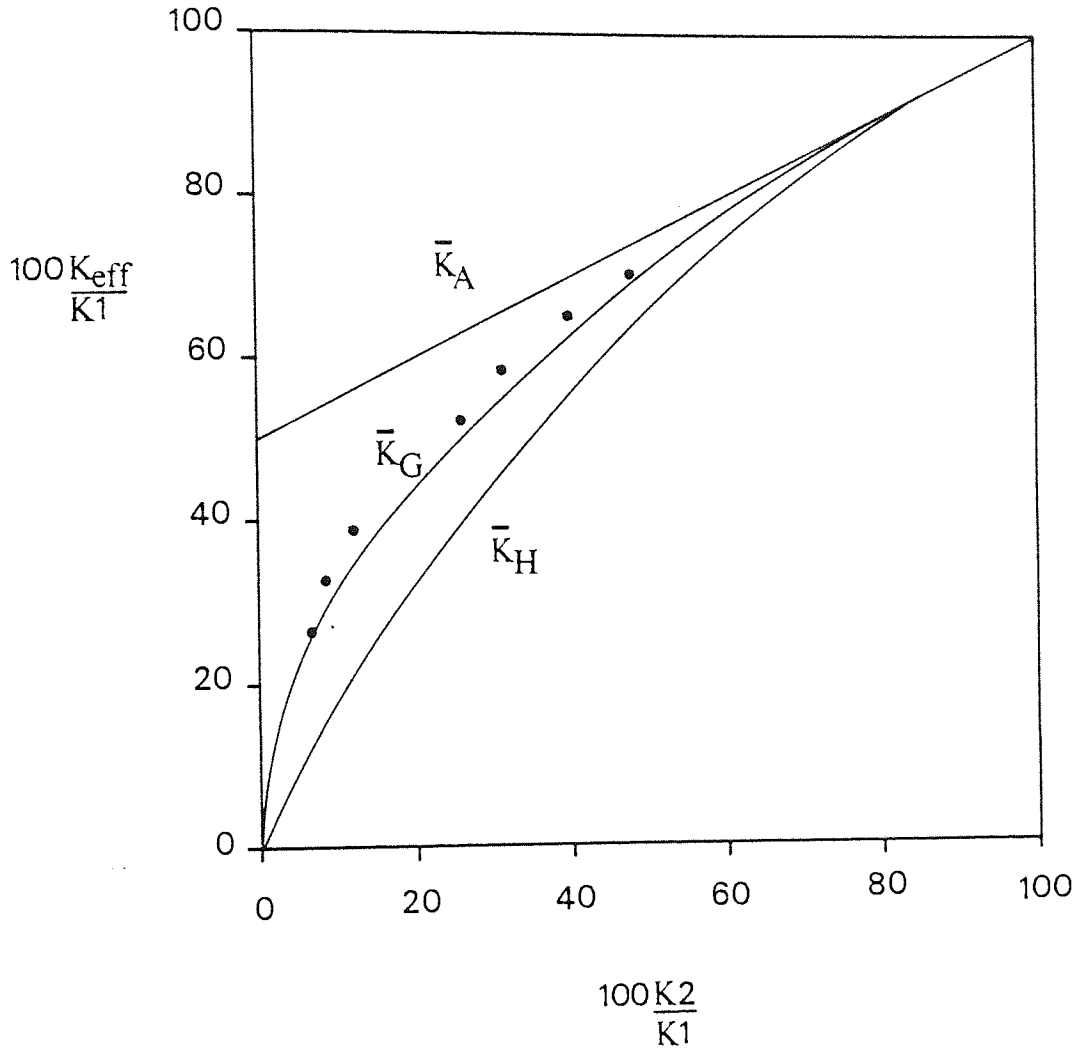

Figure 6.2 Variation of equivalent permeability K_{eff} with permeability ratio. Symbols indicate the results of an anologue experiment for the case of oblique flow, after Cardwell and Parsons (1945)

By considering the general case of a block of porous medium containing any number of different conductivities and any type of directional variation, Cardwell and Parsons demonstrated that the equivalent hydraulic conductivity still lies between the harmonic and arithmetic means of the individual block values. Based on a similar arrangement of permeability cells, Marshall (1962) has developed an expression for the equivalent permeability of heterogeneous media.

The results of the Monte Carlo simulations of Warren and Price (1961), on steady state groundwater flow, have suggested that the geometric mean ($\overline{K}_G$) of the individual block hydraulic conductivities is capable of representing the nonuniform system. Freeze (1975) disputed these claims in his analysis of transient, one dimensional saturated flow and concluded that, under such conditions, an equivalent uniform media is undefinable.

Analyzing steady flow using spectral perturbation methods, Gutjhar et al. (1978) developed analytical expressions for effective hydraulic conductivities under log normal distributions. They have shown that, for problems of low amplitude, the effective conductivity of a two dimensional system is equal to $\overline{K}_G$, the value for the three dimensional case being slightly larger.

Dagan (1979) has also suggested that the geometric mean of the conductivity distribution is the best estimate of the effective hydraulic conductivity in two dimensional steady uniform flow. Dagan's equivalent parameter for three dimensional flow was close to $\overline{K}_G$ for media of low variability, although an effective conductivity over four times larger than $\overline{K}_G$ was found to be suitable for large amplitude cases.

The results of the Monte Carlo analysis of two dimensional steady saturated flow by Smith and Freeze (1979b) showed that a geometric mean conductivity may only be

suitable under strict conditions such as uniform flow. For more realistic situations $\overline{K}_G$ was found to underestimate the flow predicted by the stochastic solution.

In their study of vertical infiltration Dagan and Bresler (1983) and Bresler and Dagan (1983a) demonstrated that effective parameters may only be meaningful under certain restrictive conditions such as steady flow. Difficulties in selecting an equivalent uniform porous medium under conditions of unsteady vertical infiltration are also reported in the earlier work of Russo and Bresler (1981a)

Yeh et al. (1985a) presented analytical expressions for the effective conductivity of three dimensional steady unsaturated flow. For soils of low variability, $\overline{K}_G$ appeared to be a suitable equivalent parameter. Larger values, however, were found to be appropriate for fields of greater nonhomogeneity. The findings of Yeh et al. thus compliment the earlier conclusions of Dagan (1979) with respect to saturated groundwater movement.

In a Monte Carlo analysis of the drainage of an unconfined aquifer, using a two dimensional saturated flow approximation, El-Kadi and Brutsaert (1985) noted that the effective hydraulic conductivity was a function of time. For small times, using the geometric mean as an equivalent parameter, the outflow of the aquifer was consistently underestimated, although $\overline{K}_G$ was found to be suitable for large times. Variability of effective parameters for unsteady saturated flow had been suggested earlier by Dagan (1982b) using analytical expressions based on perturbation analysis. Dagan had concluded that, for the case of constant head initial conditions, the initial effective conductivity is equal to the arithmetic mean of the log normal distribution. After some time, termed the relaxation time, the effective conductivity is reduced to a value corresponding to that at steady state. Example calculations by Dagan (1982b) showed that typical values of the relaxation time for three dimensional flows are likely to be in the order of several minutes.

A summary of the findings of the several studies discussed is presented in table 6.1. The inequality term (>) shown in this table refers to cases of high variability. The geometric mean of the log normal distribution appears to be a suitable estimate of an effective parameter for most systems examined. This is not surprising as $\overline{K}_G$ is the arithmetic mean of the log transformed conductivities. Difficulties in determining an equivalent uniform medium for one dimensional unsteady flows are apparent. However, for multidimensional unsteady flows, which are clearly of more practical interest, effective parameters appear plausible.

Effective parameters for problems of multidimensional variably saturated flow are clearly lacking in the literature. The applicability of effective parameters to soils showing distinct zones of preferential flow, as discussed in Chapter 5, has also not received attention.

6.2 APPLICABILITY OF EFFECTIVE PARAMETERS FOR HILLSLOPE RUNOFF GENERATION

In order to assess the validity of effective parameters in physically based models of hillslope hydrology, the following two part procedure was adopted. (i) Taking a single realization of soil variability from the cases described in Chapter 4 and 5, attempt to select a suitable equivalent uniform porous medium for a given event. (ii) Changing the initial conditions and event, determine whether the selected effective hydraulic conductivity remains valid.

It is important to note the idea used within this study of determining effective parameters for *single* realizations of spatial variability. Previous studies, such as those discussed earlier in section 6.1 have addressed the problem of effective parameters to describe the average response of a given system, that is, the expected result. In

Table 6.1 Summary of findings of several previous studies of effective parameters

Source	Flow system	Effective hydraulic conductivity (K_{eff})
Cardwell and Parsons (1945)	2D steady saturated	$K_{eff} \approx \overline{K}_G$
Warren and Price (1961)	3D steady saturated (low variability)	$K_{eff} \approx \overline{K}_G$
Gutjhar et al (1978)	2D steady saturated 3D steady saturated	$K_{eff} = \overline{K}_G$ $K_{eff} \geq \overline{K}_G$
Dagan (1979)	2D steady saturated 3D steady saturated	$K_{eff} = \overline{K}_G$ $K_{eff} \geq \overline{K}_G$
Smith and Freeze (1979b)	2D uniform steady saturated	$K_{eff} = \overline{K}_G$
Yeh et al (1985a)	3D steady unsaturated	$K_{eff} \geq \overline{K}_G$
Freeze (1975)	1D unsteady saturated	not definable
Russo and Bresler (1981a)	1D unsteady unsaturated	not definable
Bresler and Dagan (1983a)	1D unsteady unsaturated	not definable
El-Kadi and Brutsaert (1985)	2D unsteady saturated (at large times)	$K_{eff} = \overline{K}_G$
Dagan(1982b)	3D unsteady saturated (at large times)	$K_{eff} \geq \overline{K}_G$

practice, it is this single realization which we wish to model since it respresents a single real hillslope or aquifer (Beven, 1981). With reference to the values of mean subsurface flow responses in tables 4.1, 4.3 and 4.5, it can be seen that the effective parameter for a collection of multiple samples is slightly greater than the geometric mean of the hydraulic conductivities (given by the population mean μ_Y), thus agreeing with previous analyses of three dimensional systems. This result is not strictly true, however, for the total flow hydrograph, as can be seen clearly by the results presented in table 4.6 for the low permeability cases. For these cases, increasing the extent of variability increases the amount of surface runoff thus lowering the effective conductivity. The importance of this result will be discussed later in this chapter.

The discussion of results will be separated into three sections, corresponding to the three conditions presented in the preceeding two chapters. These conditions are spatial variability in high permeability soils (section 4.2.4.1), spatial variability in low permeability soils (section 4.2.4.2) and soils showing distinct areas of preferred flow (section 5.3). The event used for the first part of the investigation procedure (event 1) is identical to that used earlier (see sections 4.2.3 and 4.2.4). For the second part of the experiment the initial condtions are described by the steady state solution obtained by prescribing the pressure head at the soil surface node points as a linear decrease from -90 cm at the base of the slope to -340 cm water at the top of the slope. The deterministic rainfall event consists of 5 hours of rainfall at an intensity of 3 mm per hour, followed by 3 hours of 8 mm per hour rainfall which precedes 12 hours of drainage. The total rainfall of this second event is thus 39 mm which is slightly greater than that of event 1 (32 mm). The main difference between the two events is the much wetter antecedent conditions and the short duration higher intensity rainfall, which together lead to the likelihood of the onset of surface runoff in all soils examined.

Although the equivalent porous medium simulations do not require three dimensional analysis, since the movement of water only occurs in a two dimensional plane, the

computing costs prohibited the use of an efficient search algorithm to determine the 'best' effective parameter. Instead, the volume of the runoff hydrograph was taken as the output variable to be matched and after selecting an approximate effective conductivity, using the results of approximately one hundred two dimensional simulations, a limited search of the parameter space was made.

6.2.1 Effective parameters for high permeability soils

A total of sixteen realizations from cases B to N in section 4.2.4.1 were selected in order to determine suitable effective parameters. Since in all these cases overland flow was seen to occur during the latter stage of the rainfall period, it was decided to attempt to match the subsurface flow volume and then determine the suitability of the effective conductivity in reproducing the peak total (subsurface plus surface) flow. The 'best' parameters are shown in table 6.2 together with the population statistics of the various cases. In this table, E1 refers to example 1 from case E, E2 to example 2 and so on.

The error of each effective parameter simulation was evaluated by four quantities: subsurface flow peak and volumetric errors and total flow peak and volumetric errors. Each error was expressed as a percentage using,

$$\text{Percentage error} = 100\% \times \frac{f - f_{eff}}{f}$$

where f is the peak or volumetric flow produced by the nonuniform case and f_{eff} is the corresponding value for the uniform simulation. Table 6.3 shows the matching errors of the event 1 simulations using the effective parameters in table 6.2. It can be seen from the values of table 6.3 that, for most cases, matching the volume of subsurface flow produces a reasonable effective conductivity for the total flow hydrograph. The effective parameters for the uncorrelated realizations E1, E3 and F2 show the greatest

Table 6.2 Effective hydraulic conductivities for selected realizations from cases (B-N)

Case	μ_Y (cm/min)	σ_Y^2	K_{eff} (cm/min)
B1	0.05	0.25	0.05197
E1	0.10	0.50	0.10304
E2	0.10	0.50	0.11118
E3	0.10	0.50	0.09891
F1	0.10	1.00	0.11929
F2	0.10	1.00	0.10055
H1	0.20	0.25	0.21323
I1	0.20	0.50	0.22159
I2	0.20	0.50	0.19948
J1	0.10	0.25	0.09358
J2	0.10	0.25	0.11882
K1	0.10	0.50	0.09412
K2	0.10	0.50	0.13051
M1	0.20	0.25	0.31794
N1	0.20	0.50	0.39065
N2	0.20	0.50	0.18914

Table 6.3 Matching errors using effective parameters for cases (B-N) for event (1)

Case	Subsurface flow		Total flow	
	Peak error (%)	Volume error (%)	Peak error (%)	Volume error (%)
B1	0.887	0.042	1.421	0.405
E1	4.495	0.007	14.264	0.185
E2	-0.360	0.022	0.575	0.032
E3	3.663	0.007	12.908	0.362
F1	0.314	-0.054	1.285	-0.039
F2	6.537	0.009	21.094	0.498
H1	-0.325	-0.011	-0.325	-0.012
I1	0.886	0.004	0.886	0.004
I2	1.649	0.006	1.649	0.006
J1	0.281	-0.020	-1.700	1.454
J2	0.815	-0.007	1.127	-0.004
K1	1.219	-0.024	3.258	2.423
K2	1.874	0.011	1.874	0.011
M1	0.374	-0.034	0.374	-0.034
N1	0.329	0.035	0.329	0.035
N2	2.040	-0.022	6.202	0.171

errors in reproducing the peak total flow. The 21.094 per cent error in peak flow for case F2 corresponds to a difference of 11.72 l/min (= 1.172% rainfall intensity) between nonuniform and uniform simulations. The unsuccessful matching of these uncorrelated cases is due to the effective conductivities being close to the threshold conductivity discussed in 4.2.4.1. For example, an effective conductivity of 0.1006 cm/min does not produce overland flow for this event, whereas the nonuniformity of case F2, taken from a sample with a mean of 0.1 cm/min, yields a peak surface runoff of 8.65 l/min. The influence of this threshold hydraulic conductivity is further demonstrated by the relatively successful effective parameters for the uncorrelated cases B1, H1, I1 and I2.

It is also clear from the results in table 6.3 that increasing the variability of the field reduces the applicablilty of the selected effective parameters, albeit to a minor extent.

The total flow hydrographs for cases E1, E3, K1 and N2 with the corresponding responses of uniform cases are shown in figures 6.3 to 6.6 respectively. It can be seen from these diagrams that the equivalent parameters are suitable throughout most of the event, any discrepancy occuring at the hydrograph peak.

Adopting the effective conductivities for event 1, the matching errors for event 2 are shown in table 6.4. The relatively low percentage errors displayed in this table suggest that the equivalent medium properties selected for event 1 remain suitable under the entirely different conditions of event 2. The maximum peak total flow error in table 6.4 is -3.409 per cent, for case N2, which is equivalent to a difference in flows of 11.72 l/min (= 5.86% maximum rainfall intensity). A comparison of the total flow hydrographs for case N2 and the selected effective parameter is shown in figure 6.7. As before, the effective value appears suitable throughout much of the event, in particular during the drying stages.

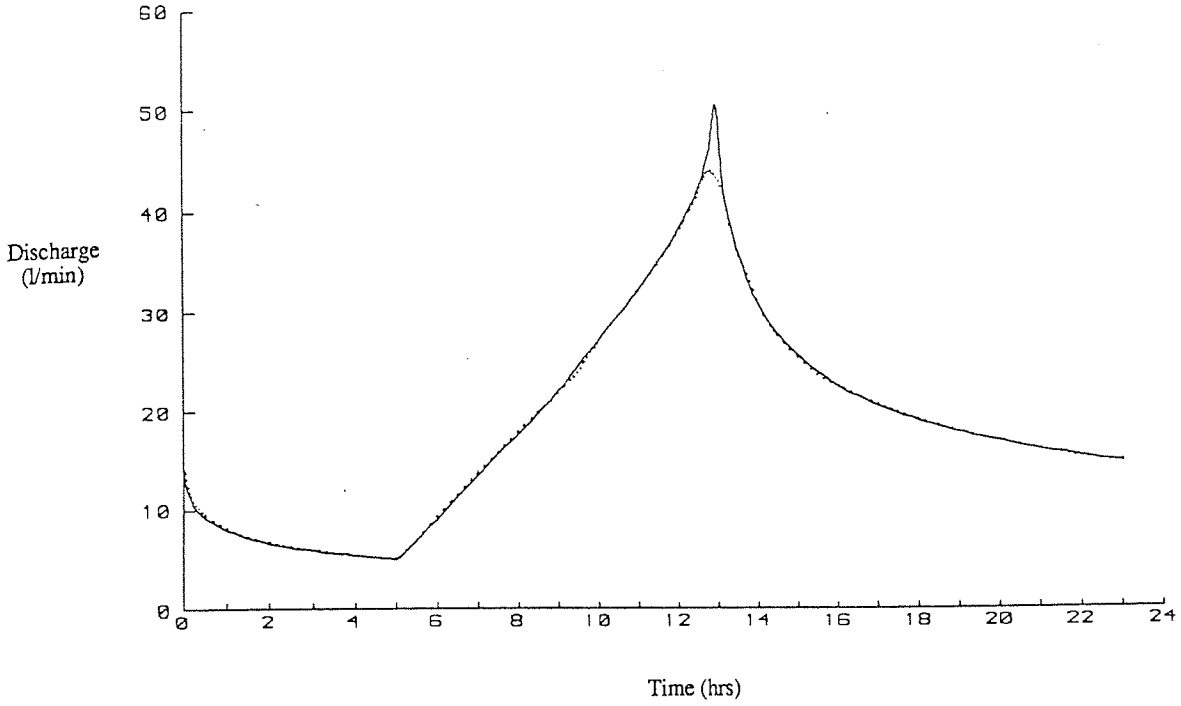

Figure 6.3 Total flow hydrographs for uniform and nonuniform media.
Solid line indicates results from case E1, event 1. Dotted line indicates effective parameter solution.

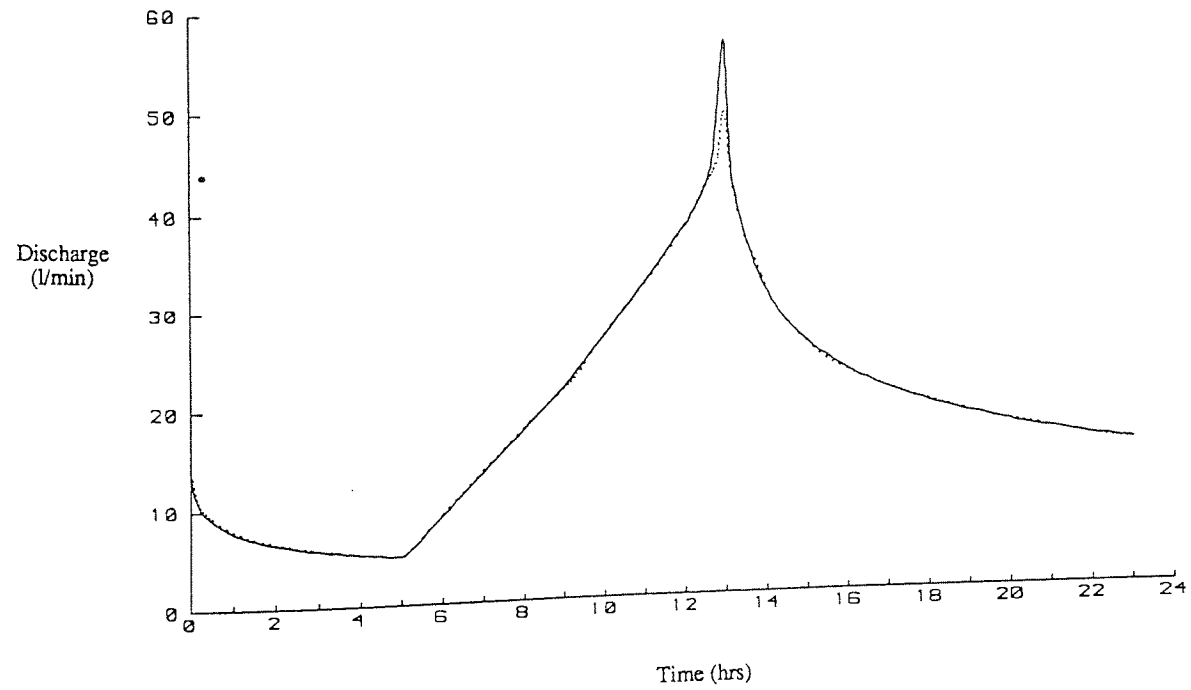

Figure 6.4 Total flow hydrographs for uniform and nonuniform media.
Solid line indicates results from case E3, event 1. Dotted line indicates effective parameter solution.

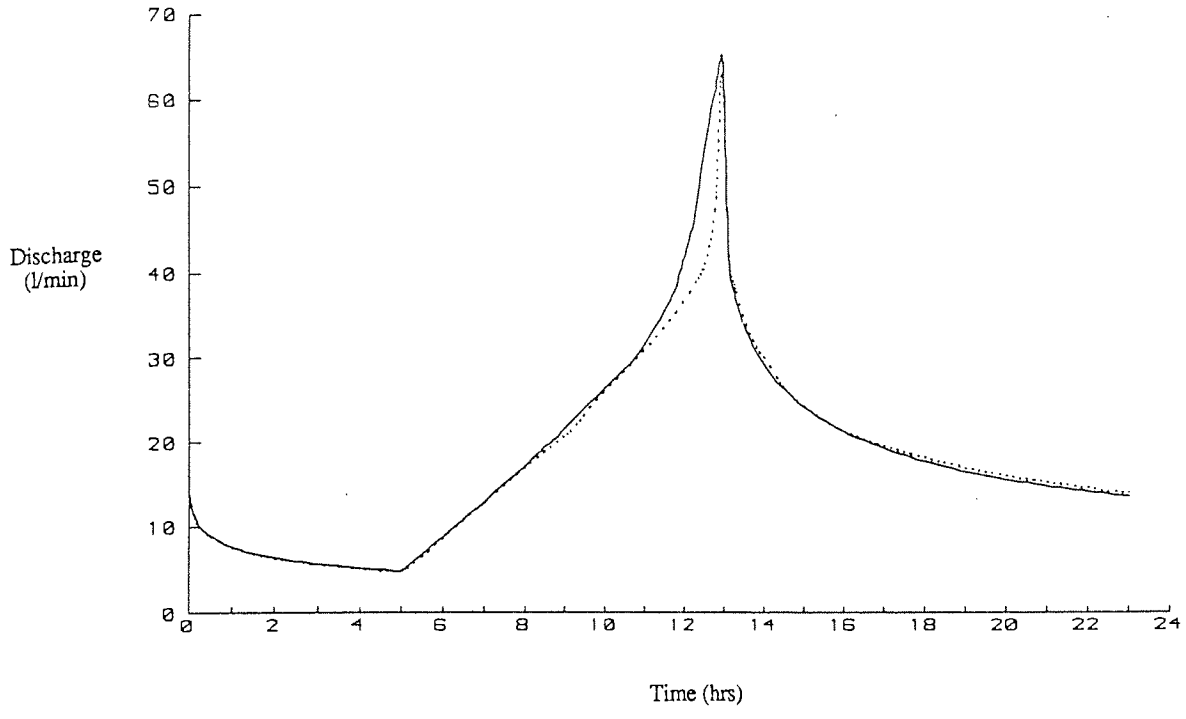

Figure 6.5 Total flow hydrographs for uniform and nonuniform media.
Solid line indicates results from case K1, event 1. Dotted line indicates effective parameter solution.

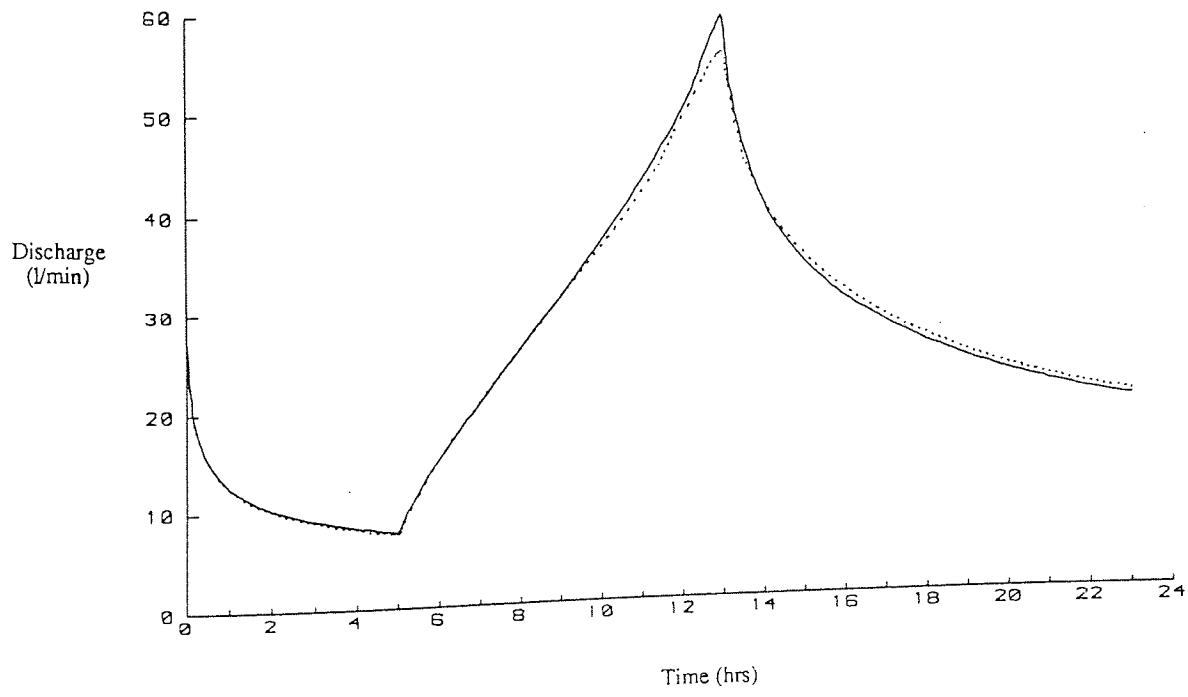

Figure 6.6 Total flow hydrographs for uniform and nonuniform media.
Solid line indicates results from case N2, event 1. Dotted line indicates effective parameter solution.

Table 6.4 Matching errors using effective parameters for cases (B-N) for event (2)

Case	Subsurface flow		Total flow	
	Peak error (%)	Volume error (%)	Peak error (%)	Volume error (%)
B1	-0.867	-0.255	0.367	-0.439
E1	0.419	0.315	0.009	-0.576
E2	1.514	0.007	1.730	-0.582
E3	-0.264	0.554	1.382	-0.004
F1	2.043	-0.229	-0.362	-0.764
F2	0.223	0.903	2.589	0.726
H1	1.218	-0.294	-1.419	-0.907
I1	1.796	-0.416	3.170	-1.025
I2	0.397	0:500	-0.832	0.815
J1	0.883	1.395	0.339	0.878
J2	1.021	0.350	0.657	-0.072
K1	2.749	2.334	-0.165	1.305
K2	1.744	0.609	0.250	-0.736
M1	0.073	-1.213	0.782	-1.699
N1	-2.767	-1.868	-2.670	-2.741
N2	2.991	1.535	-3.409	2.246

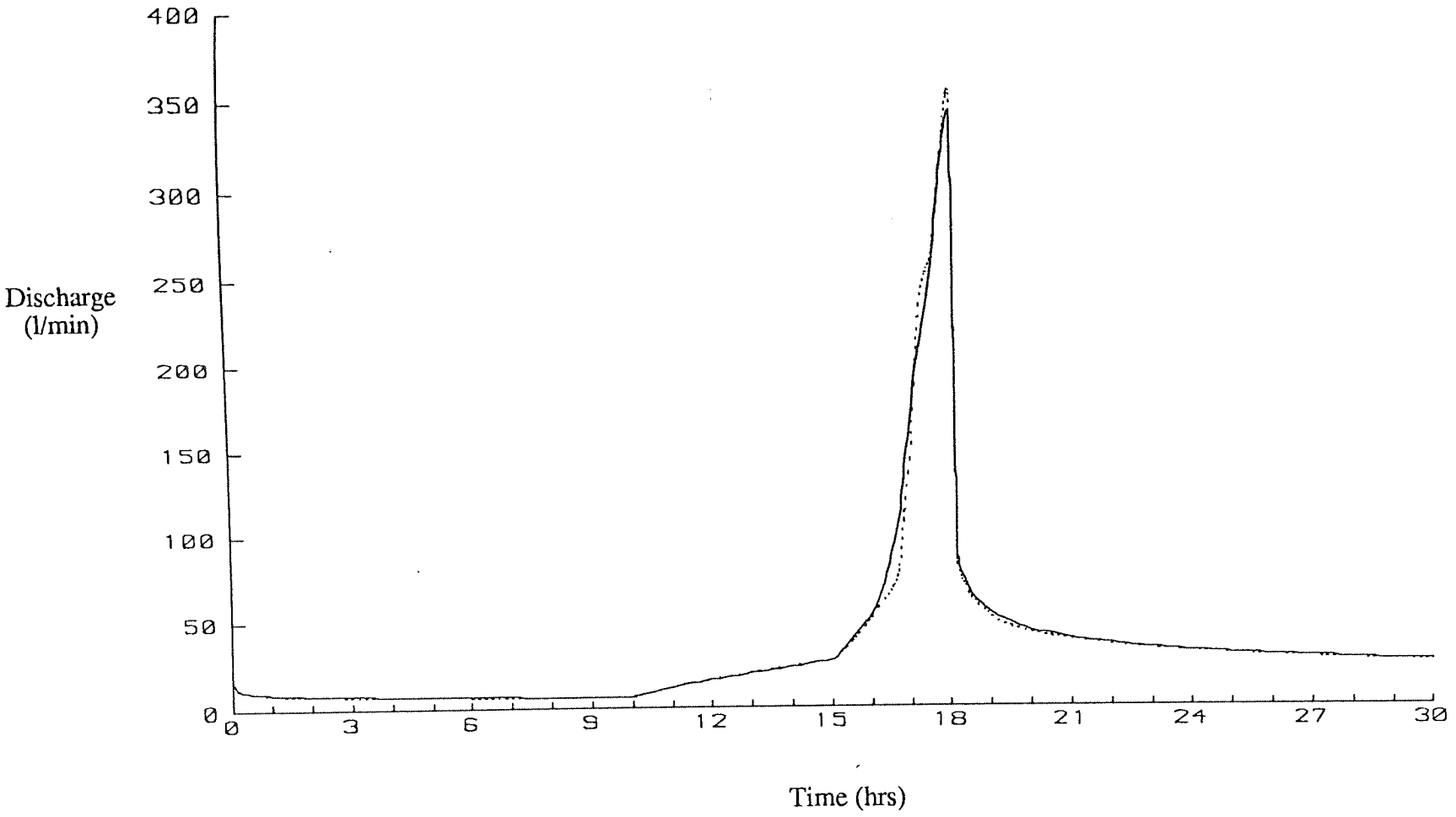

Figure 6.7 Total flow hydrographs for uniform and nonuniform media.
Solid line indicates results from case N2, event 2. Dotted line indicates effective parameter solution.

The harmonic ($\overline{K}_H$), geometric ($\overline{K}_G$) and arithmetic ($\overline{K}_A$) means of the hydraulic conductivity values for each of the sixteen stochastic fields are shown in table 6.5. For most cases, the effective parameter (K_{eff}) is greater than the geometric mean of the distribution. This agrees with the conclusion of previous analyses on simpler flow systems. In four cases (J2, K2, M1 and N1) the effective conductivity is greater than the arithmetic mean. These four cases are examples of highly correlated media and demonstrate the effect of large areas of high conductivity near the base of the slope on the resulting equivalent permeability.

Increasing the variability or autocorrelation of the stochastic field appears to amplify the difference between $\overline{K}_G$ and K_{eff}, although specific trends cannot be evaluated due to the limited number of realizations examined. The most notable result is the fact that under the two events examined, effective parameters were found to be generally suitable under various fields of spatial variability.

6.2.2 Effective parameters for low permeability soils

Five realizations from cases P to S were selected for analysis of effective parameters under conditions of infiltration excess flow. Adopting the same procedure as the previous investigation on high permeability soils, attempts were first made to determine effective values capable of reproducing the volume of subsurface flow. However, since in the examples presented in this section overland flow dominates the hydrograph, the procedure was repeated using the volume of the total flow hydrograph as the matching factor. Conclusions regarding the suitability of effective parameters for both flow types could then be drawn from the results.

The effective hydraulic conductivities for the five cases are shown in table 6.6 together with the population statistics of the conductivity fields. Within this section, P1 refers

Table 6.5 Sample properties for individual realizations from cases (B-N)

Case	K_{eff} (cm/min)	$\overline{K}_H$ (cm/min)	$\overline{K}_G$ (cm/min)	$\overline{K}_A$ (cm/min)
B1	0.05197	0.04416	0.05013	0.05690
E1	0.10304	0.07824	0.10029	0.12855
E2	0.11118	0.07851	0.10041	0.12841
E3	0.09891	0.07835	0.10004	0.12773
F1	0.11929	0.06149	0.10057	0.16450
F2	0.10055	0.06137	0.10005	0.16311
H1	0.21323	0.17736	0.20057	0.22683
I1	0.22159	0.15702	0.20081	0.25681
I2	0.19948	0.15670	0.20007	0.25545
J1	0.09358	0.08533	0.09513	0.10646
J2	0.11882	0.08184	0.09161	0.10256
K1	0.09412	0.07469	0.09319	0.11626
K2	0.13051	0.07050	0.08835	0.11072
M1	0.31794	0.19434	0.21826	0.24512
N1	0.39065	0.17942	0.22630	0.28543
N2	0.18914	0.14938	0.18637	0.23253

Table 6.6 Effective hydraulic conductivities for selected realizations from cases (P-S)

Case	μ_Y (cm/min)	σ_Y^2	K_{eff} (cm/min)
P1	0.005	0.50	0.00546
R1	0.005	0.25	0.00760
R2	0.005	0.25	0.00411
S1	0.005	0.50	0.00908
S2	0.005	0.50	0.00380
PP1	0.005	0.50	0.00465
RR1	0.005	0.25	0.00480
RR2	0.005	0.25	0.00342
SS1	0.005	0.50	0.00445
SS2	0.005	0.50	0.00290

to example 1 of case P, using the subsurface flow hydrograph volume as the output variable of interest as before and PP1 refers to the same case analyzed using the *total* flow hydrograph volume. It can be seen from the values of K_{eff} in table 6.6 that there is a considerable difference between the two effective parameters of a given field.

The matching errors for the ten effective conductivities for event 1 are displayed in table 6.7. A further five cases PP1' to SS2' were also examined. These refer to identical soil properties of cases PP1 to SS2 but differ in the magnitude of surface runoff velocity used to route overland flow. A velocity of 30.0 cm/min was used for these five cases, which corresponds to a likely value on vegetated slopes (see for example Newson and Harrison, 1978; Beven et al., 1984). The overland flow velocity of 250.0 cm/min adopted for the other ten case is more charcteristic of unvegetated slopes. Since the only difference in the responses of case PP1 and PP1', etc is the surface flow routing, the total flow rate is the only output variable affected. Thus, only the matching errors of peak total flow are recorded in table 6.7 for cases PP1' to SS2'.

The unsuitability of reproducing both subsurface flow and total flow hydrographs using a single equivalent porous medium can be seen from the large errors reported in table 6.7. The magnitude of these errors is much greater than those noted earlier in the case of high permeability soil. For example, the 34.724 per cent peak total flow error for case S2 is equivalent to a difference in flow rates of 61.78 l/min (= 6.178% rainfall intensity).

The different results of the two types of effective parameters are demonstrated further in figures 6.8 and 6.9 for cases S2 and SS2 respectively. Matching the subsurface flow in figure 6.8 clearly fails to reproduce the time of onset and rate of the surface runoff. Further examples of effective parameter results for cases PP1 and SS1 are shown in figures 6.10 and 6.11 respectively. The underestimation of subsurface flow rates caused by reducing the effective conductivity to produce greater overland flow

Table 6.7 Matching errors using effective parameters for cases (P-S) for event (1)

Case	Subsurface flow		Total flow	
	Peak error (%)	Volume error (%)	Peak error (%)	Volume error (%)
P1	1.634	-0.788	14.604	16.563
R1	-1.821	-0.696	13.428	16.172
R2	-1.172	0.395	28.494	29.305
S1	-3.160	-0.239	23.198	23.784
S2	-6.621	0.594	34.724	41.115
PP1	16.236	15.115	7.477	1.723
RR1	35.954	34.572	0.215	-1.040
RR2	16.140	20.710	4.585	2.589
SS1	49.242	48.040	3.597	0.774
SS2	18.716	30.104	1.297	3.693
PP1'			4.063	
RR1'			2.813	
RR2'			9.825	
SS1'			1.497	
SS2'			-0.533	

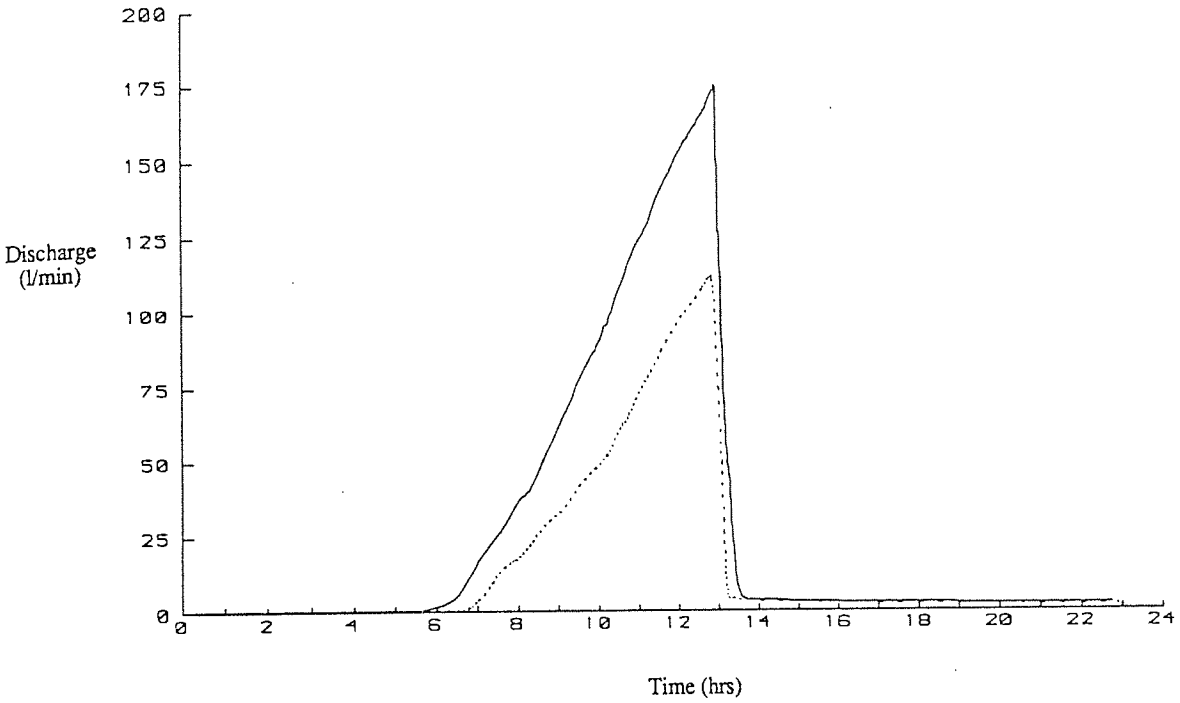

Figure 6.8 Total flow hydrographs for uniform and nonuniform media.
Solid line indicates results from case S2, event 1. Dotted line indicates effective parameter solution.

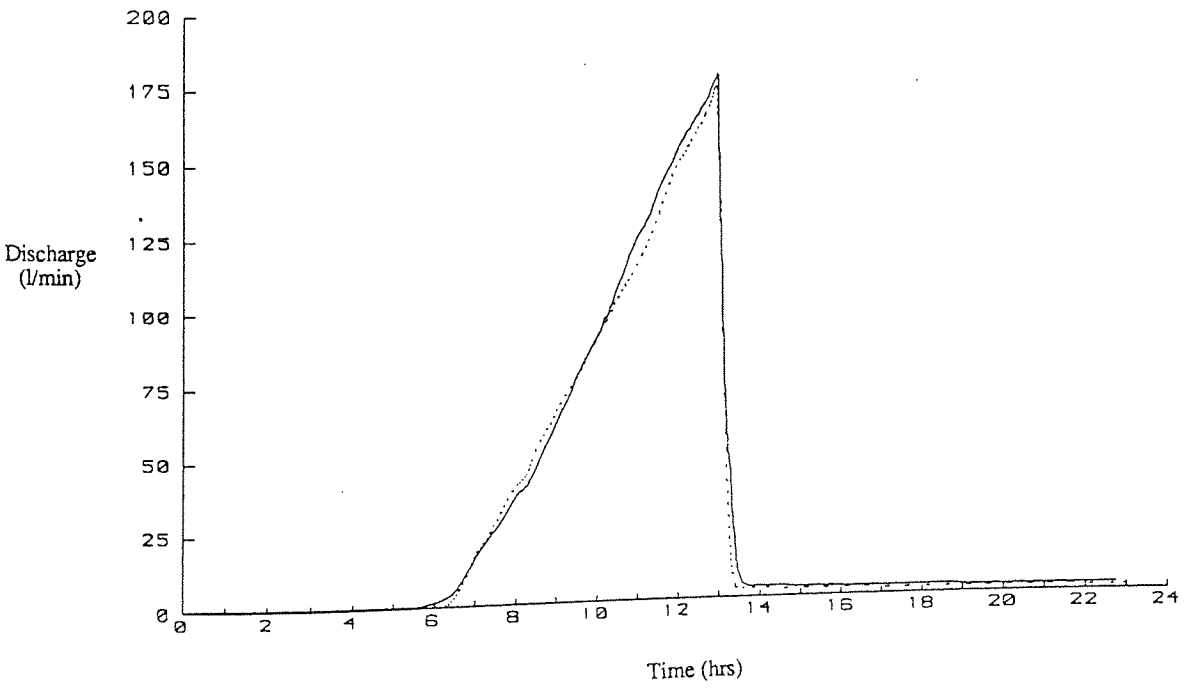

Figure 6.9 Total flow hydrographs for uniform and nonuniform media.
Solid line indicates results from case SS2, event 1. Dotted line indicates effective parameter solution.

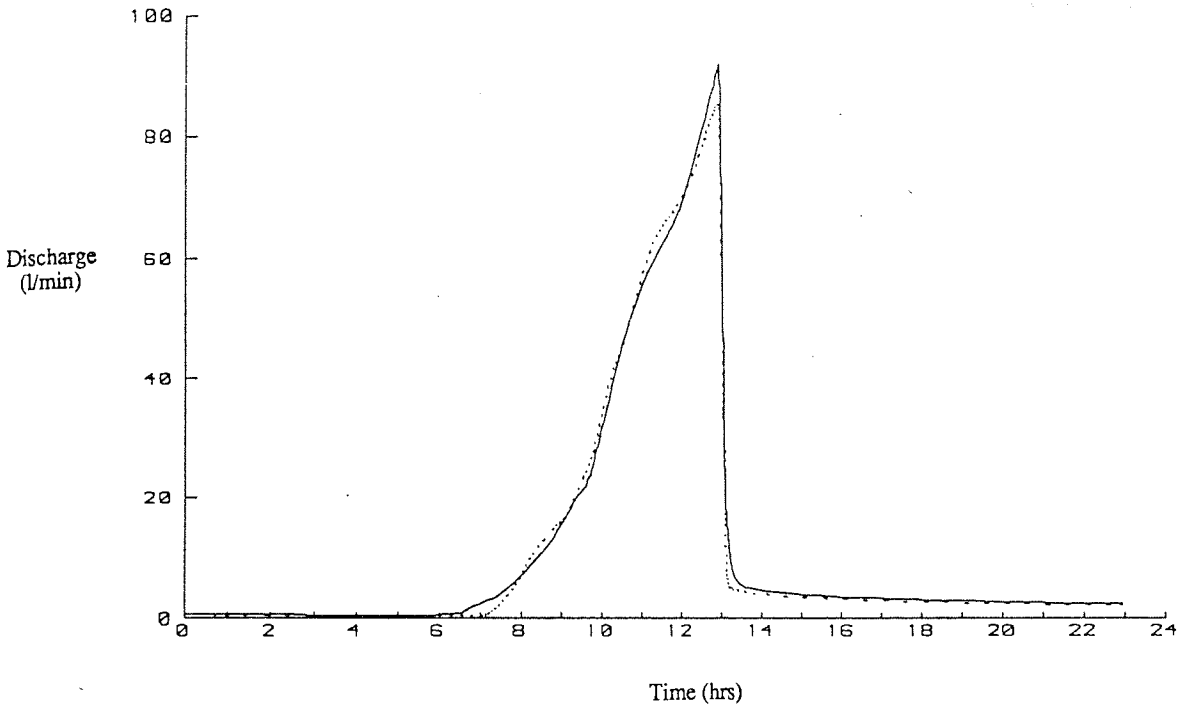

Figure 6.10 Total flow hydrographs for uniform and nonuniform media.
Solid line indicates results from case PP1, event 1. Dotted line indicates effective parameter solution.

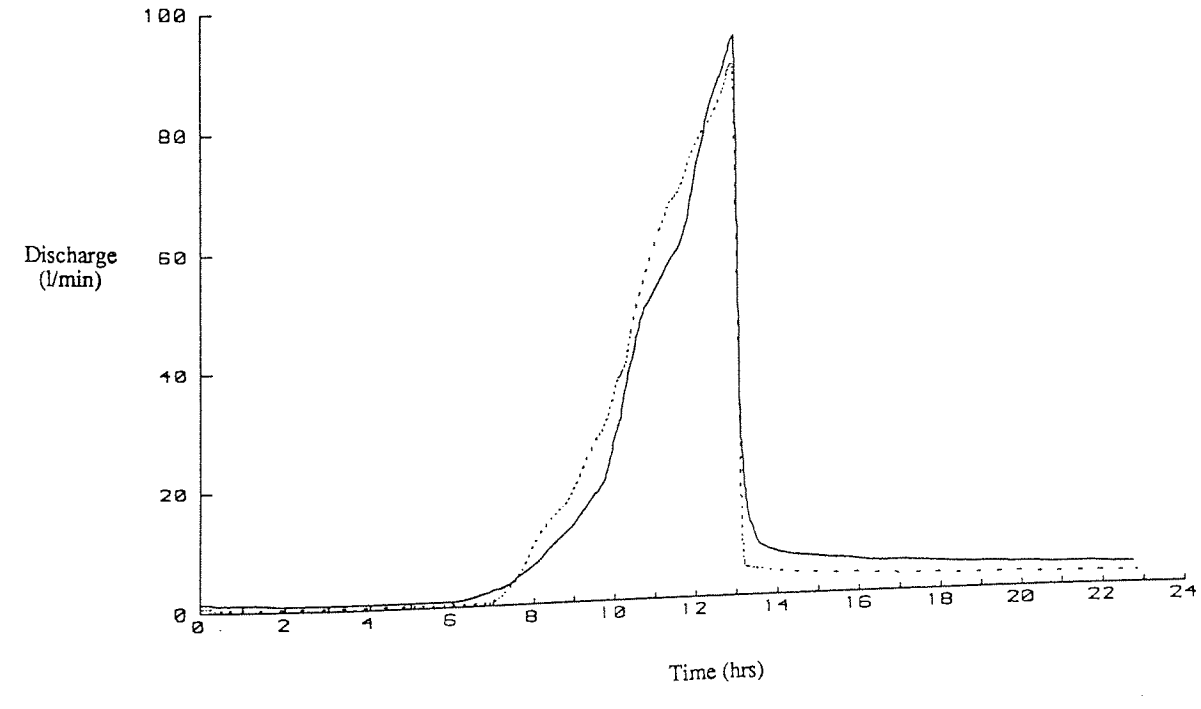

Figure 6.11 Total flow hydrographs for uniform and nonuniform media.
Solid line indicates results from case SS1, event 1. Dotted line indicates effective parameter solution.

volumes can be seen clearly in figure 6.11.

Using the same effective parameters, the matching errors for event 2 are shown in table 6.8. The suitability of reproducing the volume of subsurface flow for cases P1 to S2 is indicated by the low errors reported. However, the effective conductivities for cases PP1 to SS2' fail to provide reasonable estimates of subsurface and surface flow quantities. In these cases the subsurface flow hydrograph is consistently underestimated and the surface flow hydrograph is consistently overestimated. The greater flow rates produced in event 2 imply a greater significance of the percentage errors in table 6.8. For example, the percentage error of -15.420 for case SS2 refers to a difference in peak total flow of 255.44 l/min (= 12.772% maximum rainfall intensity). This underestimation of total flow is shown clearly in figures 6.12 to 6.14. Examples of effective parameter solutions for the low surface runoff velocity case SS2' are shown in figures 6.15 and 6.16 for event 1 and 2 respectively.

The overestimation of surface runoff using effective hydraulic conductivities determined from a lower intensity storm can be explained by considering the range of conductivities, in a given distribution, which contribute to the generation of overland flow. For event 1 the effective parameter will lie within a certain range shown as the shaded region of the frequency distribution in figure 6.17a. For the higher intensity storm of event 2 the range of contributing permeability values increase (figure 6.17b). Thus the effective conductivity is underestimated, resulting in an overestimation of surface runoff.

The sample properties for the individual realizations from cases P to S are shown in table 6.9. As in the case of high permeability soils, an effective hydraulic conductivity greater than the geometric mean of the distribution is required to reproduce the subsurface flow hydrograph volumetrically. However, in order to estimate the total flow hydrograph, an effective parameter much less than the geometric mean is required. The justification of single effective parameter values is not apparent.

Table 6.8 Matching errors using effective parameters for cases (P-S) for event (2)

Case	Subsurface flow		Total flow	
	Peak error (%)	Volume error (%)	Peak error (%)	Volume error (%)
P1	2.331	-0.081	5.581	9.943
R1	-1.077	0.559	36.137	44.473
R2	-8.875	1.289	-1.069	3.732
S1	-0.180	1.817	47.326	57.771
S2	-27.381	0.437	-0.891	4.487
PP1	16.820	14.842	-8.243	-13.894
RR1	36.082	35.932	-14.202	-19.643
RR2	9.662	20.771	-12.745	-15.517
SS1	50.921	50.230	-23.309	-31.377
SS2	41.519	32.336	-15.420	-20.353
PP1'			-9.136	
RR1'			-17.011	
RR2'			-1.222	
SS1'			-24.398	
SS2'			-6.429	

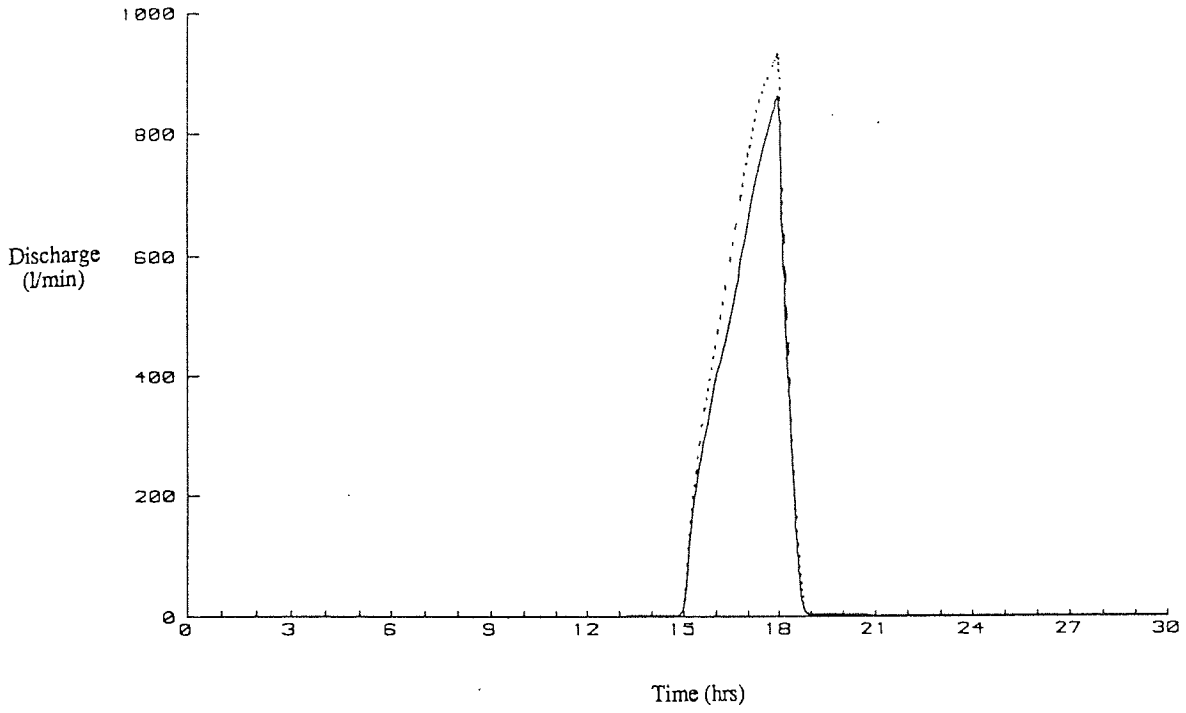

Figure 6.12 Total flow hydrographs for uniform and nonuniform media.
Solid line indicates results from case PP1, event 2. Dotted line indicates effective parameter solution.

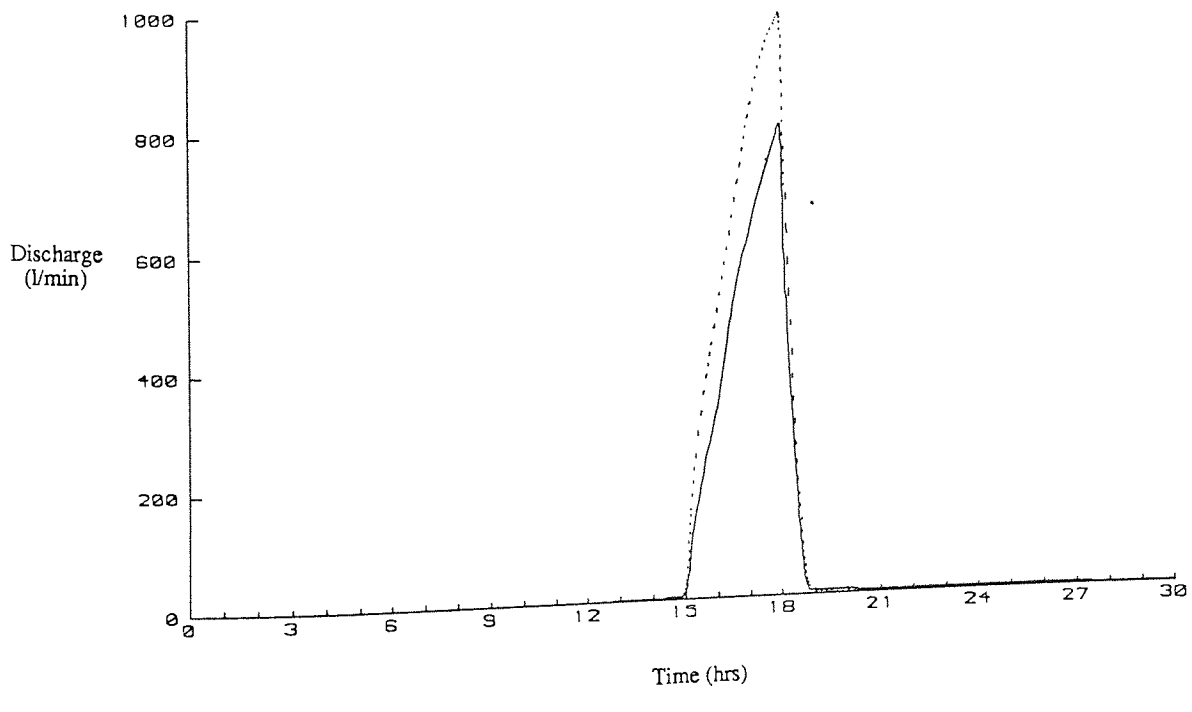

Figure 6.13 Total flow hydrographs for uniform and nonuniform media.
Solid line indicates results from case SS1, event 2. Dotted line indicates effective parameter solution.

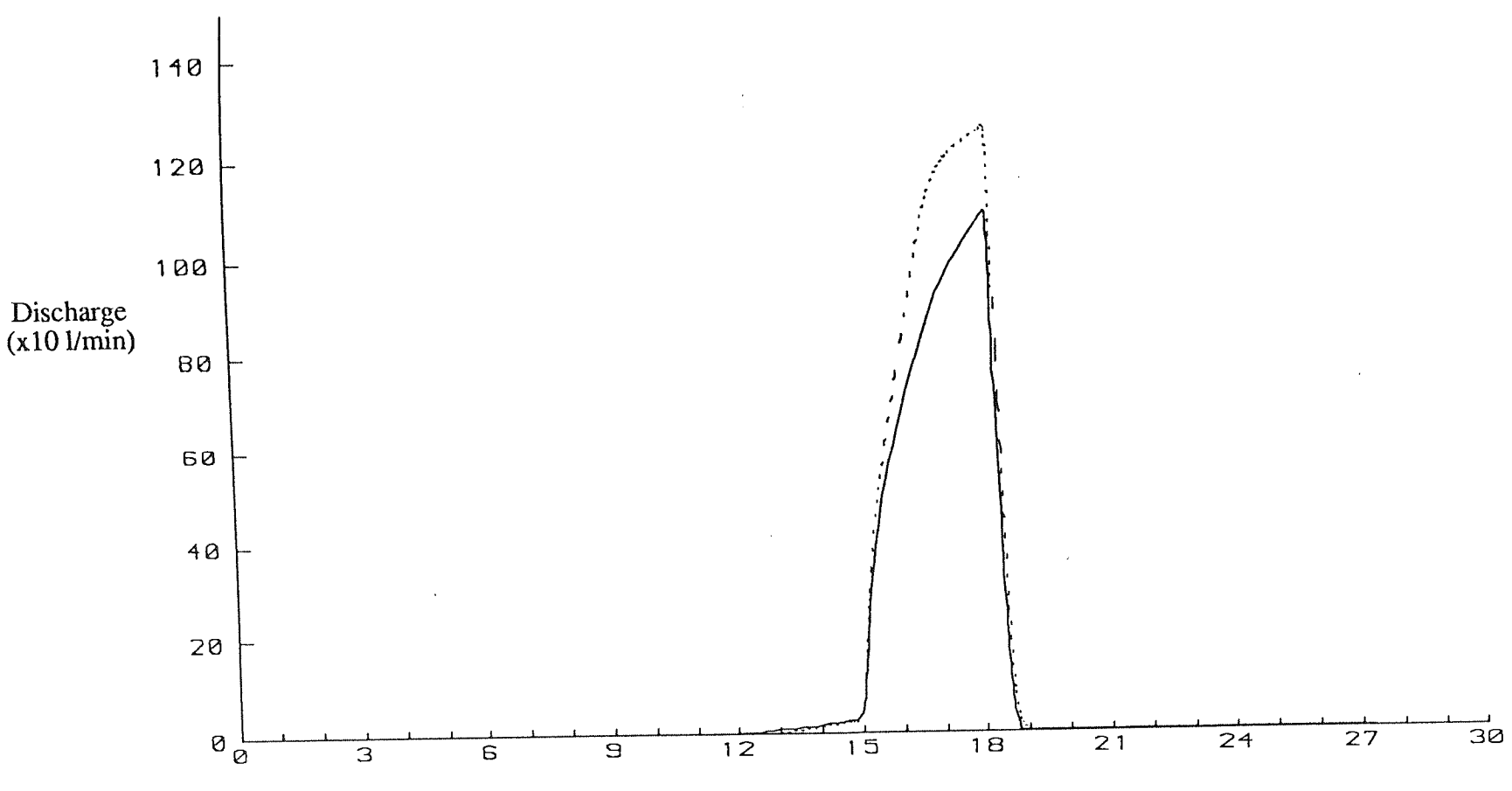

Figure 6.14 Total flow hydrographs for uniform and nonuniform media.
Solid line indicates results from case SS2, event 2. Dotted line indicates effective parameter solution.

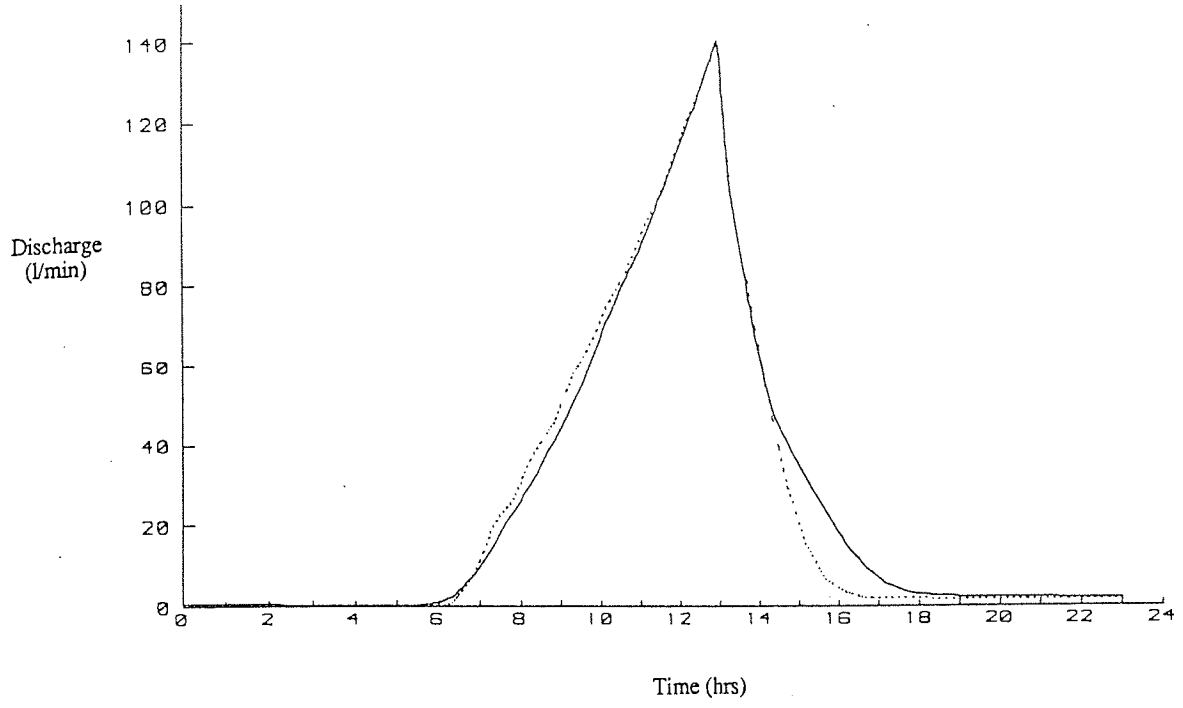

Figure 6.15 Total flow hydrographs for uniform and nonuniform media.
Solid line indicates results from case SS2', event 1. Dotted line indicates effective parameter solution.

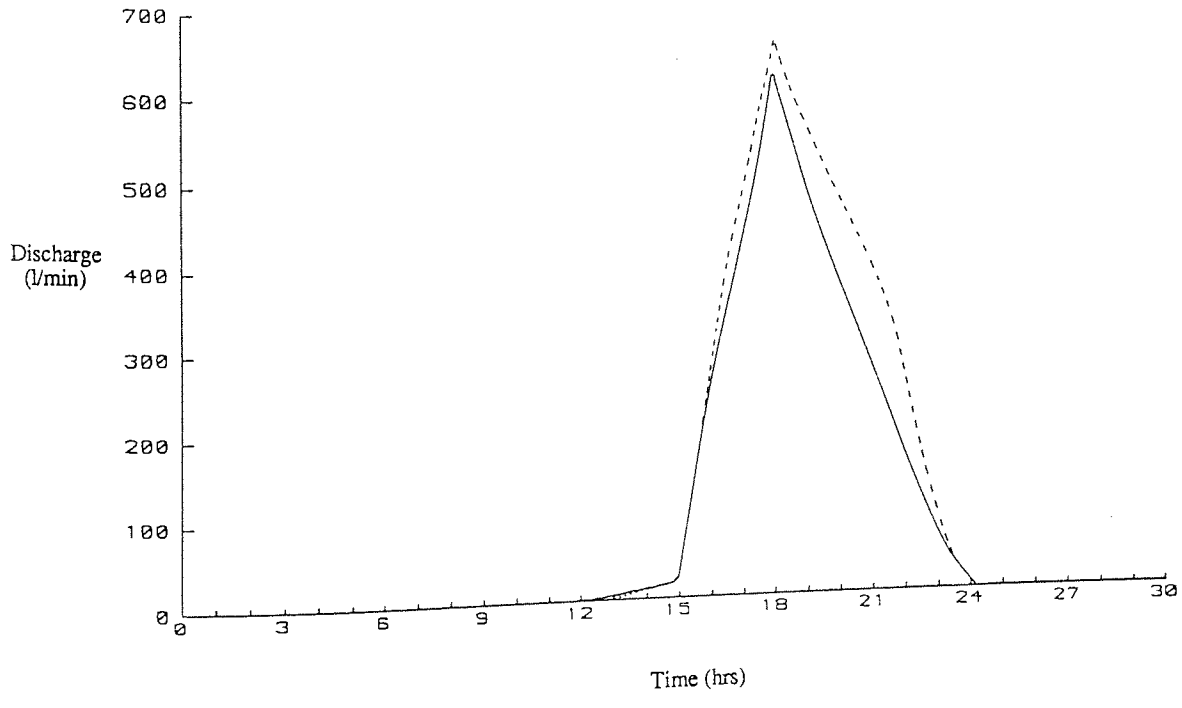

Figure 6.16 Total flow hydrographs for uniform and nonuniform media.
Solid line indicates results from case SS2', event 2. Dotted line indicates effective parameter solution.

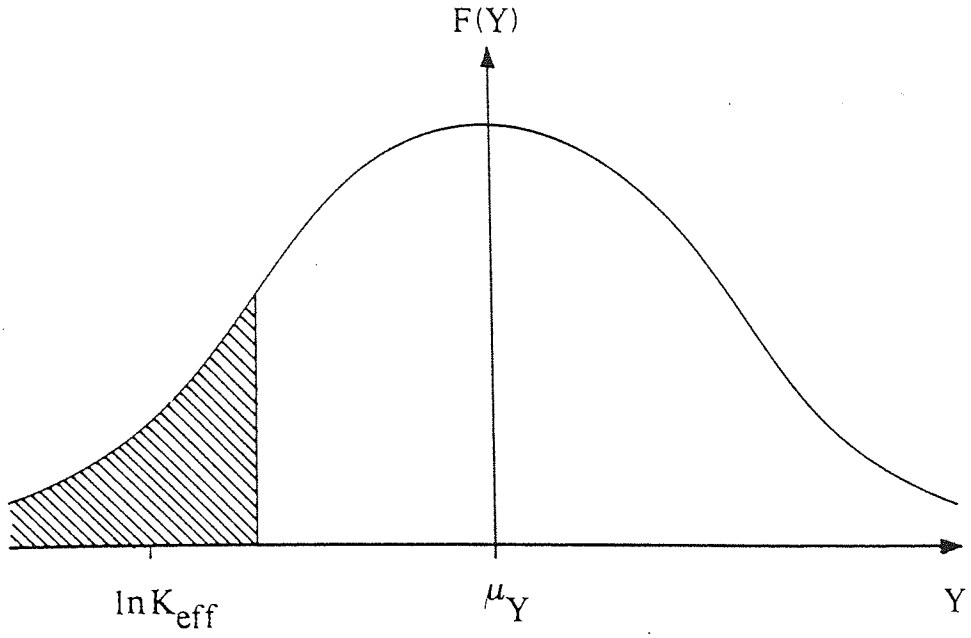

(a)

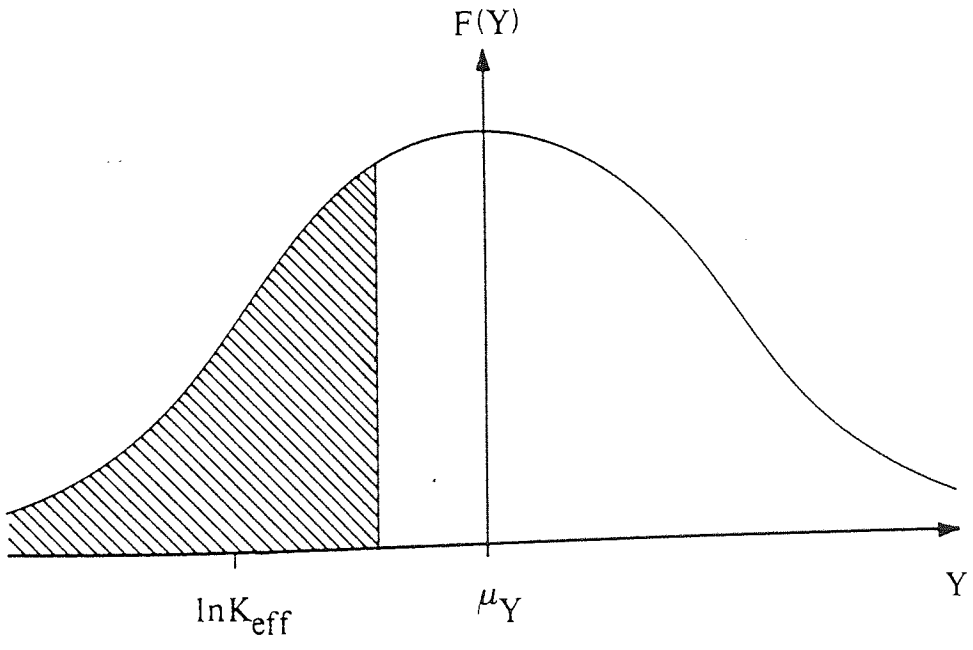

(b)

Figure 6.17 The influence of event conditions on effective parameters for infiltration excess runoff. (a) Low intensity storm. (b) High intensity storm.

Table 6.9 Sample properties for individual realizations from cases (P-S)

Case	K_{eff} (cm/min)	$\overline{K}_H$ (cm/min)	$\overline{K}_G$ (cm/min)	$\overline{K}_A$ (cm/min)
P1	0.00546	0.00393	0.00502	0.00642
R1	0.00760	0.00486	0.00546	0.00613
R2	0.00411	0.00364	0.00404	0.00449
S1	0.00908	0.00449	0.00566	0.00714
S2	0.00380	0.00300	0.00370	0.00456
PP1	0.00465	0.00393	0.00502	0.00642
RR1	0.00480	0.00486	0.00546	0.00613
RR2	0.00342	0.00364	0.00404	0.00449
SS1	0.00445	0.00449	0.00566	0.00714
SS2	0.00290	0.00300	0.00370	0.00456

6.2.3 Effective parameters for soils showing zones of preferential flow

One realization from each of cases T and U was chosen for determination of effective parameters. Matching the subsurface flow hydrograph volume, the equivalent conductivities were found to be 0.09104 and 0.07743 cm/min for cases T1 and U1 respectively. The effective values show significant deviation from the mean conductivity of the soil surrounding the area of preferred flow (= 0.05 cm/min).

The matching errors for cases T1 and U1 for event 1 are presented in table 6.10. The zone of high permeability in case T1 has clearly more effect than that of U1 , the 10.365 per cent peak total flow error is equivalent to a difference of 7.77 l/min between uniform and nonuniform responses. The total flow hydrographs for the two realizations together with the corresponding effective parameter results are shown in figures 6.18 and 6.19. The subsurface flow repsonses using the equivalent permeabilities compare well with the results of the nonuniform slopes. However, increasing the equivalent conductivity to account for the area of preferred flow clearly reduces the quantity of surface runoff and delays the time of onset of surface saturation.

Table 6.11 displays the matching errors of the hydrographs for event 2. Surprisingly the subsurface flow responses to the uniform slopes show significant error, unlike the cases discussed in the previous two sections. The subsurface flow rates are consistently underestimated by the effective parameters, although an overestimation of surface runoff reduces the errors of the total flow hydrograph. The total flow hydrographs for case T1 and the suggested equivalent medium are shown in figure 6.20. The responses compare favourably. Such close agreement would not be expected under a rainfall intensity approximating the conductivity of the soil surrounding the area of preferred flow, as under such conditions considerable surface runoff originating from infiltration excess would be produced on the nonuniform

Table 6.10 Matching errors using effective parameters for cases (T,U) for event (1)

Case	Subsurface flow		Total flow	
	Peak error (%)	Volume error (%)	Peak error (%)	Volume error (%)
T1	0.560	-0.008	10.365	4.327
U1	1.004	-0.018	-0.095	2.520

Table 6.11 Matching errors using effective parameters for cases (T,U) for event (2)

Case	Subsurface flow		Total flow	
	Peak error (%)	Volume error (%)	Peak error (%)	Volume error (%)
T1	11.427	11.390	-2.517	6.417
U1	5.355	5.100	-0.088	2.294

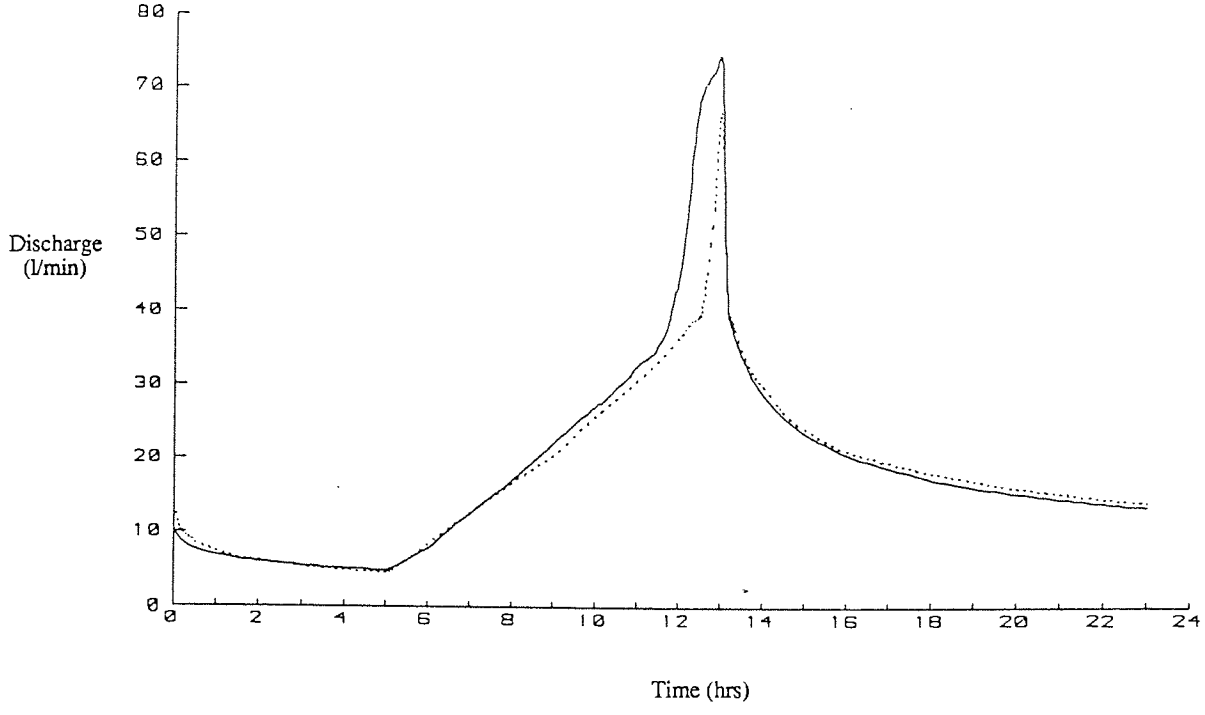

Figure 6.18 Total flow hydrographs for uniform and nonuniform media.
Solid line indicates results from case T1, event 1. Dotted line indicates effective parameter solution.

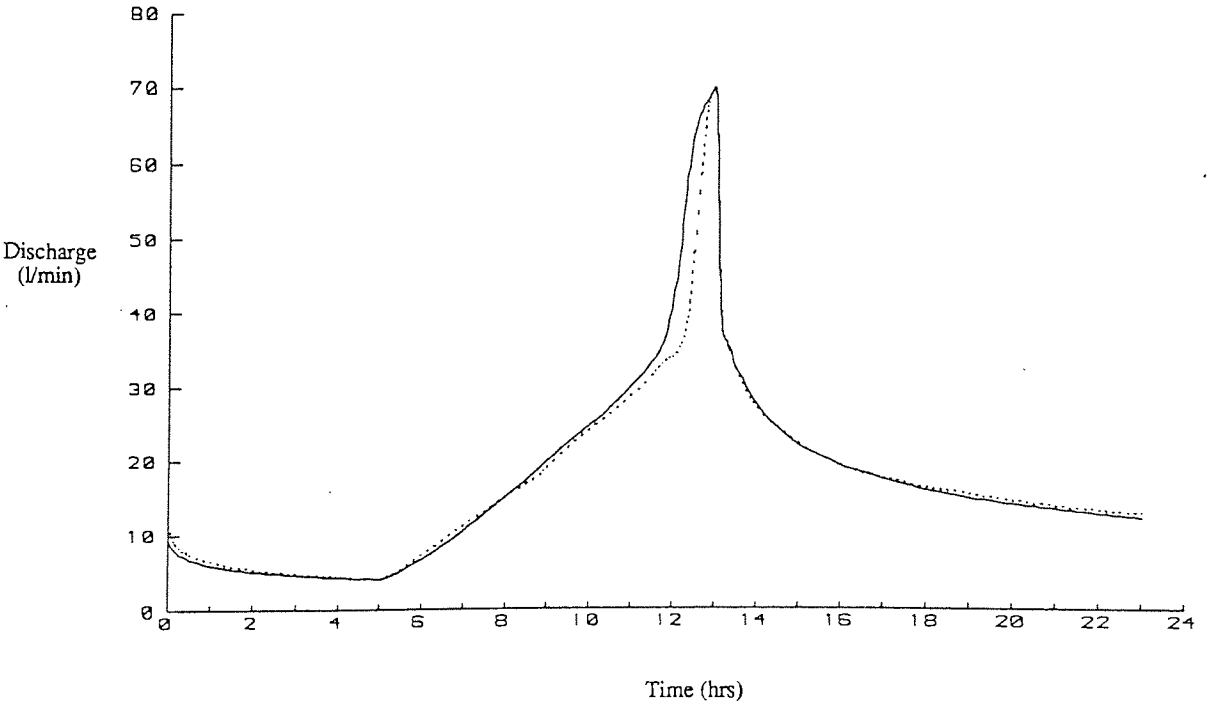

Figure 6.19 Total flow hydrographs for uniform and nonuniform media.
Solid line indicates results from case U1, event 1. Dotted line indicates effective parameter solution.

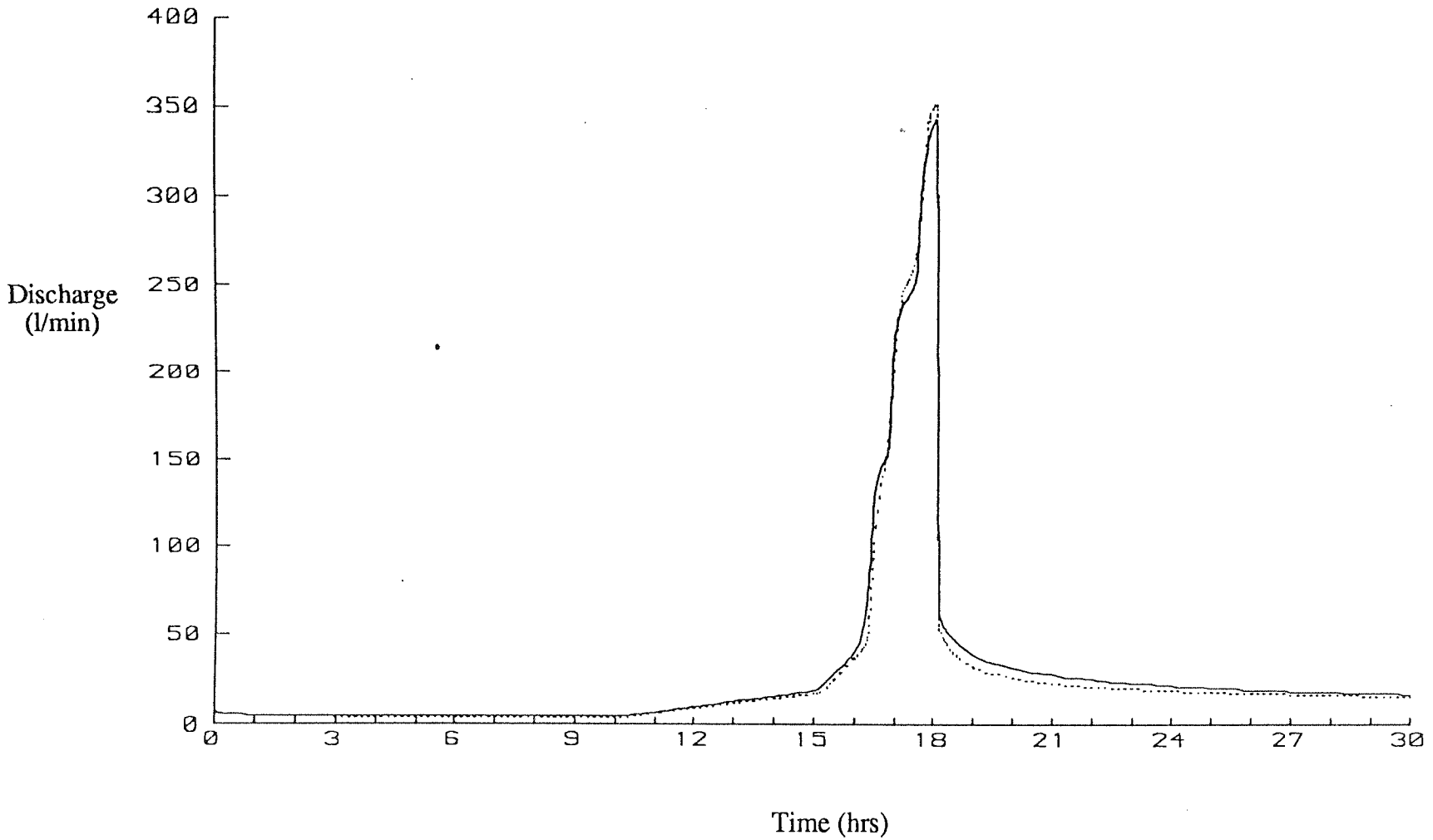

Figure 6.20 Total flow hydrographs for uniform and nonuniform media.
Solid line indicates results from case T1, event 2. Dotted line indicates effective parameter solution.

slopes. Overland flow generated on the uniform soil would be limited to a confined area of surface saturation at the base of the slope.

6.3 SUMMARY AND CONCLUSIONS

Previous studies of effective parameters have directed attention to simplified generalized flow domains, such as steady saturated groundwater movement. Investigations of three dimensional variably saturated flow in porous media are not evident in the literature. Furthermore, analyses of hillslope flow processes using effective parameters are scarce, although the results of such studies are clearly important if current physically based modelling techniques of catchment hydrology are to be recognized as practical tools.

Investigations of groundwater movement have suggested that the geometric mean of a log normally spatially distributed saturated hydraulic conductivity field provides a reasonable estimate of an equivalent uniform property. Although a greater value may be necessary for stochastic fields of high variability. The time dependent nature of effective permeabilities has also been postulated for unsteady flow systems.

There are two major differences between the analysis presented herein and in previous studies. Firstly, the complexity of the flow domain under investigation, in terms of the number of spatial dimensions and flow processes recognized, is much greater than those investigated earlier. Secondly, the concept of effective parameters of single realizations, representing individual soil formations, adopted in this study has previously been overlooked.

Using the results from various hydraulic conductivity fields presented in Chapters 4 and 5, attempts were made to select suitable equivalent soil properties capable of reproducing the response to a single event. In the case of high permeability soils,

effective parameters were found to give reasonable estimates under a variety of hydraulic conductivity fields. These values were also shown to be suitable for a completely different event. For low permeability soils, characterized by the domination of the hydrograph by surface runoff, a single effective parameter was not found to be capable of reproducing both subsurface and surface flow hydrographs. Matching the subsurface flow, in this case, consistently underestimated the surface runoff, matching the total flow hydrograph underestimated the subsurface flow response. Application of the selected effective parameters to a second event revealed the event dependency of the equivalent properties.

The event dependent nature of the effective parameters was also noted in the case of soils displaying distinct zones of preferred flow, although the matching errors reported in this case were much smaller than those for the low permeability soils.

The results of this study therefore suggest that under nonuniform homogeneous soil formations, the subsurface flow response to a single hillslope may be represented by that of a single effective hydraulic conductivity. The value of this effective parameter may not be obtained explicitly from the statistics of the distribution, although it is likely to be greater than the geometric mean of the log normally distributed conductivity field. In fact such a result is not surprising as lumped conceptual models have shown to work well in many cases. For inhomogeneous soils such as those showing localized areas of high conductance, effective parameters may not be appropriate. Further investigations are clearly required.

In the case of low permeability soils, single effective parameter values appear invalid for the modelling of both flow processes. Under conditions of infiltration excess flow a minimum of two parameters may be necessary to reproduce both peak flows and low base flows.

Chapter 7

Conclusions

7.1 INTRODUCTION

Over the past decade much attention has been devoted to the development of distributed physically based models of catchment hydrology. A number of these models, such as the Systēme Hydrologique Europēen (SHE) and the Institute of Hydrology Distributed Model (IHDM), have now reached the testing stage and will soon be available for industrial applications. The ability to simulate responses of ungauged catchments is only provided within a physically based framework, however physically based models require vast amounts of data and computing resources in comparison to earlier generations of catchment models. Loage and Freeze (1985) have recently demonstrated that physically based models may not have any advantage over simpler models on gauged catchments. In fact, unless investigating the effects of catchment changes, the relative inexpensive costs and familiarity of less complex models offer distinct advantages on gauged catchments. Physically based models, therefore, can play a useful role in the engineering and hydrological societies, however, several limitations are inherent with the current physically based modelling strategy.

Ample evidence of soil spatial variability is presented in the literature, the incorporation of which is permissible in physically based models, although immense data requirements have at present restricted the use of this information. It is generally assumed that areas of the flow domain can be represented by some equivalent soil property (or effective model parameter). Along similar lines, treating nodal areas of the model grid as homogeneous zones is based on the assumption that the model equations developed at the micro scale are valid at the model grid scale. In the case of the SHE model this may be in the order of 250 m x 250 m. Empirical equations such as Darcy's Law may not be valid at the model grid scale, or indeed at the micro scale.

In a discussion of the validity of current modelling techniques, Beven (1986) remarked that,

> "For now, it is sufficient to conclude that the current generation of distributed physically based models are lumped conceptual models".

The use of Darcy's Law also requires thorough justification if one is to attempt to model catchments composed of soils containing macropores or displaying distinct areas of preferred flow through natural soil pipes.

7.2 IMPLICATIONS FOR CURRENT PHYSICALLY BASED MODELLING

This study set out to investigate the applicability of current physically based modelling techniques on two related phenomena, namely soil spatial variability and zones of preferential flow. The investigation was carried out at the hillslope scale to assess the effects of soil spatial variabilty and preferential flow on hillslope hydrology and then determine whether the concept of effective model parameters can be justified at this scale.

In order to carry out the necessary hydrological simulations a fully three dimensional model of variably saturated flow through porous media was developed. The model is based on the Galerkin approximation of the finite element method and allows detailed analysis of the complex hillslope hydrological processes. Accessibility to the vector processor of a CDC Cyber 205 supercomputer permitted numerical solutions on grids containing several thousand node points. A hypothetical hillslope segment was developed for the purpose of this study, soil properties of the hillslope were based on measured values of real soils.

There are many studies in the literature on the effect of spatial variability of soil properties, in particular saturated hydraulic conductivity, on groundwater flow. Using either Monte Carlo simulation or analytical expressions based on perturbation methods, various degrees of complexity have been previously analyzed. It is clear from the results of these investigations that increasing the number of spatial dimensions of the flow problem reduces the effect of any soil nonuniformity, although analyses of three dimensional flow domains are scarce. The study of spatial variability of hydraulic conductivity presented herein is the first to examine three dimensional unsteady flow in variably saturated media. Moreover, the specific application to hillslope hydrology is more directly related to the problem of catchment modelling than several previous studies of generalized flow domains.

Adopting a suitable range of statistical parameters (means, variances and autocovariances) of hydraulic conductivity fields suggested by previous field studies, a number of random fields were generated within the hillslope using the turning bands method. The response of the hillslope to a single deterministic event was then evaluated for several realizations of a given stochastic field. Operational costs of the three dimensional analysis limited the number of realizations to ten, which gave a reasonable impression of the variation of responses.

Two distinct mechanisms of hillslope runoff generation were addressed. In the first case, categorized by relatively high permeability soils, the effects of spatial variability were slight. Significant differences between individual realization responses were only noted in highly correlated media. Much greater effects were evident in the case of low permeability soils, for which the discharge hydrograph was dominated by surface runoff. The variability of hydraulic head throughout the soil mass was also shown to be considerably larger for low permeability soils. In both cases the variation of runoff between realizations was noted to be time dependent. Limiting the study to a single deterministic event restricts the generality of the results presented herein, however it appears that under conditions of high permeability the effects of spatial variability are

likely to average out over the flow domain. In the case of low permeability soils, the variance and autocovariance of the soil formation are important model parameters. Increasing the autocorrelation of the hydraulic conductivity distribution in both high and low permeability soils had an effect equivalent to increasing the variance.

The phenomenon of zones of preferential flow was addressed in Chapter 5. Very few studies have attempted to assess the importance of such zones either in the form of natural soil pipes or areas of very high permeability. Barcelo and Nieber (1981) have shown that a single soil pipe within a hypothetical hillslope segment may have a significant effect on the resulting subsurface flow hydrograph. The validity of the pipe flow equation used in their study raises some doubt. In addition, the hydrological interaction of the soil mass and pipe was simplified to the extent that only recharge from the saturated soil matrix was considered.

A number of possible approaches to the problem of determining the effects of zones of preferential flow were postulated. The most suitable was found to be similar to that used in the study of soil spatial variability. By specifying some functional form of a hydraulic conductivity distribution, an artificial zone of high permeability was introduced into an otherwise homogeneous soil. Such a representation is comparable to the 'percolines' observed by Bunting (1961). Using the same hillslope segment and event conditions as in the earlier study of soil variability, two different three dimensional fields of high hydraulic conductivity were investigated. Introducing a random component to these trends, ten realizations of each distribution were simulated, although little difference between the results of each realization was observed.

In comparison with the results from the nonuniform homogeneous formations, introducing an area of high permeability had a maximum effect of increasing the peak subsurface flow by 28 per cent. However, the effect on total runoff was less significant due to the reduction in surface runoff in the case of preferred flow. The

total volume of runoff was increased by approximately 30 per cent. Little effect on the shape of the discharge hydrograph was noted in both cases. The area of high permeability had a much greater influence on the moisture profiles within the soil mass. Significant variation in moisture content with depth demonstrated the effect of an impeding layer of low conductivity at the base of the slope. Such an effect was only observed near the centre of the hillslope, the zone of preferred flow apparently had little area of influence. As expected, the effect of preferred flow was more significant during the wetting stage of the event, moisture profiles at distances over 30 metres from the base of the slope at the end of the ten hour drainage period were similar to those in the homogeneous field.

The general conclusion drawn from this short study of zones of preferential flow is that such a phenomenon makes a significant contribution to hillslope hydrology. Over simplification of the hillslope processes in current physically based models may produce erroneous predictions.

Using the results from the studies of soil variability in Chapters 4 and 5, the concept of equivalent uniform hillslopes was investigated in Chapter 6. Previous studies of groundwater movement have suggested the suitability of effective soil properties, although analyses have been limited to relatively simple flow systems. Furthermore, specific studies of effective parameters in catchment modelling are not evident in the literature. By investigating the representation of an individual realization of soil variability by a uniform hillsope, as used in current modelling techniques, it is felt that the results presented herein are likely to be of greater practical value than previous multi-realization analyses of generalized flow domains.

The study of equivalent hillslopes was separated into sections referring to three types of soil formations, which were high mean permeability soils, low mean permeability soils and soils displaying zones of high conductivity. In the first case, characterized by subsurface flow domination of the hydrograph, effective permeabilities were found

to be suitable for a single deterministic rainfall event. Generally, errors in producing the hydrograph from a hillslope of nonuniform soil properties were found to be relatively small, any major differences arising at the onset of surface runoff in the nonuniform fields. In order to test the suitability of the selected uniform properties, a comparison of the responses of an entirely different event was made. Both subsurface and surface flow (produced by surface saturation) hydrographs were represented successfully for this second event. The determination of suitable effective parameters, given *a priori* estimates of the field variability is clearly important if accurate predictions are to be made on real catchments. A comparison of the effective values and the properties of the represented stochastic fields, however, revealed the complexity of the problem. In general, the equivalent hydraulic conductivities were found to be greater than the geometric mean of the log normally distributed block conductivities, agreeing with the results of previous investigations. Specific relationships between the effective parameters and the sample properties could not be evaluated due to the limited number of realizations under examination.

For the case of low mean permeability soils, characterized by the domination of the runoff hydrograph by infiltration excess overland flow, single effective parameters were not capable of reproducing both subsurface and surface flows. An equivalent property selected to match the volume of subsurface runoff from the first event was found to be reasonably consistent for the second event. However, for both events the total flow was underestimated in all cases. Attempts to use the volume of total runoff as the matching factor also proved unsuccessful. The effective parameter simulations in this case were found to consistently underestimate the subsurface flow, moreover, the event based dependency of such an effective hydraulic conductivity was demonstrated. A comparison of the effective parameter values with the sample properties for each realization revealed that, as in the case of high permeability soils, the effective subsurface flow parameters were greater than the geometric mean conductivity. The effective total flow parameters, however, were much less than the geometric mean, in fact, for the first event, the harmonic mean conductivity provided a

better estimate. The results clearly demonstrate that, in the case of infiltration excess flow dominating the hydrograph, single effective parameters are inappropriate in current physically based models. Under such conditions one may be able to reproduce a number of observed events using effective model parameters, although the accuracy of the simulations of sub processes will be in doubt. One may then discover grossly erroneous predictions during other hydrological events.

In the case of soils showing zones of preferred flow, effective parameters for subsurface flow responses were shown to be event dependent, unlike the previous soils examined. The area of high conductivity is more significant under high intensity storms thus increasing the magnitude of the required effective conductivity. In doing so the amount of surface runoff is underestimated. Therefore, as in the case of low permeability soils, reasonable predictions of observed events may only be expected under similar conditions if single effective parameters are to be used.

Further work is required to assess the effect of soil variability under various conditions for a number of soil types. Investigations at the catchment scale would also provide useful information. In fact, under the guidance of the author, the model described in Chapter 3 is currently being used at Princeton University, USA for such a study.

7.3 IMPLICATIONS FOR FUTURE PHYSICALLY BASED MODELLING

If one assumes the applicability of effective parameters in the modelling of hillslope runoff generation, the determination of such values is clearly of practical concern. If historic records exist for a catchment then these may be used to determine effective parameters for inclusion within a rainfall runoff model such as the IHDM. Since the effective parameters so derived may bear no formal relationship to the soil properties measured in the field, the rainfall runoff model cannot be considered to be physically

based. Using a more detailed model, such as that used throughout this study, one may be able to determine the formal relationships between the effective parameters of the conceptualized model and the field measured properties.

If the hydrological regime of a catchment is changed then modelling the response of that catchment using historical data is much more difficult. If relationships between effective and measured parameters are established, as described above, then the same relationships may hold for the new regime.

In applying physically based models to ungauged catchments, the determination of effective properties poses greater problems. One may find that under certain conditions of spatial variability the mean of several field measurements provide a suitable effective parameter. Nevertheless, it appears unlikely that single hydrological predictions from physically based models will provide design information of suitable accuracy for future engineering works. There will undoubtably be uncertainty in these predictions. If the extent of uncertainty can be evaluated and is shown to be reasonably small then models based on the physics of the catchment may provide useful design tools.

Data is now becoming available (see for example Rawls et al., 1983; Cosby et al., 1984) relating soil properties, including variances, to textural classes. Knowledge of the various soil textures within a catchment may then be able to provide estimates of the model parameters. .Using the uncertainty of the model parameters, methods such as that of Rosenbleuth (1975) could be used to determine the uncertainty in model predictions.

This study has shown that effective parameters may not be appropriate in the modelling of hillslope runoff generation when infiltration excess surface runoff is a dominating mechanism, although the occurrences of such a process are likely to be isolated to a minority of catchments. Under such conditions a minimum of two

effective parameters are necessary if accurate predictions of both subsurface and surface flows are required. One possible solution to this problem is to form a composite hydrograph from a number of simulations. For example, combining the results of two independent simulations, obtained for uniform soils of different properties, is likely to provide less error in the predicted overall response than using a single simulation. If the nature of the spatial variability were known *a priori* then suitable properties of the uniform media may be selected according to the probability distribution, for example, $K_s = \mu \pm \sigma$ for the case above. The combination of the multiple simulations would clearly require calibration from previous records. In addition, the stationarity of the combination function is necessary if future predictions are to be made. Such an approach undermines the true to life nature thought to exist in current physically based models, although future research into ideas such as this is required before these models can be accepted as engineering tools.

There is also serious doubt about the validity of representing real soils containing macropores with a matrix flow model. Sloan and Moore (1984) suggest that a simple storage model based on the kinematic assumption is more suitable than a Richards equation formulation for modelling subsurface stormflow through soils containing macropores, due to the rapid response of the former model. However, adopting such an approach conceptualizes the model further.

It appears unlikely in the short term that equations of greater theoretical justification will be made available to hydrological modellers. By exploring possible enhancements to the present modelling strategy in conjuction with applications to real catchments we must quantify the future role of current physically based models and assess the economic viability of using such models as engineering tools.

The increasing availability of high speed computer hardware will permit large scale applications of physically based models to real world problems. In addition, data bases such as those provided by remote sensing techniques are likely to be invaluable sources of information for future studies. The potential for further research is there, it should be capitalized upon.

Appendix 1

Infiltrometer data

Table A1.1 Variation of final infiltration rates over Eastergrounds field

Infiltrometer plot	Final infiltration rate A ($x10^{-4}$ cm/s)	Ln A
1	2.332	0.847
2	15.038	2.711
3	0.801	-0.222
4	8.230	2.108
5	21.447	3.066
6	7.707	2.042
7	0.851	-0.161
8	1.829	0.604
9	1.108	0.103
10	8.562	2.147
11	11.762	2.465
12	13.261	2.585
13	4.033	1.395
14	6.961	1.940
15	6.265	1.835
16	4.750	1.558
17	0.517	-0.660
18	6.179	1.821
19	0.168	-1.784
20	15.985	2.772
21	2.130	0.756
22	1.906	0.645
23	1.675	0.516
24	13.062	2.570
25	18.171	2.900
26	6.728	1.906
27	27.512	3.315
28	4.921	1.594
29	36.959	3.610
30	1.375	0.318
31	1.448	0.370
32	1.242	0.217

Table A1.2 Final infiltration rates along 100 metre transect

Infiltrometer plot	Distance from plot 4 (m)	Final infiltration rate A ($x10^{-4}$ cm/s)	Ln A
4	0.00	8.230	-7.103
33	10.00	3.313	-8.012
5	20.00	21.447	-6.145
34	30.00	1.909	-8.564
6	40.00	7.707	-7.168
58	41.25	14.110	-6.563
57	42.50	1.778	-8.635
56	43.75	1.941	-8.547
55	45.00	13.763	-6.588
54	46.25	9.828	-6.925
53	47.50	0.682	-9.593
52	48.75	1.112	-9.104
35	50.00	3.744	-7.890
51	51.25	0.907	-9.308
50	52.50	0.933	-9.280
49	53.75	7.513	-7.194
48	55.00	1.472	-8.824
47	56.25	2.145	-8.447
46	57.50	3.259	-8.029
45	58.75	0.917	-9.297
7	60.00	0.851	-9.372
38	61.25	4.345	-7.741
39	62.50	1.220	-9.011
40	63.75	2.046	-8.494
41	65.00	1.740	-8.656
42	66.25	1.391	-8.880
43	67.50	4.056	-7.810
44	68.75	0.283	-10.473
36	70.00	2.295	-8.219
59	71.25	4.695	-7.664
60	72.50	1.872	-8.583
61	73.75	0.669	-9.612
62	75.00	1.389	-8.882
63	76.25	1.888	-8.575
64	77.50	0.247	-10.602
65	78.75	0.493	-9.918
8	80.00	1.829	-8.607
66	81.25	1.548	-8.773
67	82.50	1.955	-8.540
68	83.75	0.404	-10.117
69	85.00	2.891	-8.149
70	86.25	6.956	-7.271
71	87.50	1.170	-9.053
72	88.75	5.568	-7.493
37	90.00	7.464	-7.200
9	100.00	1.108	-9.108

Appendix 2

Program listings

This appendix contains the listings of three computer files: (i) the finite element code (VSAT3D), (ii) an example mesh data generation program (INDAT), (iii) the necessary data file for INDAT.

VSAT3D is written in CDC's FORTRAN 200 and will thus only operate on the CDC Cyber 205. The main data source for this code is provided by first executing INDAT which will operate on any ANSI FORTRAN 77 system. Further information of the data requirements of VSAT3D can be found in the COMMENT statements of the listing.

Copies of both source codes on magnetic tape or diskette may be obtained by writing to either of the two addresses below. A scalar version of VSAT3D, written in ANSI FORTRAN 77, is also available.

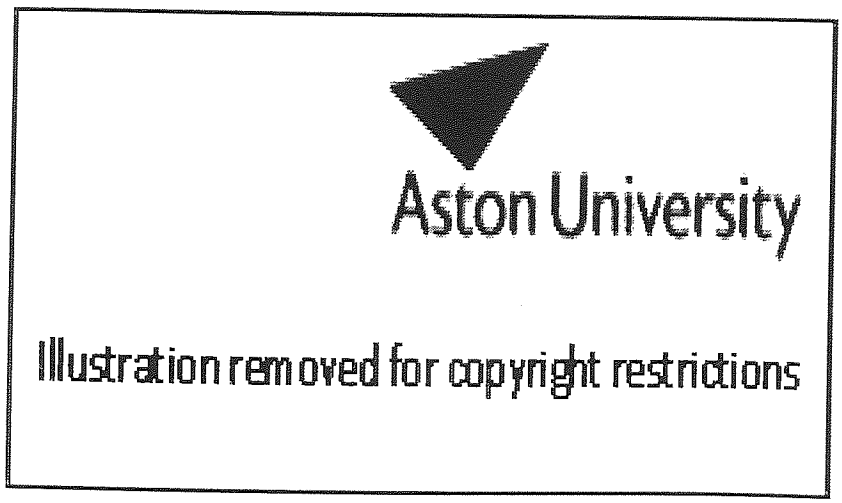

Listing of VSAT3D

```
      PROGRAM VSAT3D(INPUT,OUTPUT,TAPE1,TAPE2,TAPE5,TAPE7,TAPE8,
     *TAPE9,TAPE4=INPUT,TAPE3=OUTPUT)
C
C-----PROGRAM VSAT3D, JULY 1986 VERSION. USING FOUR POINT GAUSS
C-----QUADRATURE IN VERTICAL DIRECTION FOR THREE DIMENSIONAL
C-----ISOPARAMETRIC ELEMENTS USING ELEMENT INDEX
C
C-----THE SIZE OF BS MUST BE AT LEAST 9*NUMNP + NUMA + NUMEL
C-----  + 97*NUMSH + 22*MAX(1,NUMNFQ).
C
C-----THE SIZE OF IBS MUST BE AT LEAST 1 + 2*NUMNP + 10*NUMEL +
C-----MAX(1,NSEEP)*(2 + MAX(1,MAXS)) + 18*MAX(1,NUMNFQ).
C
C-----THE SIZE OF EACH ARRAY IN COMMON/MAT/ MUST BE AT LEAST NUMMAT.
C
C
C-----PROGRAM MAIN SCALARS :-
C
C     NUMA      SIZE OF ARRAY A
C     NUMNP     NUMBER OF NODE POINTS
C     NUMEL     NUMBER OF ELEMENTS
C     NUMMAT    NUMBER OF SOIL TYPES
C     NSEEP     NUMBER OF SEEPAGE FACES
C     NDIM      MAX(1,NSEEP)
C     MAXSP     MAX(1,MAXIMUM NUMBER OF NODES ON A SEEPAGE FACE)
C     NUMSH     NUMBER OF ELEMENT SHAPES
C     NUMNFQ    NUMBER OF BOUNDARY NODES WITH NON-ZERO FLUX
C     NQ        MAX(1,NUMNFQ)
C     HED       JOB TITLE
C     SUBHED    JOB SUBTITLE
C     MAXIT     MAXIMUM NUMBER OF ITERATIONS PER TIME STEP
C     MAXIT2    MAXIMUM NUMBER OF ITERATIONS PER TIME STEP BEFORE
C               REDUCTION IN TIME STEP
C     INTBAL    CONTINUITY CHECK INTERVAL
C     INTPRIN   NODE INFORMATION PRINTOUT INTERVAL
C     INTQPR    NODAL FLUX INFORMATION PRINTOUT INTERVAL
C     DT        INITIAL TIME STEP
C     DTMAX     MAXIMUM TIME STEP
C     DTMIN     MINIMUM TIME STEP
C     TMAX      TIME AT END OF SIMULATION
C     TOL       ITERATION TOLERANCE
C     DTQS      TIME INTERVAL FOR SURFACE FLOW ROUTING (DTQS .LE. DTMIN)
C     DELMAX    MAXIMUM POSSIBLE DELAY TIME OF SURFACE FLUXES
C
C-----PROGRAM ARRAYS :-
C
C     A         CONDUCTANCE ARRAY
C     B         RHS OF FE EQUATION
C     AFLUX     COMPACT CONDUCTANCE ARRAY FOR FLUX CALCULATIONS
C     BFLUX     RHS FOR FLUX CALCULATIONS
C     C         DUMMY ARRAY
C     D         F MATRIX IN FE EQUATION
C     DUMY      DUMMY ARRAY
C     P         NEW PRESSURE HEAD VALUES
C     P1        OLD PRESSURE HEAD VALUES
C     X,Y,Z     COORDINATES OF NODE POINTS
C     Q         UNKNOWN FLUXES
C     QX        SPECIFIED FLUXES
C     DET       DETERMINANT FOR EACH ELEMENT SHAPE
C     DINT      DERIVATIVES AT EACH GAUSS POINT OF EACH SHAPE
C     CELEM     HYDRAULIC CONDUCTIVITY FOR EACH ELEMENT
C     DELAY     DELAY TIMES OF EACH SURFACE NODE
C     KODE      CODE FOR EACH NODE POINT
C               = -2 POTENTIAL SEEPAGE FACE
C               =  0 SPECIFIED FLUX
```

```
C              =  1 SPECIFIED HEAD
C              =  2 SEEPAGE FACE
C     KX       ELEMENT CORNER NODES AND SOIL TYPE
C     NP       NODE NUMBERS FOR SEEPAGE FACES
C     NSP      NUMBER OF NODES ON EACH SEEPAGE FACE
C     KODES    DIRECTION OF FLOW AT EACH SEEPAGE FACE
C              =  -1 FLOW DIRECTED OUT
C              =   1 FLOW DIRECTED IN
C     LD       INDEX FOR CONDUCTACE MATRIX
C     NODEQ    INDEX FOR COMPACT CONDUCTANCE MATRIX
C     QSDEL    DELAYED SURFACE FLUXES
C
C  UNSATURATED SOIL PROPERTIES (MAT COMMON BLOCK)
C
C  THETA(PSI)=RESID+(POR-RESID)*ATHET/(ATHET+(-PSI)^BTHET)   (PSI < PSIL)
C  THETA(PSI)=POR*(1+PSI*BETA-GAMMA*PSI*PSI)   (PSIL < PSI < 0)
C  KREL(PSI) =APERM/(APERM+(-PSI)^BPERM)   (PSI < 0)
C
C-----INPUT FILES :-
C
C     UNIT 1   UNFORMATTED FILE FROM DATA GENERATION PROGRAM
C     UNIT 4   FORMATTED JOB DATA
C     UNIT 5   FORMATTED HYFRAULIC CONDUCTIVITY DATA
C     UNIT 8   UNFORMATTED INITIAL PRESSURE HEAD DISTRIBUTION OR
C              RESTART DATA
C
C-----OUTPUT FILES :-
C
C     UNIT 2   FORMATTED PRESSURE HEADS AT SELECTED TIMES
C     UNIT 3   TIME STEP INFORMATION (MAIN OUTPUT FILE)
C     UNIT 7   UNFORMATTED FILE FOR RESTART DUMP
C     UNIT 9   FORMATTED DISCHARGE DATA
C
C
      PARAMETER(NBS=682500,NIBS=48500)
      CHARACTER*80 HED,SUBHED
      COMMON BS(NBS),IBS(NIBS)
      COMMON /MAT/POR(1),RESID(1),ATHET(1),BTHET(1),APERM(1),
     *BPERM(1),BETA(1),GAMMA(1),PSIL(1)
C
C-----INITIALIZE ARRAYS
C
      DO 5 I=0,NBS-1,65535
      LENGTH=MIN(NBS-I,65535)
      BS(I+1;LENGTH)=0.0
5     CONTINUE
      DO 7 I=0,NIBS-1,65535
      LENGTH=MIN(NIBS-I,65535)
      IBS(I+1;LENGTH)=0
7     CONTINUE
      NERR=0
      IFAIL=0
      REWIND 1
      READ(1) NUMA,NUMNP,NUMEL,NUMMAT,NSEEP,NDIM,MAXSP,NUMNFQ,NQ,
     *NUMSH,HED,SUBHED
C
C-----EVALUATE DIMENSIONS FOR REAL ARRAYS
C
      N1=1+NUMA
      N2=N1+NUMNP
      N3=N2+18*NQ
      N4=N3+NQ
      N5=N4+NUMNP
      N6=N5+NUMNP
      N7=N6+NUMNP
      N8=N7+NUMNP
```

```
      N9=N8+NUMNP
      N10=N9+NUMNP
      N11=N10+NUMNP
      N12=N11+NUMNP
      N13=N12+NQ
      N14=N13+NQ
      N15=N14+NUMSH
      N16=N15+96*NUMSH
      N17=N16+NUMEL
C
C-----EVALUATE DIMENSIONS FOR INTEGER ARRAYS
C
      I1=1+NUMNP
      I2=I1+10*NUMEL
      I3=I2+NDIM*MAXSP
      I4=I3+NDIM
      I5=I4+NDIM
      I6=I5+NUMNP+1
C
C-----CHECK DIMENSIONS OF ARRAYS IN BLANK COMMON
C
      NBSC=N17+NQ
      NIBSC=I6+18*NQ
      IF (NBSC .GT. NBS) THEN
        WRITE(3,10) NBS,NBSC
10      FORMAT(//1H ,'----------ERROR IN SIZE OF BS----------',
     */1H ,'ARRAY SIZE IS',I10/1H ,'ARRAY SIZE SHOULD BE',I10)
        STOP'DIMENSION ERROR'
      END IF
      IF (NIBSC .GT. NIBS) THEN
        WRITE(3,20) NIBS,NIBSC
20      FORMAT(//1H ,'----------ERROR IN SIZE OF IBS----------',
     */1H ,'ARRAY SIZE IS',I10/1H ,'ARRAY SIZE SHOULD BE',I10)
        STOP'DIMENSION ERROR'
      END IF
      CALL SETUP (BS(1),BS(N1),BS(N2),BS(N3),BS(N4),BS(N5),BS(N6),
     *BS(N7),BS(N8),BS(N9),BS(N10),BS(N11),BS(N12),BS(N13),BS(N14),
     *BS(N15),BS(N16),BS(N17),IBS(1),IBS(I1),IBS(I2),IBS(I3),IBS(I4),
     *IBS(I5),IBS(I6),NUMNP,NUMA,NUMEL,NUMMAT,NSEEP,NDIM,MAXSP,NUMNFQ,
     *NQ,NUMSH,HED,SUBHED,NERR,IFAIL)
      IF (NERR .NE. 0) WRITE(3,110) NERR
      IF (IFAIL .NE. 0) WRITE(3,120) IFAIL
110   FORMAT(//1H ,'NERR =',I3)
120   FORMAT(//1H ,'IFAIL =',I7)
      IF (NERR .GT. 0) STOP'TOLERANCE ERROR'
      IF (IFAIL .GT. 0) STOP'CONDUCTANCE MATRIX IS SINGULAR'
      IF (IFAIL .LT. 0) STOP'CONDUCTANCE MATRIX IS INDEFINITE'
      STOP
      END
```

```
C
C
C>>>>>>>>>>>>>>>>>>>>>>>>>>SETUP SUBROUTINE<<<<<<<<<<<<<<<<<<<<<<<<<<<<
C
C-----SETS THE DIMENSIONS OF ALL ARRAYS IN BLANK COMMON.
C-----CALL SUBROUTINES FOR EACH TIME STEP UNTIL TIME TMAX IS REACHED,
C-----OUTPUT CAN THEN BE SENT TO AN UNFORMATTED FILE FOR RESTARTING
C-----PURPOSES LATER ALSO AT TIME TMAX FORMATTED OUTPUT IS SENT ON
C-----UNIT 2 FOR LATER INVESTIGATION OF RESULTS.
C
C
      SUBROUTINE SETUP (A,B,AFLUX,BFLUX,C,D,DUMY,P,P1,X,Y,Z,Q,QX,DET,
     *DINT,CELEM,DELAY,KODE,KX,NP,NSP,KODES,LD,NODEQ,NUMNP,NUMA,NUMEL,
     *NUMMAT,NSEEP,NDIM,MAXSP,NUMNFQ,NQ,NUMSH,HED,SUBHED,NERR,IFAIL)
      PARAMETER (NQSDEL=2000)
      CHARACTER*80 HED,SUBHED,HED1*3
      DIMENSION A(NUMA),B(NUMNP),AFLUX(18,NQ),BFLUX(NQ),C(NUMNP),
     *D(NUMNP),DUMY(NUMNP),P(NUMNP),P1(NUMNP),X(NUMNP),Y(NUMNP),
     *Z(NUMNP),Q(NQ),QX(NQ),DET(NUMSH),DINT(3,8,4,NUMSH),
     *CELEM(NUMEL),KODE(NUMNP),KX(10,NUMEL),NP(MAXSP,NDIM),NSP(NDIM),
     *KODES(NDIM),LD(0:NUMNP),NODEQ(18,NQ),DELAY(NQ),QSDEL(NQSDEL)
      COMMON /MAT/POR(1),RESID(1),ATHET(1),BTHET(1),APERM(1),
     *BPERM(1),BETA(1),GAMMA(1),PSIL(1)
C
C-----READ JOB PARAMETERS
C
      READ(4,10) HED1
10    FORMAT(A)
      IF (HED1 .EQ. 'RES') GO TO 40
      HED1='XXX'
      READ(4,20) MAXIT,MAXIT2,INTBAL,INTPRIN,INTQPR
20    FORMAT(5I5)
      MAXIT2=MIN(MAXIT,MAXIT2)
      READ(4,30) DT,DTMAX,DTMIN,TMAX,TOL
      READ(4,30) DTQS,DELMAX
30    FORMAT (8E10.3)
      IF (DTQS .GT. DTMIN) DTQS=DTMIN
C
C-----CHECK ON SIZE OF QSDEL ARRAY
C
      NDELAY=INT(DELMAX/DTQS)+1
      I=INT(TMAX/DTQS)+NDELAY
      IF (I .LE. NQSDEL) GO TO 40
33    WRITE(3,35) I,NQSDEL
35    FORMAT(1H ,'--------------ERROR IN QSDEL ARRAY SIZE-----------',
     *'---'/1H ,'ARRAY SIZE IS',I8/1H ,'ARRAY SIZE SHOULD BE',I8)
      STOP
40    WRITE(3,50) HED,SUBHED,NUMNP,NUMEL,NUMMAT,NUMNFQ,NUMSH,
     *INTBAL,INTPRIN,MAXIT,TOL
50    FORMAT(1H0,20X,A/1H ,20X,A///
     *1H ,'NUMBER OF NODE POINTS---------',I4//
     *1H ,'NUMBER OF ELEMENTS------------',I4//
     *1H ,'NUMBER OF MATERIALS-----------',I4//
     *1H ,'NUMBER OF BOUNDARY FLUX NODES-',I4//
     *1H ,'NUMBER OF ELEMENT SHAPES------',I4//
     *1H ,'CONTINUITY CHECK INTERVAL-----',I4//
     *1H ,'OUTPUT INTERVAL---------------',I4//
     *1H ,'MAX NUMBER OF ITERATIONS------',I4//
     *1H ,'ITERATION TOLERANCE-----------',E10.3//)
C
C-----READ DATA
C
55    READ(5,10) HED
      READ(5,60) (CELEM(N),N=1,NUMEL)
60    FORMAT(5E15.6)
```

```
      READ(1) X,Y,Z,Q,QX,DET,DINT,DELAY,KODE,KX,NP,NSP,KODES,LD,
     *NODEQ,POR,RESID,ATHET,BTHET,APERM,BPERM,BETA,GAMMA,PSIL
      WRITE(9,65) HED,SUBHED
65    FORMAT(1H ,20X,A/1H ,20X,A/1H ,5X,'TIME',9X,'QSUB',
     *9X,'QSUR',9X,'QTOT',9X,'STOT',9X,'QTOT')
      IF (HED1 .EQ. 'RES') GO TO 250
      REWIND 8
      READ(8) P
      P1(1;NUMNP)=P(1;NUMNP)
C
C-----SET UP FOR TIME INTEGRATION
C
      QSDEL(1;NQSDEL)=0.0
      TINT=0.0
      QINCUM=0.0
      QOUTCUM=0.0
      LA=1
      TIME=DT
      IPRINT=1
      IQPRINT=1
      IBAL=1
70    WRITE(3,80) HED,SUBHED,TIME,LA
80    FORMAT (/////20X,A/20X,A//40X,'TIME=',E13.5,5X,'TIME STEP =',
     *I4/40X,'**************************************'//)
C
C-----FORM AND SOLVE EQUATIONS
C
      ITER=0
      CALL FORSOL (A,B,AFLUX,BFLUX,C,D,DUMY,P,P1,Z,Q,QX,DET,DINT,
     *CELEM,DELAY,QSDEL,KODE,KX,NP,NSP,KODES,LD,NODEQ,NUMNP,
     *NUMA,NUMEL,NUMMAT,MAXIT,INTBAL,INTPRIN,NSEEP,NDIM,MAXSP,NUMNFQ,
     *NQ,NUMSH,NERR,IFAIL,LA,TIME,DT,DT1,ITER,QIN,QOUT,TOL,IBAL,
     *IPRINT,INTQPR,IQPRINT,NQSDEL,DTQS,TINT)
C
C-----IF SOLUTION HAS NOT CONVERGED JUMP OUT OF LOOP
C
      IF (NERR .GT. 0) GO TO 160
C
C-----IF ERROR IN EQUATION SOLVER ROUTINE THEN RETURN
C
      IF (IFAIL .NE. 0) RETURN
C
C-----OUTPUT INFLOW AND OUTFLOW RESULTS
C
      QINCUM=QINCUM+QIN
      QOUTCUM=QOUTCUM+QOUT
      WRITE(3,115) QOUTCUM,QINCUM
115   FORMAT (///1H ,'CUMMULATIVE OUTFLOW FROM CATCHMENT IS--',E13.5//
     *1H ,'CUMMULATIVE INFLOW INTO CATCHMENT IS---',E13.5///)
      IF (ABS(TIME-TMAX) .LE. 0.001*DT) GO TO 160
C
C-----SET UP FOR NEW TIME STEP
C
130   LA=LA+1
      IBAL=IBAL+1
      IPRINT=IPRINT+1
      IQPRINT=IQPRINT+1
      DT1=DT
C
C-----REDUCE TIME STEP IF
C-----(1) UNSATISFACTORY CONVERGENCE
C-----(2) RESTARTED WITH NEW CONDITIONS
C
      IF (ITER .GE. MAXIT2 .OR. NERR .LT. 0 .OR. HED1 .NE. 'XXX') THEN
        DT=0.5*DT
        IF (DT .LT. DTMIN) DT=DTMIN
```

```
      ELSE
        DT=1.4*DT
        IF (DT .GT. DTMAX) DT=DTMAX
      END IF
      IF ((TIME+DT) .GT. TMAX .OR. ABS(TMAX-TIME-DT) .LT. 0.2*DT) THEN
        DT=TMAX-TIME
        TIME=TMAX
      ELSE
        TIME=TIME+DT
      END IF
      HED1='XXX'
      NERR=0
      GO TO 70
160   IF (IPRINT .NE. 0) THEN
        WRITE(3,170)
170     FORMAT(/////1H0,4(1H ,'  NODE',4X,'HEAD',9X,'PSI     ')//)
        DUMY(1;NUMNP)=P(1;NUMNP)+Z(1;NUMNP)
        WRITE(3,180) (N,DUMY(N),P(N),N=1,NUMNP)
180     FORMAT(I8,2E12.5,I7,2E12.5,I7,2E12.5,I7,2E12.5)
      END IF
      WRITE(2,185) HED,SUBHED,NUMNP,TIME
185   FORMAT(1H ,20X,A/1H ,20X,A/1H ,'NUMBER OF NODE POINTS =',I5/
     *1H ,'TIME =',E10.3)
      WRITE(2,190) (N,KODE(N),P(N),N=1,NUMNP)
190   FORMAT(I6,I5,E12.5,2I5,E12.5,2I5,E12.5)
      IF (NERR .GT. 0) GO TO 230
      READ(4,220) HED1
220   FORMAT(A)
      IF (HED1 .EQ. 'END') RETURN
      IF (HED1 .EQ. 'CON') GO TO 270
230   REWIND 7
      WRITE(7) MAXIT,MAXIT2,INTBAL,INTPRIN,DT,DTMAX,DTMIN,TOL,TIME,
     *QINCUM,QOUTCUM,LA,IPRINT,IBAL,INTQPR,IQPRINT,TINT,DTQS,NDELAY
      WRITE(7) P,P1,Q,QX,QSDEL,KODE
      RETURN
C
C-----RESTART AND READ IN NEW BOUNDARY CONDITIONS
C
250   READ(8) MAXIT,MAXIT2,INTBAL,INTPRIN,DT,DTMAX,DTMIN,TOL,TIME,
     *QINCUM,QOUTCUM,LA,IPRINT,IBAL,INTQPR,IQPRINT,TINT,DTQS,NDELAY
      READ(8) P,P1,Q,QX,QSDEL,KODE
270   READ(4,290) TMAX,DTMAX1
290   FORMAT(2E10.3)
      I=INT((TMAX-TIME)/DTQS)+NDELAY
      IF (I .GT. NQSDEL) GO TO 33
      I1=INT((TIME-TINT)/DTQS)
      DO 300 I=1,NDELAY
      J=I1+I
300   QSDEL(I)=QSDEL(J)
      NVEC=NQSDEL-NDELAY
      QSDEL(NDELAY+1;NVEC)=0.0
      TINT=TIME
      IF (DTMAX1 .GT. 0.0) DTMAX=DTMAX1
370   FORMAT(I5,E20.6)
      NODQX=0
390   READ(4,370) N,VALUE
      IF (N .LT. 1) GO TO 130
400   NODQX=NODQX+1
      NODE=NODEQ(1,NODQX)
      IF (N .GT. NODE) GO TO 400
      QX(NODQX)=VALUE
      GO TO 390
      END
```

```
C
C
C>>>>>>>>>>>>>>>>>>>>>>>>>>>FORSOL SUBROUTINE<<<<<<<<<<<<<<<<<<<<<<<<<<<
C
C-----FORMS EQUTIONS IN AX=B FORM AND SOLVES. MODIFIES CONDITIONS ON
C-----SEEPAGE FACES, REPEATS UNTIL REQUIRED TOLERANCE IS ACHIEVED.
C
C
      SUBROUTINE FORSOL (A,B,AFLUX,BFLUX,C,D,DUMY,P,P1,Z,Q,QX,DET,DINT,
     *CELEM,DELAY,QSDEL,KODE,KX,NP,NSP,KODES,LD,NODEQ,NUMNP,NUMA,
     *NUMEL,NUMMAT,MAXIT,INTBAL,INTPRIN,NSEEP,NDIM,MAXSP,NUMNFQ,NQ,
     *NUMSH,NERR,IFAIL,LA,TIME,DT,DT1,ITER,QIN,QOUT,TOL,IBAL,IPRINT,
     *INTQPR,IQPRINT,NQSDEL,DTQS,TINT)
      PARAMETER (TOL2=0.01)
      DIMENSION A(NUMA),B(NUMNP),AFLUX(18,NQ),BFLUX(NQ),C(NUMNP),
     *D(NUMNP),DUMY(NUMNP),P(NUMNP),P1(NUMNP),Z(NUMNP),Q(NQ),DELAY(NQ),
     *DET(NUMSH),QX(NQ),DINT(3,8,4,NUMSH),CELEM(NUMEL),KODE(NUMNP),
     *KX(10,NUMEL),NP(MAXSP,NDIM),NSP(NDIM),KODES(NDIM),LD(0:NUMNP),
     *NODEQ(18,NQ),ALOC(8,8),BLOC(4),DLOC(4),LM(8),PLM(8),QSDEL(NQSDEL)
      COMMON /MAT/POR(1),RESID(1),ATHET(1),BTHET(1),APERM(1),
     *BPERM(1),BETA(1),GAMMA(1),PSIL(1)
C
C-----EXTRAPOLATION OF P VALUES
C
      IF (LA .EQ. 1) GO TO 6
      T3=TIME-0.5*DT
      T2=TIME-DT
      DTIT=LOG10(TIME/T3)/LOG10(TIME/T2)
      IF (LA .LT. 4) THEN
        DTT=0.5*DT/DT1
      ELSE
        T1=T2-DT1
        DTT=LOG10(T3/T2)/LOG10(T2/T1)
      END IF
      DUMY(1;NUMNP)=P(1;NUMNP)+DTT*(P(1;NUMNP)-P1(1;NUMNP))
      P1(1;NUMNP)=P(1;NUMNP)
      P(1;NUMNP)=DUMY(1;NUMNP)
C
C-----CHECK FOR MODIFICATION OF SURFACE FLUXES
C
6     DO 9 I=1,NUMNFQ
      NOD=NODEQ(1,I)
      IF (KODE(NOD) .EQ. 1) THEN
        IF (Q(I) .GE. QX(I)) THEN
          Q(I)=0.0
          KODE(NOD)=0
        END IF
      ELSE IF (KODE(NOD) .EQ. 0 .AND. P(NOD) .GE. 0.0) THEN
        P(NOD)=0.0
        P1(NOD)=0.0
        KODE(NOD)=1
      END IF
9     CONTINUE
C
C-----INITIALISE ARRAYS
C
      IF (LA .EQ. 1) GO TO 25
10    B(1;NUMNP)=0.0
      D(1;NUMNP)=0.0
      DO 20 I=0,NUMA-1,65535
      LENGTH=MIN(NUMA-I,65535)
      A(I+1;LENGTH)=0.0
20    CONTINUE
C
C-----FOR EACH ELEMENT ADD LOCAL SYSTEM OF EQUATIONS TO GLOBAL SYSYTEM.
```

```
C
25     M=1
       POROS=POR(1)
       ATHETA=ATHET(1)
       BTHETA=BTHET(1)
       BMINUS=BTHETA-1.0
       APOR2=BTHETA*ATHETA*(POR(1)-RESID(1))
       APERMM=1.0/APERM(1)
       BPERMM=BPERM(1)
       BETAM=BETA(1)
       GAMMAM=GAMMA(1)
       PSILM=PSIL(1)
       SMCFIX=BETAM*POROS
       DO 50 N=1,NUMEL
       IF (KX(9,N) .NE. M) THEN
         M=KX(9,N)
         POROS=POR(M)
         ATHETA=ATHET(M)
         BTHETA=BTHET(M)
         BMINUS=BTHETA-1.0
         APOR2=ATHETA*BTHETA*(POR(M)-RESID(M))
         APERMM=1.0/APERM(M)
         BPERMM=BPERM(M)
         BETAM=BETA(M)
         GAMMAM=GAMMA(M)
         PSILM=PSIL(M)
         SMCFIX=BETAM*POROS
       END IF
         DO 30 I=1,8
         LM(I)=KX(I,N)
30       PLM(I)=P(LM(I))
       ISHAP=KX(10,N)
       DETL=DET(ISHAP)
       CSATM=CELEM(N)*DETL
       CALL LOCAL (ALOC,BLOC,DLOC,PLM,DINT(1,1,1,ISHAP),POROS,
      *ATHETA,BTHETA,BMINUS,APERMM,BPERMM,APOR2,BETAM,GAMMAM,PSILM,
      *SMCFIX)
       DO 31 L=1,4
       BLOCI=BLOC(L)*CSATM
       DLOCI=DLOC(L)*DETL
       I1=LM(L)
       I2=LM(L+4)
       B(I1)=B(I1)+BLOCI
       B(I2)=B(I2)+BLOCI
       D(I1)=D(I1)+DLOCI
31     D(I2)=D(I2)+DLOCI
       DO 33 L=1,8
       I=LM(L)
       LDI=LD(I)
         DO 32 LL=1,8
         K=I-LM(LL)
         IF (K .GE. 0) A(LDI-K)=A(LDI-K)+ALOC(L,LL)*CSATM
32       CONTINUE
33     CONTINUE
50     CONTINUE
C
C-----FORM EFFECTIVE MATRIX EQUATION
C
       DTR=1.0/DT
       D(1;NUMNP)=D(1;NUMNP)*DTR
       B(1;NUMNP)=D(1;NUMNP)*P1(1;NUMNP)-B(1;NUMNP)
       DO 70 N=1,NUMNP
       LDN=LD(N)
70     A(LDN)=A(LDN)+D(N)
C
C-----ADD CONTRIBUTION OF A AND B TO AFLUX AND BFLUX
```

```
C
      DO 100 N=1,NUMNFQ
      NOD=NODEQ(1,N)
      IF (KODE(NOD) .LT. 1 .OR. KODE(NOD) .GT. 2) THEN
        B(NOD)=B(NOD)+QX(N)
      ELSE
        LDN=LD(NOD)
        AFLUX(1,N)=A(LDN)
        BFLUX(N)=B(NOD)
        B(NOD)=B(NOD)+Q(N)
          DO 80 I=2,18
          NODI=NODEQ(I,N)
          IF (NODI .LT. 1) GO TO 100
          IF (NODI .LT. NOD) THEN
            LDI=LDN-NOD+NODI
          ELSE
            LDI=LD(NODI)-NODI+NOD
          END IF
80        AFLUX(I,N)=A(LDI)
      END IF
100   CONTINUE
C
C-----ADJUST B VECTOR FOR FIXED HEAD NODES
C
      IF (ITER .GE. 1) THEN
        WHERE (KODE(1;NUMNP) .GT. 0) B(1;NUMNP)=C(1;NUMNP)
      ELSE
        WHERE (KODE(1;NUMNP) .GT. 0) B(1;NUMNP)=P(1;NUMNP)
      END IF
C
C-----SOLVE EQUATIONS
C
      CALL SKYSOL (A,B,DUMY,P,KODE,LD,NUMNP,NUMA,IFAIL)
      IF (IFAIL .NE. 0) RETURN
C
C-----DETERMINE UNKNOWN BOUNDARY FLUXES
C
      DO 200 N=1,NUMNFQ
      NOD=NODEQ(1,N)
      IF (KODE(NOD) .LT. 1 .OR. KODE(NOD) .GT. 2) GO TO 200
      QN=AFLUX(1,N)*P(NOD)-BFLUX(N)
        DO 150 I=2,18
        NOD=NODEQ(I,N)
        IF (NOD .LT. 1) GO TO 180
150     QN=QN+AFLUX(I,N)*P(NOD)
180   Q(N)=QN
200   CONTINUE
      ITER=ITER+1
C
C-----MODIFY CONDITIONS ON SEEPAGE FACES
C
      DO 500 I=1,NSEEP
      ICHECK=0
      NS=NSP(I)
      NOD=0
        DO 480 J=1,NS
        N=NP(J,I)
400     NOD=NOD+1
        IF (N .GT. NODEQ(1,NOD)) GO TO 400
        IF (KODE(N) .NE. -2) GO TO 450
        IF (P(N) .LT. 0.0) ICHECK=1
        IF (ICHECK .GT. 0) GO TO 480
        KODE(N)=2
        P(N)=0.0
        P1(N)=0.0
        GO TO 480
```

```
450      IF (KODE(N) .NE. 2) GO TO 480
         IF (ICHECK .GT. 0) GO TO 470
         IF ((Q(NOD) .LT. 0.0 .AND. KODES(I) .LT. 0) .OR.
     *     (Q(NOD) .GT. 0.0 .AND. KODES(I) .GT. 0)) GO TO 480
470      KODE(N)=-2
         Q(NOD)=0.0
         ICHECK=1
480      CONTINUE
500    CONTINUE
C
C-----CHECK FOR MODIFICATION OF SURFACE FLUXES
C
       DO 530 I=1,NUMNFQ
       NOD=NODEQ(1,I)
       IF (KODE(NOD) .EQ. 1) THEN
         IF (Q(I) .GE. QX(I)) THEN
           Q(I)=0.0
           KODE(NOD)=0
         END IF
       ELSE IF (KODE(NOD) .EQ. 0 .AND. P(NOD) .GE. 0.0) THEN
         P(NOD)=0.0
         P1(NOD)=0.0
         KODE(NOD)=1
       END IF
530    CONTINUE
C
C-----ITERATE TO IMPROVE SOLUTION
C
       IF (ITER .EQ. 1) GO TO 538
       D(1;NUMNP)=C(1;NUMNP)
       C(1;NUMNP)=VABS(P(1;NUMNP)-C(1;NUMNP);C(1;NUMNP))
       NODMAX=Q8SMAXI(C(1;NUMNP))+1
       EPSLON=C(NODMAX)
       WRITE(3,535) ITER,EPSLON,NODMAX
535    FORMAT (//1H ,'MAXIMUM CHANGE IN PRESSURE HEAD DURING ITERATION',
     *I3,' WAS',E13.5,' AT NODE',I8)
       IF (EPSLON .LE. TOL .OR. ITER .GE. MAXIT) GO TO 540
C
C-----CHECK FOR OSCILLATION ABOUT SOLUTION
C
       IF ((EPSLON-EPSLON1) .LT. -1.0E-4 .OR. ITER .EQ. 2) GO TO 537
       WHERE ((P(1;NUMNP) .LT. 0.0 .AND. D(1;NUMNP) .GT. 0.0) .OR.
     *        (P(1;NUMNP) .GT. 0.0 .AND. D(1;NUMNP) .LT. 0.0))
          P(1;NUMNP)=0.0
          P1(1;NUMNP)=0.0
       OTHERWISE
         P(1;NUMNP)=0.5*(P(1;NUMNP)+D(1;NUMNP))
       END WHERE
       WRITE(3,536)
536    FORMAT(1H ,20X,'**********WARNING FORCED CONVERGENCE**********'/)
       NERR=-1
       GO TO 540
C
C-----DOMAIN RESTRICTION SECTION
C
537    IF (ITER .EQ. 2) THEN
         WHERE (C(1;NUMNP) .LE. TOL2 .AND. KODE(1;NUMNP) .EQ. 0)
     *  KODE(1;NUMNP)=4
       END IF
538    C(1;NUMNP)=P(1;NUMNP)
C
C-----INTERPOLATE P VALUES TO GET ESTIMATE OF P AT K+1/2
C
       IF (LA .EQ. 1) THEN
         P(1;NUMNP)=0.5*(P(1;NUMNP)+P1(1;NUMNP))
       ELSE
```

```
        P(1;NUMNP)=P(1;NUMNP)+DTIT*(P1(1;NUMNP)-P(1;NUMNP))
      END IF
C
C-----GO TO START FOR NEXT ITERATION
C
      EPSLON1=EPSLON
      GO TO 10
540   WHERE (KODE(1;NUMNP) .EQ. 4) KODE(1;NUMNP)=0
C
C-----CONTINUITY CALCULATIONS
C
      IF (IBAL .EQ. INTBAL) THEN
        WRITE(3,542) ITER
542     FORMAT(////1H ,'CONTINUITY CALCULATIONS AT ITERATION',I3/
     *  1H ,'---------------------------------------')
        CALL CONTIN (P,P1,Q,QX,DET,KODE,KX,NODEQ,NUMNP,NUMEL,NUMMAT,
     *  NUMNFQ,NQ,NUMSH,DT,STOT,QTOT)
        IBAL=0
      END IF
C
C-----PRINT RESULTS
C
      IF (IPRINT .EQ. INTPRIN) THEN
        WRITE(3,545)
545      FORMAT(/////1H0,4(1H ,'  NODE',4X,'HEAD',9X,'PSI    ')//)
         DUMY(1;NUMNP)=P(1;NUMNP)+Z(1;NUMNP)
         WRITE(3,546) (N,DUMY(N),P(N),N=1,NUMNP)
546      FORMAT(I8,2E12.5,I7,2E12.5,I7,2E12.5,I7,2E12.5)
        IPRINT=0
      END IF
      THALF=TIME-0.5*DT
      IF (IQPRINT .EQ. INTQPR) THEN
        WRITE(3,580) THALF
580     FORMAT(////1H ,'NODAL FLUXES AT TIME',E13.5/1H ,6(1H ,'  NODE',
     *  3X,'DISCHARGE ')//)
        J=0
        N=0
585     N=N+1
        IF (N .GT. NUMNFQ) GO TO 588
        J=J+1
        IF (Q(N) .NE. 0.0) THEN
          PLM(J)=Q(N)
          LM(J)=NODEQ(1,N)
        ELSE
          J=J-1
        END IF
        IF (J .LT. 6) GO TO 585
588     WRITE(3,590) (LM(I),PLM(I),I=1,J)
        J=0
        IF (N .LT. NUMNFQ) GO TO 585
590     FORMAT(I8,E13.5,I7,E13.5,I7,E13.5,I7,E13.5,I7,E13.5,I7,E13.5)
        IQPRINT=0
      END IF
      T2=TIME-TINT
      T1=T2-DT
      QSIN=0.0
      QIN=0.0
      QSUB=0.0
      QSUR=0.0
      DO 800 I=1,NUMNFQ
      QIN=QIN+QX(I)
      QI=Q(I)
      NOD=NODEQ(1,I)
C
C-----SEEPAGE FACE FLOW ADDED TO SUBSURFACE FLOW (QSUB)
C-----THEN CHECKS ARE MADE ON FLOW TYPES OF ALL NON-FIXED
```

```
C-----FLUX NODES WITH KODE=1
C
      IF (KODE(NOD) .EQ. 2) THEN
        QSUB=QSUB-QI
      ELSE IF (KODE(NOD) .EQ. 1) THEN
        QXI=QX(I)
        TDEL=DELAY(I)
        I1=INT((T1+TDEL)/DTQS)+1
        I2=INT((T2+TDEL)/DTQS)
          DO 760 II=I1,I2
760       QSDEL(II)=QSDEL(II)+QXI-QI
        IF (QI .GT. 0.0) QSIN=QSIN+QI
      ELSE
        QSIN=QSIN+QX(I)
      END IF
800   CONTINUE
C
C-----CHECK ON ADDITION OF DELAYED DISCARGE TO SURFACE FLOW (QSUR)
C
      I1=INT(T1/DTQS)+1
      I2=INT(T2/DTQS)
      QSUM=0.0
      DO 820 I=I1,I2
820   QSUM=QSUM+QSDEL(I)
      QSUR=QSUR+QSUM/REAL(I2-I1+1)
      QOUT=QSUB+QSUR
      WRITE(9,850) THALF,QSUB,QSUR,QOUT,STOT,QTOT
850   FORMAT(E14.5,5E13.5)
      WRITE(3,900) QSUB,QSIN,QSUR,QOUT,QIN
900   FORMAT(///1H ,'TOTAL SUBSURFACE OUTFLOW IS ',E19.5//1H ,
     *'TOTAL SOIL INFLOW IS        ',E19.5///1H ,'TOTAL SURFACE ',
     *'RUNOFF IS     ',E19.5///1H ,'TOTAL OUTFLOW IS            ',
     *E19.5///1H ,'TOTAL INFLOW IS',13X,E19.5//)
      IF (EPSLON .GT. TOL .AND. ITER .GE. MAXIT .AND. NERR .EQ. 0)
     *NERR=1
      RETURN
      END
```

```
C
C
C
C>>>>>>>>>>>>>>>>>>>>>>>>LOCAL SUBROUTINE<<<<<<<<<<<<<<<<<<<<<<<<<<<<<<<<
C
C-----EVALUATES LOCAL MATRIX EQUATION FOR ELEMENT N
C
C
      SUBROUTINE LOCAL (ALOC,BLOC,DLOC,PLM,DINTL,POROS,ATHETA,
     *BTHETA,BMINUS,APERMM,BPERMM,APOR2,BETAM,GAMMAM,PSILM,SMCFIX)
      DIMENSION ALOC(8,8),BLOC(4),DLOC(4),PLM(8),DINTL(3,8,4)
      COMMON /BASIS/ SHAP(4,4)
      ALOC(1,1;64)=0.0
      DO 25 I=1,4
      BLOC(I)=0.0
25    DLOC(I)=0.0
C
C-----LOOP ON GAUSS POINTS
C
      DO 1000 K=1,4
      PK=0.0
        DO 100 I=1,4
100     PK=PK+SHAP(I,K)*(PLM(I)+PLM(I+4))
      IF (PK .LT. PSILM) THEN
        PKM=-PK
        RELK=1.0/(1.0+APERMM*PKM**BPERMM)
        THET=1.0/(ATHETA+PKM**BTHETA)
        SMC=APOR2*PKM**BMINUS*THET*THET
      ELSE IF (PK .LT. 0.0) THEN
        PKM=-PK
        RELK=1.0/(1.0+APERMM*PKM**BPERMM)
        SMC=POROS*(2.0*GAMMAM*PKM+BETAM)
      ELSE
        RELK=1.0
        SMC=SMCFIX
      END IF
        DO 700 I=1,8
          DO 600 J=I,8
          SUM=0.0
            DO 550 L=1,3
550         SUM=SUM+DINTL(L,I,K)*DINTL(L,J,K)
600       ALOC(I,J)=ALOC(I,J)+SUM*RELK
700     CONTINUE
        DO 800 I=1,4
800     DLOC(I)=DLOC(I)+SHAP(I,K)*SMC
        DO 950 I=1,4
950     BLOC(I)=BLOC(I)+DINTL(3,I,K)*RELK
1000  CONTINUE
C
C-----ADD VALUES TO SYMMETRICAL LOCAL ARRAYS
C
      DO 1200 I=2,8
        DO 1100 J=1,I-1
1100    ALOC(I,J)=ALOC(J,I)
1200  CONTINUE
      RETURN
      END
```

```
C
C
C>>>>>>>>>>>>>>>>>>>>>>>>>>>>SKYSOL SUBROUTINE<<<<<<<<<<<<<<<<<<<<<<<<<<<<
C
C-----FACTORISE AND SOLVE EQUATIONS USING METHOD FROM FELLIPA(1975)
C
C
      SUBROUTINE SKYSOL(A,B,DUMY,P,KODE,LD,NUMNP,NUMA,IFAIL)
      DIMENSION A(NUMA),DUMY(NUMNP),LD(0:NUMNP),B(NUMNP),P(NUMNP),
     *KODE(NUMNP)
      REAL TVEC(2)
      BIT BVEC(1)
      DESCRIPTOR TVEC,BVEC
      DATA EPSMAC/5.688E-14/
C
C-----COMPUTE SQUARED LENGTHS OF UNCONSTRAINED ROWS
C
      IF (KODE(1) .LT. 1) THEN
        DUMY(1)=A(1)*A(1)
      ELSE
        DUMY(1)=0.0
      END IF
      DO 1000 I=2,NUMNP
      IF (KODE(I) .GT. 0) THEN
        DUMY(I)=0.0
      ELSE
        II=LD(I)
        DUMY(I)=A(II)*A(II)
        M=II-I
        K=MAX(1,LD(I-1)-M+1)
        L=I-1
        NVEC=L-K+1
        ASSIGN TVEC(1),.DYN. NVEC
        ASSIGN TVEC(2),.DYN. NVEC
        ASSIGN BVEC(1),.DYN. NVEC
        BVEC(1)=KODE(K;NVEC) .LT. 1
        TVEC(1)=A(M+K;NVEC)*A(M+K;NVEC)
        TVEC(2)=Q8VMASK(TVEC(1),0.0,BVEC(1);TVEC(2))
        DUMY(I)=DUMY(I)+Q8SSUM(TVEC(2))
        TVEC(1)=DUMY(K;NVEC)+TVEC(1)
        DUMY(K;NVEC)=Q8VCTRL(TVEC(1),BVEC(1);DUMY(K;NVEC))
        J=L+1
800     FREE
      END IF
1000  CONTINUE
C
C-----FACTORISE
C
      IF (KODE(1) .GT. 0) GO TO 1500
      TOLROW=EPSMAC*SQRT(DUMY(1))
      IF (A(1) .LE. 0.0) IFAIL=-1
      IF (ABS(A(1)) .LT. TOLROW) IFAIL=1
      IF (IFAIL .NE. 0) RETURN
      A(1)=1.0/A(1)
1500  DO 4000 J=2,NUMNP
      IF (KODE(J) .GT. 0) GO TO 4000
      JJ=LD(J)
      D=A(JJ)
      JMJ=LD(J-1)
      JK=JJ-JMJ
      KU=JK-1
      IJK=J-JK
        DO 2000 K=1,KU
        I=IJK+K
        DUMYK=0.0
```

```
        IF (KODE(I) .GT. 0) GO TO 2000
        II=LD(I)
        M=MIN(II-LD(I-1),K)-1
        IJ=JMJ+K
        IF (M .EQ. 0) THEN
          DUMYK=A(IJ)
        ELSE
          DUMYK=A(IJ)-Q8SDOT(A(II-M;M),DUMY(K-M;M))
        END IF
        A(IJ)=DUMYK*A(II)
2000    DUMY(K)=DUMYK
C
C-----COMPUTE DIAGONAL ELEMENT D
C
      D=D-Q8SDOT(A(JMJ+1;KU),DUMY(1;KU))
C
C-----SINGULARITY TEST
C
      TOLROW=EPSMAC*SQRT(DUMY(J))
      IF (ABS(D) .GT. TOLROW) GO TO 2500
      IFAIL=J
      RETURN
2500  A(JJ)=1.0/D
C
C-----POSITIVE DEFINITNESS CHECK
C
      IF (D .GT. 0.0) GO TO 4000
      IFAIL=-J
      RETURN
4000  CONTINUE
C
C-----END OF FACTORISATION SECTION
C
      P(1;NUMNP)=B(1;NUMNP)
C
C-----RHS MODIFICATION
C
      DO 5000 I=1,NUMNP
      IF (KODE(I) .LT. 1) GO TO 5000
      II=LD(I)
      BI=B(I)
      IF (BI .EQ. 0.0) GO TO 5000
      K=I-II+LD(I-1)+1
        DO 4900 J=K,NUMNP
        IF (KODE(J) .GT. 0) GO TO 4900
        JJ=LD(J)
        M=J-I
        IF (M .LT. 0) THEN
          P(J)=P(J)-A(II+M)*BI
        ELSE
          IJ=JJ-M
          IF ((IJ-LD(J-1)) .GT. 0) P(J)=P(J)-A(IJ)*BI
        END IF
4900    CONTINUE
5000  CONTINUE
C
C-----FORWARD SUBSTITUTION PASS
C
      IF (KODE(1) .GT. 0) P(1)=0.0
      DO 5500 I=2,NUMNP
      IF (KODE(I) .LT. 1) THEN
        II=LD(I)
        IMI=LD(I-1)+1
        M=II-IMI
        P(I)=P(I)-Q8SDOT(A(IMI;M),P(I-M;M))
      ELSE
```

```
        P(I)=0.0
      END IF
5500  CONTINUE
C
C-----SCALING PASS
C
      DO 6000 I=1,NUMNP
      II=LD(I)
6000  P(I)=A(II)*P(I)
C
C-----BACK SUBSTITUTION PASS
C
      DO 7000 I=NUMNP,2,-1
      IF (KODE(I) .LT. 1) THEN
        II=LD(I)
        M=II-LD(I-1)-1
        PI=P(I)
        P(I-M;M)=P(I-M;M)-A(II-M;M)*PI
      ELSE
        P(I)=B(I)
      END IF
7000  CONTINUE
      IF (KODE(1) .GT. 0) P(1)=B(1)
      RETURN
      END
```

```
C
C
C>>>>>>>>>>>>>>>>>>>>>>>>>>CONTIN SUBROUTINE<<<<<<<<<<<<<<<<<<<<<<<<<<
C
C-----EVALUATES CONINUITY CHECK OVER ENTIRE MESH USING FOUR POINT GAUSS
C-----QUADRATURE.
C
C
      SUBROUTINE CONTIN (P,P1,Q,QX,DET,KODE,KX,NODEQ,NUMNP,NUMEL,NUMMAT,
     *NUMNFQ,NQ,NUMSH,DT,STOT,QTOT)
      DIMENSION P(NUMNP),P1(NUMNP),Q(NQ),QX(NQ),DET(NUMSH),
     *KX(10,NUMEL),KODE(NUMNP),NODEQ(18,NQ),PLM(8),P1LM(8)
      COMMON /MAT/POR(1),RESID(1),ATHET(1),BTHET(1),APERM(1),
     *BPERM(1),BETA(1),GAMMA(1),PSIL(1)
      COMMON /BASIS/ SHAP(4,4)
C
C-----DETERMINE NET SOIL FLUX
C
      QTOT=0.0
      DO 5 I=1,NUMNFQ
      NOD=NODEQ(1,I)
      IF (KODE(NOD) .GT. 0) THEN
        QTOT=QTOT+Q(I)
      ELSE
        QTOT=QTOT+QX(I)
      END IF
5     CONTINUE
      QTOT=QTOT*DT
      STOT=0.0D0
C
C-----LOOP ON ELEMENTS TO DETERMINE CHANGE IN STORAGE OVER TIME DT
C
      M=1
      POROS=POR(1)
      ATHETA=ATHET(1)
      BTHETA=BTHET(1)
      RESIDM=RESID(1)
      BETAM=BETA(1)
      GAMMAM=GAMMA(1)
      PSILM=PSIL(1)
      ATHPOR=ATHETA*(POROS-RESIDM)
      DO 100 N=1,NUMEL
      IF (KX(9,N) .NE. M) THEN
        M=KX(9,N)
        POROS=POR(M)
        ATHETA=ATHET(M)
        BTHETA=BTHET(M)
        RESIDM=RESID(M)
        BETAM=BETA(M)
        GAMMAM=GAMMA(M)
        PSILM=PSIL(M)
        ATHPOR=ATHETA*(POROS-RESIDM)
      END IF
        DO 30 I=1,8
        II=KX(I,N)
        PLM(I)=P(II)
30      P1LM(I)=P1(II)
      ISHAP=KX(10,N)
C
C-----LOOP ON GAUSS POINTS
C
      DETK=DET(ISHAP)
        DO 70 K=1,4
        PK=0.0
        P1K=0.0
```

```
          DO 40 I=1,4
          PK=PK+SHAP(I,K)*(PLM(I)+PLM(I+4))
40        P1K=P1K+SHAP(I,K)*(P1LM(I)+P1LM(I+4))
        IF (PK .LT. PSILM) THEN
          THET=RESIDM+ATHPOR/(ATHETA+(-PK)**BTHETA)
        ELSE IF (PK .LT. 0.0) THEN
          THET=POROS*(1.0+BETAM*PK-GAMMAM*PK*PK)
        ELSE
          THET=POROS*(1.0+BETAM*PK)
        END IF
        IF (P1K .LT. PSILM) THEN
          THET1=RESIDM+ATHPOR/(ATHETA+(-P1K)**BTHETA)
        ELSE IF (P1K .LT. 0.0) THEN
          THET1=POROS*(1.0+BETAM*P1K-GAMMAM*P1K*P1K)
        ELSE
          THET1=POROS*(1.0+BETAM*P1K)
        END IF
        STOT=STOT+(THET-THET1)*DETK
70      CONTINUE
100   CONTINUE
C
C-----CALCULATE ERRORS
C
      PMB=0.0
      IF (ABS(QTOT) .LT. 1.0E-22) GO TO 170
      PMB=100.0*(STOT-QTOT)/QTOT
      WRITE(3,160) PMB
160   FORMAT(1H ,'MASS CONTINUITY ERROR IS',E13.5,'PERCENT')
170   WRITE(3,180) STOT,QTOT
180   FORMAT(1H ,'NET CHANGE IN STORAGE IS',E13.5,
     *'    NET INFLOW IS',E13.5)
      RETURN
      END
```

```
C
C
C>>>>>>>>>>>>>>>>>>>>>>>>>>>>>>>>BLOCK DATA<<<<<<<<<<<<<<<<<<<<<<<<<<<<<<<<
C
C-----PROVIDES DATA FOR COMMON BLOCK BASIS
C
      BLOCK DATA
      PARAMETER (E=0.125,RT=0.57735026918963,SX=1.0/6.0,R=SX+RT*0.25,
     *S=SX-RT*0.25,T=1.0/12.0,U=(1.0+RT)/8.0,V=(1.0-RT)/8.0)
      COMMON /BASIS/ SHAP(4,4)
      DATA SHAP/R,T,S,T,T,R,T,S,S,T,R,T,T,S,T,R/
      END
```

Listing of INDAT

```
      PROGRAM INDAT(INPUT,OUTPUT,TAPE1,TAPE4=INPUT,TAPE3=OUTPUT)
C
C-----PROGRAM INDAT, JULY 1986 VERSION. GENERATES DATA FOR
C-----VSAT3D FOR ANY ELEMENT SHAPE AND DUMPS ON UNFORMATTED FILE
C-----USING ELEMENT SHAPES
C
C-----THE SIZE OF BS MUST BE AT LEAST 5*NUMNP + 97*NUMSH
C----- + 3*MAX(1,NUMNFQ) + MAX(1,NUMFX).
C
C-----THE SIZE OF IBS MUST BE AT LEAST 1 + 2*NUMNP + 10*NUMEL +
C-----MAX(1,NSEEP)*(2 + MAX(1,MAXS)) + 18*MAX(1,NUMNFQ) + MAX(1,NUMFX).
C
C-----THE SIZE OF EACH ARRAY IN COMMON/MAT/ MUST BE AT LEAST NUMMAT.
C
      PARAMETER(NBS=500000,NIBS=100000)
      CHARACTER*80 HED,SUBHED
      COMMON BS(NBS),IBS(NIBS)
      COMMON /MAT/POR(1),RESID(1),ATHET(1),BTHET(1),APERM(1),
     *BPERM(1),BETA(1),GAMMA(1),PSIL(1)
C
C-----INITIALIZE ARRAYS
C
      DO 5 I=1,NBS
5     BS(I)=0.0
      DO 10 I=1,NIBS
10    IBS(I)=0
      READ(4,20) HED
      READ(4,20) SUBHED
20    FORMAT (A)
      READ(4,30) NUMNP,NUMEL,NUMMAT,NSEEP,MAXS,NUMNFQ,NUMFX,NUMSH
30    FORMAT (8I5)
      NDIM=MAX(1,NSEEP)
      MAXSP=MAX(1,MAXS)
      NQ=MAX(1,NUMNFQ)
      NX=MAX(1,NUMFX)
C
C-----EVALUATE DIMENSIONS FOR REAL ARRAYS
C
      N1=1+NUMNP
      N2=N1+NUMNP
      N3=N2+NUMNP
      N4=N3+NUMNP
      N5=N4+NUMNP
      N6=N5+NQ
      N7=N6+NQ
      N8=N7+NUMSH
      N9=N8+96*NUMSH
      N10=N9+NQ
C
C-----EVALUATE DIMENSIONS FOR INTEGER ARRAYS
C
      I1=1+NUMNP
      I2=I1+10*NUMEL
      I3=I2+NDIM*MAXSP
      I4=I3+NDIM
      I5=I4+NDIM
      I6=I5+NUMNP+1
      I7=I6+18*NQ
      CALL SETUP (BS(1),BS(N1),BS(N2),BS(N3),BS(N4),BS(N5),BS(N6),
     *BS(N7),BS(N8),BS(N9),BS(N10),IBS(1),IBS(I1),IBS(I2),IBS(I3),
     *IBS(I4),IBS(I5),IBS(I6),IBS(I7),NUMNP,NUMEL,NUMMAT,NSEEP,NDIM,
     *MAXSP,NUMNFQ,NUMFX,NQ,NX,NUMSH,HED,SUBHED)
      STOP
      END
```

```
C
C
C>>>>>>>>>>>>>>>>>>>>>>>>>>SETUP SUBROUTINE<<<<<<<<<<<<<<<<<<<<<<<<<<<<<<
C
C-----SETS THE DIMENSIONS OF ALL ARRAYS IN BLANK COMMON.
C
C
      SUBROUTINE SETUP (P,P1,X,Y,Z,Q,QX,DET,DINT,DELAY,QXX,KODE,KX,NP,
     *NSP,KODES,LD,NODEQ,NODEX,NUMNP,NUMEL,NUMMAT,NSEEP,NDIM,MAXSP,
     *NUMNFQ,NUMFX,NQ,NX,NUMSH,HED,SUBHED)
      CHARACTER*80 HED,SUBHED
      DIMENSION P(NUMNP),P1(NUMNP),X(NUMNP),Y(NUMNP),Z(NUMNP),Q(NQ),
     *QX(NQ),DET(NUMSH),DINT(3,8,4,NUMSH),KODE(NUMNP),KX(10,NUMEL),
     *NP(MAXSP,NDIM),NSP(NDIM),KODES(NDIM),LD(0:NUMNP),NODEQ(18,NQ),
     *NODEX(NX),DELAY(NQ),QXX(NX)
      COMMON /MAT/POR(1),RESID(1),ATHET(1),BTHET(1),APERM(1),
     *BPERM(1),BETA(1),GAMMA(1),PSIL(1)
      WRITE(3,50) HED,SUBHED,NUMNP,NUMEL,NUMMAT,NUMNFQ,NUMFX,NUMSH
50    FORMAT(1H0,20X,A/1H ,20X,A///
     *1H ,'NUMBER OF NODE POINTS--------',I4//
     *1H ,'NUMBER OF ELEMENTS-----------',I4//
     *1H ,'NUMBER OF MATERIALS----------',I4//
     *1H ,'NUMBER OF NODE POINTS WITH'/
     *1H ,'UNKNOWN FLUX-----------------',I4//
     *1H ,'NUMBER OF NODE POINTS WITH'/
     *1H ,'FIXED FLUX-------------------',I4//
     *1H ,'NUMBER OF ELEMENT SHAPES-----',I4//)
C
C-----READ AND GENERATE DATA
C
      CALL GENDAT (X,Y,Z,Q,QX,DELAY,QXX,KODE,KX,NP,NSP,KODES,LD,NODEQ,
     *NODEX,NUMNP,NUMEL,NSEEP,NDIM,MAXSP,NUMNFQ,NUMFX,NQ,NX,NUMSH)
      CALL OUTDAT (X,Y,Z,Q,QX,DET,DINT,DELAY,KODE,KX,NP,NSP,KODES,LD,
     *NODEQ,NUMNP,NUMEL,NUMMAT,INT,NSEEP,NDIM,MAXSP,NUMNFQ,NQ,NUMSH)
C
C-----OUTPUT DATA TO UNFORMATTED FILE
C
      NUMA=LD(NUMNP)
      REWIND 1
      WRITE(1) NUMA,NUMNP,NUMEL,NUMMAT,NSEEP,NDIM,MAXSP,NUMNFQ,NQ,
     *NUMSH,HED,SUBHED
      WRITE(1) X,Y,Z,Q,QX,DET,DINT,DELAY,KODE,KX,NP,NSP,KODES,LD,NODEQ,
     *POR,RESID,ATHET,BTHET,APERM,BPERM,BETA,GAMMA,PSIL
C
C-----OUTPUT BLANK COMMON REQUIREMENTS
C
      NBS=9*NUMNP+NUMA+NUMEL+22*NQ+97*NUMSH
      NIBS=1+2*NUMNP+10*NUMEL+NDIM*(2+MAXSP)+18*NQ
      WRITE(3,100) NBS,NIBS
100   FORMAT(///1H ,'BLANK COMMON REQUIREMENTS'/1H ,'--------------',
     *'------------'/1H ,'THE SIZE OF ARRAY BS IN VSAT3D MUST BE',
     *' AT LEAST',I10/1H ,'THE SIZE OF ARRAY IBS IN VSAT3D MUST BE',
     *' AT LEAST',I9)
      RETURN
      END
```

```
C
C
C>>>>>>>>>>>>>>>>>>>>>>>>>>>SUBROUTINE OUTDAT<<<<<<<<<<<<<<<<<<<<<<<<<<
C
C-----INPUTS DATA FOR EACH MATERIAL TYPE AND OUTPUTS ALL DATA TO
C-----FORMATTED FILE ALSO GENERATES JACOBIAN DATA FOR EACH GAUSS POINT.
C
C
      SUBROUTINE OUTDAT (X,Y,Z,Q,QX,DET,DINT,DELAY,KODE,KX,NP,NSP,KODES,
     *LD,NODEQ,NUMNP,NUMEL,NUMMAT,INT,NSEEP,NDIM,MAXSP,NUMNFQ,NQ,
     *NUMSH)
      DIMENSION X(NUMNP),Y(NUMNP),Z(NUMNP),Q(NQ),DELAY(NQ),
     *DET(NUMSH),DINT(3,8,4,NUMSH),KODE(NUMNP),KX(10,NUMEL),
     *LD(0:NUMNP),NODEQ(18,NQ),NP(MAXSP,NDIM),NSP(NDIM),
     *KODES(NDIM),QX(NQ),RINV(3,3)
      COMMON /MAT/POR(1),RESID(1),ATHET(1),BTHET(1),APERM(1),
     *BPERM(1),BETA(1),GAMMA(1),PSIL(1)
      COMMON /BASIS/ DSHAP(3,4,4)
C
C-----MATERIAL PROPERTIES
C
      WRITE(3,20)
20    FORMAT(///1H ,'MATERIAL PROPERTIES ARE'//)
      DO 40 M=1,NUMMAT
      READ(4,30) POR(M),ATHET(M),BTHET(M),RESID(M),APERM(M),BPERM(M)
30    FORMAT(6E10.3)
      READ(4,35) BETA(M),GAMMA(M),PSIL(M)
35    FORMAT(3E10.3)
40    WRITE(3,50) M,POR(M),ATHET(M),BTHET(M),RESID(M),
     *APERM(M),BPERM(M),BETA(M),GAMMA(M),PSIL(M)
50    FORMAT(1H ,'MATERIAL ',I3//1H ,'POROSITY  ',E13.5/1H ,
     *'ATHETA    ',E13.5/1H ,'BTHETA    ',E13.5/1H ,'RESID M.C.',
     *E13.5/1H ,'APERM     ',E13.5/1H ,'BPERM     ',E13.5/1H ,
     *'BETA',6X,E13.5/1H ,'GAMMA     ',E13.5/1H ,'LIMIT PSI ',
     *E13.5///)
C
C-----BOUNDARY FLUX DATA
C
      IF (NUMNFQ .LT. 1) GO TO 82
      WRITE(3,55)
55    FORMAT(1H ,'BOUNDARY FLUX NODES'//1H ,' NODE',
     *5X,'INITIAL VALUE',40X,'NODES CONNECTED TO',36X,'DELAY TIME'/
     *1H ,8X,'UNFIXED',7X,'FIXED')
      DO 65 N=1,NUMNFQ
      WRITE(3,61) NODEQ(1,N),Q(N),QX(N),(NODEQ(I,N),I=2,18),DELAY(N)
61    FORMAT(I6,2E12.4,I7,16I5,E12.4)
65    CONTINUE
C
C-----SEEPAGE FACE INFORMATION
C
82    IF (NSEEP .LT. 1) GO TO 100
      WRITE(3,83)
83    FORMAT(///1H ,'SEEPAGE FACE INFORMATION'/)
      DO 90 I=1,NSEEP
      WRITE(3,87) I,NSP(I),KODES(I)
87    FORMAT(///1H ,'SEEPAGE FACE NUMBER---',I5,15X,
     *'NUMBER OF NODES--------',I5,'    SEEPAGE FACE CODE-----',
     *I5/1H ,'NODE NUMBERS')
      NS=NSP(I)
      WRITE(3,88) (NP(J,I),J=1,NS)
88    FORMAT(14X,I6,17I5)
90    CONTINUE
C
C-----NODE POINT INFORMATION
C
```

```
100   WRITE(3,110)
110   FORMAT(////1H ,'NODAL POINT INFORMATION'///1H ,'   NODE NO.',5X,
     *'KODE',7X,'X',14X,'Y',14X,'Z'//)
      DO 190 I=1,NUMNP
190   WRITE(3,200) I,KODE(I),X(I),Y(I),Z(I)
200   FORMAT(2I10,3E15.6)
C
C-----ELEMENT INFORMATION
C
      WRITE(3,330)
330   FORMAT(////1H ,'ELEMENT INFORMATION'///1H ,'ELEMENT',34X,'CORNER',
     *'  NODES',32X,'MATERIAL',5X,'SHAPE NO.'//)
      DO 395 N=1,NUMEL
      WRITE(3,390) N,(KX(I,N),I=1,10)
390   FORMAT(I6,I15,7I8,2I14)
395   CONTINUE
C
C-----EVALUATE JACOBIAN INFORMATION FOR ELEMENT SHAPES
C
      DO 700 N=1,NUMSH
      READ(4,400) XE,YE,ZE
400   FORMAT(3E10.3)
      WE=YE/6.0
      DET(N)=XE*YE*ZE*0.25
      XE=2.0/XE
      YE=2.0/YE
      ZE=2.0/ZE
      IF (WE .NE. 0.0) THEN
        TE=-0.50*YE*ZE*WE
      ELSE
        TE=0.0
      END IF
      UE=YE-TE
      VE=YE+TE
C
C-----EVALUATE DN/DX,DN/DY,DN/DZ ARRAYS AT EACH GAUSS POINT FOR FOUR
C-----POINT SCHEME
C
      RINV(1,1)=XE
      RINV(2,1)=0.0
      RINV(3,1)=0.0
      RINV(1,2)=0.0
      RINV(2,2)=YE
      RINV(3,2)=0.0
      RINV(1,3)=0.0
      RINV(2,3)=TE
      RINV(3,3)=ZE
C
C-----LOOP ON GAUSS POINTS
C
        DO 600 K=1,4
          DO 500 I=1,4
            DO 490 J=1,3
            SUM=0.0
              DO 480 L=1,3
480           SUM=SUM+RINV(J,L)*DSHAP(L,I,K)
490         DINT(J,I,K,N)=SUM
500       CONTINUE
          DO 550 I=1,4
          DINT(1,I+4,K,N)=-DINT(1,I,K,N)
          DINT(2,I+4,K,N)=DINT(2,I,K,N)
550       DINT(3,I+4,K,N)=DINT(3,I,K,N)
600     CONTINUE
700   CONTINUE
      RETURN
      END
```

```
C
C
C>>>>>>>>>>>>>>>>>>>>>>>>>>SUBROUTINE GENDAT<<<<<<<<<<<<<<<<<<<<<<<<<<<<
C
C-----GENERATES DATA
C
      SUBROUTINE GENDAT (X,Y,Z,Q,QX,DELAY,QXX,KODE,KX,NP,NSP,KODES,LD,
     *NODEQ,NODEX,NUMNP,NUMEL,NSEEP,NDIM,MAXSP,NUMNFQ,NUMFX,NQ,NX,
     *NUMSH)
      DIMENSION X(NUMNP),Y(NUMNP),Z(NUMNP),Q(NQ),QX(NQ),DELAY(NQ),
     *KODE(NUMNP),KX(10,NUMEL),NP(MAXSP,NDIM),NSP(NDIM),KODES(NDIM),
     *LD(0:NUMNP),NODEQ(18,NQ),NODEX(NX),XX(16),YY(24),ZZ(10),IDUM(28),
     *NODD(4),NODL(4),QXX(NX)
      DATA ZZ/0.0,12.5,25.0,37.5,50.0,62.5,75.0,87.5,97.5,100.0/
      YY(1)=0.0
      YY(2)=5.0
      YY(3)=170.0
      YY(4)=335.0
      YY(5)=500.0
      DO 2 I=6,24
2     YY(I)=YY(I-1)+500.0
      XX(1)=0.0
      DO 3 I=2,16
3     XX(I)=XX(I-1)+1000.0
      SLOPE=1.0/6.0
      NNX=16
      NNY=24
      NNZ=10
      NEX=NNX-1
      NEY=NNY-1
      NEZ=NNZ-1
      NXY=NNX*NNY
      NXZ=NNX*NNZ
      NYZ=NNY*NNZ
C
C-----GENERATE X,Y AND Z COORDS
C
      N=0
      DO 120 K=1,NNY
      YYK=YY(K)
      ZDATUM=YYK*SLOPE
        DO 110 J=1,NNX
        XXJ=XX(J)
          DO 100 I=1,NNZ
          N=N+1
          X(N)=XXJ
          Y(N)=YYK
100       Z(N)=ZZ(I)+ZDATUM
110     CONTINUE
120   CONTINUE
C
C-----GENERATE ELEMENT NODE NUMBER ARRAY KX
C
      NMUL=NNX*NNZ
      N=0
      DO 420 I=1,NEY
        DO 410 J=1,NEX
        NFACT=J*NNZ+NMUL*(I-1)
          DO 400 K=1,NEZ
          N=N+1
          KX(1,N)=NFACT+K
          KX(2,N)=KX(1,N)+NXZ
          KX(3,N)=KX(2,N)+1
          KX(4,N)=KX(1,N)+1
          KX(5,N)=KX(1,N)-NNZ
```

```
          KX(6,N)=KX(2,N)-NNZ
          KX(7,N)=KX(6,N)+1
          KX(8,N)=KX(5,N)+1
          KX(9,N)=1
400       CONTINUE
410     CONTINUE
420   CONTINUE
C
C-----GENERATE ELEMENT SHAPE INDEX
C
      K=0
      DO 450 I=1,NEY
      IF (I .EQ. 1) THEN
        I1=1
        I2=2
        I3=3
      ELSE IF (I .LT. 5) THEN
        I1=4
        I2=5
        I3=6
      ELSE
        I1=7
        I2=8
        I3=9
      END IF
        DO 440 J=1,NEX
          DO 430 N=1,7
          K=K+1
430       KX(10,K)=I1
        K=K+1
        KX(10,K)=I2
        K=K+1
        KX(10,K)=I3
440     CONTINUE
450   CONTINUE
C
C-----ZERO KODE VECTOR
C
      DO 600 I=1,NUMNP
600   KODE(I)=0
C
C-----EVALUATE LD THE POSITION VECTOR FOR ARRAY A
C
      LD(0)=0
      LD(1)=1
      DO 700 I=2,NUMNP
      MAXD=0
        DO 680 N=1,NUMEL
        ICHECK=0
        NMIN=NUMNP
          DO 670 L=1,8
          IF (KX(L,N) .EQ. I) ICHECK=1
          IF (KX(L,N) .LT. NMIN) NMIN=KX(L,N)
670       CONTINUE
        IF (ICHECK .EQ. 0) GO TO 680
        II=I-NMIN
        IF (II .GT. MAXD) MAXD=II
680     CONTINUE
      LD(I)=LD(I-1)+MAXD+1
700   CONTINUE
C
C-----GENERATE NON-FIXED FLUX VALUES AND CONDENSED NODE
C-----NUMBERING ARRAY NODEQ
C
      DO 703 I=1,NUMNFQ
        DO 702 J=1,18
```

```
702       NODEQ(J,I)=0
703     CONTINUE
        KK=0
        K=0
        DO 710 I=1,NNX
          DO 705 J=1,NNZ-1
          KK=KK+1
          K=K+1
          Q(K)=0.0
          KODE(KK)=-2
705       NODEQ(1,K)=KK
        K=K+1
        Q(K)=0.0
        KK=KK+1
        NODEQ(1,K)=KK
710     CONTINUE
        DO 712 I=1,NNY-1
        KK=NNZ+NXZ*I
          DO 711 J=1,NNX
          K=K+1
          Q(K)=0.0
          NODEQ(1,K)=KK
711       KK=KK+NNZ
712     CONTINUE
        DO 790 I=1,NUMNFQ
          DO 713 J=1,28
          IDUM(J)=0
713       CONTINUE
        NOD=NODEQ(1,I)
        K=0
          DO 730 N=1,NUMEL
            DO 715 J=1,8
            IF (KX(J,N) .EQ. NOD) GO TO 720
715         CONTINUE
            GO TO 730
720         DO 725 L=1,8
            KXLN=KX(L,N)
            IF (KXLN .EQ. NOD) GO TO 725
            K=K+1
            IDUM(K)=KXLN
725         CONTINUE
730       CONTINUE
          DO 740 L=1,27
          II=IDUM(L)
            DO 735 K=L+1,28
            IF (IDUM(K) .GE. II) GO TO 735
            II=IDUM(K)
            IDUM(K)=IDUM(L)
            IDUM(L)=II
735         CONTINUE
740       CONTINUE
        K=1
          DO 750 L=1,28
          IDL=IDUM(L)
          IF (IDL .EQ. 0 .OR. IDL .EQ. NODEQ(K,I)) GO TO 750
          K=K+1
          NODEQ(K,I)=IDUM(L)
750       CONTINUE
790     CONTINUE
C
C-----ASSIGN TIME DELAYS TO DELAY ARRAY
C
        DO 800 I=1,NUMNFQ
        QX(I)=0.0
        NODE=NODEQ(1,I)
800     DELAY(I)=Y(NODE)/30.0
```

```
C
C-----GENERATE NODEX AND QX FOR FIXED FLUX NODES
C
      Q1=0.5/240.0
      K=0
      DO 900 I=1,NUMFX
      K=K+NNZ
      QXX(I)=0.0
900   NODEX(I)=K
      DO 1000 N=1,NUMEL
      ICHECK=0
        DO 920 J=1,8
        KXJN=KX(J,N)
        L=0
910     L=L+1
        IF (KXJN .EQ. NODEX(L)) GO TO 915
        IF (L .LT. NUMFX) GO TO 910
        GO TO 920
915     ICHECK=ICHECK+1
        NODD(ICHECK)=KXJN
        NODL(ICHECK)=L
920     CONTINUE
      IF (ICHECK .LT. 4) GO TO 1000
      N1=NODD(1)
      N2=NODD(2)
      N3=NODD(3)
      N4=NODD(4)
      XMAX=MAX(X(N1),X(N2),X(N3),X(N4))
      XMIN=MIN(X(N1),X(N2),X(N3),X(N4))
      YMAX=MAX(Y(N1),Y(N2),Y(N3),Y(N4))
      YMIN=MIN(Y(N1),Y(N2),Y(N3),Y(N4))
      QSCALE=Q1*(XMAX-XMIN)*(YMAX-YMIN)
        DO 930 I=1,4
        L=NODL(I)
930     QXX(L)=QXX(L)+QSCALE
1000  CONTINUE
C
C-----ASSIGN FIXED FLUX VALUES TO Q ARRAY
C
      DO 1010 I=1,NUMFX
      NODE=NODEX(I)
      NOD=0
1005  NOD=NOD+1
      IF (NODEQ(1,NOD) .LT. NODE) GO TO 1005
      QX(NOD)=QXX(I)
1010  CONTINUE
C
C-----SEEPAGE FACE DATA
C
      DO 1100 I=1,NSEEP
      K=NNZ*(I-1)
      KODES(I)=-1
      NSP(I)=NNZ-1
        DO 1050 J=1,NSP(I)
        K=K+1
        NP(J,I)=K
1050    CONTINUE
1100  CONTINUE
      RETURN
      END
```

```
C
C
C>>>>>>>>>>>>>>>>>>>>>>>>>>>>>>>>BLOCK DATA<<<<<<<<<<<<<<<<<<<<<<<<<<<<<<<<
C
C-----PROVIDES DATA FOR COMMON BLOCK BASIS
C
      BLOCK DATA
      PARAMETER (RT=0.57735026918963,SX=1.0/6.0,R=SX+0.25*RT,
     *S=SX-0.25*RT,T=1.0/12.0,U=(1.0+RT)/8.0,V=(1.0-RT)/8.0)
      COMMON /BASIS/ DSHAP(3,4,4)
      DATA DSHAP/R,-U,-U,T,U,-V,S,V,V,T,-V,U,T,-U,-V,R,U,-U,T,V,U,S,-V,
     *V,S,-V,-V,T,V,-U,R,U,U,T,-U,V,T,-V,-U,S,V,-V,T,U,V,R,-U,U/
      END
```

INDAT data file

```
        M E S H  ( 7 )  T R A N S I E N T  S I M U L A T I O N
                  UNITS IN CENTIMETRES AND MINUTES
3840 3105    1   16    9  528  384    9
     0.57    1924.8     1.247     0.245   14.7516    0.9569
1.754E-05 1.702E-01-3.382E-05
   1000.0       5.0      12.5
   1000.0       5.0      10.0
   1000.0       5.0       2.5
   1000.0     165.0      12.5
   1000.0     165.0      10.0
   1000.0     165.0       2.5
   1000.0     500.0      12.5
   1000.0     500.0      10.0
   1000.0     500.0       2.5
```

References

Abbot, M.B., I.R. Warren, K.H. Jensen, T. Jonch-Clausen and K. Havno, Coupling of unsaturated and saturated zone models, *Proc XVIII IAHR Congress*, Cagliari, Italy, Subject D.C., p119-125, 1979.

Akan, A.O. and B.C. Yen, Mathematical model of shallow water flow over porous media, *J. Hyd. Div. ASCE*, 107, p479-494, 1981.

Andersson, J. and A.M. Shapiro, Stochastic analysis of one dimensional steady state unsaturated flow: A comparison of Monte Carlo and perturbation methods, *Water Resources Res.*, 19 (1), p121-133, 1983.

Aparcio, F.J. and M. Berezowsky, A distributed rainfall - runoff model, *Proc. 4th International Conf. Finite Elements in Water Resources*, Hannover, W.Germany, p(4-3)-(4-12), 1982.

Atkinson, T.C., Techniques for measuring subsurface flow on hillslopes, in *Hillslope Hydrology*, edited by M.J. Kirkby, Wiley, 1978.

Babalola, O., Spatial variability of soil water properties in tropical soils of Nigeria, *Soil Sci.*, 126 (5), p269-279, 1978.

Babu, D.K. and G.F. Pinder, A finite element - finite difference alternating direction algorithm for three dimensional groundwater transport, *Adv. in Water Resources*, 7, p116-119, 1984.

Baker, F.G. and J. Bouma, Variability of hydraulic conductivity in two subsurface horizons of two silt loam soils, *Soil Sci. Soc. Am. J.*, 40, p219-222, 1976.

Bakr, A.A., L.W. Gelhar, A.L. Gutjhar and J.R. MacMillan, Stochastic analysis of spatial variability in subsurface flows 1. Comparison of one and three dimensional flows, *Water Resources Res.*, 14 (2), p263-271, 1978.

Barcelo, M.D. and J.L. Nieber, Simulation of the hydrology of natural pipes in a soil surface, *Amer. Soc. Agric. Eng.*, Pap No. 81-2028, 1981.

Barcelo, M.D. and J.L. Nieber, Influence of a soil pipe network on catchment Hydrology, *Proc. Fourth Int. Conf. on Finite Elements in Water Resources*, Hannover, W. Germany, p(10-3)-(10-14), 1982.

Bartlett, M.S., *The statistical analysis of spatial pattern*, Chapman and Hall, 1975.

Beven, K.J., A deterministic, spatially distributed model of catchment hydrology, *PhD thesis*, School of Environ. Sci., University of East Anglia, 1975.

Beven, K.J., Hillslope hydrographs by the finite element method, *Earth Surf. Processes*, 2, p13-28, 1977.

Beven, K.J., Comments on 'A stochastic - conceptual analysis of rainfall - runoff processes on a hillsope' by R.A. Freeze, *Water Resources Res.*, 17 (2), p431-432, 1981

Beven, K.J., Introducing spatial variability into TOPMODEL: Theory and preliminary results, *Unpublished rept.*, Dept. Environ. Sci., Univ. Virginia, USA, 1983.

Beven, K.J., Comments on models, physically-based models, and SHE, *Unpublished manuscript*, Dept. Environ. Sci., Univ. Lancaster, U.K., 1986.

Beven, K.J. and M.J. Kirkby, A physically based, variable contributing area model of basin hydrology, *Hydrol. Sci. Bull.*, 24 (1), p43-69, 1979.

Beven, K.J. and P. Germann, Water flow in macropores: II A combined flow model, *J. Soil. Sci.*, 32, p15-29, 1981.

Beven, K.J. and P.E. O'Connel, On the role of physically - based distributed modelling in hydrology, *Institute of Hydrology rept. 81*, Institute of Hydrology, UK, 1982.

Beven, K.J. and P. Germann, Macropores and water flow in soils, *Water Resources Res.*, 18 (5), p1311-1325, 1982.

Beven, K.J. and E.M. Morris, The Institute of Hydrology distributed model, *Institute of Hydrology rept. in preperation*, Institute of Hydrology, UK, 1986.

Beven, K.J., R. Warren and J. Zaoui, SHE: Towards a methodology for physically - based distributed forecasting in hydrology, *Proc. Oxford Symp.*, IAHS publ. no. 129, p133-137, 1980.

Beven, K.J., M.J. Kirkby, N. Schofield and A.F. Tagg, Testing a physically - based flood forecasting model (TOPMODEL) for three U.K. catchments, *J. Hydrol.*, 69, p119-143, 1984.

Bouma, J. and L.W. Decker, A method for measuring the vertical and horizontal Ksat of clay soils with macropores, *Soil Sci. Soc. Am. J.*, 45, p662-663, 1981.

Bouma, J., C.F.M. Belmans and L.W. Dekker, Water infiltration in a silt loam subsoil with vertical worm channels, *Soil Sci. Soc. Am. J.*, 46, p917-921, 1982.

Brakensiek, D.L., Hydrodynamics of overland flow and non - prismatic channels, *Trans. ASAE*, 9 (1), p119-122, 1966.

Brebbia, C.A. and S.Walker, *Boundary Element Techniques in Engineering*, Butterworth and Co., 1980.

Bresler, E. and G. Dagan, Unsaturated flow in spatially variable fields 2. Application of water flow models to various fields, *Water Resources Res.*, 19 (2), p421-428, 1983a.

Bresler, E. and G. Dagan, Unsaturated flow in spatially variable fields 3. Solute transport models and their application to two fields, *Water Resources Res.*, 19 (2), p429-435, 1983b.

Brooks, R.H. and A.T.Corey, Hydraulic properties of porous media, *Hydrol. pap. 3*, 27pp, Agric. Eng. Dept., Colorado State Univ., Colorado, USA, 1964.

Bruch, J.C., Two dimensional unsteady flow in unsaturated porous media, *Proc. First Int. Conf. on Finite Elements in Water Resources*, Princeton Univ.,USA, 1976.

Brutsaert, W., Probability laws for pore - size distributions, *Soil Sci.*, 101 (2), p85-92, 1966.

Brutsaert, W., The permeability of a porous medium determined from certain probability laws for pore size distribution, *Water Resources Res.*, 4 (2), p425-434, 1968.

Brutsaert, W. and A.I. El-Kadi, The relative importance of compressibility and partial saturation in unconfined groundwater flow, *Water Resources Res.*, 20 (3), p400-408, 1984.

Bunting, B.T., The role of seepage moisture in soil formation, slope development and stream initiation, *Am. J. Sci.*, 259, p503-518, 1961.

Butcher, D.P., The field verification of topographic indeces for use in hillslope runoff models., *Phd thesis*, Dept. Geography, Huddersfield Polytechnic, U.K., 1986.

Burt, T.P., Three simple and low - cost instruments for measurement of soil moisture properties, *Occasional paper 8*, 24pp, Dept. Geography, Huddersfield Polytechnic, U.K., 1978.

Cardwell, W.L. and R.L. Parsons, Average permeabilities of heterogeneous oil sands, *Trans. AIME*, 160, p34-43, 1945.

Carvallo, H.O, D.K. Cassel, J. Hammond and A. Bauer, Spatial variability of in situ unsaturated hydraulic conductivity of Maddock sandy loam, *Soil Sci.*, 121 (1), p1-8, 1976.

Childs, E.C. and N. Collis-George, The permeability of porous materials, *Proc. Royal Soc.*, A201, p392-405, 1950.

Contractor, D.N., B.B. Ross and V.O. Shanholtz, A finite element watershed model to predict storm hydrographs, sediment erosion and transport, *Proc. Third Int. Conf. on Finite Elements in Water Resources*, Oxford, Miss., USA, 1980.

Cooley, R.L., A finite difference method for variably saturated porous media: Application to a single pumping well, *Water Resources Res.*, 7 (6), p1607-1625, 1971.

Cooley, R.L., Some new procedures for numerical solution of variably saturated flow problems, *Water Resources Res.*, 19 (5), p1271-1285, 1983.

Cosby, B.J., G.M. Hornberger, R.B. Clapp and T.R. Ginn, A statistical exploration of the relationships of soil moisture characteristics to the physical properties of soils, *Water Resources Res.*, 20 (6), p682-690, 1984.

Cusham, J.H., Comments on 'Three-dimensional stochastic analysis of macro dispersion in aquifers', *Water Resources Res.*, 19 (6), p1641-1642, 1983.

Cusham, J.H., D. Kirkham and R.F. Keller, A Galerkin in time, linearized finite element model of 2-dimensional unsaturated porous media drainage, *Soil Sci. Soc. Am. J.*, 43, p638-641, 1979.

Dagan, G., Models of groundwater flow in statistically homogeneous porous formations, *Water Resources Res.*, 15 (1), p47-63, 1979.

Dagan, G., Stochastic modelling of groundwater flow by unconditional and conditional probabilities 1. Conditional simulation and the direct problem, *Water Resources Res.*, 18 (4), p813-833, 1982a.

Dagan, G., Analysis of flow through heterogeneous random aquifers 2. Unsteady flow in confined aquifers, *Water Resources Res.*, 18 (5), p1571-1585, 1982b.

Dagan, G. and E. Bresler, Unsaturated flow in spatially variable fields 1. Derivation of models of infiltration and redistribution, *Water Resources Res.*, 19 (2), p413-420, 1983.

Dettinger, M.D. and J.L. Wilson, First order analysis of uncertainty in numerical models of groundwater flow. Part 1 Mathematical development, *Water Resources Res.*, 17 (1), p149-161, 1981.

Dillon, P.J. and J.L. Ligget, An ephermal stream-aquifer interaction model, *Water Resources Res.*, 19 (3), p621-626, 1983.

Edwards, W.M., R.R. Van der Ploeg and W. Ehlers, A numerical study of noncapillary-sized pores upon infiltration, *Soil Sci. Soc. Am. J.*, 43, p851-856, 1979.

Ehlers, W., Observations on eartworm channels and infiltration on tilled and untilled loes soil., *Soil Sci.*, 119 (3), p242-249, 1975.

El-Kadi, A. and W. Brutsaert, Applicability of effective parameters for unsteady flow in nonuniform aquifers, *Water Resources Res.*, 21 (2), p183-189, 1985.

Emmet, W.W., Overland flow, in *Hillslope Hydrology*, edited by M.J. Kirkby, Wiley, 1978.

Eraslan, A.V., I.H. Erhan and W.L. Lin, A fast transient, two dimensional, discrete element rainfall runoff model for channelized, composite subsurface-surface flows in valleys with steep terain, in *Proc. Int. Symp. on Rainfall-Runoff Modeling*, Mississippi, USA, 1981.

Eriksson, E. and H. Grip, in *Comparison of Forest Water and Energy Exchange Models*, edited by S. Halldin, p213-224, 1979.

Faust, C.R. and J.W. Mercer, Groundwater modelling: Numerical models, *Groundwater*, 18 (4), p395-409, 1980.

Fellipa, C.A., Solution of linear equations with skyline stored symmetric matrix, *Computers and Structures*, 5, p13-30, 1975.

Fogg, G.E., E.S. Simpson and S.P. Neuman, Aquifer modelling by numerical methods applied to an Arizona groundwater basin, *rept PB-298 962*, Univ. Arizona, Arizona, USA, 1979.

Fread, D.L., Flood routing: A synopsis of past, present and future capability. In: Rainfall runoff relationships, *Proc. Int. Symp. Rainfall Runoff Modeling*, Mississippi, USA, p521-542, 1981.

Freeze, R.A., Three-dimensional, transient, saturated-unsaturated flow in a groundwater basin, *Water Resources Res.*, 7 (2), p347-366, 1971.

Freeze, R.A., Role of subsurface flow in generating surface runoff. I Baseflow contributions to channel flow, *Water Resources Res.*, 8 (3), p609-623, 1972a.

Freeze, R.A., Role of subsurface flow in generating surface runoff. II Upstream source areas, *Water Resources Res.*, 8 (5), p1272-1283, 1972b.

Freeze, R.A., A stochastic-conceptual analysis of one-dimensional groundwater flow in a nonuniform homogeneous media, *Water Resources Res.*, 11 (5), p725-741, 1975.

Freeze, R.A., Mathematical models of hillslope hydrology, in *Hillslope Hydrology*, edited by M.J. Kirkby, Wiley, 1978.

Freeze, R.A., A stochastic-conceptual analysis of rainfall runoff processes on a hillslope, *Water Resources Res.*, 16 (2), p391-408, 1980.

Frind, E.O. and M.J. Verge, Three dimensional modelling of groundwater flow systems, *Water Resources Res.*, 14 (4), p844-856, 1978.

Gardner, W.R., Some steady state solutions of the unsaturated moisture flow equation with application to evaporation from a water table, *Soil Sci.*, 85, p228-232, 1958.

Gelhar, L.W., Effects of hydraulic conductivity variations on groundwater flows, *Proc. Second Int. IAHR Symp. on Stochastic Hydraulics*, Lund, Sweden, 1976.

Gelhar, L.W. and C.L. Axness, Three-dimensional stochastic analysis of macrodispersion in aquifers, *Water Resources Res.*, 19 (1), p161-180, 1983.

Gelhar, L.W. and C.L. Axness, Reply, *Water Resources Res.*, 19 (6), p1643-1644, 1983.

Germann, P. and K.J. Beven, Water flow in soil macropores: I An experimental approach, *J. Soil Sci.*, 32, p1-13, 1981.

Gilding, B.H., The soil moisture zone in a physically-based hydrologic model, *Adv. Water Resources*, 6, p36-43, 1983.

Gillham, R.W., A. Klute and D.F. Heermann, Measurement and numerical simulation of hysteretic flow in a heterogeneous porous medium, *Soil Sci. Soc. Am. J.*, 43 (6), p1061-1067, 1979.

Gilman, K. and M. Newson, *Soil Pipes and Pipeflow - A Hydrological Study in Upland Wales*, Res. Monographs 1, Brit. Geomorphological Res. Group, Geobooks, Norwich, UK, 1980.

Green, W.H. and G.A. Ampt, Studies on soil physics: I Flow of air and water through soils, *J. Agric. Sci.*, 4, p1-24, 1911.

Gupta, S.K. and K.K. Tanji, A three dimensional Galerkin finite element solution of flow through multiaquifers in Sutter Basin, California, *Water Resources Res.*, 12 (2), p155-162, 1976.

Gureghian, A.B., A two dimensional finite element solution scheme for the saturated-unsaturated flow with applications to flow through ditch-drained soils, *J. Hydrol.*, 50, p333-353, 1981.

Gutjhar, A.L., Stochastic models of subsurface flow: Log linearized gaussian models are "exact" for covariances, *Water Resources Res.*, 20 (12), p1909-1912, 1984.

Gutjhar, A.L. and L.W. Gelhar, Stochastic models of subsurface flow: Infinite versus finite domains and stationarity, *Water Resources Res.*, 17 (2), p337-350, 1981.

Gutjhar, A.L., L.W. Gelhar, A.A. Bakr and J.L. MacMillan, Stochastic analysis of spatial variability in subsurface flows. 2 Evaluation and application, *Water Resources Res.*, 14 (5), p953-959, 1978.

Hammermeister, D.P., G.F. Kling and J.A. Vomocil, Perched water tables on hillslides in Western Oregon: II Preferential downslope movement of water and anions, *Soil Sci. Soc. Am. J.*, 46, p819-826, 1982.

Haverkamp, R. and M. Vauclin, A comparative study of three forms of the Richard equation used for predicting one-dimensional infiltration into unsaturated soil, *Soil Sci. Soc. Am. J.*, 45, p13-20, 1981.

Hayhoe, H.N., Study of the relative efficiency of finite difference and Galerkin techniques for modeling soil-water transfer, *Water Resources Res.*, 14 (1), p97-102, 1978.

Heatwole, C.D., V.O. Shanholtz and B.B. Ross, Finite element model to describe overland flow on an infiltrating watershed, *Trans. ASAE*, 25 (3), p630-637, 1982.

Herrling, B. and H.M. Leismann, Finite element computation of unsaturated and saturated groundwater flow in stratified aquifers, *Proc. Fifth Int. Conf. on Finite Elements in Water Resources*, Vermont, USA, 1984.

Hillel, D., *Soil and water. Physical principles and processes*, Academic press, 1971.

Holtan, H.N., A concept for infiltration estimates in watershed engineering, *Agric. Res. Serv. USDA*, ARS 41-51, 1961.

Hornung, U. and W. Messing, A predictor-corrector alternating-direction implicit method for two dimensional unsteady saturated-unsaturated flow in porous media, *J. Hydrol.*, 47, p317-323, 1980.

Hosseinpour, Z and M. Amein, Finite element computation of two-dimensional unsteady flow for river problems, *Proc. Fifth Int. Conf. on Finite Elements in Water Resources*, Vermont, USA, 1984.

Hromadka, T.V. and G.L. Guymon, Some effects of linearizing the unsaturated soil moisture transfer diffusivity model, *Water Resources Res.*, 16 (4), p643-650, 1980.

Hromadka, T.V. and G.L. Guymon, Improved linear trial function finite element model of soil moisture transport, *Water Resources Res.*, 17 (3), p504-512, 1981.

Hromadka, T.V., G.L. Guymon and G.C. Pardoen, Nodal domain integration model of unsaturated two-dimensional soil water flow: Development, *Water Resources Res.*, 17 (5), p1425-1430, 1981.

Huyakorn, P.S., S.D. Thomas and B.M. Thompson, Techniques for making finite elements competitive in modelling variably saturated porous media, *Water Resources Res.*, 20 (8), p1099-1115, 1984.

Jayawardena, A.W., On the application of the finite element method to catchment modelling, *PhD. thesis,* Univ. London, 281pp, 1975.

Jensen, S.E., Model ETFOREST for calculating actual evapotranspiration, in *Comparison of Forest Water and Energy Exchange Models*, edited by S. Halldin, p165-172, 1979.

Jensen, K.H. and T. Jonch-Clausen, Unsaturated flow and evapotranspiration modeling as a component of the European Hydrologic System (SHE), in Modelling components of the hydologic cycle, *Proc. Int. Symp. on Rainfall-Runoff Modeling*, Mississippi, USA, p235-253, 1981.

Jonch-Clausen, T., SHE Systeme Hydrologique Eurpeen. A short description, *Danish Hydraulic Institute Report*, 1979.

Jones, A.A., Soil piping and stream channel initiation, *Water Resources Res.*, 7 (3), p603-610, 1971.

Jones, A.A., Soil piping and the subsurface initiation of stream channel networks, *PhD thesis*, Cambridge Univ, UK, 1976.

Jovic, V., Groundwater balance simulation by finite element method, *Proc. XVIII Congress IAHR*, Cagliari, Italy, subject DC, p153-160, 1979.

Kawahara, M. and T. Yokoyama, Finite element method for direct runoff flow, J. *Hyd. Div. ASCE*, 106, p519-534, 1980.

Keller, H.M., Model comparison to estimate consumptive use, in *Comparison of Forest Water and Energy Exchange Models*, edited by S. Halldin, p225-235, 1979.

King, I.P., Finite element models for unsteady flow routing through irregular channels, *Proc. First Int. Conf. on Finite Elements in Water Resources*, Princeton Univ.,USA, 1976.

King, I.P., Strategies for finite element modelling of three dimensional hydrodynamic systems, Adv. *Water Resources*, 8, p69-76, 1985.

Kirkby, M.J., *Hillslope Hydrology*, Wiley, 1978.

Kirkham, D., Flow of ponded water into drain tubes in soil overlying an impervious layer, *Trans. Am. Geophys. Union*, 30 (3), p369-385; 1949.

Lam, L. and D.G. Fredlund, Saturated-unsaturated transient finite element seepage model for geotechnical engineering, *Adv. in Water Resources*, 7 (3), p132-136, 1984.

Law, J., A statistical approach to the interstitial heterogeneity of sand reservoirs. *Trans. AIME*, 155, p202-222, 1944.

Li, E.A., V.O. Shanholtz and D.N. Contractor, Generating rainfall excess based on readily determinable soil and land use characteristics, *Trans. ASAE*, 20 (6), p1070-1077, 1977.

Ligget, J.A. and P.L.F. Liu, *Boundary Integral Equation Method for Porous Media Flow*, Allen and Unwin, 1983.

Linsey, R.K. and N.H. Crawford, Computer simulation of a synthetic streamflow record on a digital computer, *Hydrol. Sci. Bull.*, Publ. 51, p526-538, 1960.

Linsey, R.K., Rainfall-runoff models - An overview, Proc. Int. Symp. on Rainfall-Runoff Modelling, *Proc. Int. Symp. on Rainfall-Runoff Modeling*, Mississippi, USA, p3-22, 1981.

Loage, K.M. and R.A. Freeze, A comparison of rainfall-runoff modeling techniques on small upland catchments, *Water Resources Res.*, 21 (2), p229-248, 1985.

McDonald, M.G. and A.W. Harbaugh, A Modular three dimesional finite-difference groundwater flow model, US Dept. of the Interior, US Geological Survey, National Center, Reston, Virginia, 1984.

Macfarlane, I.C., *Muskeg Engineering Handbook*, Univ. Toronto Press, Ontario, Canada, 1969,

Mantoglou, A. and J.L. Wilson, Simulation of random fields with the turning bands method, *Tech. Rept. 264*, Dept. Civil Eng., Mass. Inst. Technol., Cambridge, Mass, USA, 1981.

Mantoglou, A. and J.L. Wilson, The turning bands method for simulation of random fields using line generation by a spectral method, *Water Resources Res.*, 18 (5), p1379-1394, 1982.

Mapa, R.B., Temporal variability of soil hydraulic properties subsequent to tillage, *Phd. thesis*, Univ. Hawaii, 216pp, 1984.

Marino, M.A., Analysis of the transient movement of water and solutes in stream-aquifer systems, *J. Hydrol.*, 49, p1-17, 1981.

Marshall, T.J., Permeability equations and their models, *Proc. Symp. on Interaction between Fluids and Particles*, London, p299-303, 1962.

Matheron, G., The intrinsic random functions and their applications, *Advan. Appl. Prob.*, 5, p439-468, 1973.

Mejia, J.M. and I. Rodriguez-Iturbe, On the synthesis of random field sampling form the spectrum: An application to the generation of hydrologic spatial processes, *Water Resources Res.*, 10 (4), p705-711, 1974.

Milly, P.C.D., Moisture and heat transport in hysteretic, inhomogeneous porous media: A matric head based formulation and a numerical model, *Water Resources Res.*, 18 (3), p489-498, 1982.

Milly, P.C.D., A mass-conservative procedure for time stepping in models of unsaturated flow, *Proc. Fifth Int. Conf. on Finite Elements in Water Resources*, Vermont, USA, 1984.

Mizell, S.A., A.L. Gutjhar and L.W. Gelhar, Stochastic analysis of spatial variability in two dimensional steady groundwater flow assuming stationary and nonstationary heads, *Water Resources Res.*, 18 (4), p1053-1067, 1982.

Mohsenisaravi, M., Forecasting subsurface water flow and storage on forested slopes using a finite element model, *Phd. dissertation*, Univ. Idaho, Idaho, USA, 1981.

Morris, E.M., Forecasting flood flows in grassy and forested basins using a deterministic distributed mathematical model, *Proc. Oxford Symp.*, IAHS publication 129, p247-255, 1980.

Morris, E.M. and J.G. Godfrey, The European Hydrological System snow routine, in *Proc. Modelling of Snow Cover Runoff*, edited by S.C. Colbeck and M. Ray, CRREL, Hanover, New Hampshire, USA, 1979.

Mosely, M.P., Streamflow generation in a forested watershed NZ, *Water Resources Res.*, 15 (4), p795-806, 1982.

Mualem, Y., A conceptual model of hysteresis, *Water Resources Res.*, 10 (3), p514-520, 1974.

Myers, J.C., A study of drainage conditions on a hillside receiving sewage plant waste water effluent at weekly intervals, *MSc. thesis*, Dept. Agronomy, Pennsylvania State Univ., Pennsylvania, USA, 1967.

Naef, F., Can we model the rainfall-runoff process today ?, *Hydrol. Sci. Bull.*, 26, p281-289, 1981.

Narasimhan, T.N. and P.A. Witherspoon, An integrated finite difference method for analysing fluid flow in porous media, *Water Resources Res.*, 12 (1), p57-64, 1976.

Narasimhan, T.N. and P.A. Witherspoon, Numerical model for saturated-unsaturated flow in deformable porous media. I Theory, *Water Resources Res.*, 13 (3), p657-664, 1977.

Narasimhan, T.N. and P.A. Witherspoon, Numerical model for saturated-unsaturated flow in deformable porous media. III Applications, *Water Resources Res.*, 14 (6), p1017-1034, 1978.

Narasimhan, T.N., P.A. Witherspoon and P.A. Edwards, Numerical model for saturated-unsaturated flow in deformable porous media. II The algorithm, *Water Resources Res.*, 14 (2), p225-261, 1978a.

Narasimhan, T.N., S.P. Neuman and P.A. Witherspoon, Finite element method for subsurface hydrology using a mixed explicit-implicit scheme, *Water Resources Res.*, 14 (5), p863-877, 1978b.

Neuman, S.P., Finite element computer programs for flow in saturated-unsaturated porous media, *Project A10-SWC-77*, Hydraulic Engineering Laboratory, Technion, Haifa, Israel, 1972.

Neuman, S.P., Saturated-unsaturated seepage by finite elements, *J. Hyd. Div. ASCE*, 99, p2233-2250, 1973.

Neuman, S.P., R.A. Feddes and E. Bresler, Finite element simulation of flow in saturated-unsaturated soils considering water uptake by plants, *Project AL0-SWC-77*, Hydraulic Engineering Laboratory, Technion, Haifa, Israel, 1974.

Newson, M.D. and J.G. Harrison, Channel studies in the Plynlimon experimental catchment, *Institute of Hydrology rept. 47*, Institute of Hydrology, UK, 1978.

Nieber, J.L., Evaluation of coefficient matrices of linear triangular elements involving unsaturated soil moisture flow, *Proc. Third Int. Conf. on Finite Elements in Water Resources*, Oxford, Miss., USA, 1980.

Nieber, J.L. and M.F. Walter, 2-dimensional soil moisture flow in a sloping rectangular region: Experimental and numerical studies, *Water Resources Res.*, 17 (6), p1722-1730, 1981.

Nielsen, D.R., J.W. Biggar and K.T. Erh, Spatial variability of field measured soil water properties, *Hilgardia*, 42, p215-259, 1973.

Orlob, G.T. and A. Ghorbanzadeh, Impact of water resource development on salinization of semi-arid lands, *Agric. Water Management*, 4, p275-293, 1981.

Overton, D.E., Simulating overland flow on hillslopes with a kinematic cascade, *Mathematical Models in Hydrology*, Volume 2, 1971.

Parker, G.G., Piping: A geomorphologic agent in landform development of the drylands, *IAHS publ. 65*, p103-113, 1963.

Philip, J.R., The theory of infiltration, 4 sorptivity and algebraic infiltration equations, *Soil Sci.*, 84, p257-264, 1957.

Philip, J.R., Theory of infiltration, *Advan. Hydroscience*, 5, p216-296, 1969.

Pickens, J.F. and R.W. Gillham, Finite element analysis of solute transport under hysteretic unsaturated flow conditions, *Water Resources Res.*, 16 (6), p1071-1078, 1980.

Pinder, G.F. and E.O. Frind, Application of Galerkin's procedure to aquifer analysis, *Water Resources Res.*, 8 (1), p108-120, 1972.

Pinder, G.F. and W.G. Gray, *Finite element simulation in surface and subsurface hydrology*, Academic Press, 1977.

Rawls, W.J., D.L. Brakensiek and N. Miller, Green Ampt infiltration parameters form soil data, *J. Hyd. Div. ASCE*, 109, p62-70, 1983.

Reeder, J.W., D.L. Freyberg, J.B. Franzini and I. Remson, Infiltration under rapidly varying surface water depths, *Water Resources Res.*, 16 (1), p97-104, 1980.

Remson, I., G.M. Hornberger and F.Z. Molz, *Numerical Methods in Subsurface Hydrology*, Wiley, 1971.

Richards, L.A., Capillary conduction of liquids through porous mediums, *Physics*, 1 (5), p318-333, 1931.

Rogers, C.C.M., K.J. Beven, E.M. Morris and M.G. Anderson, Sensitivity analysis, calibration and predictive uncertainty of the Institute of Hydrology Distributed Model, *J. Hydrol.*, 81, p179-191, 1985.

Rogowski, A.S., Watershed physics: Soil variability criteria, *Water Resources Res.*, 8 (4), p1015-1023, 1972.

Rosenblueth, E., Point estimates for probability moments, *Proc. National Academy Sci. USA*, 72 (10), p3812-3814, 1975.

Ross, B.B., D.N. Contractor and V.O. Shanholtz, A finite element model of overland flow and channel flow for assessing the hydrological impact of landuse change, *J. Hydrol.*, 41, p11-30, 1979.

Rovey, C.E.K., Numerical model of flow in a stream aquifer system, *Hydrology paper 74*, Colorado State Univ., Colorado, USA, 1975.

Rubin, J., Theoretical analysis of two dimensional transient flow of water in unsaturated and partly unsaturated soils, *Soil Sci. Soc. Am. Proc.*, 32 (5), p607-615, 1968.

Russo, D. and E. Bressler, Effect of field variability in soil hydraulic properties on solutions of unsaturated water and salt flows, *Soil Sci. Soc. Am. J.*, 45, p675-681, 1981a.

Russo, D. and E. Bressler, Soil hydraulic properties as stochastic processes. I An analysis of field spatial variability, *Soil Sci. Soc. Am. J.*, 45, p682-687, 1981b.

Russo, D. and E. Bressler, Soil hydraulic properties as stochastic processes. II Errors of estimates in a heterogeneous field, *Soil Sci. Soc. Am. J.*, 46, p20-26, 1982.

Sagar, B., Galerkin finite element procedure for analysing flow through random media, *Water Resources Res.*, 14 (6), p1035-1044, 1978.

Sai, J.O., Effect of capillary hysteresis and spatial variability of hydraulic conductivity on two dimensional hillslope moisture flow, *Phd. dissertation*, Texas A and M Univ., USA, 1982.

Samuels, P.G., Two dimensional modelling of flood flows using the finite element method, *Proc. Int. Conf. Hydraulic aspects of Floods and Flood Control*, Cranfield, UK, 1983.

Samuels, P.G. and R.K. Price, FLUCOMP - A numerical river flow model, in *Engineering Software Proc. 1st Int. Conf.*, Southampton Univ, UK, p303-319, 1979.

Saxton, K.E., Mathematical modeling of evapotranspiration on agricultural watersheds, In: Modeling Components of Hydrologic Cycle, *Proc. Int. Symp. Rainfall Runoff Modeling*, Mississippi, USA, p183-204, 1981.

Scotter, D.R., Preferential solute movement through larger soil voids. I Some computations using simple theory, *Australian J. Soil Research*, 16, p257-267, 1978.

Shanholtz, V.O., B.B. Ross and J.C. Carr, Effect of spatial variability on the simulation of overland and channel flow, *Trans. ASAE*, 24 (1), p124-133, 1981.

Sharma, M.L. and R.J. Luxmore, Soil spatial variability and its consequences on simulated water balance, *Water Resources Res.*, 15 (6), p1567-1573, 1979.

Sharma, M.L., G.A. Gander and C.G. Hunt, Spatial variability of infiltration in a watershed, *J. Hydrol.*, 45, p101-122, 1980.

Sloan, P.G. and I.D. Moore, Modelling subsurface stormflow on steeply forested watersheds, *Water Resources Res.*, 20 (12), p1815-1822, 1984.

Smith, L., A stochastic analysis of steady state groundwater flow in a bounded domain, *Phd. thesis*, Univ. British Columbia, Vancouver, Canada, 325pp, 1978.

Smith, L. and R.A. Freeze, Stochastic analysis of steady state groundwater flow in a bounded domain. 1 One dimensional simulations, *Water Resources Res.*, 15 (3), p521-528, 1979a.

Smith, L. and R.A. Freeze, Stochastic analysis of steady state groundwater flow in a bounded domain. 2 Two dimensional simulations, *Water Resources Res.*, 15 (6), p1543-1559, 1979b.

Smith, R.E. and D.A. Woolhiser, Mathematical simulation of infiltrating watersheds, *Hydrol. Paper 47*, Colorado State Univ., Colorado, USA, 1971.

Smith, R.E. and R.H.N. Hebbert, A Monte Carlo analysis of the hydrologic effects of spatial variability of infiltration, *Water Resources Res.*, 15 (2), p419-429, 1979.

Stauffer, F., Numerical simulation of infiltration onto porous media and response of the water table, *Proc. Fourth Int. Conf. on Finite Elements in Water Resources*, Hannover, W. Germany, 1982.

Stauffer, F. and D. Job, Infiltration in geschichteten boden und reaktion des grundwasserspiegels experiment und simulation, *Report 18-82*, Insitut fur Hydromechanik und Wasserwirtschaft eth Zurich, Zurich, Switzerland, 1982.

Stockton, J.G., Spatial variability of soil hydrologic parameters, *MSc. thesis*, Dept. Agric. Chemistry and Soils, Univ. Arizona, Arizona, USA, 1971.

Taylor, C., A computer simulation of direct run-off, *Proc. First Int. Conf. on Finite Elements in Water Resources*, Princeton Univ.,USA, 1976.

Thomas, R.G., Groundwater models, *Irrigation and drainage paper 21*, Food and Agric. Organization of the United Nations, Rome ,1973.

Todsen, M., Numerical studies of two dimensional saturated/unsaturated drainage models, *J. Hydrol.*, 20, p311-326, 1973.

Trescot, P.C., G.F. Pinder and S.P. Larson, Finite-difference model for aquifer simulation in two dimensions with results of numerical experiments, *US Geological Survey Techniques of Water Resouces Investigations*, Book 7, Ch. C1, 1976.

Troake, R.P. and D.E. Walling, The natural history of the Slapton Ley nature reserve. VII The hydrology of the Slapton Wood stream: a preliminary report, *Field studies*, 3, 719-740, 1973.

Trudgill, S.T., The natural history of the Slapton Ley nature reserve. XVI The soils of Slapton Wood, *Field studies*, 5, 1983.

Tyson, R.G., Groundwater management for the nations future - computer simulation of groundwater basins, *J. Hyd. Div. ASCE*, 90, p59-77, 1964.

Van Genuchten, M. Th., A comparison of numerical solutions of the one dimensional unsaturated-saturated flow and mass transport, *Proc. Third Int. Conf. on Finitè Elements in Water Resources*, Oxford, Miss., USA, 1980.

Vauclin, M., D. Khanji and G. Vachaud, Experimental and numerical study of a transient two-dimensional unsaturated-saturated water table recharge problem, *Water Resources Res.*, 15 (5), p1089-1101, 1979.

Viera, S.R., D.R. Nielsen and J.W. Biggar, Spatial variability of field measured infiltration rate, *Soil Sci. Soc. Am. J.*, 45, 1040-1048, 1981.

Warren, J.E. and H.S. Price, Flow in heterogeneous porous media, *Soc. Petrol. Eng. J.*, 1, p153-169, 1961.

Webster, R. and H.E. Cuanalo de la C, Soil transect correlograms of North Oxfordshire and their interpretation, *J. Soil Sci.*, 26, p176-194, 1975.

Whittle, P., On stationary processes in the plane, *Biometrika*, 41, p434-449, 1954.

Woolhiser, D.A. and J.A. Ligget, Unsteady one-dimensional flow over a plane - The rising hydrograph, *Water Resources Res.*, 3 (3), p753-771, 1967.

Yeh, G.T., An interstitial water transport model in aquifer systems by finite element method, *Proc. Int. Conf. Water Resources Development*, Taipei, Taiwan, China, 1980.

Yeh, T.C.J., L.W. Gelhar and A.L. Gutjhar, Stochastic analysis of unsaturated flow in heterogeneous soils. 1 Statistically isotropic media, *Water Resources Res.*, 21 (4), p447-456, 1985a.

Yeh, T.C.J., L.W. Gelhar and A.L. Gutjhar, Stochastic analysis of unsaturated flow in heterogeneous soils. 2 Statistically anisotropic media with variable α, *Water Resources Res.*, 21 (4), p457-464, 1985b.

Youngs, E.G., an estimation of sorptivity for sorptivity for infiltration studies from moisture movement consideration, *Soil Sci.*, 106, p157-163, 1968.

Zaslavsky, D. and G. Sinai, Surface hydrology: IV Flow in a sloping layered soil, *J. Hyd. Div. ASCE*, 107, p53-64, 1981.

List of symbols

Listed below are the most commonly used symbols. Other symbols are defined where they appear in the text.

a	Parameter of relative hydraulic conductivity function.
A	Parameter of relative moisture content function.
A	Final infiltration rate.
A_{ij}	Coefficient of finite element matrix **A**.
b	Parameter of relative hydraulic conductivity function.
B	Parameter of relative moisture content function.
B_i	Coefficient of finite element vector **B**.
C	Specific moisture capacity.
CV_q	Coefficient of variation of flow rate.
CV_Q	Coefficient of variation of volume of flow.
CV_ψ	Coefficient of variation of pressure head.
e	Element number.
$E\{\}$	Expected operator.
f	Function.
F	Frequency.
F_{ij}	Coefficient of finite element matrix **F**.
h	Hydraulic head.
$\tilde{h}$	Perturbation of h.
i	Node number.
i	Infiltration rate.
$\mathbf{J}$	Jacobian of the transformation from global to local coordinates.
$\lvert \mathbf{J} \rvert$	Determinant of **J**.
k	Intrinsic permeability.
K_{eff}	Effective hydraulic conductivity.
K_r	Relative hydraulic conductivity.
K_s	Saturated hydraulic conductivity.
$\mathbf{K}_s$	Saturated hydraulic conductivity tensor.
$\bar{K}_A$	Arithmetic mean of block hydraulic conductivities.

$\overline{K}_G$	Geometric mean of block hydraulic conductivities.
$\overline{K}_H$	Harmonic mean of block hydraulic conductivities.
L	Differential operator.
n	Number of node points.
N_i	Shape function for node i.
q	Discharge rate.
$\bar{q}$	Mean discharge rate.
Q	Volume of discharge.
Q_i	Coefficient of finite element vector **Q**.
$\overline{Q}$	Mean volume of discharge.
r	Pore radius.
R	Region.
R	Residual.
R^e	Region of element e.
s_e	Pore size density function.
S	Boundary surface.
S_e	Effective saturation.
S_q	Standard deviation of flow rates.
S_Q	Standard deviation of flow volumes.
S_r	Residual saturation.
S_ψ	Standard deviation of pressure head values.
S^e	Boundary surface of element e.
t	Time.
u	Function.
W_ε	Weight coefficient for Gauss quadrature.
W_η	Weight coefficient for Gauss quadrature.
W_ζ	Weight coefficient for Gauss quadrature.
x	Horizontal axis.
y	Horizontal axis.
Y	Ln (K_s) or Ln (final infiltration rate).
z	Vertical axis.
α_Y	Autocorrelation parameter of the variation of Y.
β	Parameter of relative moisture content function.

γ	Parameter of relative moisture content function.
ε	Local coordinate axis.
η	Local coordinate axis.
ζ	Local coordinate axis.
θ	Moisture content.
θ_{res}	Residual moisture content.
θ_s	Saturated moisture content.
Θ	Function.
μ_Y	Mean of Y.
ρ_{xy}	Autocorrelation of $\ln(K_s)$ in x-y plane.
ρ_z	Autocorrelation of $\ln(K_s)$ in z axis.
ρ_ι	Autocorrelation at lag ι.
σ^2_Y	Variance of Y.
Φ	Function.
ψ	Pressure head.
ψ_i	Nodal pressure head.
ψ_o	Air entry pressure head.
$\overline{\psi}$	Mean pressure head.
Δ	Increment.
∇	Laplace operator.